Imperial College London

Assessment of new *in vitro* and *in vivo* models for mumps virus replication

Lauren Parker, BSc (Honours)

This thesis is submitted in fulfilment of the requirements of Imperial College London for the degree of Doctor of Philosophy (PhD)

Imperial College London
Department of Medicine
Section of Virology
St Mary's Campus
Norfolk Place
London
W2 1PG

January 2013

DECLARATION OF ORIGINALITY

I, Lauren Parker, declare that the work presented in this thesis is entirely my own except where appropriately referenced, and that none of this work has previously been submitted to Imperial College or any other university for any other degree.

ACKNOWLEDGEMENTS

I would first and foremost like to thank my supervisors Dr Silke Schepelmann (NIBSC) and Dr Mike Skinner (Imperial College London). Silke has encouraged and helped me to become independent in my research, Mike has always helped me to view my research in a different light and to think "outside the box", and both have instilled my self-confidence over the past three years.

There are many of my colleagues at NIBSC who have helped me in some way during my PhD, but in particular I would like to thank Dr Phil Minor for taking an interest in my project, and always being able to make time for me whether it be to read over my upgrade report and thesis chapters or simply to talk through ideas and results. I owe an enormous amount of thanks and gratitude to Sarah Gilliland and Ruth Harvey for their friendship and constant support in and out of work over the past three years. They made me feel so welcome when I moved to NIBSC and I wouldn't have got this far without them. I'd also like to thank NIBSC for funding me during this project.

I would not be where I am now if not for my long-suffering boyfriend Mark and of course, my parents Mike and Wilma. Mark has been a continuous source of encouragement and support, and I cannot thank him enough for leaving his job and friends to move to London with me so I could fulfil my wish of doing this PhD. There are not enough ways to say thank you to my parents that will suffice, and therefore I am dedicating this PhD thesis to them and hope it will give them a small idea as to how grateful I am for everything they have done for me and how much they mean to me.

ABSTRACT

Mumps virus (MuV) is a paramyxovirus which causes mumps, a communicable disease in humans characterised by pain and swelling of the parotid gland(s). Suspected mumps cases are confirmed by PCR detection of MuV nucleotide sequences followed by virus isolation using Vero cells. Veros are the "gold-standard" for MuV isolation however they may select for attenuated or adapted virus variants and produce genetically altered viruses unsuitable for research, although this has never been confirmed. A cell line investigation was performed to assess genetic stability, viral fitness and plaque phenotype of MuV through serial passage in a panel of cell lines including Veros. Primary *ex-vivo* human airway epithelial cultures were infected with different MuV strains to investigate their susceptibility to MuV. The data presented here shows mutations in MuV introduced during passage through Vero and other continuous cell lines for the first time and suggests alternative cell lines for MuV propagation. HAE cells are demonstrated to be capable of isolating MuV from a clinical sample and producing progeny virus with superior genetic similarity to the parent virus when compared with Vero's.

No animal model exists for MuV therefore *in vivo* knowledge of the virus is limited. Ferrets are established as a successful model for influenza virus. MuV and influenza share certain biological features such as utilisation of sialic acid as the cellular receptor and both are negative-sense single-stranded RNA viruses. This suggests that ferrets may be useful as a MuV model. Ferrets were assessed as an *in vivo* mumps model by investigation of clinical signs, virus shedding and recovery from tissues, serum antibody response and detectable immune response in PBMCs. The data presented here demonstrate that ferrets elicit a mumps-specific neutralising antibody response and mount a cytokine response consistent with viral infection, however due to lack of clinical symptoms, virus shedding and virus recovery from tissues, the ferret model is very limited in its usefulness for MuV research.

TABLE OF CONTENTS

Title Page.....1
Declaration of Originality.....2
Acknowledgements.....3
Abstract..... 4
List of Figures.....10
List of Tables.....12
Abbreviations.....13

1. Introduction.....16

1.1 A Brief History of Mumps.....16

1.2 Mumps Pathogenesis and Disease.....17

1.3 Diagnosis of Mumps.....18

1.4 Mumps Epidemiology.....18

1.5 Mumps Vaccines.....19

1.6 Mumps Virus Taxonomy and Physical Properties.....22
1.6.1 Taxonomy.....22
1.6.2 Viral Genome.....22
1.6.3 Virus Structure.....23

1.7 Mumps Virus Proteins.....24
1.7.1 Nucleoprotein.....24
1.7.2 V/P/I Proteins.....25
1.7.3 Matrix Protein.....26
1.7.4 Fusion Protein.....26
1.7.5 Haemagglutinin-neuraminidase Protein.....27
1.7.6 Small Hydrophobic Protein.....28
1.7.7 Large Protein.....29

1.8 Virus Infection of Host Cells.....29
1.8.1 Virus Attachment and Entry.....29
1.8.2 Virus Transcription and Replication.....31
1.8.3 The Host Cell Anti-Viral Response to Infection.....32
1.8.4 Host Range Determination.....35

1.9 *In Vitro* Mumps Research.....36
1.9.1 Studies of Mumps Virus in Cell Substrates.....36
1.9.2 Defective Interfering Particles.....38

1.10 *In Vivo* Mumps Research....39
1.10.1 Experimental Animal Models....39
1.10.2 Mumps and Ferrets....41

1.11 Fundamental Mumps Research....43

1.12 PhD Project Aims....45

2. Materials and Methods....46

2.1 Materials....46
2.1.1 Eukaryotic Cell Lines....46
2.1.2 Cell Culture Media....49
2.1.3 Viruses....51
2.1.4 Standard and Real-time PCR Primers and Probes....51
2.1.5 Molecular Biology Reagents, Chemicals and Buffers....53

2.2 Cell Culture....57
2.2.1 Routine Cell Culture....57
2.2.2 Routine Maintenance of MucilAir™ HAE Cells....57
2.2.3 Preparation of Primary Cells....58

2.3 Routine *In Vitro* Virology....58
2.3.1 Virus Infection of Cells in 96-well Plates....58
2.3.2 Virus Infection of Cells and Preparation of Progeny Virus....59
2.3.3 Passaging of Viruses through Cell Lines....60
2.3.4 Infection of MucilAir™ HAE Cells....60
2.3.5 Titration of Viruses....61
2.3.6 Plaque Reduction Neutralisation (PRN) Assays....61

2.4 Routine Molecular Virology....63
2.4.1 RNA Extraction....63
2.4.2 Reverse-Transcriptase (RT) PCR....63
2.4.3 Standard PCR....64
2.4.4 PCR Product Purification....65
2.4.5 Sequencing Reactions....66
2.4.6 Preparation of Standard Curves for Real-Time Quantitative RT-PCR....66
2.4.7 Real-Time Quantitative RT-PCR....67
2.4.8 SYBR® Green Real-Time RT-PCR....67

2.5 Immunohistochemistry....68
2.5.1 Optimisation of Antibody Dilutions....68
2.5.2 Staining of MucilAir™ Histological Sections....69

2.6 Sialic Acid Investigations....69

2.6.1 Sialic Acid Quantification Bioassay.....69
2.6.2 Fluorescence Activated Cell Sorting (FACS) Analysis.....71
2.6.3 Sialic Acid Blocking.....71

2.7 Human Cytokine ELISA.....72

2.8 *In Vivo* Virology.....73
2.8.1 Animals.....73
2.8.2 Blood Sample Processing.....74
2.8.3 Nasal Wash Processing.....75
2.8.4 Urine Sample Processing.....75
2.8.5 Faeces Sample Processing.....75
2.8.6 Oral Swab Processing.....75
2.8.7 Tissue Homogenate Preparation.....76
2.8.8 Preparation of Tissue Homogenates Spiked with Mumps Virus.....77

3. Results – *In Vitro*.....78

3.1 Initial Cell Line Screen.....79
3.1.1 Cell Line Screen Using a GFP-Expressing Mumps Virus.....79
3.1.2 Cell Line Screen Using Representative Wild-Type and Vaccine Mumps Viruses.....82

3.2 Mumps Virus Serial Passage Through Various Cell Lines.....85
3.2.1 Vero.....86
3.2.2 A549 (BVDV).....89
3.2.3 A549 (PIV5-V).....91
3.2.4 CaCO2.....94
3.2.5 Hep 2C.....97
3.2.6 MCF-7.....99
3.2.7 PANC-1.....101
3.2.8 HGT-1.....102
3.2.9 RD.....104
3.2.10 BSC-1.....107
3.2.11 COS-7.....109
3.2.12 LLC-MK2.....112
3.2.13 MA-104.....114
3.2.14 B95a.....118
3.2.15 BHK-21.....120
3.2.16 JH4 Clone 1.....122
3.2.17 MDCK.....125

3.3 Assessment of Plaque Formation on Various Cell Lines.....127

3.4 Sialic Acid Investigations.....129
3.4.1 Sialic Acid Bioassay.....129

3.4.2 FACS Analysis.....131
3.4.3 Infection of MDCK-SIAT1 Cells with Mumps Virus.....135
3.4.4 Sialic Acid Blocking.....136

3.5 Experimental Infection of MucilAir™ HAE with Mumps Virus.....140
3.5.1 Infection of HAE with Representative Wild-Type and Vaccine Mumps Viruses.....140
3.5.2 Isolation of Clinical Mumps Virus using HAE Cells.....143
3.5.3 Immunohistochemistry of HAE Cell Sections Infected with Mumps Virus.....145
3.5.3.1 Optimisation of Antibody Dilutions.....145
3.5.3.2 Immunofluorescence Staining of HAE Cell Sections.....147
3.5.4 Comparison of HAE and Vero Cells for Isolation of Clinical Mumps Virus.....149

3.6 Results Summary.....153

3.7 Discussion.....160
3.7.1 Cell Line Screen.....160
3.7.2 Sialic Acid Studies.....168
3.7.3 HAE Cell Investigation.....170

4. Results – *In Vivo*.....174

4.1 Ferret Study A.....175
4.1.1 Clinical Signs of Infection.....175
4.1.2 Isolation of Virus from Nasal Washes, Urine and Faeces.....179
4.1.3 PRN Assays.....179
4.1.4 Recovery of Virus from day 28 Ferret Tissues.....183

4.2 Ferret Study B.....187
4.2.1 Heat-inactivation of Mumps Virus.....187
4.2.2 PRN Assays.....188

4.3 Ferret Study C.....193
4.3.1 Isolation of Virus from Oral Swabs.....193
4.3.2 Recovery of Virus from Ferret Tissues.....194
4.3.3 Spiking of Uninfected Ferret Tissue Homogenates with Mumps Virus.....197
4.3.4 Detection of Mumps Virus in Ferret PBMCs.....199
4.3.5 Detection of Cytokines in Ferret PBMCs.....200
4.3.6 Human Cytokine ELISA.....202

4.4 Ferret Study D.....204
4.4.1 Recovery of Virus from Ferret Tissue Homogenates.....204

4.5 Results Summary.....208

4.6 Discussion.....209

5. Concluding discussion.....217

References.....220

LIST OF FIGURES

Figure 1 – MuV genome organisation
Figure 2 – Schematic representation of a MuV virion
Figure 3 – GFP expression levels of various cell lines infected with GFP-MuV over 10 days
Figure 4 – Representative wild-type (Mu90) and vaccine (RIT 4385) progeny virus titres from various cell lines
Figure 5 – P1 to P5 progeny virus titres (Vero)
Figure 6 – P1 to P5 plaque morphologies (Vero)
Figure 7 – P1 to P5 progeny virus titres (A549 (BVDV))
Figure 8 – P1 to P5 plaque morphologies (A549 (BVDV))
Figure 9 – P1 to P5 progeny virus titres (A549 (PIV5-V))
Figure 10 – P1 to P5 plaque morphologies (A549 (PIV5-V))
Figure 11 – P1 to P5 progeny virus titres (CaCO2)
Figure 12 – P1 to P5 plaque morphologies (CaCO2)
Figure 13 – P1 to P5 progeny virus titres (Hep 2C)
Figure 14 – P1 to P5 plaque morphologies (Hep 2C)
Figure 15 – P1 to P5 progeny virus titres (MCF-7)
Figure 16 – P1 to P5 plaque morphologies (MCF-7)
Figure 17 – P1 to P5 progeny virus titres (PANC-1)
Figure 18 – P1 to P5 plaque morphologies (PANC-1)
Figure 19 – P1 to P5 progeny virus titres (HGT-1)
Figure 20 – P1 to P5 plaque morphologies (HGT-1)
Figure 21 – P1 to P5 progeny virus titres (RD)
Figure 22 – P1 to P5 plaque morphologies (RD)
Figure 23 – P1 to P5 progeny virus titres (BSC-1)
Figure 24 – P1 to P5 plaque morphologies (BSC-1)
Figure 25 – P1 to P5 progeny virus titres (COS-7)
Figure 26 – P1 to P5 plaque morphologies (COS-7)
Figure 27 – P1 to P5 progeny virus titres (LLC-MK2)
Figure 28 – P1 to P5 plaque morphologies (LLC-MK2)
Figure 29 – P1 to P5 progeny virus titres (MA-104)
Figure 30 – P1 to P5 plaque morphologies (MA-104)
Figure 31 – P1 to P5 progeny virus titres (B95a)
Figure 32 – P1 to P5 plaque morphologies (B95a)
Figure 33 – P1 to P5 progeny virus titres (BHK-21)
Figure 34 – P1 to P5 plaque morphologies (BHK-21)
Figure 35 – P1 to P5 progeny virus titres (JH4 Clone 1)
Figure 36 – P1 to P5 plaque morphologies (JH4 Clone 1)
Figure 37 – P1 to P5 progeny virus titres (MDCK)
Figure 38 – P1 to P5 plaque morphologies (MDCK)
Figure 39 – MuV plaque morphologies on various cell lines
Figure 40 – Sialic acid quantification bioassay data
Figure 41 – Control cell lines FACS data
Figure 42 – FACS analysis data, DIG glycan differentiation of various cell lines

Figure 43 – MDCK-SIAT1 progeny virus titres
Figure 44 – α2,3 sialic acid blocking assay data
Figure 45 – α2,3 and α2,6 sialic acid blocking assay data
Figure 46 – Representative wild-type and vaccine progeny MuV titres from HAE cells
Figure 47 – Progeny virus plaque morphologies from HAE cells (Mu90 and RIT 4385)
Figure 48 - Clinical MuV titres from HAE cells
Figure 49 – Progeny virus plaque morphologies from HAE cells (AFZ315)
Figure 50 – Optimal dilutions for immunofluorescence antibodies
Figure 51 – Confocal images of HAE cells infected with MuV
Figure 52 – Clinical MuV titres from HAE and Vero cells
Figure 53 – Ferret study A summary
Figure 54 – Ferret clinical signs data
Figure 55 – Ferret plaque reduction neutralisation assay data (study A)
Figure 56 – Ferrets 1 to 6, day 28 tissues real-time PCR data
Figure 57 – Live versus heat-inactivated MuV real-time PCR data
Figure 58 – Ferret study B summary
Figure 59 – Ferret plaque reduction neutralisation assay data (study B)
Figure 60 – Influenza PR8 and MuV HPA1.1/P1V challenge plaque reduction neutralisation assay data
Figure 61 – Ferret study C summary
Figure 62 – Ferrets 1.1 to 1.8 tissues real-time PCR data
Figure 63 – Limit of detection mumps virus in ferret tissues by real-time RT-PCR
Figure 64 – Ferrets 1.1 to 1.8 PBMCs real-time PCR data
Figure 65 – Detection of cytokines in ferret PBMCs SYBR® Green real-time PCR data
Figure 66 – Measurement of cytokine levels in basal HAE cell samples, ELISA data
Figure 67 – Ferret study D summary
Figure 68 – Ferrets 1 to 4 tissues real-time PCR data (study D)

LIST OF TABLES

Table 1 – Amino acid name abbreviations and symbols
Table 2 – Mumps vaccines in recent use
Table 3 – Eukaryotic cell lines
Table 4 – Cell culture and maintenance media
Table 5 – Viruses
Table 6 – Standard PCR primers
Table 7 – Real-time PCR primers
Table 8 – In-house chemicals and reagents
Table 9 – Standard preparation for sialic acid bioassay
Table 10 – Ferret tissues analysed
Table 11 – Cell lines selected from initial screen for further investigation
Table 12 – Amino acid substitutions in P5 progeny virus proteins (Vero)
Table 13 - Amino acid substitutions in P5 progeny virus proteins (A549 (BVDV))
Table 14 - Amino acid substitutions in P5 progeny virus proteins (A549 (PIV5-V))
Table 15 - Amino acid substitutions in P5 progeny virus proteins (CaCO2)
Table 16 - Amino acid substitutions in P5 progeny virus proteins (Hep 2C)
Table 17 - Amino acid substitutions in P5 progeny virus proteins (MCF-7)
Table 18 - Amino acid substitutions in P5 progeny virus proteins (HGT-1)
Table 19 - Amino acid substitutions in P5 progeny virus proteins (RD)
Table 20 - Amino acid substitutions in P5 progeny virus proteins (BSC-1)
Table 21 - Amino acid substitutions in P5 progeny virus proteins (COS-7)
Table 22 - Amino acid substitutions in P5 progeny virus proteins (LLC-MK2)
Table 23 - Amino acid substitutions in P5 progeny virus proteins (MA-104)
Table 24 - Amino acid substitutions in P5 progeny virus proteins (B95a)
Table 25 - Amino acid substitutions in P5 progeny virus proteins (BHK-21)
Table 26 - Amino acid substitutions in P5 progeny virus proteins (JH4 Clone 1)
Table 27 - Amino acid substitutions in P5 progeny virus proteins (MDCK)
Table 28 – Mean number of MuV plaques formed on various cell lines
Table 29 – Amino acid substitutions in N, F, HN and SH proteins of HAE and Vero AFZ315 progeny viruses
Table 30 – Summary of identical amino acid substitutions in P5 Mu90 MuVs from various cell lines
Table 31 – Summary of identical amino acid substitutions in P5 RIT 4385 MuVs from various cell lines

ABBREVIATIONS

A - adenine
ABI – Applied Biosystems
ADAR - dsRNA-specific adenosine deaminase
APOBEC3G - apolipoprotein B mRNA-editing enzyme-catalytic polypeptide 3G
ATCC – American Type Tissue Culture Collection
BD – Becton Dickinson
BSA – bovine serum albumin
BSD – Biological Services Division
BVDV – Bovine viral diarrhoeal virus
C - cytosine
$CaCl_2$ – calcium chloride
CARD – caspase-recruiting domain
CDV – Canine distemper virus
CEF – chicken embryo fibroblast
CMC – carboxymethylcellulose
CNS – central nervous system
CPE – cytopathic effect
CRP – C-reactive protein
CSF – cerebrospinal fluid
DEPC – diethyl pyrocarbonate
DI – defective interfering particles
DIG – digoxigenin
DMEM – Dulbecco's Minimum Essential Medium
DNA – deoxyribose nucleic acid
dNTP – deoxynucleotide
dsRNA – double-stranded RNA
EBI – European Bioinformatics Institute
ECACC – European Collection of Cell Cultures
EDTA – ethylenediamine tetra acetic acid
ELISA – enzyme-linked immunosorbent assay
EMBL – European Molecular Biology Laboratory
F – fusion protein or gene
F_0 – fusion protein inactive precursor
F_1 – carboxy-terminal subunit of F
F_2 – amino-terminal subunit of F
FACS – fluorescence-activated cell sorting
FCS – foetal calf serum
FDA – Food and Drug Administration
FI – fluorescence intensity
FITC – fluorescein isothiocyanate
G - guanine
GAPDH – glyceraldehyde 3-phosphate dehydrogenase
GFP – green fluorescent protein
GFP-MuV – GFP-expressing mumps virus
GSK – GlaxoSmithKline
HAE – human airway epithelial cells
HIV – human immunodeficiency virus
HN – haemagglutinin – neuraminidase protein or gene
HPA – Health Protection Agency

hPIV2 – human parainfluenza virus type 2
hPIV3 – human parainfluenza virus type 3
hPIV5 – human parainfluenza virus type 5
HRP – horse radish peroxidase
IFN - interferon
IL – interleukin
IPS-1 – interferon-β promoter stimulator
IRF-3 – interferon regulatory factor 3
JAK – Janus kinase
JL-2 – Jeryl-Lynn 2
JL-5 – Jeryl-Lynn 5
KCl – potassium chloride
kDa – kilo Daltons
KH_2PO_4 – monopotassium phosphate
L – large (polymerase) protein or gene
L-3 – Leningrad 3 mumps strain
L-15 – Liebovitz-15 medium
LO-1 – London-1 mumps virus
LPG2 – Laboratory of physiology and genetics 2
L-Zagreb – Leningrad-Zagreb mumps strain
M – matrix protein or gene
MAA – Maackia amurensis agglutinin
mda-5 – melanoma-differentiation-associated protein 5
MEM – Minimum Essential Medium
$MgCl_2$ – magnesium chloride
MMR – Measles, Mumps and Rubella vaccine
$MnCl_2$ – manganese chloride
MOI – multiplicity of infection
mRNA – messenger RNA
MuV – mumps virus
MV – measles virus
N – nucleoprotein/nucleocapsid or gene
Na_2HPO_4 – sodium phosphate dibasic
NaCl – sodium chloride
NCBI – National Centre for Biotechnology Information
NDV – Newcastle disease virus
NF-κB – nuclear factor-kappa B
NIBSC – National Institute for Biological Standards and Control
NiV – Nipah virus
NPro – N-terminal protease fragment
nt - nucleotide
OD – optical density
P – phosphoprotein or gene
PAMPs – pathogen-associated molecular patterns
PBMC – peripheral blood mononuclear cells
PBS – phosphate buffered saline
PCR – polymerase chain reaction
pfu – plaque forming units
PKR - protein kinase dsRNA-regulated
PRN – plaque reduction neutralisation
PRRs – pattern recognition receptors

PVR – poliovirus receptor
RdRp – RNA-dependent RNA polymerase
RIG-I – Retinoic acid inducible gene I
RNA – ribonucleic acid
RNP – ribonucleoprotein complex
RPMI – Roswell Park Memorial Institute
RSV – Respiratory Syncytial virus
RT – reverse transcription
SA – sialic acid
SeV – Sendai virus
SH – small hydrophobic protein or gene
SILAC – stable isotope labelling of amino acids in cell culture
SNA – Sambucus nigra agglutinin
SPR – surface plasmon resonance
ssRNA – single-stranded RNA
STAT – signal transducer and activator of transcription
SV-40 – Simian virus 40
T – thymine
Taq – *Thermus aquaticus*
TBE – Tris borate EDTA
TBS – Tris-buffered saline
TLR – Toll-like receptor
Tris - tris (hydroxymethyl) aminomethane
VLP – virus-like particle
ZO-1 – zonula occludens-1

Table 1 - Amino acid name abbreviations and symbols

Name	Abbreviation	Symbol
Alanine	Ala	A
Arginine	Arg	R
Asparagine	Asn	N
Aspartate	Asp	D
Cysteine	Cys	C
Glutamate	Glu	E
Glutamine	Gln	Q
Glycine	Gly	G
Histidine	His	H
Isoleucine	Ile	I
Leucine	Leu	L
Lysine	Lys	K
Methionine	Met	M
Phenylalanine	Phe	F
Proline	Pro	P
Serine	Ser	S
Threonine	Thr	T
Tryptophan	Trp	W
Tyrosine	Tyr	Y
Valine	Val	V

CHAPTER 1 – INTRODUCTION

1.1 A Brief History of Mumps

Mumps is one of the oldest human illnesses known, and is thought to have been first recorded by Hippocrates in the 5th century B.C in his Book of Epidemics. He described a painful epidemic illness with swelling of the testes in male patients, and around the neck and jaw, which is likely to be a description of the most characteristic symptom of mumps that we know today, swelling of the parotid gland(s). During the late 18th century, a physician named Robert Hamilton made the first association between mumps and its implication in central nervous system (CNS) disease during documentation of a fatal case (Hamilton, 1790). In 1908, a causative agent for mumps was suggested by Granata (first cited in (Wollstein, 1916)), who reported that the illness may be caused by a filterable pathogen after experiments using rabbits resulted in swelling of the parotid glands following direct inoculation with filtrate from a patient. In 1933, Johnson and Goodpasture carried out a series of experiments showing that mumps is caused by a virus (Johnson & Goodpasture, 1934). Briefly, they inoculated Rhesus Macaques via the Stenson's duct with saliva collected from a patient, and the animals were sacrificed upon development of swelling of the parotid glands. Homogenates were prepared from the parotid glands for passage through more animals. To fulfil Koch's Postulates, bacteria free material from the infected parotid glands of the macaques was inoculated into groups of volunteer children via intranasal and oral routes. Saliva samples were taken from children demonstrating clinical symptoms and parotid swelling, and these were inoculated into healthy Rhesus Macaques who then once again, demonstrated the symptoms of mumps (Johnson & Goodpasture, 1935). These findings and the development of using embryonated eggs (Habel, 1945) and tissue culture systems (Henle & Deinhardt, 1955) for isolation of the virus increased knowledge and understanding of mumps infection, and led to the development of the live attenuated mumps vaccine strain in 1967, and thus a steady worldwide decline in the number of cases of mumps.

1.2 Mumps Pathogenesis and Disease

Mumps is traditionally known as a childhood illness and is characterised primarily by pain and swelling of the parotid gland(s) which may be unilateral or bilateral. Although this is by no means the only symptom, it is the most common characteristic in terms of diagnosis. Approximately one third of mumps cases are asymptomatic, however in those cases presenting symptoms, parotitis is evident in approximately 95% of these (Philip *et al.*, 1959). It is generally a mild, self-limiting illness however in a small number of cases, more severe complications such as meningitis or encephalitis can occur due to CNS involvement, and it has been known to be a major cause of childhood deafness. Orchitis occurs in approximately 15-30% of male patients and oophoritis in 5% of female patients (Hviid *et al.*, 2008). The virus is also capable of infecting a multitude of other tissues including the brain, heart, liver, pancreas, spleen, and kidneys. Humans are the only reservoir for the virus.

Mumps virus (MuV) is transmitted via droplet spread or from direct contact with an infectious patient therefore large groups of people living closely together are required for an outbreak of the disease to occur. The primary site of virus replication is the upper respiratory epithelium such as those found in the nasal epithelia or salivary glands. After initial replication, the virus spreads to local lymphoid tissues and then disseminates via a transient primary viraemia, which most likely occurs in T cells (Fleischer & Kreth, 1982). This allows MuV to spread to other organs resulting in a systemic illness, frequently being associated with localisation to the kidneys, pancreas, heart, testes, CNS and of course the parotid glands, however the virus is capable of infecting almost all tissue and organ types. The infection has also been shown to remain localised to the respiratory tract in some cases (Foy *et al.*, 1971).

The incubation period ranges from 15-24 days with virus being shed in saliva from approximately five days prior to the onset of clinical symptoms and five days after symptoms have subsided (Chiba *et al.*, 1973). MuV can also be detected in the urine of patients up to 14 days after the onset of clinical symptoms (Utz *et al.*, 1958) and has been detected in breast milk (Kilham, 1951).

1.3 Diagnosis of Mumps

With regards to clinical diagnosis, acute uni- or bilateral parotitis is the most common symptom of mumps disease. However, infection by other viruses such as Epstein-Barr (Lee *et al.*, 1997), human immunodeficiency virus (HIV) (Santra, 2009) and influenza A virus (Krilov & Swenson, 1985) has also been associated with parotitis, but these viruses are easily distinguishable from MuV by virus culture or serological techniques. Mumps is a reportable disease and by UK law, samples must be collected from suspect patients by health professionals to be sent for confirmatory diagnosis by laboratory methods.

Worldwide, suspected mumps cases are currently confirmed by RT-PCR detection of MuV nucleotide sequences, serological methods using patient sera or virus isolation from clinical samples (the most commonly used is saliva). Serological assays such as complement fixation, haemagglutinin-inhibition and virus neutralisation can be used, but mumps-specific IgG and IgM immune responses are commonly measured using ELISA methodology (Ukkonen *et al.*, 1981). However these are only easily performed when using patient sera taken at the acute phase of infection.

Vero cells are currently the "gold-standard" for MuV isolation and propagation. These cells are known to be deficient in the production of interferon (Desmyter *et al.*, 1968) and it is likely that this feature makes them so permissive for MuV infection.

1.4 Epidemiology of Mumps

Mumps is endemic worldwide with cases peaking in winter and spring months, however it is reported throughout the entire year. Historically, the disease was most commonly reported amongst children between the ages of 5 and 9 years old but in recent years there has been a resurgence in the number of reported mumps cases and with it, a change in the most commonly affected age group from 5 – 9 to 15 – 24. This is likely to be due to the fact that individuals in this age group were

too old to receive the two-dose schedule of vaccine when it was introduced in 1988, or only received one dose. The question of whether or not the mumps comeback is actually due to waning immunity has been raised many times in the last decade. Waning immunity is defined as the loss of protective antibodies over time and has been blamed for several recent mumps outbreaks (Cohen *et al.*, 2007) (Dayan *et al.*, 2008) however, a study in which cellular and humoral immunity were measured in a group of individuals 21 years after receiving a first vaccination demonstrated reduced humoral immunity but persistence of highly protective anti-mumps cellular immune responses (Jokinen *et al.*, 2007). Mumps is rarely seen in infants under the age of 1 year old, which is thought to be as a result of the presence of maternal antibodies (Plotkin & Rubin, 2008). The most recent figures from the Health Protection Agency (HPA) UK advise that in England and Wales for the quarter April to June 2012, there were 930 laboratory-confirmed cases of mumps from a total of 1564 reported and tested (HPA, 2012).

1.5 Mumps Vaccines

Mumps is a vaccine-preventable disease and when used appropriately, the scheduled two doses of the current trivalent MMR (Measles-Mumps-Rubella) vaccines are a highly effective means of keeping disease outbreaks at bay.

Formalin-inactivated killed vaccines were used during the 1950's and 1960's and this was the first documented means of protection against MuV by vaccination (Plotkin & Wharton, 1999). The use of these kinds of MuV vaccines did not last long however, with the development of live attenuated vaccines by serial passage of wild-type isolates in embryonated hens eggs or tissue culture during the late 1960's. The Jeryl Lynn (JL) strain was the first live MuV to be used as a mumps vaccine. It was derived from a throat culture isolate taken from the daughter of the scientist responsible for development of the vaccine at Merck and Co. and was attenuated by serial passage through chicken

embryo fibroblasts (CEFs) after initial isolation in embryonated hens eggs (Buynak & Hilleman, 1966). Sequence analysis of JL MuV revealed that the virus is actually a mixed population of two very distinct isolates which have been designated Jeryl Lynn 2 (JL-2) and Jeryl Lynn 5 (JL-5) (Afzal *et al.*, 1993) (Chambers *et al.*, 2009). The JL strain of MuV is the most commonly used worldwide in trivalent MMR vaccines at the time of writing, manufactured by Merck and Co as M-M-R II (Merck & Co, 2004). GlaxoSmithKline (GSK) Biologicals also manufacture a trivalent MMR vaccine, Priorix®, which has been used in the UK and throughout Europe since the late 1990's. The MuV strain used in Priorix® is designated RIT 4385 and is a pure population of JL-5 obtained by selective dilution of the mixed population JL virus and passage through CEFs (Tillieux *et al.*, 2009). Although these two are the most commonly used, there have been many other live attenuated MuV vaccines used in recent years and these are summarised in Table 2.

Table 2 – Live attenuated MuV vaccines in recent use

Virus strain	Growth/passage history	Genotype	Reference
Hoshino	Isolation in embryonated hens eggs, serial passage in CEFs	B	(Makino *et al.*, 1976)
Jeryl Lynn	Isolation in embryonated hens eggs, serial passage in CEFs	A	(Buynak & Hilleman, 1966)
Leningrad-3 (L-3)	Isolation and passage in primary guinea pig kidney cells, further serial passage in Japanese quail embryo fibroblasts	Distinct	(Smorodintsev, 1960) (WHO, 2007)
Leningrad-Zagreb (L-Zagreb)	Further serial passage of Leningrad-3 strain in CEFs	Distinct	(Beck *et al.*, 1989)
S79	Three further serial passages of JL in CEFs	A	(Fu *et al.*, 2009)
RIT 4385	Selective dilution and passage in CEFs of Jeryl Lynn	A	(Tillieux *et al.*, 2009)

Rubini	Isolation in WI-38 cells followed by serial passage in embryonated hens eggs and MRC-5 cells	A	(Gluck *et al.*, 1986)
Urabe AM9	Isolation and serial passage in embryonated hens eggs and CEFs	B	(Yamanishi *et al.*, 1970)

The genotypes for L-3 and L-Zagreb vaccine strains have been described as distinct in Table 2 as they form a phylogenetically separate group and a genotype has yet to be designated. Although the genotypes of MuV attenuated vaccine strains are varied, the virus is said to be serologically monotypic, therefore protection against one strain or genotype will infer immunity to all MuVs (Rubin *et al.*, 2006).

Some of these vaccine viruses have been associated with adverse events and as a result their use has either been restricted or withdrawn in many countries. The L-Zagreb and parental L-3 strains have been associated with vaccine-related aseptic meningitis (Cizman *et al.*, 1989) and mumps disease (Bakker & Mathias, 2001), as well as horizontal transmission of the vaccine viruses (Atrasheuskaya *et al.*, 2006) (Kaic *et al.*, 2008). Data linking L-Zagreb with vaccine-related meningitis (da Cunha *et al.*, 2002) was later shown to be inconclusive, however the virus was still found to cause mumps-like illness (Kulkarni *et al.*, 2005). These vaccines are still manufactured for use by the Serum Institute of India. The Rubini strain of MuV has also been associated with mumps outbreaks in previously vaccinated populations (Strohle *et al.*, 1997) (Goh, 1999) (Pons *et al.*, 2000) and this virus is rarely used now in vaccines. The Urabe AM9 live attenuated vaccine virus was shown to be a mixture of MuVs varying at one amino acid residue in the haemagglutinin-neuraminidase protein (Brown & Wright, 1998) and has been associated with neurovirulence and vaccine-related meningitis (Furesz & Contreras, 1990) (Ueda *et al.*, 1995) (Miller *et al.*, 1993). Vaccines containing Urabe AM9 were withdrawn from use in the UK, Canada and many other countries (Schmitt *et al.*, 1993). The JL and

RIT 4385 strains have not been associated with vaccination-related illness or complications (Hviid *et al.*, 2008).

The molecular basis of attenuation of MuVs from wild-type to vaccine strain is not fully understood other than serial passage in various types of tissue culture or embryonated hens eggs results in a loss of cytopathic effects (Plotkin & Rubin, 2008).

1.6 Mumps Virus Taxonomy and Physical Properties

1.6.1 Taxonomy

Mumps virus is a non-segmented, negative-sense, single-stranded RNA (ssRNA) virus belonging to the order *Mononegavirales*, family *Paramyxoviridae*, sub-family *Paramyxovirinae*, and genus *Rubulavirus*. Other members of this genus include human parainfluenza virus 5 (hPIV5), human parainfluenza virus types 2 (hPIV2), 4a (hPIV4a) and 4b (hPIV4b) and Porcine rubulavirus. Antigenic cross-reactivity and the presence of neuraminidase activity are the biological features necessary for classification in the *Rubulavirus* genus (Lamb & Parks, 2007). The family *Paramyxoviridae* contains many other important pathogenic viruses of humans and animals including measles virus (MV), human respiratory syncytial virus (RSV), human parainfluenza virus type 3 (hPIV3), Sendai virus (SeV), Newcastle disease virus (NDV) and the recently eradicated Rinderpest virus.

1.6.2 Viral Genome

The MuV genome is 15,384 nucleotides in length and encodes proteins in the following order: nucleocapsid (interchangeable with nucleoprotein throughout this thesis) (N), V, phospho- (P) and I proteins, membrane (M), fusion (F), small hydrophobic (SH), haemagglutinin-neuraminidase (HN) and large (L) proteins (Figure 1).

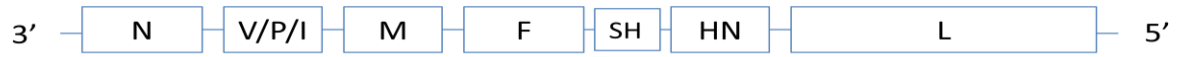

Figure 1 - Schematic representation of MuV genome organisation. Viral genome proceeds from 3’ to 5’ end in the order: nucleoprotein, V/P/I, matrix, fusion, small hydrophobic, haemagglutinin-neuraminidase and large genes.

Each gene is separated by untranslated regions (UTRs) of varying lengths consisting of gene end (GE) sequences containing transcriptional and translational stop signals. These stop signals are followed by gene start (GS) sequences containing transcriptional and translational start signals for the next gene (Elango *et al.*, 1988).

There are currently 13 different reported mumps genotypes designated A-M, however only 11 of these are actually different as a result of duplicative reporting from different research groups (Jin *et al.*, 2005; Santos *et al.*, 2008). The SH protein demonstrates the most genomic variation and is therefore commonly used for genotyping MuV strains (Yeo *et al.*, 1993).

1.6.3 Virus Structure

MuV forms spherical or pleomorphic virions ranging in size from approximately 100 to 600 nm. The virus consists of a helical ribonucleoprotein (RNP) core and a host-cell derived lipid membrane. The RNP core consists of the RNA genome associated with the N, P and L proteins. The viral envelope is studded with F and HN glycoprotein projections which extend approximately 12 to 15 nm from the virus surface and can be visualised by electron microscopy (Lamb & Parks, 2007). The SH protein is incorporated into the lipid envelope (Elliot *et al.*, 1989) (Elango *et al.*, 1988), while the matrix protein is situated between the RNP core and lipid envelope. A schematic diagram of a representative MuV virion demonstrating the locations of the major viral proteins is shown in Figure 2.

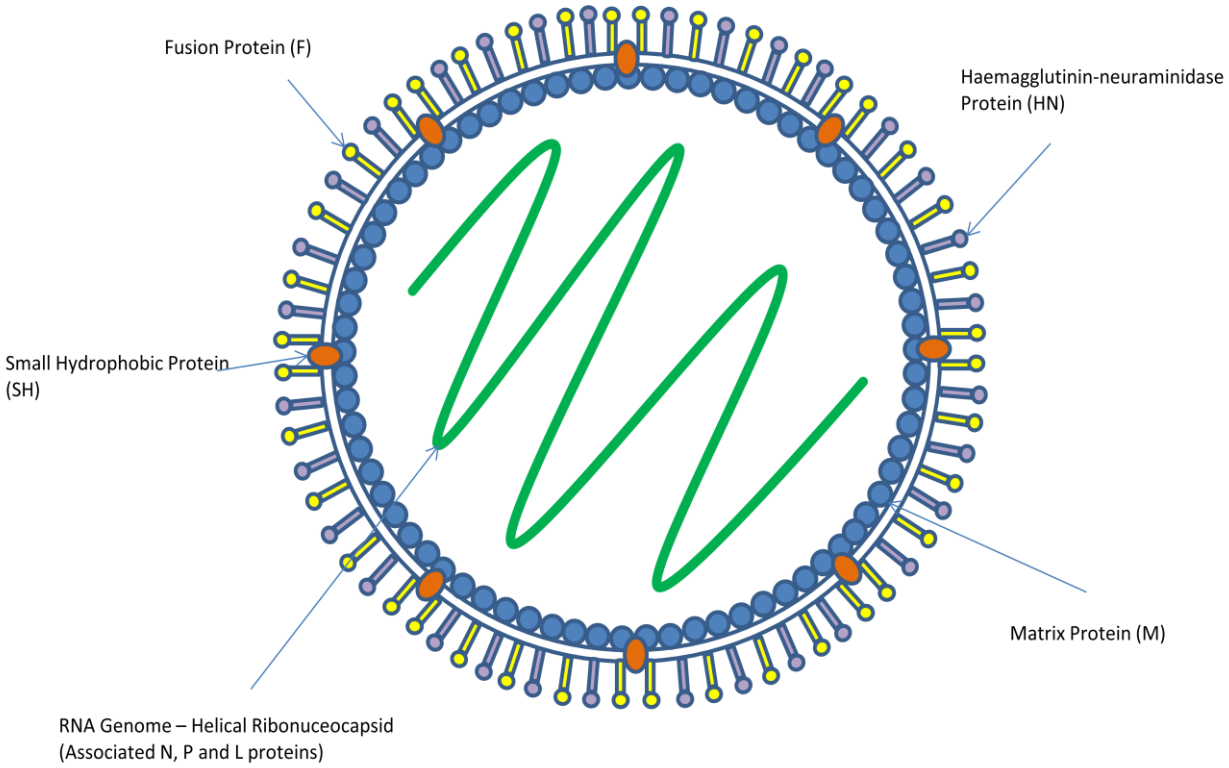

Figure 2 – Schematic representation of a MuV virion. A typical mumps virus virion consisting of helical RNP core comprising N, P, and L proteins, structural matrix protein underneath surface of viral envelope, and the surface fusion and HN glycoproteins.

1.7 Mumps Virus Proteins

The protein products from each of the MuV genes play essential roles in the survival and life cycle of the virus.

1.7.1 Nucleoprotein

The N gene encodes a 549 amino acid nucleoprotein of approximately 61-73 kilo Daltons (kDa) (Tanabayashi *et al.*, 1990) and is the first unit of the MuV genome to be transcribed. The primary

function of the nucleoprotein is to form a complex with the P and L proteins and the viral RNA genome, which results in the formation of the biologically active helical capsid structure which is required for RNA synthesis. “Naked” viral RNA, so-called because of a lack of nucleocapsid, is unable to replicate and cause infection in a host cell which indicates the importance of the N protein in the life cycle of MuV. The protein also has a protective role in preventing the action of host cell proteases upon the virus (Carbone & Rubin, 2007).

1.7.2 V/P/I Proteins

The three distinct V, P and I proteins are transcribed from the V/P/I gene by a process known as RNA editing, which differs from the transcription method of all of the other MuV proteins. The V protein is produced from a faithful V/P/I gene transcript, however co-transcriptional addition of two non-template guanine (G) nucleotides is necessary for production of the P protein, and addition of four non-template G nucleotides produces the I protein. (Takeuchi *et al.*, 1988) (Paterson & Lamb, 1990). The accuracy of these insertions has previously been demonstrated to differ between MuV strains (Elliott *et al.*, 1990). RNA editing results in the V, P and I proteins having the same amino-termini but different carboxy-termini.

The V protein is 224 amino acids in length and approximately 25-28 kDa (Takeuchi *et al.*, 1990). It plays a major role in the circumvention of the host cell interferon (IFN) response and has been demonstrated to interfere with the activities of signal transducers and activators of transcription 1 (STAT-1) (Horvath, 2004a; Kubota *et al.*, 2002; Nishio *et al.*, 2002) as well as interacting with melanoma differentiation associated protein 5 (mda-5) to inhibit interferon production via the IFN-β promoter (Andrejeva *et al.*, 2004). It has also been suggested that the MuV V protein plays a role in altering the activities of caspase-9 in the apoptosis pathway (Rosas-Murrieta *et al.*, 2011) and in suppressing interleukin-6 (IL-6) production (Xu *et al.*, 2012).

The P protein is 391 amino acids in length and approximately 41-47 kDa (Takeuchi *et al.*, 1988). Its main function is as part of the transcriptase complex, in association with the MuV L protein (section 1.6.7).

The I protein is 171 amino acids long and has a molecular weight of 19 kDa. Studies investigating the role of the I protein are lacking, and currently its function is unknown.

1.7.3 Matrix Protein

The M gene of MuV encodes the structural matrix protein which is 375 amino acids in length and has an approximate molecular weight of 41-47 kDa (Elliot *et al.*, 1989). The M protein plays a crucial role in virion assembly and structure, and it has been inferred from studies on the related paramyxoviruses NDV (Nagai *et al.*, 1976) and SeV (Sanderson *et al.*, 1994) that it serves to connect the viral genetic information and associated proteins (N, P and L) with the cytoplasmic tails of the envelope surface glycoproteins (F and HN). This interaction between the F and HN cytoplasmic tails and the viral genome has also been demonstrated for hPIV5 (Schmitt *et al.*, 1999). The M protein of MuV has also been shown to be essential for virus-like particle (VLP) formation (Li *et al.*, 2009) and due to its importance in virion assembly, is likely to play an important role in mediating virus budding (Takimoto & Portner, 2004).

1.7.4 Fusion Protein

The F protein is one of two MuV envelope surface glycoproteins and exists in a pre-cursor form designated as F_0 which is 538 amino acids in length and approximately 64-74 kDa (Elliot *et al.*, 1989) with a membrane anchor region of 30 hydrophobic residues in the C terminus (Waxham *et al.*, 1987). F_0 is biologically inactive until it is cleaved between amino acids 102 and 103 at the R-R-H-K-R motif sequence by host cell proteases after transport from the endoplasmic reticulum through to the trans-Golgi network (Gardner *et al.*, 2007) to form two smaller proteins designated F_1 and F_2 (Herrler & Compans, 1982) (Merz *et al.*, 1983).

The protease(s) responsible for this cleavage step in the MuV life cycle is furin or furin-like proteases (Nakayama, 1997). Furin is an ubiquitous subtilisin-like endoprotease that specifically recognises and acts upon the R-R-K-K-R motif, and is responsible for F_0 cleavage in other paramyxoviruses such as hPIV5V (Klenk & Garten, 1994), hPIV3 (Ortmann *et al.*, 1994) and MV (Watanabe *et al.*, 1995). The protease-dependent cleavage event transforms the F protein into its active state by an irreversible conformational change which causes the amino terminus of the F_1 sub-protein containing the highly conserved hydrophobic fusion peptide to become exposed (Scheid & Choppin, 1974) (Hsu *et al.*, 1981) (Novick & Hoekstra, 1988).

The crystal structure of the MuV F protein core has been solved, and was shown to comprise a complex of a six-helix bundle with a central hydrophobic coiled-coil formed of three heptad repeat (HR) peptides, with another three HR peptides situated against the hydrophobic grooves on the surface of the coiled-coil (Liu *et al.*, 2006). F_1 and F_2 are linked by disulphide bonds and drive cell to cell and virus to cell fusion, which results in entry of the viral genomic information, and are therefore essential for virus spread (Morrison, 2003).

Different MuV strains demonstrate varying extents of cytopathic effect (CPE) by cell fusion, and the amino acid residue serine at position 195 of the F protein has been linked with the amount of fusogenicity shown during infection of host cells (Tanabayashi *et al.*, 1993). This finding may be strain or host-cell specific though, as a leucine residue at position 383 of the F protein of a wild-type MuV strain was shown to be essential for fusion in B95a cells (Yoshida & Nakayama, 2010).

1.7.5 Haemagglutinin-neuraminidase Protein

The HN protein is the second envelope glycoprotein located on the surface of MuV and is 582 amino acids in length with an approximate molecular weight of 74-80 kDa (Waxham *et al.*, 1988). The H (haemagglutinin) portion of the protein is responsible for viral attachment and entry to the host cell by recognition of the sialic acid cellular receptor, so therefore plays a major role in infection. The N

portion (neuraminidase) cleaves sialic acid residues and prevents self-agglutination of released viruses. The N terminus of the HN protein contains a hydrophobic sequence of 19 amino acids responsible for the anchoring of the protein in the virus envelope (Waxham *et al.*, 1988) and potential glycosylation sites of the HN protein have been identified (Kovamees *et al.*, 1989). Monomers of HN have a membrane proximal stalk consisting of a 4-helix bundle, a straight N terminus region and a super-coiled C terminus (Bose *et al.*, 2011) (Yuan *et al.*, 2011) linked to a globular head with a six-blade propeller structure that is characteristic of all paramyxovirus HN proteins (Crennell *et al.*, 2000) (Lawrence *et al.*, 2004) (Yuan *et al.*, 2005).

The MuV HN protein is the major antigenic determinant of the virus, with antibodies directed against this target being entirely capable of neutralising MuV (Orvell, 1978) (Orvell, 1984) (Server *et al.*, 1982). Genetic markers of neurovirulence and neuroattenuation have been frequently associated with alterations in the HN protein sequence of wild-type MuV (Cusi *et al.*, 1998) (Malik *et al.*, 2009) and the attenuated vaccine Urabe AM9 strain (Malik *et al.*, 2009) (Shah *et al.*, 2009).

The HN protein also has fusion promoter activity, and it was previously inferred from studies on related paramyxoviruses that F and HN proteins associate prior to fusion and the F protein is only released upon the binding of HN to the sialic acid receptor (Connaris *et al.*, 2002; Gravel & Morrison, 2003). In recent years it has been demonstrated that viruses related to MuV such as hPIV3 and NDV may rely on activity at a second receptor binding site on the globular head of the HN protein to initiate activation of the F protein (Porotto *et al.*, 2007) (Porotto *et al.*, 2012).

1.7.6 Small Hydrophobic Protein

The SH protein is the smallest MuV gene product, being just 57 amino acids long and with an approximate molecular weight of 6 kDa (Elliot *et al.*, 1989). As previously mentioned, the SH protein demonstrates the most genomic variability and is most commonly used for genotyping MuV strains. Although this protein is membrane associated, it is non-structural and has been shown to be non-

essential for virus growth (Takeuchi *et al.*, 1996). However, the MuV SH protein has recently been discovered to play a role in the prevention of apoptosis of infected host cells by targeting ataxin-1 ubiquitin-like interacting protein 4 (Woznik *et al.*, 2010) and was identified as having a role as a virulence factor, when it was discovered that deleting this gene in a molecular clone of MuV resulted in the virus becoming attenuated (Malik *et al.*, 2011). In the paramyxovirus RSV, it has been suggested that the SH protein plays a role in membrane permeabilisation as a viroporin (Carter *et al.*, 2010).

1.7.7 Large Protein

The largest gene of the MuV genome encodes the L protein, which is 2261 amino acids in length and approximately 180-200 kDa (Okazaki *et al.*, 1992). The primary function of this protein is as part of the viral transcription machinery, whereby P and L proteins bind to one another to form the RNA dependant RNA polymerase (RdRp) transcriptase complex and associate with the N protein and genomic material to form the helical RNP virus core. This has been inferred from research carried out on the related paramyxoviruses SeV (Gotoh *et al.*, 1989) and NDV, in which functional P and L proteins were both required in order to initiate transcription of the N gene (Hamaguchi *et al.*, 1983).

1.8 Virus Infection of Host Cells

1.8.1 Virus Attachment and Entry

Entry of MuV into a host cell consists of two main events, which are binding to the host cell and membrane fusion. The cellular receptor for MuV is sialic acid (SA), based on the observation that the sialidase (neuraminidase) of *Vibrio cholerae* acted as a “receptor-destroying” enzyme and protected the host cell from infection (Markwell, 1991). SA is expressed on the surface of most cells which reflects on the ability of MuV to be able to infect almost all cell and tissue types. Sialic acid-containing molecules exist in varying analogues with different linkages, including sialylα2,3 lactose

and sialylα2,6 lactose (Villar & Barroso, 2006), and it is currently unknown as to which type of linkage, if either, MuV has a greater affinity for. SA is the cellular receptor for paramyxoviruses containing an HN protein such as hPIV5, hPIV3 and NDV, however for the rest that contain only an H (haemagglutinin only) protein such as MV, a specific protein is required for binding to a host cell (Iorio & Mahon, 2008). Both wild-type and attenuated vaccine MVs utilises signal-lymphocyte activating molecule (SLAM) (Tatsuo *et al.*, 2000) and vaccine viruses also use human membrane cofactor 46 (CD46) as a cellular receptor (Naniche *et al.*, 1993). The human protein EphrinB2 has been shown to act as the receptor for Nipah virus infection of micro vascular endothelial cells (Negrete *et al.*, 2005).

Receptor binding affinity of human and avian influenza viruses has been well characterised, and it is now understood that human viruses exhibit preferential binding to α2,6-linked sialic acid residues while avian viruses bind to α2,3-linked molecules (Rogers & Paulson, 1983) (Connor *et al.*, 1994). In recent years, this has been further confirmed and investigated by infecting *ex-vivo* models of the human airway epithelium with different human and avian influenza viruses, and using lectin staining to determine the localisation of the differing SA moieties. These studies found that ciliated cells express mainly α2,3-linked and non-ciliated cells express primarily α2,6-linked SA residues (Matrosovich *et al.*, 2004) (Thompson *et al.*, 2006). The fact that these types of cell models are highly similar to the *in vivo* situation, allows for the results from studies such as these to be translated directly to influenza infection in the human host. Human airway epithelial (HAE) cell models have also been used for experimental infection and pathogenesis studies of MuV-related paramyxoviruses including RSV (Zhang *et al.*, 2002), hPIV3 (Zhang *et al.*, 2005) (Palermo *et al.*, 2009) and hPIV5 (Zhang *et al.*, 2011), and therefore may be suitable for MuV research.

Alterations to the amino acid sequence of the MuV HN protein have been well-documented with regards to their effects on receptor-binding. Amino acid change S466D was shown to reduce receptor binding affinity and neuraminidase activity in a wild-type MuV (Malik *et al.*, 2007) and

amino acid change E335K in the HN protein has also been demonstrated to alter receptor binding specificity of the Urabe strain of MuV (Reyes-Leyva *et al.*, 2007). Two variants of the MuV Urabe AM9 strain differing by a single amino acid in the HN glycoprotein were shown to exhibit different affinities for the α2,3 and α2,6 linked molecules (Reyes-Leyva *et al.*, 2007).

The HN glycoprotein serves as the attachment protein, recognising the SA receptor and binding to it. Once binding has occurred and the fusion of the viral and host cell membranes has been mediated, RNPs enter into the cytoplasm. The exact mechanism of fusion mediation by the MuV F protein is unclear, however studies on CDV, MV and MuV F protein-expressing Vero cells have suggested that the F_1 subunit is proteolytically further to F_{1A} and F_{1B} and that this action may aid in the formation of F protein "pores" in the host cell membrane, allowing entry of the viral genomic information (von Messling *et al.*, 2004).

Once the MuV RNPs have entered the host cell, virus replication and transcription can take place.

1.8.2 Virus Transcription and Replication

Virus replication occurs in the cell cytoplasm where the RdRp transcriptase complex uses the MuV nucleocapsid (complex of N, P and L proteins) as the template molecule to synthesis complementary positive-sense mRNAs and full length RNA from the negative-sense genome. The viral RdRp initially acts on a single promoter at the 3' end of the genomic RNA, synthesises the positive-sense leader RNA and terminates at the end of the leader region before acting upon the GS sequence at the start of the N gene. The positive-sense full length RNA (anti-genome) is used as the template for the new negative-sense MuV genomic RNA. The leader sequence and N mRNA are the first to be transcribed, with the L gene mRNA being last. Transcription of MuV and all other non-segmented –ssRNA viruses occurs by what is called a stop-start mechanism. This means that the RdRp does not disengage from the template upon release of the mature mRNA, and instead remains bound to the template and scans for the next GS site in the untranslated region (Cordey & Roux, 2006). Since the RdRp can only

initiate at the 3' end of the genome, decreasing quantities of monocistronic mRNAs are synthesised for genes located further from the 3' end. This results in the formation of a transcription gradient in which the concentration of N mRNA is greatest and the subsequent mRNA transcripts are reduced in relation to their distance from the 3' end promoter (Rassa & Parks, 1998) (Hausmann *et al.*, 1999).

Replication cannot take place until the primary transcription has taken place and a critical amount of N and P proteins are present (Conzelmann, 1998). Synthesis of the genomic RNA requires the RdRp to effectively "ignore" the GS and GE signal sites and continue along the template producing a full-length complementary RNA (Lamb & Parks, 2007). This occurs by the encapsidation of the 5' end of the positive-sense leader RNA, which results in the RdRp being unable to recognise GS and GE sites and instead reads through the whole template producing an full-length RNA transcript (Lamb & Parks, 2007).

It was first discovered using SeV that paramyxoviruses replicate under a phenomenon referred to as the Rule of Six (Calain & Roux, 1993) in which the number of nucleotides in the viral genome must be divisible by six in order for efficient replication to take place. Therefore, if during the RNA editing process to produce the V/P/I gene (section 1.7.2) six nucleotides exactly are not introduced, the virus may be incapable of efficient replication (Kolakofsky *et al.*, 1998).

1.8.3 The Host Cell Anti-Viral Response to Infection

Upon infection by a virus, cells initiate an antiviral response by producing interferons (IFN) and cytokines or chemokines. These are protein or glycoprotein molecules secreted by the cell in order to limit or inhibit viral replication and exist as type I (α/β), type II (γ) or type III (λ) IFNs. RNA viruses, including the paramyxoviruses, are recognised by the host cell by melanoma-differentiation-associated gene 5 (mda-5) and retinoic acid inducible gene I (RIG-I) like receptors (RLRs) which then initiate a signalling cascade involving a number of molecules to induce IFN responses, which is reviewed in (Yoneyama *et al.*, 2004) (Takeuchi & Akira, 2008) and (Jensen & Thomsen, 2012). RIG-I

and mda-5 recognise structures or molecules known as pathogen-associated molecular patterns (PAMPs) on or produced by double-stranded RNA (dsRNA) viruses. Specifically, 5' triphosphate single stranded RNA produced by viral polymerases has been demonstrated to act as the ligand for RIG-I sensing of RNA viruses (Hornung *et al.*, 2006) (Pichlmair *et al.*, 2006). Pattern recognition receptors (PRRs) are molecules expressed on the surface of innate immune cells and are equally important in innate immunity as they are also responsible for sensing PAMPs. One example of a PRR is toll-like receptor 3 (TLR3), which is expressed on cell surfaces and is capable of sensing PAMPs upon virus infection (Dunlevy *et al.*, 2010). However it is RIG-I that is essential for recognition of MuV and the paramyxoviruses. Upon recognition of PAMPs, RIG-I and mda-5 are both recruited to the IFN-β promoter stimulator (IPS-1) which in turn activates several transcription factors including interferon regulatory factor3 (IRF-3) and nuclear factor (NF)-κB. IRF-3 and NF-κB regulate type I IFN expression and cytokine production respectively (Kawai *et al.*, 2005). IFN and cytokine molecules bind to their specific receptors which in turn results in stimulation of the Janus kinase (JAK)-signal transducer and activator of transcription (STAT) signalling pathway which is reviewed in (Darnell *et al.*, 1994) and (Shuai & Liu, 2003). Briefly, binding of a cytokine or IFN to a specific cellular receptor causes dimerization and activation of JAK tyrosine kinases. Once activated, the JAKs phosphorylate tyrosine residues on the receptor and this creates sites for the localisation of the STAT proteins, which are a family of latent cytoplasmic transcription factors. The next stage in the JAK-STAT pathway is the phosphorylation and resultant dimerization of the STATs causing them to move into the nucleus and activate gene transcription.

Many viruses have the ability to circumvent the IFN response to some extent, usually by means of a protein(s) which can interfere with the host cell's antiviral response. The roles that the V protein of paramyxoviruses play in these processes has been well documented (Gotoh *et al.*, 2002) (Horvath, 2004a) (Horvath, 2004b) (Ramachandran & Horvath, 2009). The MuV V protein acts to interfere with the IFN response by targeting STAT proteins for degradation (Kubota *et al.*, 2001) (Kubota *et al.*, 2005b) (Nishio *et al.*, 2002) and the association of MuV-V with the protein RACK1 (Kubota *et al.*,

2002) results in antiviral signalling disruption by interfering with the formation of the STAT-1, RACK1 and IFN receptor complex. More specifically, the V protein of MuV has been demonstrated to suppress transcription of IL-6 by targeting STAT-3 for degradation by ubiquitylation (Ulane *et al.*, 2003). MuV V also targets STAT-1 for proteasome-mediated degradation by interaction of the CYS-rich C-terminus (Kubota *et al.*, 2001) however it does not fully degrade STAT-1 but only decreases the levels of the protein (Kubota *et al.*, 2005a). Paramyxovirus V proteins have recently been found to bind to a helicase demonstrating homology to RIG-I and mda-5 called laboratory of physiology and genetics 2 (LPG2) which resulted in the inhibition of RIG-I-dependent IFN signalling (Childs *et al.*, 2012). The V protein can also bind to, and thus prevent mda-5 from activating the IFN-β promoter (Andrejeva *et al.*, 2004). However, the MuV Enders strain which is known to encode a V protein that inhibits IFN action was demonstrated to be sensitive to IFN despite the functional V protein (Young *et al.*, 2009) and more recently, MuV V has been revealed not to inhibit the activities of IRF-3 (Irie *et al.*, 2012). This indicates that other antiviral factors are also involved in the host cell response. Analysis of cytokine levels in cases of mumps meningitis showed elevated levels of IFN-γ, interleukin (IL)-2, IL-6, IL-8, IL-10, IL-12 and IL-13 in CSF (Ichiyama *et al.*, 2005) (Martin *et al.*, 1991) (Asano *et al.*, 2011) indicating that the cytokine response cannot be entirely avoided. For example, the cytidine deaminase apolipoprotein B mRNA-editing enzyme-catalytic polypeptide 3G (APOBEC3G) exerts an antiviral effect on MuV with a fully functional V protein and inhibits transcription and protein expression (Fehrholz *et al.*, 2012).

Viral proteins involved in circumvention of the host cell antiviral response are not restricted to paramyxoviruses. Another example of a protein such as this is the N-terminal protease fragment (NPro) of Bovine viral diarrhoeal virus (BVDV) which is known for its ability to block signalling of IFN-α and IFN-β (Gil *et al.*, 2006) and has been demonstrated to specifically inhibit DNA-binding of IRF-3 and by doing so, causes it to be targeted for enzymatic degradation (Hilton *et al.*, 2006).

1.8.4 Host Range Determination

In very simple terms, the host range of a virus is determined by proteins of the both the virus and the host. These factors can provide restrictions to, or act in favour of the virus and include the presence of a suitable receptor(s), the antiviral response of the host to infection and properties at the gene level of the virus or host. These are important due to their role in maintaining species-specificity of viruses and can prevent viruses from "jumping" from one species host to another (E.g. animal to human).

The first stage in the infection of a host cell by any virus is binding to the suitable receptor upon the cell surface, and if this is not available then infection will not occur. Sialic acid, the MuV and influenza virus receptor is ubiquitously expressed and in abundance, however in the case of influenza A, if a specific type of sialic acid linkage is not available then infection of the host cell becomes more difficult. Human influenza viruses preferentially bind α2,6 whereas avian and equine viruses bind α2,3 linkages, and recognition of α2,3 sialic acid has been demonstrated to be critical for virus replication in horses (Suzuki *et al.*, 2000) which makes this factor a host range determinant. The human poliovirus receptor (PVR) acts as the host range determinant for polio, which can only naturally infect humans and primates. However, introduction of the PVR into the mouse genome results in mice becoming susceptible to polio infection (Ren *et al.*, 1990).

Host restriction factors are inhibitory to viral replication and are most commonly associated with components of the innate, anti-viral immune system. Section 1.8.3 discusses the host cell anti-viral response in greater detail with emphasis on MuV and its evasion of certain aspects of the innate pathway by the V protein. The V protein of NDV acts in a similar manner to MuV V as an IFN antagonist, and has previously been reported to act as a host range determinant as the activities of V are restricted to avian cells (Park *et al.*, 2003). The host range of hPIV5 has also been demonstrated to be restricted by the action of the V protein. STAT1 is efficiently targeted by the V protein and degraded in human cells, however due to the differences between human and murine STAT2, STATs

are unable to be fully degraded by hPIV5 in murine cells which has an inhibitory effect on virus replication, thus effectively restricting its host range (Parisien *et al.*, 2002).

Specific amino acids in viral proteins can also be associated with determination of host range, one example of this being the amino acid at position 627 of the PB2 polymerase protein of influenza A. It was observed by the authors that all avian influenza viruses contain a glutamic acid at this position and all human influenza viruses contain a lysine at position 627 (Subbarao *et al.*, 1993).

1.9 *In Vitro* Mumps Research

1.9.1 Studies of MuV in Cell Substrates

As mentioned in section 1.3, Vero cells are currently the "gold-standard" for isolation and cultivation of MuV from clinical samples, and they are also the standard cell line used for growth of MuVs in the laboratory. Their permissiveness for infection is likely due to their defectiveness in IFN production (Emeny & Morgan, 1979). Although Vero cells are commonly used, it has been suggested that they may be selective, insensitive and unsuitable for the production of virus isolates to be used in research (Afzal *et al.*, 2005). A previous study also demonstrated that Vero cells produce virus populations that are different from the original parent virus when serially passaged (Yates, 1995) and passage of a wild-type MV through Vero cells was reported to cause a functional change in the viral haemagglutinin protein (Bankamp *et al.*, 2008). These suggestions about the effect that Vero cells may have on MuV during passage have not been confirmed.

The study in which concerns were raised over the use of Vero cells (Afzal *et al.*, 2005) was carried out in order to assess alternative cell lines for MuV propagation including CaCO2 (human colorectal adenocarcinoma), PLC/PRF/5 (human liver hepatoma) and NCI-H292 (human lung carcinoma) using techniques such as plaque assays, immunofluorescence staining and electron microscopy. The authors suggested that due to the small number of cell lines investigated and the limited

experiments carried out, a much larger scale study would be required to obtain more conclusive results however this has not yet been carried out. Studies investigating the genetic stability of MuV during serial passage are extremely limited. MuV protein synthesis has been analysed in Vero cells (Herrler & Compans, 1982) (Rima *et al.*, 1980) and CEFs (Naruse *et al.*, 1981) and was shown to be highly similar in both cells with very slight differences in the electrophoretic mobilities of proteins between MuV strains and not cell lines. A later study in which MuVs were adapted to either Vero cells or embryonated hen eggs, reported differences in RNA production during culture in Vero cells (Afzal *et al.*, 1990), however the results were inconclusive and did not provide definitive answers about the interaction of MuV with these cells. Genetic characterisation of a wild-type MuV grown on MRC-5 (human lung) cells after four passages through the amniotic cavity of embryonated hens eggs suggested that by passage four there were two virus variants present, however whether this was due to natural heterogeneous variations or an early laboratory contamination was inconclusive (Ivancic *et al.*, 2004).

Several other cell lines have been assessed for their suitability of wild-type MuV isolation, and Vero and LLC-MK2 (Rhesus monkey kidney) cells were shown to be equally efficient using the shell vial method (Reina *et al.*, 2001) which is an indirect immunofluorescence method that requires acetone fixation of cells and so no live virus is recovered using this technique. The cell line NCI-H292 was shown to be permissive for culture of different strains and serotypes of paramyxoviruses (Castells *et al.*, 1990), and the marmoset lymphoblastic cell line B95a has also been used for MuV isolation from clinical samples during an outbreak of the disease (Knowles & Cohen, 2001). HeLa (human cervical carcinoma) cells have been successfully manipulated to stably express the HN and F proteins of MuV (Hishiyama *et al.*, 1996) and several different strains of MuV were demonstrated to propagate successfully in continuous human stomach carcinoma cell lines (Kato, 1981). These studies all indicate that there are cell substrates available that may be suitable for MuV isolation and culture other than Vero or CEFs. As mumps is a solely human illness, MuV may replicate more efficiently and stably when grown in cell lines of human origin.

A highly sensitive cell culture system for MuV would be of great use. The factors which make a cell line capable of supporting MuV growth and replication are currently unknown.

1.9.2 Defective Interfering Particles

Defective interfering (DI) particles are viral genomes that are incomplete, and missing some of the genetic information of the parent virus due to polymerase errors causing internal deletions during the replication process. DI particles are an unavoidable product of virus replication and have been implicated in the establishment and maintenance of persistent viral infections (Huang & Baltimore, 1970). In non-segmented negative-sense ssRNA viruses, DI particles are known to exist as either copy-back or internal deletion genomes, reviewed in (Lazzarini *et al.*, 1981). Copy-back DI genomes lack the 3' end of the genomic RNA, and instead have a complementary 5' sequence in its place, whereas internal deletion DI genomes retain the correct 5' and 3' sequence ends. DI virus particles cannot successfully infect cells by themselves, and they require co-infection with the parent virus for replication.

As discussed in section 1.7.2, RIG-I is heavily involved in the host cell IFN response, and DI genomes of RNA viruses have been shown to induce the activities of RIG-I and increase IFN activation and production (Johnston, 1981) (Strahle *et al.*, 2006) (Chen *et al.*, 2010).

DI particles generated from SeV replication have been well-characterised (Re *et al.*, 1983) (Hsu *et al.*, 1985) (Engelhorn *et al.*, 1993) and DI genomes of hPIV5 have been previously studied to show that the adherence of the nucleotide lengths of the viral genome to the Rule of Six enhances DI replication efficiency (Murphy & Parks, 1997). MuV has also been demonstrated to generate DI particles during persistent infection of continuous human cell lines with the vaccine strain L-3 (Andzhaparidze *et al.*, 1982). The presence of large populations of DI particles can result in the production of lower infectious progeny virus titres and the von Magnus phenomenon describes how high MOIs results in the generation of large quantities of DI particles in tissue culture (Von Magnus,

1954). Therefore, virus infection *in vitro* using a low MOI can reduce the likelihood of DI genomes being produced.

1.10 *In Vivo* Mumps Research

Humans are the only known natural reservoir of MuV. No animal model has been developed for MuV (Carbone & Rubin, 2007), and conclusive *in vivo* experimental data and knowledge of the virus and infection is therefore limited. The search for an animal model has been on-going for a long time and although experimental data on mumps has been obtained from *in vivo* studies in the past, results have been inconclusive or the studies were not designed to investigate in such a way that the data could be translated into human disease. Studies have been carried out using Rhesus Macaque, cat, guinea pig, hamster, rat and mouse models.

1.10.1 Experimental Animal Models

In 1915, Wollstein demonstrated that it was possible to cause a pathological condition in cats similar to that found in humans with parotitis that was suspected to be caused by MuV, by inoculating the animals with patient material via the parotid gland and the testes (Wollstein, 1916). After seven days the animals demonstrated tenderness and swelling of the parotid gland and testes and an increased white blood cell count which was taken to be indicative of an immune response. The authors were unable to show that MuV was the causal agent of the parotitis. Other viruses have been found to cause swelling of the parotid glands such as influenza (Bastien *et al.*, 2009) (Krilov & Swenson, 1985) and Epstein Barr (Lee *et al.*, 1997) therefore the data obtained from cats was inconclusive. This was substantiated by a later study in which kittens were injected with MuV into the parotid gland and were found to demonstrate no signs of illness, no virus was recovered and no serum antibody response was detected (Enders *et al.*, 1945).

Both suckling and pregnant hamsters have been experimentally infected with MuV. Several different egg-adapted MuV strains have been demonstrated to be neurovirulent in new born hamsters (McCarthy *et al.*, 1980), infecting neurons and choroid plexus cells, and upon intravenous inoculation of pregnant hamsters with MuV isolated from human breast milk, the uterus and placenta of all test animals became infected but no virus was recovered from the foetus or other tissues (Ferm & Kilham, 1963).

MuV has been shown to replicate in guinea pig primary cells (Gavitt & Bird, 1967) and the animals have also demonstrated an antibody response to MuV (Enders *et al.*, 1945) (van der Veen & Sonderkamp, 1965) (Tokuda, 1957). In addition to this, MuV has also been recovered from the brains and testes of guinea pigs after intracerebral and intra-testicular inoculation with an egg-adapted strain of the virus, and neutralising antibodies were detected at day eight post-infection after the intracerebral route of administration (Tokuda, 1957).

Suckling mice were shown to exhibit a serum antibody response when infected with mumps (Overman, 1954), and the virus has been shown to replicate in the lungs, salivary glands, heart, liver, testes and spleen of infected mice (Tsurudome *et al.*, 1987), however, the MuV strains used in both of these studies were selectively replicated by several passages of the virus through mouse brains or in the murine cell line L929. Other studies using a murine experimental model also required to adapt virus strains by passaging through mouse and hamster brains (Kilham & Murphy, 1952). In many studies carried out to experimentally inoculate mice with MuV the infection has been shown to be abortive (Tsurudome *et al.*, 1987) (Yamada *et al.*, 1984).

Mumps vaccine viruses such as the Urabe AM9 and L-3 strains, have been linked to cases of meningitis in vaccine recipients (Balraj & Miller, 1995), and the *in vivo* neurovirulence test is one of the pre-clinical safety requirements for new or candidate live attenuated mumps vaccines (WHO, 1994). Because of the neurovirulent potential of wild-type MuV and its association with meningitis, it is important that we have an in-depth understanding of this phenotype. The MuV neurovirulence

test has traditionally been performed using non-human primates such as Rhesus Macaques however results obtained have in some instances not correlated with the actual outcome in human vaccine recipients (Afzal *et al.*, 1999) or the difference in data obtained for wild-type and vaccine strains has not been statistically significant (Rubin *et al.*, 1999). In recent years neonatal rats have been studied as an alternative model. An international collaborative study between the Centre for Biologics Evaluation and Research at the Food and Drug Administration (FDA) and the National Centre for Biological Standards and Control (NIBSC) used a panel of wild-type and live attenuated vaccine MuV strains to inoculate neonatal rats intra-cranially before analysing the brains at 25 days post infection for severity of hydrocephalus. The results demonstrated that the rat neurovirulence test was reproducible and gave correct correlations between the MuV strain and neurovirulent potential (Rubin *et al.*, 2005). Neonatal rats have also been used to screen a panel of recombinant MuVs in order to investigate genetic markers of neurovirulence (Sauder *et al.*, 2011).

1.10.2 Mumps and Ferrets

Ferrets (*Mustela furo*) have been used successfully as an experimental model for several pathogenic bacteria and viruses. Experimental infection with the bacterium *Campylobacter jejuni* was demonstrated to reproduce similar disease to that observed in humans (Fox *et al.*, 1987) and ferrets have also been used to investigate immunity to this organism (Bell & Manning, 1990). Aerosolised *Mycobacterium bovis* has been used to vaccinate ferrets to demonstrate their suitability as an animal model for assessing tuberculosis vaccines in wildlife species (McCallan *et al.*, 2011). Ferrets are also susceptible to infection with SARS coronavirus and have been used in transmission studies (Martina *et al.*, 2003) and vaccine efficacy studies (Kobinger *et al.*, 2007).

The ferret model is frequently used to investigate Morbillivirus infection, immunity and host-interactions (Pillet *et al.*, 2009). Although these animals are not susceptible to measles, they are a natural host for CDV, which is a canine virus closely related to MV. CDV infection of ferrets produces the same clinical symptoms as measles in humans. Because of this, ferrets have been suggested as a

model for testing candidate vaccines for MV and other paramyxoviruses. Vaccination of ferrets with recombinant vaccinia and canarypox viruses expressing fusion and haemagglutinin (HA) proteins of CDV was shown to result in a 100% survival rate, as well as no viraemia and high titres of neutralising antibodies when challenged with CDV (Stephensen *et al.*, 1997). More recently, this *in vivo* model has been used to demonstrate that infection-enhancing lipopeptides Pam3CSK4 and PHCSK4 can be employed as adjuvants to increase the immune response to a CDV vaccination with a view to using ferrets to assess other live attenuated paramyxovirus vaccines (Nguyen *et al.*, 2012). Ferrets can also be successfully infected with Nipah virus (NiV), another member of the family *Paramyxoviridae*, and have been used to assess prevention of NiV infection and disease using Chloroquine (Pallister *et al.*, 2009).

Ferrets are established in the field of virology as a successful animal model for studying influenza virus infection, pathogenesis and transmission (Maher & DeStefano, 2004) and (Matsuoka *et al.*, 2009). This *in vivo* model is thought to be the most accurate in terms of an animal representing human influenza infection. The ferret respiratory tract has been characterised and shown to have similar patterns of α2,3 and α2,6 SA expression to those found in the human respiratory tract (Piazza *et al.*, 1991; van Riel *et al.*, 2007). MuV and influenza are known to have similar biological properties, and until the 1950's, both were considered to be members of the same virus family and MuV was referred to as *Myxovirus parotidis* (Andrewes *et al.*, 1955). Both are negative-sense, single stranded RNA viruses which utilise sialic acid as the host cell receptor, and have proteins with haemagglutinin and neuraminidase activities.

In early experiments, ferrets inoculated with MuV by injection into the testicles were reported to show no signs of illness or serum antibody response (Enders *et al.*, 1945). However, ferrets that were infected intranasally with an egg-adapted MuV Enders strain were shown to illicit a serum antibody response and infection resulted in a type of bronchiolitis similar to that caused by some strains of influenza. Infectious virus was also recovered from nasal washings, turbinates and lung samples at

days 3 and 4 post infection (Gordon *et al.*, 1956). These differences in results may have been due to differing routes of infection. Cultured ferret cell lines from the brain and lungs have shown susceptibility to infection by paramyxoviruses (Trowbridge *et al.*, 1985), and preliminary data from our laboratory suggests that ferrets mount an immune response to MuV (unpublished data). Based on all of this, ferrets have the potential to be an effective animal model for MuV infection.

An effective animal model would be of great use for studying pathogenesis, virulence, tissue tropism and persistence of MuV. It could also be useful for assessing attenuated vaccines.

1.11 Fundamental Mumps Research

Although mumps cases have been documented for hundreds of years, and vaccines have been available for over 60 years, specific virological data on MuV is somewhat lacking. Much of the knowledge available from the literature is inferred from research carried out on other paramyxoviruses, in particular the closely related hPIV5 which is often referred to as a prototypical rubulavirus and paramyxovirus. The lack of a sensitive cell culture model and an effective animal model are two reasons contributing to this lack of knowledge in the field of mumps research and the availability of effective *in vitro* and *in vivo* models would allow fundamental virological research to be carried out.

For example, although a MuV vaccine is available with a high uptake rate and demonstrated efficacy, the mechanism of how live MuVs become attenuated enough to become vaccine viruses and how these vaccines work are questions that are currently unanswered. Specific data on basic aspects of the life cycle of the virus such as fusion and budding processes are only inferred from data on other paramyxoviruses, and as useful as this information has been, we cannot know for certain that MuV operates in precisely the same manner. One recent example of how MuV has been demonstrated to differ from related paramyxoviruses is in its ability to avoid restriction in release of VLPs by tetherin,

whereas Sendai and Nipah viruses were both shown to be sensitive to tetherin action (Kong *et al.*, 2012). MuV pathogenesis data availability is also sparse, and an effective animal model would allow conclusive studies to be carried out on sites of viral replication, transmission, and viral spread within the host to name but a few. *In vivo* studies could also be employed to investigate immune responses to mumps, another area about which little is known.

1.12 Project Aims

The aims of this project are:

- To investigate a panel of cell lines and identify those which are suitable for supporting MuV growth and replication, and are capable of producing high titre progeny virus from clinical isolates which have very similar genotypic and phenotypic properties to the parent virus.
- To identify a cell line(s) that could be used as an alternative to Vero cells in diagnostic laboratories.
- To determine what changes are made to MuV at the genome level upon serial passage in Vero cells
- To determine some of the molecular reasons for a cell line being suitable for MuV propagation (for example: preferences for different types of sialic acid linkage)
- To assess ferrets as an animal model for MuV infection.

CHAPTER 2 – MATERIALS AND METHODS

2.1 Materials

2.1.1 Eukaryotic Cell Lines

The cell lines used are detailed in Table 3.

Table 3 – Eukaryotic Cell Lines

Origin	Cell Line	Source	Reference
Human	A549; *Lung carcinoma*	Professor Rick Randall, University of St Andrews	(Foster *et al.*, 1998)
	A549 (expressing NPro protein of BVDV); *Lung carcinoma*	Professor Rick Randall, University of St Andrews	(Young *et al.*, 2003)
	A549 (expressing V protein of hPIV-5); *Lung carcinoma*	Professor Rick Randall, University of St Andrews	(Young *et al.*, 2003)
	IMR-90; *Lung (foetal)*	NIBSC, Ref No 770501*	(Nichols *et al.*, 1977)
	MRC-5; *Lung (foetal)*	NIBSC, Ref No 660902*	(Jacobs *et al.*, 1970)
	NCI-H292; *Lung carcinoma*	NIBSC, Ref No 000724*	(Carney *et al.*, 1985) (Banks-Schlegel *et al.*, 1985)
	Ca Ski; *Cervical carcinoma*	NIBSC, Ref No 920702*	(Pattillo *et al.*, 1977)
	Hep 2C; *Cervical carcinoma*	NIBSC, Ref No 740502*	(Moore *et al.*, 1955)
	MucilAir™ Human Airway Epithelial (HAE) cells	Epithelix Sarl, Switzerland	(Huang *et al.*, 2011)
	MCF-7; *Breast carcinoma*	NIBSC, Ref No 000410*	(Soule *et al.*, 1973)
	Detroit 562; *Pharyngeal carcinoma*	ECACC, Cat No 87042205	(Peterson *et al.*, 1971)
	PANC-1; *Pancreatic carcinoma*	ECACC, Cat No 87092802	(Lieber *et al.*, 1975)
	293T; *Kidney (SV-40 transformed)*	NIBSC, Ref No 000617*	(Graham *et al.*, 1977)
	CaCO2; *Colorectal adenocarcinoma*	NIBSC, Ref No 010310*	(Fogh *et al.*, 1977a) (Fogh *et al.*, 1977b)

	HGT-1; *Stomach carcinoma*	NIBSC, Ref No 890101*	(Laboisse *et al.*, 1982)
	NT2/D1; *Testes carcinoma*	NIBSC, Ref No 030211*	(Andrews *et al.*, 1984)
	RD; *Muscle rhabdomyosarcoma*	NIBSC, Ref No 990825*	(McAllister *et al.*, 1969)
Non-Human Primate	BSC-1; *African Green Monkey kidney*	NIBSC, Ref No 890602*	(Hopps *et al.*, 1963)
	COS-7; *African Green Monkey kidney (SV-40 transformed)*	Professor Salvador Moncada, UCL Cancer Institute	(Gluzman, 1981)
	CV-1; *African Green Monkey kidney*	Professor Geoff Smith, Imperial College London	(Jensen *et al.*, 1964)
	DBS-FcL2; *African Green Monkey lung*	ECACC, Cat No 90112815	(Wallace *et al.*, 1973b) (Wallace *et al.*, 1973a)
	Vero; *African Green Monkey kidney*	NIBSC, Ref No 880101*	(Yasumura & Kawakita, 1963)
	DBS-FrhL2; *Rhesus Monkey lung*	ECACC, Cat No 89101303	(Wallace *et al.*, 1973b) (Wallace *et al.*, 1973a)
	LLC-MK2; *Rhesus Monkey kidney*	ECACC, Cat No 85062804	(Hull *et al.*, 1956) (Hull *et al.*, 1962)
	MA-104; *Rhesus Monkey kidney (foetal)*	NIBSC, Ref No 820402*	(Whitaker & Hayward, 1985)
	B95a; *Marmoset lymphoblast*	NIBSC, Ref No 001026*	(Miller *et al.*, 1972)
Other	2° Ferret Lung	NIBSC, Ref No 860401*	N/A
	Mpf; *Ferret brain*	ATCC, Cat No ATCC-CRL-1656	(Trowbridge *et al.*, 1982)
	L20B; *Mouse L cell (expressing polio virus receptor)*	NIBSC, Ref No 910705*	(Pipkin *et al.*, 1993) (Mendelsohn *et al.*, 1986)

	L929; *Mouse L cell*	NIBSC, Ref No 810101*	(Sanford *et al.*, 1948)
	LtK-; *Mouse L cell*	NIBSC, Ref No 920501*	(Kit *et al.*, 1963)
	TM3; *BALB/C mouse testis Leydig cell*	ECACC, Cat No 91060526	(Mather, 1980)
	BHK-21; *Syrian Hamster kidney*	ECACC, Cat No 85011433	(MacPherson, 1963)
	CHO-K1; *Chinese Hamster ovary*	ECACC, Cat No 85051005	(Kao & Puck, 1968; Puck *et al.*, 1958)
	JH4 Clone 1; *Guinea Pig lung*	ECACC, Cat No 86070201	(Hoying, 1975)
	MDCK; *Canine kidney*	NIBSC, Ref No 821104*	(Madin & Darby, 1958)
	MDCK-SIAT1; *Canine kidney over-expressing α2,6 sialyltransferase*	Carolyn Nicholson, NIBSC	(Matrosovich *et al.*, 2003)
	RK-13; *Rabbit kidney*	NIBSC, Ref No 750402*	(Beale *et al.*, 1963)
Primary	CEF; *Chicken embryo fibroblast*	Institute for Animal Health, Compton via Dr Marc Davies, Imperial College London	N/A
	Kidney; *Cynomolgus Macaque*	Prepared at NIBSC (Lauren Parker)	N/A
	Testes; *Cynomolgus Macaque*	Prepared at NIBSC (Lauren Parker)	N/A
Ex-Vivo	MucilAir™ Human Airway Epithelial (HAE) cells	Epithelix Sarl, Switzerland	N/A

* NIBSC Ref No refers to in-house cell bank number

N/A - not applicable

2.1.2 Cell Culture Media

Cell culture and maintenance media are detailed in Table 4.

Table 4 – Cell Culture and Maintenance Media

Media used in cell culture/routine maintenance	**Cell Line**
Minimum Essential Medium (MEM) (Sigma Aldrich, UK) 10% (v/v) Foetal Calf Serum (FCS) (Sigma Aldrich, UK) 2% (w/v) 200 mM L-Glutamine (Sigma Aldrich, UK)	2° Ferret Lung 293T BHK-21 BSC-1 Ca Ski CaCO2 CV-1 DBS FcL2 DBS FrhL2 Detroit 562 HGT-1 Hep 2 Hep 2 C IMR-90 JH4 Clone 1 L20B LLC-MK2 MA-104 MCF-7 MDCK MRC-5 RD Vero
Dulbecco's Minimum Essential Medium (DMEM) (Sigma Aldrich, UK) 10% (v/v) FCS (Sigma Aldrich, UK) 2% (w/v) 200 mM L-Glutamine (Sigma Aldrich, UK)	A549 A549 (BVDV) A549 (PIV5-V) B95a

	COS-7 LtK- NT2/D1 PANC-1
Roswell Park Memorial Institute (RPMI 1640) (Sigma Aldrich, UK) 10% (v/v) FCS (Sigma Aldrich, UK) 2% (w/v) 200 mM L-Glutamine (Sigma Aldrich, UK)	L929 NCI-H292
MEM (Sigma Aldrich, UK) 14% (v/v) Lamb Serum (Sigma Aldrich, UK) 2% (w/v) 200 mM L-Glutamine (Sigma Aldrich, UK)	Mpf
Ham's F12 (Sigma Aldrich, UK) 5% (v/v) Horse Serum (Life Technologies™ UK) 2.5% (v/v) FCS (Sigma Aldrich, UK) 2% (w/v) 200 mM L-Glutamine (Sigma Aldrich, UK)	TM3
DMEM (Sigma Aldrich, UK) 20% (v/v) FCS (Sigma Aldrich, UK) 2% (w/v) 200 mM L-Glutamine (Sigma Aldrich, UK) 1% (w/v) 10,000 units/mL Penicillin-Streptomycin (Sigma Aldrich, UK) 1% (w/v) 250 mM Amphotericin B (Sigma Aldrich, UK) 0.5 mg/mL Gentamicin (Life Technologies™ UK)	All primary cells
BioWhittaker® UltraCULTURE™ (Lonza, USA) 2%(w/v) 200 mM L-Glutamine (Sigma Aldrich, UK)	RK-13
MucilAir™ Culture Medium (Epithelix Sarl, Switzerland)	MucilAir™ HAE cells

Minimal Essential Medium (MEM, Sigma Aldrich UK) containing 4% (v/v) foetal calf serum (FCS, Sigma Aldrich UK), 2% (w/v) 200 mM L-Glutamine (Sigma Aldrich, UK), 1% (w/v) 10,000 units/mL Penicillin-Streptomycin (Sigma Aldrich, UK) and 1% (w/v) 250 mM Amphotericin B (Sigma Aldrich, UK) was used as a negative control for uninfected cells and for preparing virus dilutions, and is designated as "infection medium" throughout the text.

2.1.3 Viruses

The viruses used are detailed in Table 5.

Table 5 – Viruses

Virus	Additional Information	Source/Reference
AFZ315	Clinical saliva sample collected from mumps patient 2 days after onset of symptoms, University of Hertfordshire 2002	NIBSC
GFP-expressing mumps (GFP-MuV)	Recombinant JL-5 mumps virus with enhanced GFP gene inserted at position 146 prior to start of N gene	Dr Ken Lemon, Queens University, Belfast
HPA 1.1/P1V	Clinical mumps isolate from nose/throat swab, 2009, passaged once on Vero cells	Dr Kevin Brown, CFI Colindale, HPA
Influenza PR8	High growth laboratory strain of Influenza A virus	NIBSC
Mu90	Clinical mumps isolate from passaged 4 times on Vero cells, original isolate known as LO-1 from North London clinic 1988	NIBSC (Afzal *et al.*, 1997)
RIT 4385	Live attenuated mumps virus component of Priorix® MMR vaccine, GSK, UK	NIBSC (Tillieux *et al.*, 2009)

2.1.4 Standard and Real-Time PCR Primers and Probes

Primers and probes used for both standard and reverse transcriptase and real-time PCR are detailed in Table 6 and Table 7, respectively. All of the listed oligonucleotides were designed using online

programme Primer3 Input v0.4.0 (http://frodo.wi.mit.edu/primer3/) and were obtained from Life Technologies™ or Eurofins MWG Operon.

Table 6 – Standard PCR Primers

Primer name	Sequence (5' to 3')	Gene	GenBank Accession number used for primer design/Reference
HN1Fw	aaaaagcaagccagaacaaa		
HN2Rv	caattcccctcaagaccaga		
HN3Fw	tcttgttcagaccgcatcag		
HN4Rv	tgtggtaggaggcaaaca	MuV HN – LO-1	X98874
RIT_HN117Fw	ttccggccactaagaaaatg		
RIT_HN1069Rv	tattccactccccactcctg		
RIT_HN947Fw	agcccacctacccagaaact		
RIT_HN1925Rv	aatgagacacgcccgtaaag	MuV HN – RIT 4385	FJ211585
F4Fw	tgatcattaatcatgaaggctttt		
F946Rv	ccaagatcctgtctggcaat		
F771Fw	cggtctaatggagggtcaga		
F1627Rv	acctgatgagatcatcgacac	MuV F – Genotype C	AY669145
RIT_F7Fw	gaccggtggtaattcgattg		
RIT_F847Rv	cctccattagaccggcact		
RIT_F804Fw	tgcagtggttcaagcaacat		
RIT_F1751Rv	aaattgcaggacgaatcacc	MuV F – RIT 4385	FJ211585
N2Fw	ggacattttgacactacctgga		
N894Rv	gtgaatgcagccaatgacag		
N775Fw	ctatgcaatggtgggtgaca		
N1707Rv	gcaattgagggtggtttgat	MuV N – Genotype C	AY669145
RIT_N1Fw	ccaaggggagaatgaatatgg		
RIT_N914Rv	tgtcacccaccattgcatag		
RIT_N798Fw	tatgcaatggtgggtgacat		
RIT_N1776Rv	acttgcaactgtgcgttttg	MuV N – RIT 4385	FJ211585
JLSH1Fw	agtagtgtcgatgatctcat		
JLSH2Rv	gctcaagccttgatcattga		

JLSH3Fw	gtcgatgatctcattaggtac		
JLSH4Rv	agctcacctaaagtgacaat	MuV SH – RIT 4385	FJ211585
GAPDHFw	aacatcatccctgcttccactggt		(Svitek & von Messling,
GAPDHRv	tgttgaagtcgcaggagacaacct	Ferret – GAPDH	2007)
IL-2Fw	tgctgctggacttacagttgctct		(Svitek & von Messling,
IL-2Rv	caattctgtggccttcttgggcat	Ferret – IL-2	2007)
IL-6Fw	caaatgtgaagacagcaaggaggca		(Svitek & von Messling,
IL-6Rv	tctgaaactcctgaagaccggtagtg	Ferret IL-6	2007)
IL-10Fw	tccttgctggaggactttaagggt		(Svitek & von Messling,
IL-10Rv	tccaccgccttgctcttattctca	Ferret IL-10	2007)

Table 7 – Real-Time PCR Primers

Primer/Probe name	**Sequence (5' – 3')**	**Gene**	**Accession number used for primer design/Reference**
JLSHF	atccaacctcccttatacctaac		
JLSHR	gatcaaaaccccagcgagagaag		
JLSHP (Probe)	FAM – tattaactataagacggcggtgcgat – BHQ1	MuV - SH	FJ211585
AFZ315SHF	gccattacctacaagactgc		
AFZ315SHR	ctggggttctgtgttgtatt		
AFZ315P (Probe)	FAM – gctgcatttgaatgatgccg – BHQ1	MuV - SH	AB618040
GAPDH535F	atcactgccacccagaagac		
GAPDH680R	gtgagcttcccattcagctc		(Svitek & von
GAPDHP (Probe)	JOE – ccactggtgcagccaaggctgtag – BHQ1	Ferret - GAPDH	Messling, 2007)

2.1.5 Molecular Biology Reagents, Chemicals and Buffers

Reagents (including assay kits) were obtained from QIAGEN® UK, Bioline UK, Roche UK, Sigma Aldrich UK, Life Technologies™ UK or Calbiochem® UK and used as detailed in the text.

Chemicals and reagents prepared in-house are detailed in Table 8.

Table 8 – In-House Chemicals and Reagents

Chemical/Reagent	Recipe
5% CMC	For 50 mL: 2.5 g (5% w/v)carboxymethylcellulose (Fisher Scientific, UK) 50 mL PBS A (1x)
FACS Buffer	2.5 g (0.5% w/v) Probumin™ BSA (Millipore, USA) 0.1 g $MgCl_2$ $6H_2O$ (Merck, UK) 0.1 g $MnCl_2$ $4H_2O$ (Merck, UK) 0.1 g $CaCl_2$ $2H_2O$ (Merck, UK) Adjust to final volume of 500 mL with distilled H_2O
FACS Fix	150 mL PBS A (1x) 325 mL distilled H_2O 25 mL 40% Paraformaldehyde (Sigma Aldrich, UK)
Methanol/Acetone (50:50)	For 500 mL: 250 mL Methanol (AnalR, UK) 250 mL Acetone (AnalR, UK)
Methyl violet	For 1 L: 200 mL IMS (Tennant, UK) 5.0 g (0.5% w/v) Methyl violet (Merck, UK) 800 mL distilled H_2O
4% Paraformaldehyde	For 500 mL: 50 mL 40% Paraformaldehyde (Sigma Aldrich, UK) 450 mL PBS A (1x)

PBS A (1x)	1.0 g NaCl (Fisher Scientific, UK) 0.25 g KCl (Merck, UK) 1.44 g Na_2HPO_4 anhydrous (Merck, UK) 0.25 g KH_2PO_4 (Merck, UK) Adjust to final volume of 1 L with distilled H_2O pH 7.5 (adjusted with NaOH or HCl)
PBS Flow	500 mL Sodium azide cell wash (Becton Dickinson, UK) 25 mL FCS (Sigma Aldrich, UK)
PBS 6-Salt	80 g NaCl (Fisher Scientific, UK) 2.0 g KCl (Merck, UK) 1.3 g $CaCl_2$ $2H_2O$ (Merck, UK) 1.0 g $MgCl_2$ $6H_2O$ (Merck, UK) 29 g Na_2HPO $12H_2O$ (Fisher, UK) 2.0 g KH_2PO_4 (Merck, UK) Adjust to final volume of 10 L with distilled H_2O
TBE (1x)	For 1 L: 100 mL 10 x TBE 900 mL distilled H_2O
TBE (10x)	109.03 g Tris Base (Fisher Scientific, UK) 55.65 g Boric Acid (Sigma Aldrich, UK) 9.31 g EDTA (Merck, UK) Adjust to final volume of 1 L with distilled H_2O pH 7.5 (adjusted with NaOH or HCl)
TBS	60.6 g Tris HCl (Merck, UK)

	13.9 g Tris Base (Merck, UK) 87.66 g NaCl (Fisher Scientific, UK) Adjust to final volume of 10 L with distilled H_2O pH 7.6 (adjusted with NaOH or HCl)

2.2 Cell Culture

2.2.1 Routine Cell Culture

Continuous cell lines listed in Table 3 were examined microscopically on a regular basis and were sub-cultured every 3 to 4 days dependent upon rate of cell growth, appearance and cell requirements for experiments. They were routinely grown in T75 flasks (Scientific Lab Supplies, UK) containing 20 mL of the relevant culture medium (Table 4).

For routine sub-culture of cells, spent medium was decanted from flasks and the cell layer washed twice with phosphate buffered saline (PBS A). Cells were then washed gently with 5 mL 0.25% Trypsin/EDTA solution (Sigma Aldrich, UK), the trypsin was decanted and flasks were incubated at 37°C, 5% CO_2 until the cells detached from the flask surface. An appropriate volume of medium for the chosen sub-culture ratio was added to each flask, cells were re-suspended and then transferred into new T75 flask(s) containing 20 mL of fresh medium.

All cell culture procedures were carried out in a class II microbiological safety cabinet using standard aseptic techniques.

2.2.2 Routine Maintenance of MucilAir™ HAE Cells

MucilAir™ are human airway epithelial (HAE) cells that have been reconstituted on a porous Transwell membrane and cultured at the air-liquid interface allowing the cells to become fully differentiated. They are polarised and form tight junctions (Huang *et al.*, 2011).

Every 2 to 3 days, the Transwell support containing the cells was transferred using sterile forceps, to a well of a fresh 24-well plate containing 0.7 mL MucilAir™ culture medium pre-warmed to 37°C. As these cells naturally produce mucus, once the Transwell was transferred into fresh medium, the mucus was washed from the cell surface by the gentle addition and removal of 100 µL sterile PBS A

pre-warmed to 37°C. This wash step was carried out 10 times. The cells were routinely incubated at 37°C, 5% CO_2.

2.2.3 Preparation of Primary Cells

Primary cells were prepared from Cynomolgus Macaque kidney and testis tissues as follows.

Tissue explants were placed in a 100 mL sterile container with 20 mL PBS A and then transferred to a petri dish containing 10 mL PBS A. Sterile scissors and forceps were used to dissect the tissues into fragments of approximately 1-2 mm in diameter which were then transferred to a 50 mL centrifuge tube containing 15 mL PBS A. The tissue pieces were washed 3 times by removing and replacing the PBS A and after the third wash, the PBS A was removed and replaced with 15 mL of 0.25% Trypsin/EDTA solution (Sigma Aldrich, UK) and incubated overnight at 4°C. After this incubation period, the tubes were incubated at 37°C for 30 min and the contents pipetted vigorously to obtain small cell clumps, before adding 15 mL primary cell culture medium (Table 4) to stop further trypsin action. The cell suspensions were centrifuged at 470 g for 5 min at room temperature, and the resulting supernatant was decanted leaving the cell pellet. The pellet was re-suspended in 50 mL of medium and a cell count was performed using a haemocytometer and the trypan blue dye-exclusion method (Strober, 2001), with a 1 in 10 dilution of cells in trypan blue (Sigma Aldrich, UK). Cells were distributed evenly between T75 flasks at a density of *ca* $1x10^5$ cells per flask and incubated at 37°C, 5% CO_2.

2.3 Routine *In Vitro* Virology

2.3.1 Virus Infection of Cells in 96-well Plates

Cells were seeded into 96-well plates (Scientific Lab Supplies, UK) at a density of *ca* $1x10^5$ cells per well in a 100 µL volume of infection medium and incubated overnight at 35°C, 5% CO_2. Cells were

examined microscopically prior to inoculation for appropriate appearance and confluency (70-90%). Virus stocks were thawed on ice and diluted in infection medium to result in an approximate MOI of 0.001 pfu (plaque forming units) per cell in a final volume of 100 µL. Spent medium was aspirated from the wells and replaced with the diluted virus inoculum, then incubated at 35°C, 5% CO_2 for *ca* 90 min. Following the incubation period, inocula were aspirated from the cells and replaced with 100 µL of infection medium per well prior to re-incubating at the previously described conditions.

2.3.2 Virus Infection of Cells and Preparation of Progeny Virus

Cells were seeded into 24 well plates or T25 flask(s) (both Scientific Lab Supplies, UK) at a density of *ca* $1x10^5$ cells in a volume of 1 mL infection medium per well for plates or 5 mL per flask, and incubated overnight at 35°C, 5% CO_2. Cells were examined microscopically prior to inoculation for appropriate appearance and confluency. Viruses were thawed on ice and diluted in infection medium to result in an approximate MOI of 0.003 pfu/cell. In the case of neat clinical isolates, 50 µL of sample was added to infection medium for inoculation. Spent media was aspirated from the cells and replaced with either 2 mL of diluted virus per T25 flask or 200 µL per well of each plate, and then incubated at 35°C, 5% CO_2 for *ca* 90 min. Following the incubation period, inocula were removed from the cells and replaced with 5 mL of infection medium per flask or 1 mL per well for 24 well plates. Cells were re-incubated at the previously described conditions.

Cells were examined microscopically on a daily basis for signs of cytopathic effect (CPE) and frozen at -80°C either when *ca* 80% CPE was evident or on day 7 post infection.

Frozen flasks or plates of cells were thawed at room temperature and the cell lysates centrifuged at 470 g for 5 min at room temperature. The resulting supernatants containing virus were aliquoted, stored at -80°C and designated as progeny virus. All progeny viruses were titrated via plaque assay on Vero cells as detailed in section 2.3.5.

2.3.3 Passaging of Viruses through Cell Lines

Mumps viruses were passaged 5 times through various cell lines. For P1 to P5, T25 flasks of each cell line were seeded, infected and aliquots of progeny virus prepared from cell lysates as described in section 2.3.2. Dilutions (1 in 50) of each progeny were prepared in infection medium prior to each passage.

2.3.4 Infection of MucilAir™ HAE Cells

Each Transwell membrane was transferred to fresh culture medium and surface mucus was washed from the cells as described in section 2.2.2. Viruses were thawed on ice and diluted in infection medium to result in an approximate MOI of 0.001 pfu/cell in a final volume of 200 µL. In the case of neat clinical isolates, 50 µL of sample was added to 150 µL of infection medium. The virus inoculum was added to the apical surface of the cells and incubated at 37°C, 5% CO_2 for *ca* 90 min.

Following the incubation period, the virus inoculum was removed from the apical cell surface by pipetting and the cells were re-incubated at the conditions previously described.

Apical and basal samples were harvested at 6, 12 and then every 24 hours for 7 days post infection. Cells were also examined microscopically for evidence of CPE at these time points.

To harvest viruses released from the apical cell surface, 300 µL of MEM pre-warmed to *ca* 37°C was added to the surface and incubated at 37°C for *ca* 30 min. Following the incubation period, the MEM was removed by pipetting and 4% (v/v) FCS, 2% (w/v) 200 mM L-Glutamine, 1% (w/v) 10,000 units/mL Penicillin-Streptomycin and 1% (w/v) 250 mM Amphotericin B were added to the sample before storing at -80°C.

To harvest viruses released from the basal cell compartments, each Transwell support was first transferred to a fresh 24-well plate containing culture medium as described in section 2.2.2. The spent cell culture medium was harvested and 4% (v/v) FCS, 2% (w/v) 200 mM L-glutamine, 1% (w/v)

10,000 units/mL Penicillin-Streptomycin and 1% (w/v) 250 mM Amphotericin B were added to the sample before storing at -80°C.

To prepare MucilAir™ cells for histological cross sectioning, each membrane was washed 3 times in PBS A and then immersed in 4% paraformaldehyde (Table 8) for 1 hour at room temperature. After the incubation period cell membranes were washed 3 times with PBS A and then stored in universal containers with 10 mL PBS A at 4°C. The fixed cells were sent to Propath UK Limited for preparation of histological slides.

2.3.5 Titration of Viruses

Viruses were titrated by plaque assay on Vero cells. Briefly, confluent T75 flasks of Vero cells were trypsinised into 50 mL infection medium and cells (1 mL per well) were added to 24-well plates. Serial 10-fold dilutions (1 in 10 to 1 in 100,000) of virus were prepared in infection medium, and 50 µL of each dilution was added to 3 wells of a 24-well plate. A negative control consisting of infection medium only was included. Cells were incubated for *ca* 3 hours at 35°C, 5% CO_2 to allow the cells to settle in the wells.

After the incubation period, inocula were aspirated from all wells and replaced with 5% CMC overlay medium (Table 8) consisting of MEM, 5% (v/v) CMC, 4% (v/v) FCS, 2% (w/v) 200 mM L-Glutamine, 1% (w/v) 10,000 units/mL Penicillin-Streptomycin, and 1% (w/v) 250 mM Amphotericin B. Cells were re-incubated at the same conditions as before. The cells were stained with methyl violet (Table 8) at 7 days post infection and the virus titres calculated from the plaque counts obtained, taking into account the volume of the inoculum and dilution factor.

2.3.6 Plaque Reduction Neutralisation (PRN) Assays

Serum samples were thawed on ice and heat-inactivated by incubating in a water bath at 56°C for 30 min to inactivate the complement pathway.

96-well plates were labelled and 150 µL of infection media was added to all wells. 150 µl of serum sample was added to the first well of the relevant sample row to create an initial 1 in 2 dilution, and using a multi-channel pipette, 150 µL of this dilution was added to the next well and mixed. This was repeated from left to right into a further 4 wells to create a range of doubling dilutions from 1 in 2 to 1 in 64. 150 µL of the serum/media mix was discarded from the last wells. 6 wells were included for a virus control each containing 150 µL infection media plus 150µL of an appropriate dilution of control mumps virus prepared in infection media. The control mumps virus was referred to throughout as the challenge virus, and 150 µL of this was then added to all remaining wells on the plate. 96-well plates containing the samples were then incubated at 4°C for *ca* 90 min.

Before the end of the incubation period, T75 flasks of confluent Vero cells were trypsinized into 50 mL of infection medium and cell suspensions were pooled.

After the incubation period, 50 µL of from each well of the 96-well plate containing sera/virus was added to 3 wells of a 24 well plate.

1.0 mL of the Vero cell suspension was then added to each well, and the 24-well plates were incubated at 35°C, 5% CO_2 for *ca* 3 hours to allow cells to settle in the wells.

After this incubation period, inocula was aspirated from all wells and replaced with 1 mL per well of 5% CMC overlay media as described in section 2.3.5. Cells were incubated at the previously described conditions for 10 days, and on day 10 post infection, cells were stained with methyl violet. Plaques were counted and the counts obtained entered into a standardised NIBSC PRN Excel spreadsheet configured with the equations required for analysis. 50% neutralising end-point titres (ND_{50}) were calculated as the serum dilution capable of reducing the mean number of plaques by 50% or greater as compared to the mean number of plaques in virus control wells using the Spearman-Karber formula (Finney, 1971).

2.4 Routine Molecular Virology

2.4.1 RNA Extraction

RNA was extracted from samples using the Trizol® LS Reagent (Life Technologies™ UK) method according to the manufacturer's instructions.

RNA was isolated using the recommended 3 volumes of Trizol® LS to 1 volume of sample.

Briefly, samples were thawed on ice and once fully thawed, Trizol® LS was added. Samples were vortexed to mix and 2 µL of glycogen (Life Technologies™ UK) was added to increase the yield of the RNA pellet. An appropriate volume of chloroform (Sigma Aldrich, UK) was added to each sample to allow phase-separation and incubated at room temperature for 5 min. Samples were then centrifuged at 18000 g for 10 min at 4°C, and the resulting top aqueous layer containing RNA was transferred to a clean nuclease free tube. An appropriate volume of isopropanol (Sigma Aldrich, UK) was added to each sample to precipitate the RNA, and incubated at -20°C for *ca* 1 hour to precipitate the RNA.

After this incubation period, samples were centrifuged at 18000 g for 10 min at 4°C, and the resulting supernatant was carefully removed by pipetting, leaving the RNA pellet. 500 µL of ice-cold 70% ethanol was added to each pellet and then centrifuged at 18000 g for 10 min at 4°C as a wash step. After this final centrifugation step, the resulting supernatant was removed carefully by pipetting and the RNA pellets were allowed to air-dry in a class II microbiological safety cabinet for 5 to 10 min. RNA pellets were re-suspended in 15-30µL diethyl pyrocarbonate (DEPC)-treated H_2O (Sigma Aldrich, UK) and stored at -20°C.

2.4.2 Reverse-Transcriptase (RT) PCR

RT-PCR was performed on RNA samples using either the QIAGEN® One-Step RT-PCR kit and protocol or Bioline MyTaq™ One-Step RT-PCR kit and protocol, both according to the manufacturer's

instructions. All primers were used at a working concentration of 10 µM and the sequences are detailed in Table 6, section 2.1.4.

For each sample to be amplified using the QIAGEN® kit, 2 µL of template RNA was added to 10 µL 5x buffer, 2 µL dNTP, 1.5 µL of each forward and reverse primer, 2 µL RT enzyme and 31 µL DEPC H_2O in a reaction tube. The RT-PCR cycle programme used was: 1) 50°C for 30 min, 2) 95°C for 15 min, 3) 94°C for 1 min followed by 50°C for 30 seconds and 72°C for 1 min. Step 3 was repeated 35 times followed by a final extension cycle of 72°C for 10 min and then held at 4°C.

For each sample to be amplified using the Bioline kit, 2 µL of template RNA was added to 25 µL 2x MyTaq™ one-step mix, 1.5 µL of each forward and reverse primer, 1 µL RiboSafe RNase inhibitor, 0.5 µL RT enzyme and 18.5 µL DEPC H_2O in a reaction tube. The RT-PCR cycle programme used was: 1) 48°C for 20 min, 2) 95°C for 1 min, 3) 95°C for 15 seconds followed by 50°C for 15 seconds and 72°C for 30 seconds. Step 3 was repeated 35 times followed by a final extension cycle of 72°C for 10 min and then held at 4°C.

All RT-PCR reactions were carried out using an Eppendorff Mastercycler® gradient machine.

RT-PCR products were analysed on a 1 x Tris-borate-EDTA (TBE) 1% agarose (Sigma Aldrich, UK) gel stained with ethidium bromide (10 mg/mL, Promega, USA), and electrophoresed for *ca* 30 min at 110 V. 5 µL of Bioline Hyper Ladder II or V was included as a marker. Gels were viewed using an Auto-Chemi® UV Transilluminator (UVP Bio-Imaging Systems). RT-PCR products were stored at -20°C.

2.4.3 Standard PCR

Standard PCR was performed on RT-PCR products (nested PCR) using the QIAGEN® HotStartTaq™ Master Mix kit and protocol according to the manufacturer's instructions. All primers were used at a working concentration of 10 µM and the sequences are detailed in Table 6, section 2.1.4.

For each sample to be amplified, 2 µL of template DNA was added to 25 µL HotStartTaq™ Master Mix, 1 µL of each forward and reverse primer and 18 µL DEPC H_2O in a reaction tube. The PCR cycle programme used was: 1) 95°C for 15 min, 2) 94°C for 30 seconds followed by 50°C for 30 seconds and 72°C for 1 min. Step 2 was repeated 35 times followed by a final extension cycle of 72°C for 10 min and then held at 4°C.

All PCR reactions were carried out using an Eppendorff Mastercycler® gradient machine.

PCR products were gel electrophoresed as described in section 2.4.2 and were stored at -20°C.

2.4.4 PCR Product Purification

RT and standard PCR products were gel purified using either the QIAGEN® QIAquick® Gel Extraction kit and protocol for microcentrifuge or the Bioline ISOLATE PCR and Gel kit, both according to the manufacturer's instructions.

For the QIAquick® Gel Extraction Kit, centrifugation conditions throughout was 18000 g for 1 min at room temperature:

DNA band(s) were excised from the gel using a sterile scalpel and weighed in a nuclease free tube. 3 volumes of Buffer QG were added per 1 volume of gel and incubated in a water bath at 50°C for *ca* 10 min, with brief vortexing every 2 to 3 min to dissolve the gel. 1 volume of isopropanol was added per 1 volume of gel and mixed via brief vortexing, and each sample was applied to a QIAquick® column placed in a collection tube and then centrifuged. The expelled liquid was discarded and 500 µL Buffer QG was added to the column which was then centrifuged. 750 µL of Buffer PE was applied to the column and centrifuged as a wash step. The flow-through liquid was discarded and the spin columns centrifuged for a final 1 min at 18000 g at room temperature. Each column was placed into a clean, nuclease free 1.5 mL microcentrifuge tube and 30 µL Buffer EB was applied to the column(s) which were left to stand for 1 min before centrifuging. The eluted purified PCR products were stored at -20°C.

When using the Bioline ISOLATE PCR and Gel kit, centrifugation conditions throughout were 10000 g for 1 min at room temperature apart from where stated otherwise:

DNA band(s) were excised from the gel using a sterile scalpel and place in a nuclease free tube. 650 µL Gel Solubilizer was added and samples were incubated in a water bath at 50°C for *ca* 10 min or until the gel was fully dissolved. 50 µL Binding Optimizer was added and vortexed briefly to mix, and then 750 µL of sample was applied to a spin column placed in a collection tube and centrifuged. The expelled liquid was discarded and any remaining sample was loaded onto the column and centrifuged. 750 µL Wash Buffer A was applied to the spin column and centrifuged, and this wash step was repeated, with any expelled liquid being discarded between each step. Spin column(s) were centrifuged for 2 min to ensure removal of Wash Buffer and then placed in a clean nuclease free tube. 30 µL Elution Buffer was applied to the Spin Column membrane and incubated at room temperature for ca 1 min before centrifugation at 6000 g for 1 min at room temperature. The eluted purified PCR products were stored at -20°C.

2.4.5 Sequencing Reactions

Purified PCR products were sent to Eurofins MWG Operon to be sequenced using the Value Read Tube Service. 15 µL of each product plus 2.25 µL of either forward or reverse primer (Table 6, section 2.1.4) at a concentration of 100 µM was provided to Eurofins for sequencing. The reactions were performed using chain termination Sanger sequencing technology and date was analysed using Lasergene8.0-SeqMan software (DNASTAR) and aligned using ClustalW software (EMBL-EBI).

2.4.6 Preparation of Standard Curves for Real-Time Quantitative RT-PCR

Standard curves were prepared for use in real-time RT-PCR as positive controls and in order to obtain an approximate limit of detection for each assay.

10 fold serial dilutions of each virus were prepared in MEM to provide a dilution range from neat virus to 10^{-7}. In order to calculate the number of pfu in each dilution, virus titres were pre-

determined via plaque assay on Vero cells (described in section 2.3.5). RNA was extracted from the viral dilutions as previously described in section 2.4.1 and standard curve samples were stored at -20°C.

2.4.7 Real-Time Quantitative RT-PCR

Real-time RT-PCR was performed on RNA samples using the QIAGEN® QuantiTect™ Probe RT-PCR kit and protocol according to the manufacturer's instructions. All primers and probes were used at a working concentration of 10 µM and the sequences are detailed in Table 7, section 2.1.4.

For each sample to be amplified, 3 µL of RNA was added to 12.5 µL 2x Master Mix, 1 µL of each forward and reverse primer, 0.5 µL probe, 0.25 µL RT enzyme and 6.75 µL DEPC H_2O in a well of a reaction plate (MicroAmp® Fast Optical 96-well reaction plate, Applied Biosystems® by Life Technologies™, UK). The RT-PCR cycle programme used was: 1) 50°C for 30 min, 2) 95°C for 15 min and 3) 94°C for 15 seconds followed by 52°C for 1 min. Step 3 was repeated 40 times.

All real-time RT-PCR reactions were carried out using an ABI 7900HT Fast Real-Time PCR machine and SDS V2.4 software (Applied Biosystems® by Life Technologies™, UK).

2.4.8 SYBR® Green Real-Time RT-PCR

SYBR® Green real-time RT-PCR was performed on RNA samples using the QIAGEN® QuantiTect SYBR® Green RT-PCR kit and protocol according to the manufacturer's instructions. All primers and were used at a working concentration of 10 µM and the sequences are detailed in Table 7, section 2.1.4.

For each sample to be amplified, 1 µL of RNA was added to 12.5 µL 2x SYBR® Green Master Mix, 0.5 µL of each forward and reverse primer, 0.25 µL RT enzyme and 10.25 µL DEPC H_2O in a well of a reaction plate (MicroAmp® Fast Optical 96-well reaction plate, Applied Biosystems® by Life Technologies™, UK). The PCR programme used was: 1) 50°C for 30 min, 2) 95°C for 15 min and 3)

94°C for 15 seconds followed by 52°C for 30 seconds and 72°C for 30 seconds. Step 3 was repeated 40 times.

All SYBR® Green RT-PCR reactions were carried out using an ABI 7900HT Fast Real-Time PCR machine and SDS V2.4 software (Applied Biosystems® by Life Technologies™, UK).

2.5 Immunohistochemistry

2.5.1 Optimisation of Antibody Dilutions

Primary and secondary antibodies were titrated to determine optimal working dilutions and diluents.

Rabbit polyclonal MuV anti-F antibody (kindly provided by Steven Rubin, FDA) and anti-β-tubulin mouse monoclonal antibody (Sigma Aldrich, UK) were diluted in PBS A containing 1% (w/v) Bovine Serum Albumin (BSA) and 1% (v/v) Tween-20 (both Sigma Aldrich, UK) or PBS A containing 5% (w/v) non-fat dried milk powder and 1% (v/v) Tween-20. Both antibodies were diluted to a range from 1 in 100 to 1 in 10,000. MuV anti-F antibody was titrated on LLC-MK2 cells (Rhesus Monkey Kidney) in 8-well chamber slides (Fisher Scientific, UK) infected with mumps virus Mu90 fixed at 72 hours post infection as described in section 2.3.4. The mouse monoclonal anti-β-tubulin antibody was titrated on MCF-7 cells (human breast adenocarcinoma) in 8-well chamber slides fixed 24 hours after seeding as described in section 2.3.4. Secondary antibodies Goat Anti-Rabbit IgG conjugated to fluorescein isothiocyanate (FITC) and Goat Anti-Mouse TEXAS RED® conjugate (both Calbiochem®, UK) were diluted in either 1% (w/v) BSA/PBS A or 5% (w/v) non-fat dried milk/PBS A over a range of 1 in 50 to 1 in 400.

All slides were mounted with glass cover slips using VECTASHIELD mounting medium (Vector Laboratories, UK) and images acquired using an Olympus IX71 fluorescence microscope and Leica camera FC345FX.

2.5.2 Staining of MucilAir™ Histological Sections

Histological sections of infected MucilAir™ HAE cells (see section 2.3.4) were received from Propath UK Limited on glass slides and de-paraffinized in xylene and ethanol and then rinsed in running tap water.

Slides were blocked in 1% (w/v) BSA/PBS A for *ca* 1 hour at room temperature. The section slides were then washed once with PBS A and co-stained with rabbit polyclonal MuV anti-F antibody and anti-β-tubulin IV mouse monoclonal antibody diluted appropriately in 1% (w/v) BSA/1% (w/v) Tween-20/PBS A, and incubated overnight at 4°C.

After the incubation period, slides were washed 3 times with ice-cold PBS A and primary antibodies were detected using FITC-Goat Anti-Rabbit IgG and Goat Anti-Mouse TEXAS RED® diluted appropriately in 1% (w/v) BSA/PBS A and incubated for *ca* 1 hour at room temperature in the dark. The sections were washed 3 times with ice cold PBS A before mounting with glass cover slips using VECTASHIELD mounting medium. Photomicrographs were obtained using a LSM 5 Pascal Axioplan 2 imaging confocal microscope and LSM Image Browser software (Zeiss).

2.6 Sialic Acid Investigations

2.6.1 Sialic Acid Quantification Bioassay

The concentration of sialic acid in a defined quantity of cells was measured using the EnzyChrom™ Sialic Acid Assay Kit (BioAssay Systems, USA) according to the manufacturer's instructions.

Briefly, one confluent T75 flask of each cell line to be analysed was trypsinized into 30 mL PBS A and centrifuged at 470 g for 5 min at room temperature to remove debris and pellet the cells. Cells were counted as described in section 2.2.3 and re-suspended at a concentration of $2x10^5$ cells in a final volume of 20 µL PBS A.

20 µL cells in PBS A were mixed with 80 µL Hydrolysis Reagent in a 1.5 mL screw cap tube and incubated in a waterbath at 80°C for 1 hour to release sialic acid bound to cell membranes. The sample was then cooled to room temperature and centrifuged at 21000 g for 1 min at room temperature. 20 µL Neutralisation Reagent was added to stop the hydrolysis reaction, mixed by vortexing and then centrifuged at 21000 g for 30 seconds at room temperature.

For the colorimetric procedure, samples and reagents were equilibrated to room temperature and a 1 mM sialic acid Standard Premix was prepared by mixing 50 µL of the 10 mM Standard with 450 µL H_2O. This was then diluted as set out in Table 9.

Table 9 – Standard Preparation for Sialic Acid Bioassay

Number	Premix + H_2O	Total Volume (µL)	Sialic Acid (mM)
1	100µL + 0µL	100	1.0
2	60µL + 40µL	100	0.6
3	30µL + 70µL	100	0.3
4	0µL + 100µL	100	0

10 µL of standards and 10µL of samples were transferred to separate wells of a clear, flat-bottomed 96 well plate (Scientific Lab Supplies, UK) in triplicate. For each reaction well, 93 µl Assay Buffer, 1 µL Dye Reagent and 1 µL Enzyme was mixed in a 1.5 mL screw cap tube, and 90 µL of this working reagent was then transferred to each reaction well and mixed gently by pipetting contents up and down several times. The reaction plate was incubated at room temperature for *ca* 1 hour and then optical density (OD) at 570 nm was measured using a FLUOstar OPTIMA plate reader (BMG LABTECH,

USA). Replicate OD readings were analysed by linear regression of the assay standard using GraphPad PRISM® 5.0 software.

2.6.2 Fluorescence Activated Cell Sorting (FACS) Analysis

Relative quantities of α2,3 and α2,6 sialic acid linkages expressed on cell surfaces was determined using the Digoxigenin (DIG) Glycan Differentiation Kit (Roche, UK) with some modifications from the manufacturer's protocol.

Briefly, one confluent T75 flask of each cell line to be analysed was trypsinized into 10 mL infection medium and centrifuged at 470 g for 5 min at room temperature to remove debris. The cell pellet was re-suspended in 20 mL PBS A and counted as described in section 2.2.3. Cells were added to 9 replicate wells of a clear, flat-bottomed 96 well plate at a concentration of $2x10^5$ cells per well in 200 µL FACS buffer (Table 8). Plates were centrifuged at 470 g for 5 min at room temperature to wash cells. The resulting supernatant was removed by over-turning the plates onto absorbent paper and the cells re-suspended by tapping the plate gently to prepare them for lectin incubation.

DIG-labelled lectins *Sambucus nigra* agglutinin (SNA) and *Maackia amurensis* agglutinin (MAA) were diluted appropriately in FACS buffer to give working concentrations of 1 µg/mL. 10 µL of SNA, MAA or FACS buffer was added to 3 of the 9 replicate wells of cells and incubated at room temperature for 30 min with gentle shaking. After the incubation period cells were washed 3 times in PBS A. 10 µL of FITC conjugated anti-DIG antibody (5 µg/mL) (Roche, UK) was added to all wells and incubated at room temperature for 30 min with gentle shaking. Cells were then washed twice in PBS Flow (Table 8) and after the final wash each well of cells was re-suspended in 200 µL FACS Fix buffer (Table 8). Samples were analysed by FACS using a BD FACSCanto™ II machine (Becton Dickinson, UK).

2.6.3 Sialic Acid Blocking

Cells were treated with lectin from MAA (Sigma Aldrich, UK) prior to infection to block α2,3 sialic acid linkages.

Briefly, cells were seeded into 24 well plates as described in section 2.3.2. Plated cells were washed once with PBS A and an appropriate volume of 1 mg/mL MAA lectin diluted in PBS A was added to each well. Control cells were treated with PBS A only. Cells were incubated at 35°C, 5% CO_2 for 1 hour before aspirating the lectin solution or control, then were washed once with PBS A and infected as described in section 2.3.2 with Mu90. Media from cells infected with Mu90 were harvested every 24 hours for 5 days and progeny virus titrated via plaque assay as described in section 2.3.5.

This experiment was also performed as described using lectin from SNA (Sigma Aldrich, UK) to block α2,6 sialic acid linkages, and with a simultaneous treatment of both MAA and SNA lectins to block both α2,3 and 6 linkages.

2.7 Human Cytokine ELISA

Levels of cytokines secreted into the basal medium of MucilAir™ cells infected with clinical mumps virus AFZ315 were measured using the Multi-Analyte ELISArray™ kit for human inflammatory cytokines (SABiosciences™, a QIAGEN® company) according to the manufacturer's instructions.

Briefly, basal samples taken at 6, 12, 24 hours and days 4, 7 and 10 post infection were centrifuged at 1000 g for 10 minutes and stored on ice. All reagents and buffers were prepared as per manufacturer's protocol and equilibrated to room temperature. 50 µL of assay buffer plus 50 µL of samples, dilution buffer (negative control) or antigen standard cocktail (positive controls) were added to the relevant wells of the ELISA plate and incubated at room temperature for 2 hours. After the incubation period, contents of all wells were decanted and each well was washed 3 times with 350 µL of wash buffer before the addition of 100µl per well of detection antibodies. ELISA plate was incubated for 1 hour at room temperature and then washed 3 times as previously described. 100 µL of Avidin-horse radish peroxidise (HRP) was added to each well and incubated in the dark at room temperature for 30 minutes before washing each well 4 times as previously described. 100 µL of

development solution was added to each well, ELISA plate incubated for 15 minutes at room temperature in the dark and the reaction then stopped by the addition of 100 µL per well of stopping solution.

The absorbance was read at 450 nm using a Multiskan Ascent plate reader and software (Thermo Scientific, UK).

2.8 *In Vivo* Virology

2.8.1 Animals

Male ferrets aged between 6 – 12 months were used in the three *in vivo* studies in this PhD project. All animal procedures were performed by fully trained and licensed NIBSC Biological Services Division (BSD) staff.

For the initial study designated A, one group of three ferrets was inoculated intranasally with *ca* $7x10^3$ pfu in 400 µL (200 µL per nostril) of neat mumps clinical sample AFZ315. A second group of three ferrets was inoculated intranasally with *ca* $2x10^4$ pfu in 400 µL (200 µL per nostril) of the RIT 4385 mumps vaccine strain diluted in MEM.

Study A ran for 28 days with pre-bleed samples collected 7 days prior to inoculation, and blood samples were taken on 7, 14, 21 and 28 days post infection. Nasal washes, urine and faeces samples were collected on days 1, 4, 7, 14, 21 and 28. On day 28, all ferrets were terminated and tissues were collected (Table 10).

For the study designated B, one group of three ferrets was inoculated intranasally with *ca* $2x10^4$ pfu in 400 µL (200 µL per nostril) of heat-inactivated RIT 4385 diluted in MEM. The virus was heat-inactivated prior to inoculation by incubating in a water bath at 60°C for 30 min.

Study B ran for 28 days with pre-bleed samples collected 9 days prior to inoculation, and blood samples were taken on 7, 14, 21 and 28 days post infection. On day 28, all ferrets were terminated.

For the study designated C, one group of eight ferrets was inoculated intranasally with *ca* $7x10^3$ pfu in 400 µL (200 µL per nostril) of neat AFZ315.

Study C ran for 14 days with pre-bleed samples collected 9 days prior to inoculation. Oral swabs were taken from all animals still on study every 24 hours for 14 days. On 1, 4, 7 and 14 days post infection, two ferrets were terminated and tissues (Table 10) and terminal bleeds collected.

The final *in vivo* investigation was designated as study D, and included four ferrets inoculated intranasally with ca $1x10^5$ pfu in 400 µL (200 µL per nostril) of AFZ315 virus harvested at day 10 post infection from MucilAir™ HAE cells.

Study D ran for 7 days. On days 4 and 7 post infection, two ferrets were terminated and tissues collected (Table 10).

2.8.2 Blood Sample Processing

Blood samples were collected in either serum-gel clotting activator tubes (Sarstedt, UK) or Becton Dickinson EDTA Vacutainers® (Fisher Scientific, UK).

Samples collected in serum-gel clotting activator tubes were allowed to clot at room temperature for 20 to 30 min. The tubes were centrifuged at 15000 g for 5 min at 4°C to separate the serum and red blood cells. Serum was carefully removed by pipetting from the top layer of the separation gel and split into 2 aliquots before being stored at -80°C.

Blood samples collected in Vacutainers® were used for peripheral blood mononuclear cell (PBMC) isolation. 4 mL ferret blood was added to 4 mL PBS A pre-warmed to 37°C and mixed by gentle inversion. The blood/PBS A mixture was deposited gently onto 4.5 mL Ficoll-Paque™ PLUS (GE Healthcare Life Sciences, UK) and centrifuged at 1400 rpm for 40 min at room temperature. PBMC's

were removed from the resulting gradient by pipetting and washed 3 times in PBS A pre-warmed to 37°C before storing at -80°C.

2.8.3 Nasal Wash Processing

Nasal washes were collected using L-15 (Liebovitz) medium (Sigma Aldrich, UK) supplemented with 2% (w/v) BSA, 2% (w/v) 200 mM L-Glutamine, 2% (w/v) 10,000 units/mL Penicillin-Streptomycin and 2% (w/v) 250 mM Amphotericin B. Samples were received on ice and split into 2 aliquots of *ca* 600 µL and stored at -80°C.

2.8.4 Urine Sample Processing

Urine samples were provided as compressed paper animal bedding soaked with urine in a 50 mL centrifuge tube on ice. 5 mL of infection medium supplemented with 50 mg/mL (v/v) Gentamicin (Life technologies™ UK) was added to each tube, and the soaked bedding/media were then transferred into a 50 mL syringe (VWR International, UK). All liquid from the bedding and syringe was then expelled back into the same collection tube. A further 4% (v/v) FCS was added to each sample before storing at -80°C.

2.8.5 Faeces Sample Processing

Faeces samples were received in 50 mL centrifuge tubes on ice. 10 mL of infection media supplemented with 50 mg/mL (v/v) Gentamicin was added to each tube and vortexed vigorously for 1 to 3 min until a homogenate was achieved. Each tube was then made up to a final volume of 50 mL with the same media and mixed well by shaking and inverting the tube several times. Faeces homogenates were stored at -80°C.

2.8.6 Oral Swab Processing

Oral swabs were taken using Sterilin pink-cap swabs containing virus transport medium sponges (Fisher Scientific, UK) and received on ice. Each swab was pressed and rubbed against the sponge for

ca 30 seconds. The sponge was removed from the tube using sterile forceps and transferred into a 15 mL centrifuge tube containing infection media supplemented with 50 mg/mL (v/v) Gentamicin. Samples were stored at -80°C.

2.8.7 Tissue Homogenate Preparation

Tissues removed from the ferrets for homogenate preparation are listed in Table 10. Tissues were received in sterile containers on ice and each was weighed and 20% homogenates prepared in infection media. To prepare the 20% homogenates, each tissue was cut into small, even fragments using sterile scalpels and forceps, and placed into Precellys 24® homogenisation tubes (Peqlab, UK) containing an appropriate volume of media. Homogenisation was carried out using a Precellys 24® cell lysis and tissue homogeniser (Bertin Technologies, France). For adrenal glands, parotid glands, lymph nodes, turbinates, salivary glands and tonsils, a programme of 1 x 3000 g for 20 s was used, and for all other tissues a programme of 1 x 4000 g for 20 s was used.

The resulting homogenates were then transferred, and pooled where necessary, into sterile containers, and an appropriate volume of infection media was added to make the final 20% homogenate. All samples were stored at -80°C.

Table 10 – Ferret Tissues Analysed

***In vivo* study A - Tissues**	***In vivo* studies C and D - Tissues**
Adrenal gland	Brain
Brain	Kidney
Colon	Lung
Heart	Lymph node**
Kidney	Pancreas
Liver	Parotid gland
Lung	Spleen

Lymph node	Testes
Pancreas	Tonsil
Parotid gland	
Salivary gland*	
Small intestine	
Spleen	
Testes	
Tongue	
Tonsil	
Turbinates	

*****BSD staff unable to locate and remove salivary glands from 2 out of 3 ferrets infected with AFZ315

**BSD staff unable to locate and remove lymph nodes from 2 out of 8 ferrets from study C

2.8.8 Preparation of Tissue Homogenates Spiked with Mumps Virus

20% homogenates of spleen, brain and kidney tissues taken from a ferret terminated on day 1 post infection during study C were spiked with a known titre of clinical mumps virus AFZ315. 10 fold serial dilutions of virus were prepared in each homogenate to provide a dilution range from 10^{-1} to 10^{-8} and RNA was extracted from each sample as described in section 2.4.1.

Spiked tissue homogenate dilutions were used as standard curve for real-time RT-PCR in order to confirm the ability of MuV to be extracted from ferret tissues and to obtain a limit of detection for quantitative real-time PCR assays.

CHAPTER 3 – IN VITRO RESULTS

Mumps virus is capable of growth in continuous cell lines, and serial passage in cell culture is the basis of attenuation for all live mumps vaccines. African Green Monkey kidney (Vero) cells are currently the "gold-standard" for MuV isolation and propagation, and it is likely that their deficiency in interferon production (Desmyter *et al.*, 1968) is the reason that they are so permissive for MuV. Although Vero cells are commonly used, it has been suggested that they may be selective, insensitive and unsuitable for the production of virus isolates to be used in research (Afzal *et al.*, 2005). A previous study also demonstrated that Vero cells produce virus populations that are different from the original parent virus (Yates, 1995). This has not been investigated further to any great extent, and one of the aims of this project was to determine how serial passage of MuVs in Vero cells affects the viral genome and plaque phenotype.

Concurrently, a cell line investigation was performed using representative wild-type and vaccine MuVs and a GFP-expressing MuV in order to identify any cell types which may offer an alternative to Vero's. As mumps is a solely human disease, it may be more stable in a human line so as well as various continuous human cell lines, *ex-vivo* human airway epithelial (HAE) cells were investigated as a model for MuV infection. HAE cells have already been well-documented for their use in experimental infections of other negative-sense ssRNA viruses, and have the potential to be useful for investigative MuV research.

It is currently unknown what factors or properties of a cell line make it suitable for efficient MuV growth and replication. Virus infection of a cell is a complex, multi-factorial process of which the initial step is binding of the virus to the host cell receptor. Sialic acid is known to be the receptor for MuV (Markwell, 1991) and exists as various analogues including α2,3 and α2,6 linked, and another aim of this project was to investigate whether or not the quantity or linkage type of expressed sialic acid on a cell's surface is a determinant of ability to successfully propagate MuV.

3.1 Initial Cell Line Screen

3.1.1 Cell Line Screen using a MuV Expressing Green Fluorescent Protein (GFP)

GFP-MuV was used to screen a panel of cell lines in order to determine which could effectively support MuV infection and protein expression. Fluorescence intensity (FI), which is indicative of both viral protein expression and cellular infection, was measured every 24 hours for 10 days. FI levels were reported as FI Units and an arbitrary value of 8,000 FI Units was designated as the value for separating high and low levels of GFP expression. Infections were performed in triplicate and values recorded were background-corrected. Data is presented as high and low GFP-expressing cell lines, with the low group being further divided into human and non-human cell lines to aid visualisation of the data, and is shown in Figure 3.

a) High GFP-expressing cell lines (>8000 FI units)

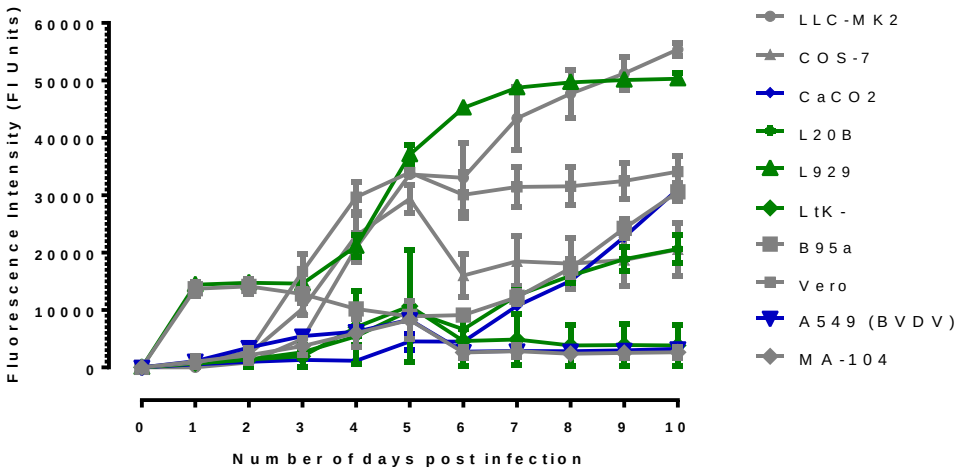

b) Low GFP-expressing cell lines (human, <8000 FI units)

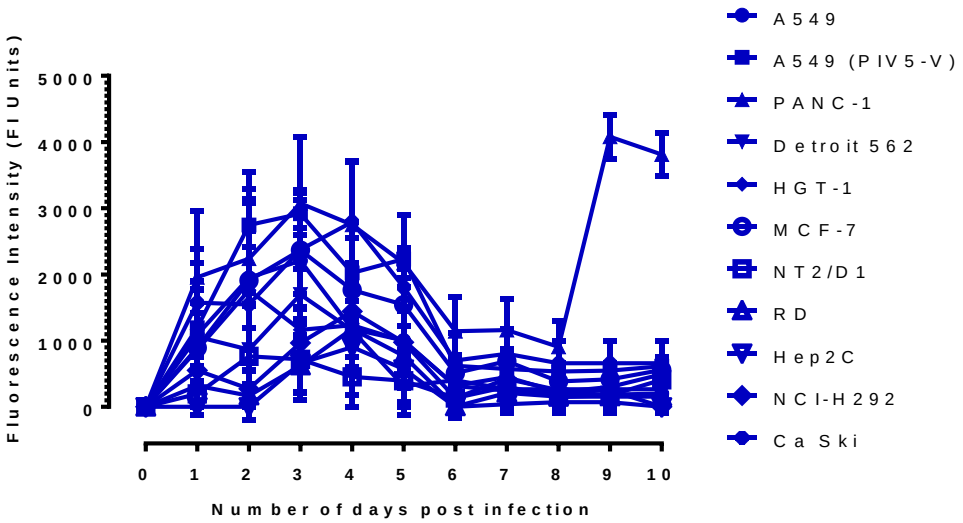

c) Low-GFP expressing cell lines (all other cells, non-human, <8000 FI)

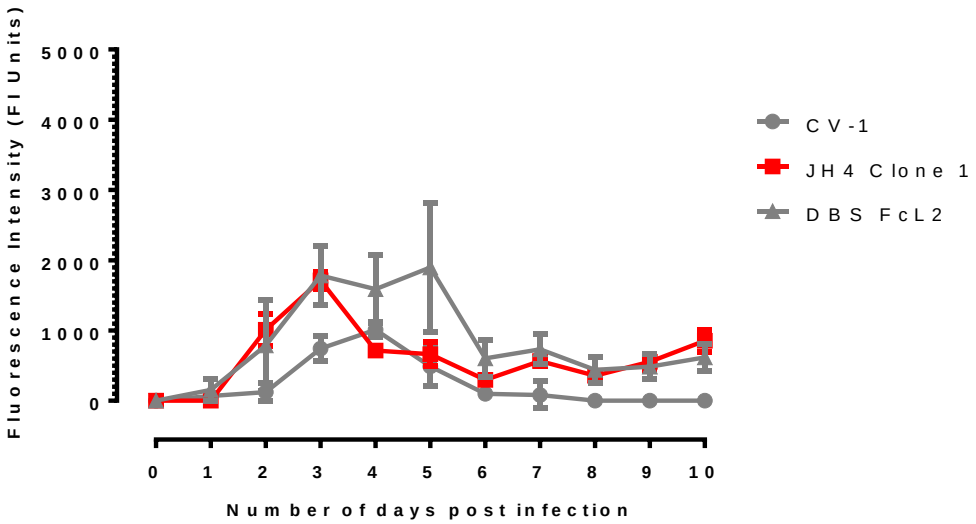

Figure 3 – GFP expression levels of various cell lines infected with GFP-MuV over 10 days. Cells were infected with GFP-expressing MuV at an MOI of 0.01 pfu per cell in triplicate in 96-well plates. Fluorescence was measured every 24 hours for 10 days using the well-scan grid mode of the BMG FLUOStar OPTIMA plate reader. GFP expression (FI units) is separated into high (a), low – human (b) and low – all other cells (c) based on an arbitrary "high" value of 8000 FI units. Values displayed represent the mean and standard deviation of triplicate readings and are background-corrected. Data in blue is from cell lines of human origin, grey data from non-human primate cell lines, murine cell lines are shown in green and all "other" cells are shown in red.

The highest recorded value was 55376 FI units on day 10 post infection of LLC-MK2 cells. The peak FI for the "gold standard" Vero cells was 33979 on day 5 post infection, and after this time point the recorded FI values reached a plateau. Several cell lines other than those shown in Figure were also infected with GFP-MuV however these exhibited no detectable GFP expression throughout the time course. Cells showing no GFP expression were MRC-5, IMR-90, 293T, RK-13, 2° Ferret Lung, Mpf, TM3, DBS FrhL2, BHK-21, MDCK, CHO-K1 and SH-SY5Y.

3.1.2 Cell Line Screen using Representative Wild-Type and Vaccine MuV's

The same panel of cell lines screened with GFP-MuV were infected with Mu90 (wild-type) and RIT 4385 (vaccine) mumps viruses at an equal MOI of 0.001 pfu per cell. This was carried out in order to determine which cells were capable of supporting MuV growth and producing high yields of infectious progeny virus. At 7 days post infection, virus was harvested from cells and titrated by plaque assay on Vero cells in triplicate. Mock-infected controls were all valid. Mu90 and RIT 4385 passage 1 progeny virus titres are shown in Figure 4.

a) Mu90 progeny virus titres

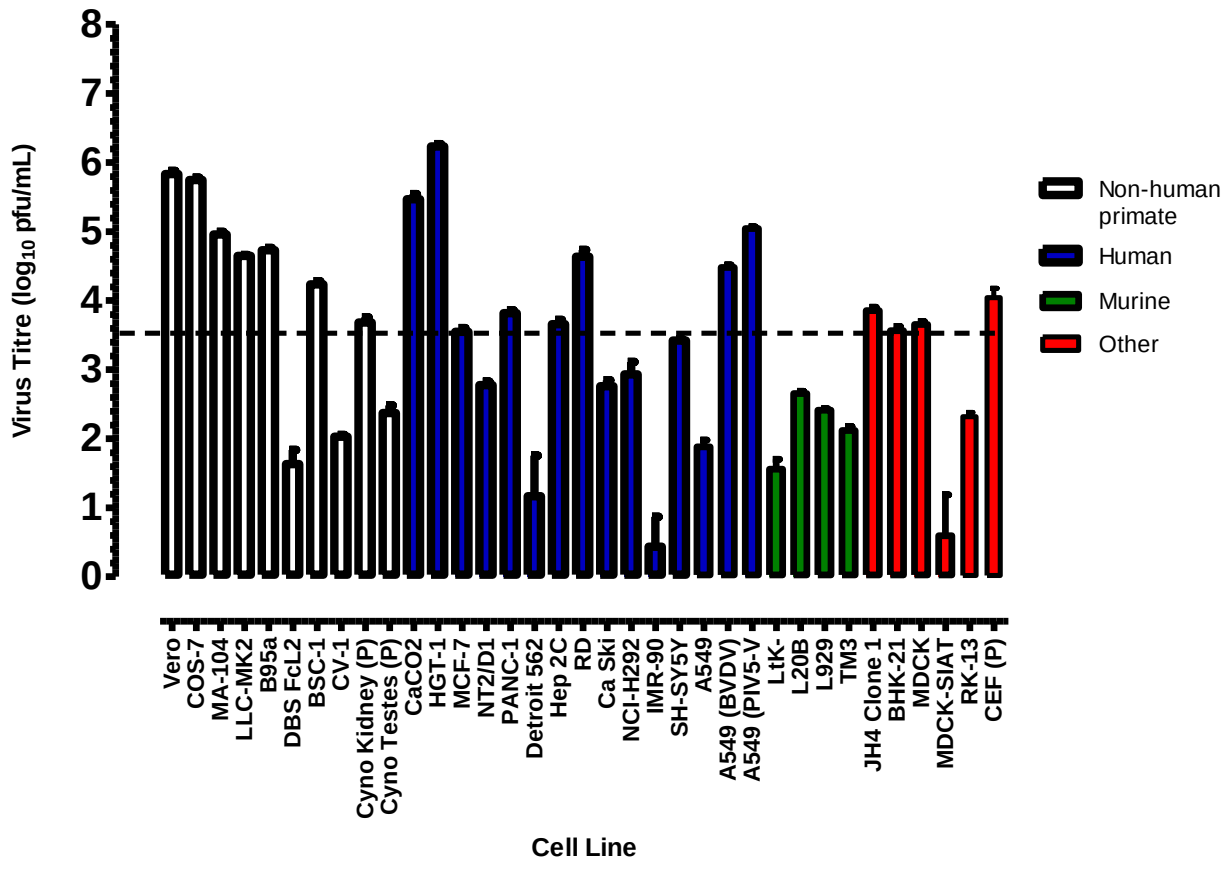

b) RIT 4385 progeny virus titres

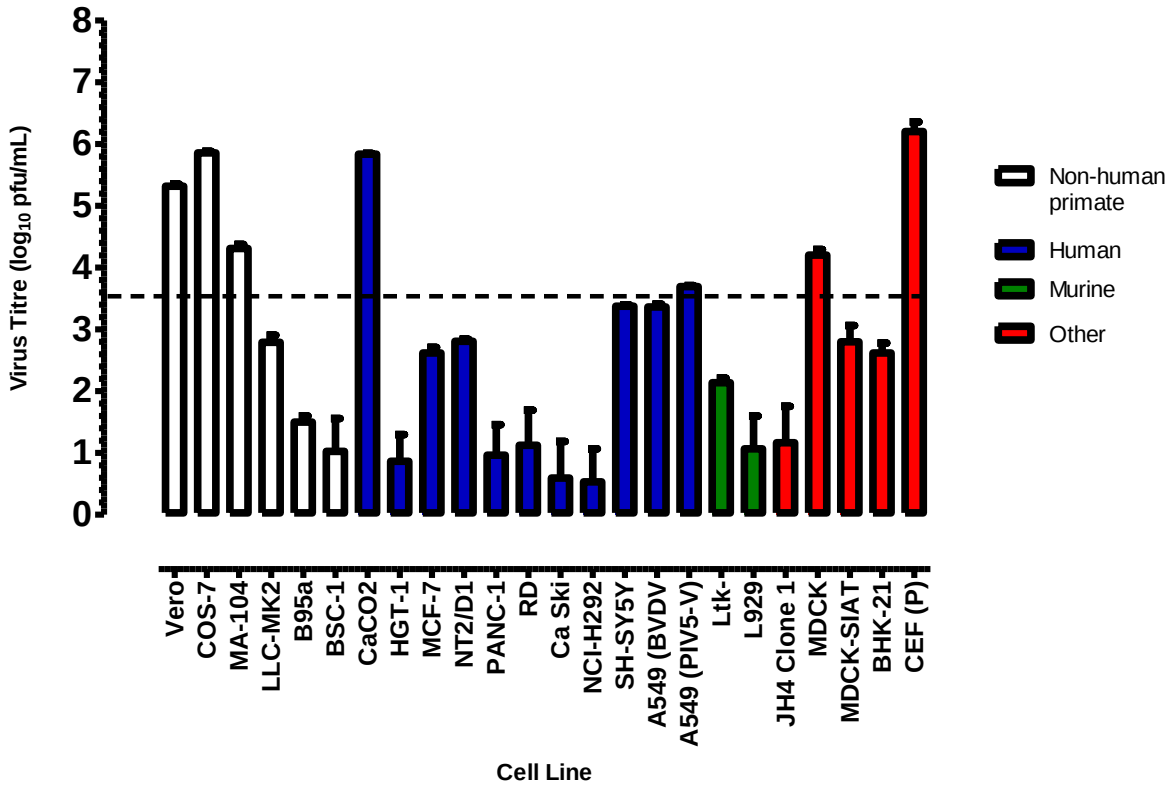

Figure 4 – MuV titres after 1 passage on various cells lines infected with either Mu90 (a) or RIT 4385 (b). Cells were infected at an MOI of 0.001 pfu per cell in triplicate and virus harvested on day 7 post infection by freeze-thawing cells and lysate clarification. P1 titres were obtained by plaque assay on Vero cells and values displayed represent the mean and standard deviation of triplicate infections. The bisecting dotted line represents the inoculum titres.

The four cell lines producing the highest titres of Mu90 virus are HGT-1 (6.23 $\log_{10}$ pfu/mL), Vero (5.83 $\log_{10}$ pfu/mL), COS-7 (5.75 $\log_{10}$ pfu/mL) and CaCO2 (5.47 $\log_{10}$ pfu/mL). However, this is not entirely mirrored by the four cell lines producing the highest RIT 4385 virus titres, which are COS-7 (5.86 $\log_{10}$ pfu/mL), CaCO2 (5.84 $\log_{10}$ pfu/mL), Vero (5.32 $\log_{10}$ pfu/mL) and MA-104 (4.31 $\log_{10}$

pfu/mL). Cell lines demonstrate a reduced ability to produce infectious RIT 4385 viruses when compared with Mu90, with the exceptions of Vero, COS-7, CaCO2, and MA-104 which all produce approximately the same titre for both. CEF cells produce higher titres of progeny RIT 4385 virus (6.20 $\log_{10}$ pfu/mL) when compared with Mu90 progeny (4.04 $\log_{10}$ pfu/mL), however this was to be expected as CEF's are the cells used to propagate RIT 4385 by the vaccine manufacturer (Tillieux *et al.*, 2009). Although only slight, LtK- cells also demonstrate an increase in titre from Mu90 progeny (1.56 $\log_{10}$ pfu/mL) to RIT 4385 progeny (2.14 $\log_{10}$ pfu/mL). MRC-5, 293T, 2° Ferret lung, CHO-K1, DBS FrhL2 and Mpf cells did not produce any infectious Mu90 or RIT 4385 progeny virus.

No obvious correlation between levels of GFP expression and ability to produce high yields of infectious progeny was observed from the data. Several high GFP-expressing cell lines produced relatively low titres of progeny MuV (L20B, L929, LtK- and Detroit 562), and several cell lines expressing lower levels of GFP produced relatively high titres of progeny MuV (HGT-1, MA-104, A549 (BVDV) and A549 (PIV5-V)).

The dotted lines bisecting graphs (a) and (b) in Figure 4 represent the titre of the inoculated virus and all cell lines producing progeny Mu90 or RIT 4385 above this threshold (3.3 $\log_{10}$ pfu/mL) were subject to further investigation. Table 11 provides a summary of these successful cells and their origin. Although primary CEF and Cynomolgus Macaque kidney cells produced high titres of progeny Mu90 virus and RIT 4385 in the case of CEFs, these cells were not studied further due to lack of availability.

Table 11 – Cell Lines Selected from Initial Screen for Further Investigation

Cell Line Origin							
Human		**Non-Human Primate**		**Murine**		**Other**	
Mu90	**RIT 4385**	**Mu90**	**RIT 4385**	**Mu90**	**RIT 4385**	**Mu90**	**RIT 4385**
A549 (BVDV)	A549 (PIV5-V)	B95a	COS-7			BHK-21	MDCK
A549 (PIV5-V)	CaCO2	BSC-1	MA-104			JH4 Clone 1	
CaCO2		COS-7	Vero			MDCK	
Hep2C		LLC-MK2					
HGT-1		MA-104					
MCF-7		Vero					
PANC-1							
RD							

The majority of the cells studied further were of human origin, followed by non-human primate and then a mixed group designated as “other” including Syrian hamster (BHK-21) guinea pig (JH4 Clone 1) and canine (MDCK) cells. No murine cell lines were used in further investigations.

3.2 Mumps Virus Serial Passage through Various Cell Lines

Passage 1 (P1) viruses obtained from designated “successful” cell lines (section 3.2.2, Table 11) were passaged through the same cells a further four times, resulting in a total of five passages. Each passage was performed independently and in triplicate, resulting in three separate virus samples per passage, per cell line. Progeny viruses from P2, P3, P4 and P5 were titrated via plaque assay on Vero cells in triplicate and plaque morphologies at each stage examined to determine any phenotypic changes. Plaque assays were performed directly on each cell line using the parent Mu90 virus in order to determine whether or not they were able to support MuV plaque formation.

RNA was isolated from cell supernatants containing virus, and nucleoprotein (N), fusion (F), haemagglutinin-neuraminidase (HN) and small hydrophobic (SH) genes from parent Mu90 and RIT 4385 viruses, and P5 viruses were analysed by RT-PCR, sequenced and the alignments compared in order to assess the genetic stability provided by each of the investigated cell lines. The specific primers used for each MuV gene are detailed in section 2.1.4, Table 6.

In all cases, mock-infected and negative controls were valid.

The following sections (3.2.1 to 3.2.17) provide a summary of the results obtained for all cell lines investigated.

3.2.1 Vero

P1 to P5 titres of Mu90 and RIT 4385 progeny viruses from Vero (African Green Monkey kidney) cells are shown in Figure 5.

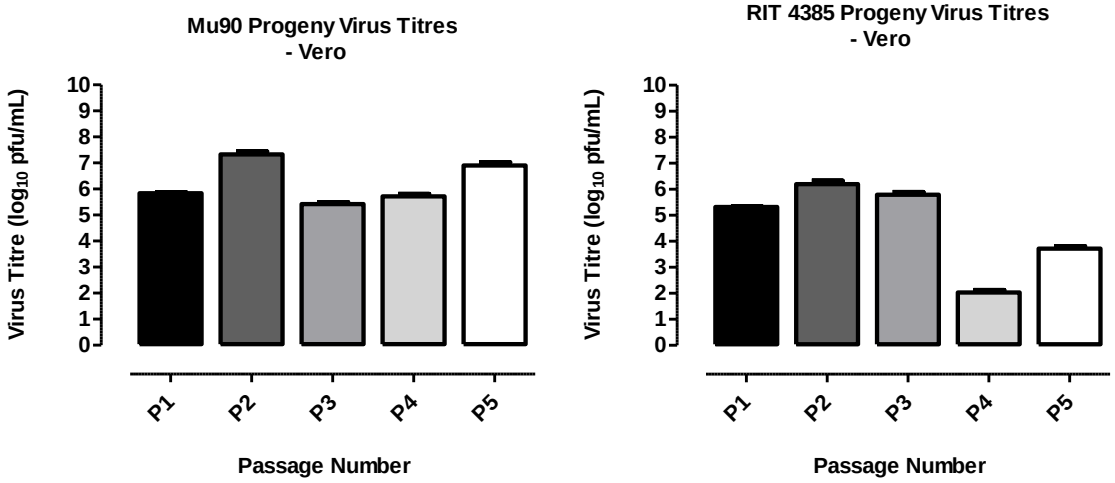

Figure 5 –Titres of Mu90 and RIT 4385 progeny viruses over 5 serial passages in Vero cells. Cells were infected with a 1 in 50 dilution of the previous passage sample (E.g. P2 used to infect P3) prepared in infection medium and virus harvested on day 7 post infection by freeze-thawing cells and lysate clarification. Progeny virus titres were obtained by plaque assay on Vero cells and values displayed represent the mean and standard deviation of triplicate, independent infections.

Mu90 progeny virus titres from Vero cells are highest at P2 (7.3 $\log_{10}$ pfu/mL) before a decrease at P3 (5.4 $\log_{10}$ pfu/mL) followed by a steady increase to 6.9 $\log_{10}$ pfu/mL at level P5. The highest titre of RIT 4385 progeny virus occurs at P2 (6.2 $\log_{10}$ pfu/mL) and the lowest at P4 (2.0 $\log_{10}$ pfu/mL).

Figure 6 demonstrates the plaque morphologies from P1 to P5 of Mu90 and RIT 4385 progeny viruses.

a) Mu90 plaque morphologies

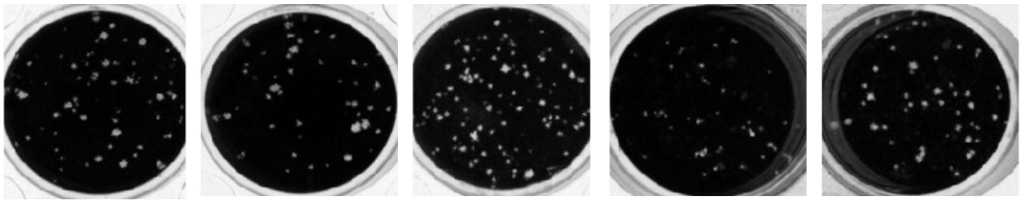

b) RIT 4385 plaque morphologies

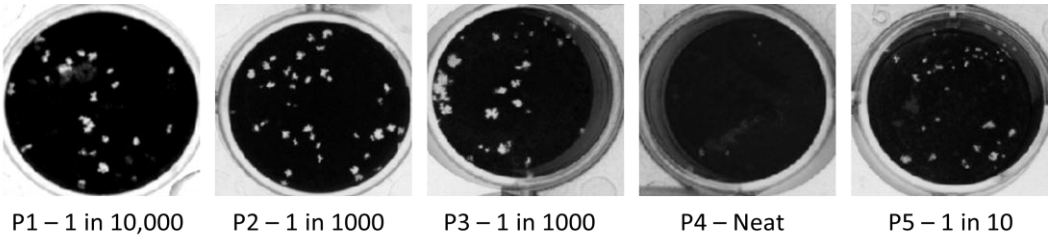

Figure 6 – Plaque morphologies of Mu90 (a) and RIT 4385 (b) progeny viruses over 5 serial passages in Vero cells. Dilutions of viruses photographed for each example of morphology at each passage are noted below each image.

Mu90 P1 plaques appear to contain a mixture of medium sized and smaller morphologies which is maintained throughout five serial passages. RIT 4385 P1 plaques appear larger and more homogeneous, however smaller plaques begin to appear in P3 and more are present by P5.

Results from the genetic stability studies in which N, F, HN and SH genes of parent and P5 viruses were sequenced and aligned are summarised in Table 12 as amino acid changes. Full nucleotide and amino acid alignments are detailed in appendices 1-8.

Table 12 – Amino acid substitutions in P5 progeny Mu90 and RIT 4385 virus proteins from Vero cells

Protein	Mu90	RIT 4385
Nucleoprotein (N)	R194I Q199H G544A D545T W546G	N/A
Fusion (F)	M140I E153K R381Q	I244T
Haemagglutinin-neuraminidase (HN)	T24A V575F	F15S V43A D151E F157L
Small hydrophobic (SH)	F48L H50R	N/A

N/A – not applicable, no substitutions

The number of mutations present indicates that the attenuated vaccine virus RIT 4385 is more genetically stable than the wild-type Mu90 virus in Vero cells.

3.2.2 A549 (BVDV)

P1 to P5 titres of Mu90 progeny viruses from A549 (BVDV) (human lung carcinoma expressing the NPro protein of BVDV) cells are shown in Figure 7. These cells did not produce high enough titres of RIT 4385 progeny virus (> 3.3 log_{10} pfu/mL) at passage 1 to be investigated further with this MuV.

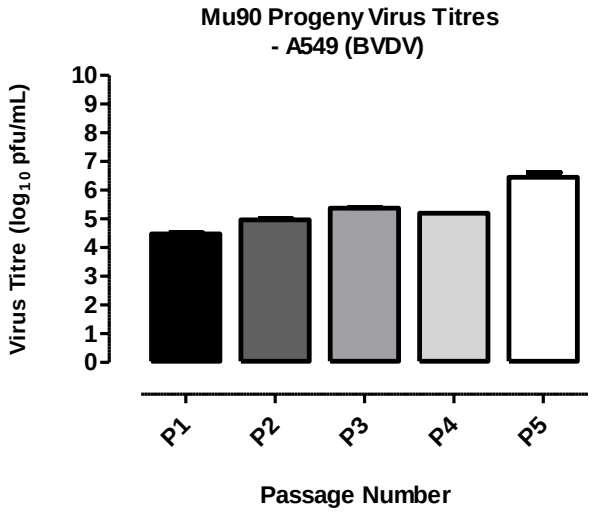

Figure 7 – Titres of Mu90 progeny viruses over 5 serial passages in A549 (BVDV) cells. Infection and titration details as per Figure 5.

Mu90 virus titres increase slightly from P1 (4.48 log_{10} pfu/mL) to P3 (5.4 log_{10} pfu/mL) and then reach their highest titres at P5 (6.5 log_{10} pfu/mL).

Figure 8 demonstrates the plaque morphologies from P1 to P5 of Mu90 progeny viruses from A549 (BVDV) cells.

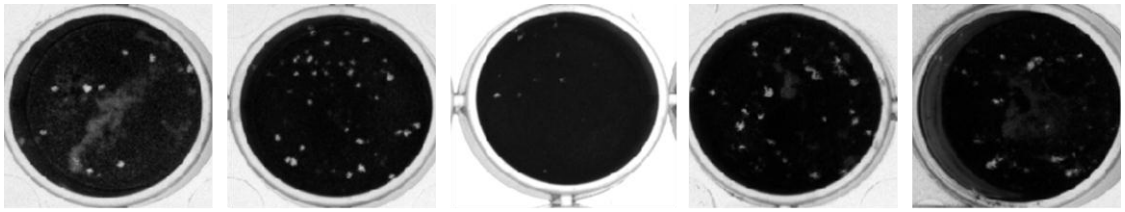

P1 – 1 in 1000 P2 – 1 in 1000 P3 – 1 in 1000 P4 – 1 in 100 P5 – 1 in 10,000

Figure 8 – Plaque morphologies of Mu90 progeny viruses over 5 serial passages in A549 (BVDV) cells. As per Figure 6.

Mu90 P1 plaques appear as a homogeneous population of round, medium-sized plaques. Smaller plaques appear at P2 and are seen throughout until P5.

Results from the genetic stability studies in which N, F, HN and SH genes of parent and P5 viruses were sequenced and aligned are summarised in Table 13 as amino acid changes. Full nucleotide and amino acid alignments are detailed in appendices 1-4.

Table 13 – Amino acid substitutions in P5 progeny Mu90 virus proteins from A549 (BVDV) cells

Protein	Mu90
Nucleoprotein (N)	E235K
	R241Q
	G264R
	Q508K
	D509X
Fusion (F)	I28M
Haemagglutinin-neuraminidase (HN)	T24A
	H94Y
	L576S
	T577N
	R578Q

	L579I
	T580D
	I581Y
	T582H
	-583L (extra amino acid)
Small hydrophobic (SH)	F48L
	H50R

Amino acid substitutions were present in all four proteins investigated in these experiments. The HN protein contained ten substitutions, making the protein one amino acid (position 583, leucine) longer than that of the parent MuV. The F protein from the P5 progeny MuV was found to be 18 amino acids shorter than that of the parental virus.

3.2.3 A549 (PIV5-V)

P1 to P5 titres of Mu90 and RIT 4385 progeny viruses from A549 (PIV5-V) (human lung carcinoma expressing V protein of PIV-5) cells are shown in Figure 9.

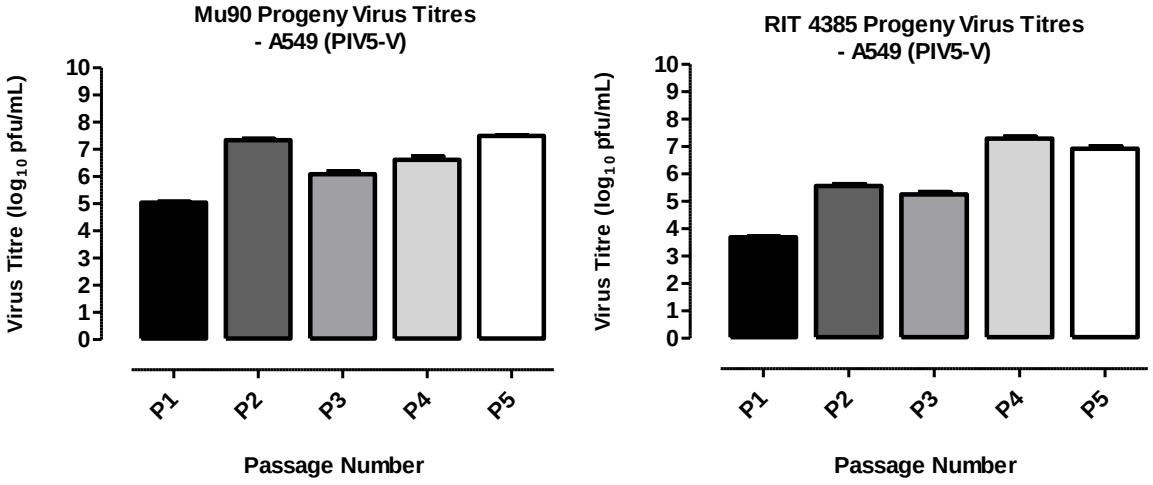

Figure 9 – Titres of Mu90 and RIT 4385 progeny viruses over 5 serial passages in A549 (PIV5-V) cells. Infection and titration details as per Figure 5.

Mu90 progeny virus titres increase from P1 (5.0 $\log_{10}$ pfu/mL) to P5 (7.5 $\log_{10}$ pfu/mL) with another peak at P2 (7.3 $\log_{10}$ pfu/mL). Titres of RIT 4385 progeny viruses increase from P1 (3.7 $\log_{10}$ pfu/mL) to P4 (7.3 $\log_{10}$ pfu/mL) and then decrease slightly at P5 (6.9 $\log_{10}$ pfu/mL).

Figure 10 demonstrates the plaque morphologies from P1 to P5 of Mu90 and RIT 4385 progeny viruses.

a) Mu90 plaque morphologies

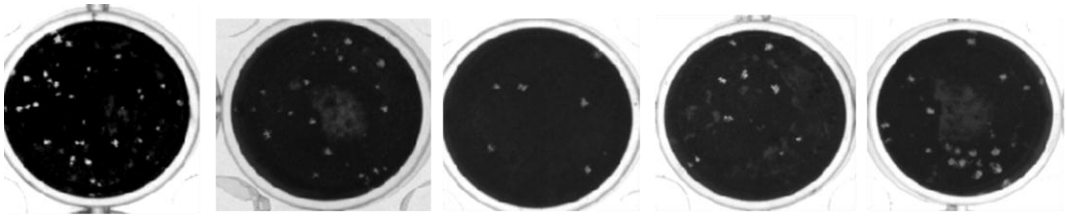

b) RIT 4385 plaque morphologies

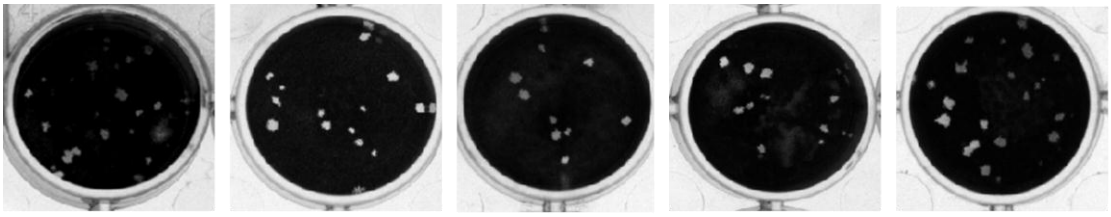

Figure 10 – Plaque morphologies of Mu90 (a) and RIT 4385 (b) progeny viruses over 5 serial passages in A549 (PIV5-V) cells. As per Figure 6.

Mu90 P1 plaques appear to contain a mixture of medium sized and smaller morphologies. The smaller plaques begin to decrease in number from P2 and are no longer evident by P5. RIT 4385 P1 plaques appear larger and more homogeneous, and this is maintained through the serial passages.

Results from the genetic stability studies in which N, F, HN and SH genes of parent and P5 viruses were sequenced and aligned are summarised in Table 14 as amino acid changes. Full nucleotide and amino acid alignments are detailed in appendices 1-8.

Table 14 – Amino acid substitutions in P5 progeny Mu90 and RIT 4385 virus proteins from A549 (PIV5-V) cells

Protein	Mu90	RIT 4385
Nucleoprotein (N)	N/A	I433T
		F451L
		V455A
		L457S
		V460A
		F468P
Fusion (F)	I536S	-539Q
Haemagglutinin-neuraminidase (HN)	T24A	S509N
	H94Y	V575C
	L576S	L576A
	T577N	A577S
	R578Q	R578Q
	L579I	L579I
	T580D	T580D
	I581Y	I581H
	T582H	T582H
	-583L (extra amino acid)	-583L (extra amino acid)
Small hydrophobic (SH)	F48L	N/A
	H50R	

N/A – not applicable, no substitutions

More mutations were present in the N protein of the P5 RIT 4385 progeny virus when compared to Mu90. The F protein of RIT 4385 P5 has an extra amino acid (position 539, glutamine) compared with

the parent and both Mu90 and RIT 4385 have nine amino acid substitutions in the HN protein. Some of these are present in both progeny virus HN proteins (R578Q, L579I, T580D and T582H) and both are also one amino acid (position 583, leucine) longer than their respective parental viruses.

3.2.4 CaCO2

P1 to P5 titres of Mu90 and RIT 4385 progeny viruses from CaCO2 (human colorectal adenocarcinoma) cells are shown in Figure 11.

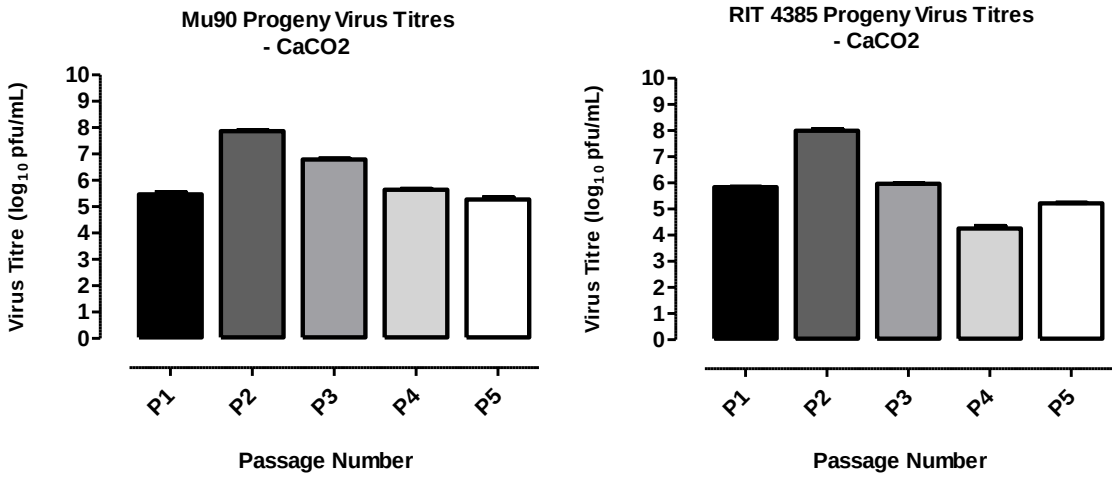

Figure 11 – Titres of Mu90 and RIT 4385 progeny viruses over 5 serial passages in CaCO2 cells.

Infection and titration details as per Figure 5.

Mu90 and RIT 4385 P1 to P5 progeny viruses from CaCO2 follow the same trend. The virus titres peak at P2 and then decrease from P3 to P5, with P5 titres being lower than P1. Mu90 titres range from a minimum of 5.3 $\log_{10}$ pfu/mL (P5) to 7.9 $\log_{10}$ pfu/mL (P2), and RIT 4385 titres from 4.3 $\log_{10}$ pfu/mL (P4) to a maximum of 8.0 $\log_{10}$ pfu/mL (P2).

Figure 12 demonstrates the plaque morphologies from P1 to P5 of Mu90 and RIT 4385 progeny viruses.

a) Mu90 plaque morphologies

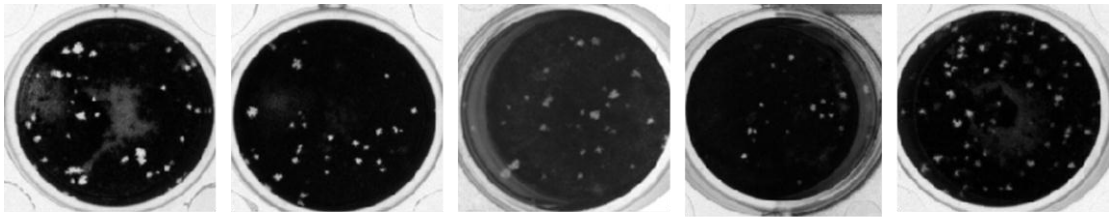

b) RIT 4385 plaque morphologies

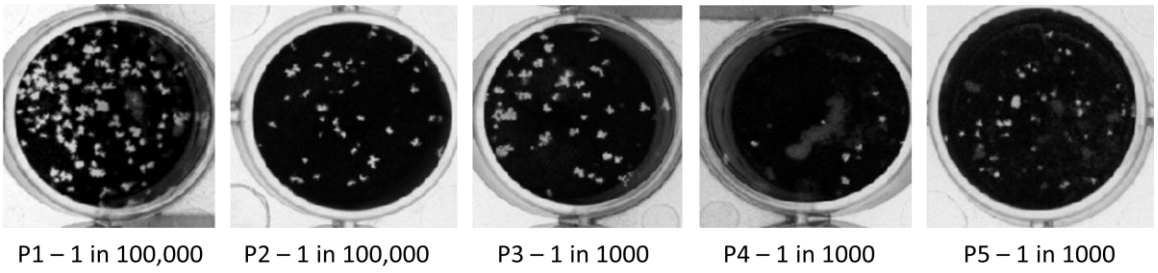

Figure 12 – Plaque morphologies of Mu90 (a) and RIT 4385 (b) progeny viruses over 5 serial passages in CaCO2 cells. As per Figure 6.

Mu90 P1 plaques appear to contain a mixture of medium sized and smaller morphologies, with the smaller plaques becoming the more dominant size by P5. RIT 4385 P1 plaques appear medium-sized with less smaller plaques however as for Mu90, the small plaque morphology is more dominant by P5.

Results from the genetic stability studies in which N, F, HN and SH genes of parent and P5 viruses were sequenced and aligned are summarised in Table 15 as amino acid changes. Full nucleotide and amino acid alignments are detailed in appendices 1-8.

Table 15 – Amino acid substitutions in P5 progeny Mu90 and RIT 4385 virus proteins from CaCO2 cells

Protein	Mu90	RIT 4385
Nucleoprotein (N)	N/A	F451L
Fusion (F)	R537T	I244T
Haemagglutinin-neuraminidase (HN)	T24A H94Y L576S T577N R578Q L579I T580D I581Y T582H -583L (extra amino acid)	N/A
Small hydrophobic (SH)	Q45H F48L H50R	N/A

N/A – not applicable, no substitutions

The RIT 4385 virus was relatively genetically stable when passaged through CaCO2 cells, compared to Mu90, with only one amino acid substitution in the N (F451L) and F (I244L) proteins. There were no substitutions in the HN or SH proteins. There were several substitutions in the HN protein of the P5 Mu90 virus, which resulted in it being one amino acid (position 583, leucine) longer than that of the parent.

3.2.5 Hep 2C

P1 to P5 titres of Mu90 progeny viruses from Hep 2C (human cervical carcinoma) cells are shown in Figure 13. These cells did not produce high enough titres of RIT 4385 progeny virus (> 3.3 log_{10} pfu/mL) at passage 1 to be investigated further with this MuV.

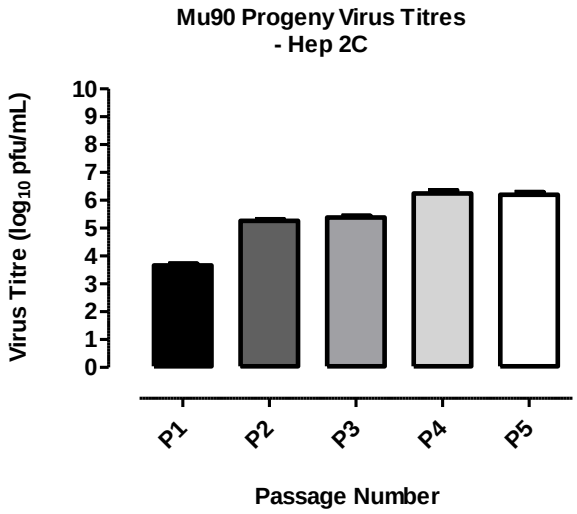

Figure 13 – Titres of Mu90 progeny viruses over 5 serial passages in Hep 2C cells. Infection and titration details as per Figure 5.

Mu90 progeny virus titres from Hep 2C cells increase steadily from P1 (3.7 log_{10} pfu/mL) to P5 (6.2 log_{10} pfu/mL).

Figure 14 demonstrates the plaque morphologies from P1 to P5 of Mu90 progeny viruses.

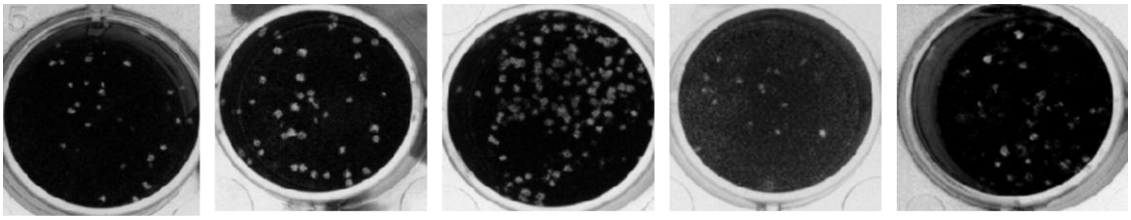

P1 – 1 in 10 P2 – 1 in 100 P3 – 1 in 100 P4 – 1 in 1000 P5 – 1 in 1000

Figure 14 – Plaque morphologies of Mu90 progeny viruses over 5 serial passages in Hep 2C cells. As per Figure 6.

Mu90 P1 plaques appear to be of a small, homogeneous population with larger morphologies present from P2 to P5.

Results from the genetic stability studies in which N, F, HN and SH genes of parent and P5 viruses were sequenced and aligned are summarised in Table 16 as amino acid changes. Full nucleotide and amino acid alignments are detailed in appendices 1-4.

Table 16 – Amino acid substitutions in P5 progeny Mu90 virus proteins from Hep 2C cells

Protein	Mu90
Nucleoprotein (N)	N/A
Fusion (F)	N/A
Haemagglutinin-neuraminidase (HN)	T24A
	H94Y
	L576S
	T577N
	R578Q
	L579I
	T580D
	I581Y
	T582H
	-583L (extra amino acid)

Small hydrophobic (SH)	F48L
	H50R

N/A – not applicable, no substitutions

There were no amino acid substitutions observed in N or F proteins from Mu90 P5 progeny virus from Hep 2C cells, however there were a total of nine in the HN protein, resulting in it being one amino acid (position 583, leucine) longer than that of the parent virus.

3.2.6 MCF-7

P1 to P5 titres of Mu90 progeny viruses from MCF-7 (human breast carcinoma) cells are shown in Figure 15. These cells did not produce high enough titres of RIT 4385 progeny virus (> 3.3 $\log_{10}$ pfu/mL) at P1 to be investigated further with this MuV.

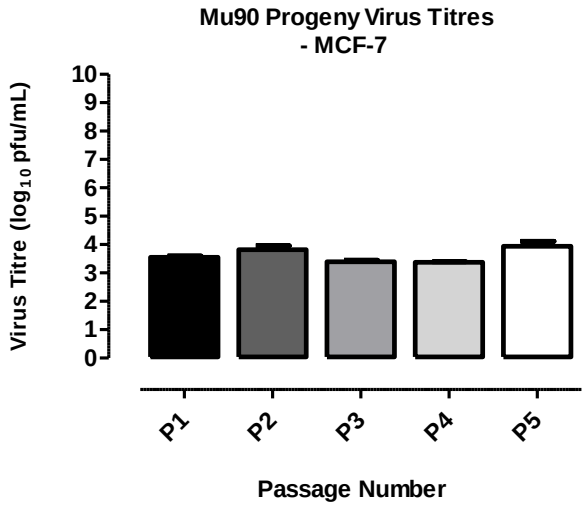

Figure 15 – Titres of Mu90 progeny viruses over 5 serial passages in MCF-7 cells. Infection and titration details as per Figure 5.

Mu90 progeny virus titre production from MCF-7 cells maintains a steady rate over P1 to P5, with only little variation. For example, the lowest titre was 3.4 log_{10} pfu/mL (P4) and the highest 3.9 log_{10} pfu/mL (P5).

Figure 16 demonstrates the plaque morphologies from P1 to P5 of Mu90 progeny viruses.

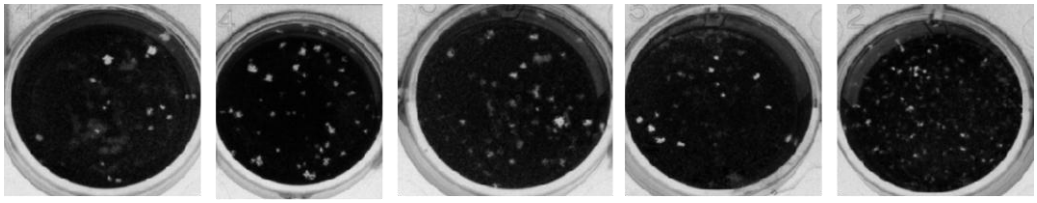

Figure 16 – Plaque morphologies of Mu90 progeny viruses over 5 serial passages in MCF-7 cells. As per Figure 6.

Mu90 P1 plaques appear to contain a mixture of medium sized and smaller morphologies, with the smaller plaques becoming the more dominant size by P5.

Results from the genetic stability studies in which N, F, HN and SH genes of parent and P5 viruses were sequenced and aligned are summarised in Table 17 as amino acid changes. Full nucleotide and amino acid alignments are detailed in appendices 1-4.

Table 17 – Amino acid substitutions in P5 progeny Mu90 virus proteins from MCF-7 cells

Protein	Mu90
Nucleoprotein (N)	G264R
Fusion (F)	A3D F4I I221M
Haemagglutinin-neuraminidase (HN)	T24A

	H94Y
	V575F
Small hydrophobic (SH)	F48L
	H50R

Amino acid substitutions were present in all four proteins investigated in these experiments.

3.2.7 PANC-1

P1 to P5 titres of Mu90 progeny viruses from PANC-1 (human pancreatic carcinoma) cells are shown in Figure 17. These cells did not produce high enough titres of RIT 4385 progeny virus (> 3.3 log_{10} pfu/mL) at P1 to be investigated further with this MuV.

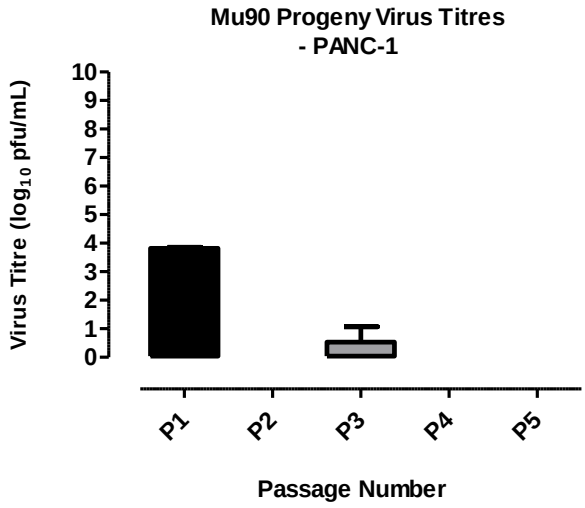

Figure 17 – Titres of Mu90 progeny viruses over 5 serial passages in PANC-1 cells. Infection and titration details as per Figure 5.

Mu90 progeny virus was only detected by plaque assay at passage levels 1 and 3, with the virus titres being 3.8 log_{10} pfu/mL and 0.5 log_{10} pfu/mL respectively.

Figure 18 demonstrates the plaque morphologies of P1 and P3 Mu90 progeny viruses.

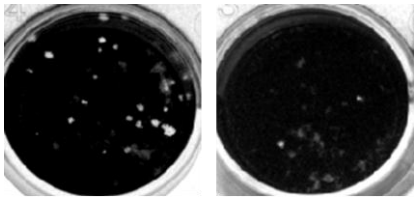

Figure 18 – Plaque morphologies of Mu90 progeny viruses from P1 and P3 in PANC-1 cells. As per Figure 6

Mu90 P1 plaques appear to contain a mixture of medium sized and smaller morphologies, with only small plaques present at P3.

Due to the fact that there was only infectious progeny virus production at passages 1 and 3, no P5 genetic stability studies were carried out using PANC-1 cells.

3.2.8 HGT-1

P1 to P5 titres of Mu90 progeny viruses from HGT-1 (human stomach carcinoma) cells are shown in Figure 19. These cells did not produce high enough titres of RIT 4385 progeny virus (> 3.3 $\log_{10}$ pfu/mL) at P1 to be investigated further with this MuV.

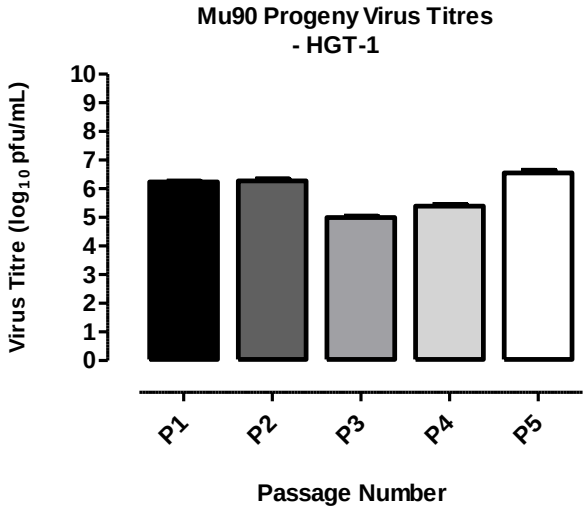

Figure 19 – Titres of Mu90 progeny viruses over 5 serial passages in HGT-1 cells. Infection and titration details as per Figure 5.

HGT-1 was the only cell line to produce higher titres of P1 progeny virus than the "gold standard" Vero cells. (6.0 $\log_{10}$ pfu/mL and 5.8 $\log_{10}$ pfu/mL respectively). HGT-1 Mu90 titres decrease at P3 (5.0 $\log_{10}$ pfu/mL) and then increase steadily to peak at P5 (6.6 $\log_{10}$ pfu/mL).

Figure 20 demonstrates the plaque morphologies from P1 to P5 of Mu90 progeny viruses.

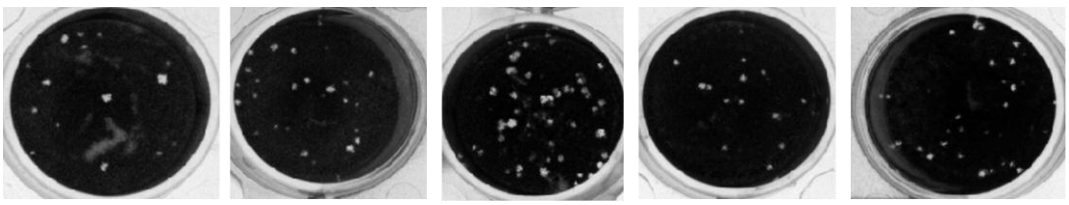

Figure 20 – Plaque morphologies of Mu90 progeny viruses over 5 serial passages in HGT-1 cells. As per Figure 6.

Mu90 P1 plaques appear to contain a mixture of medium sized and smaller morphologies, with the smaller plaques becoming the more dominant size by P5.

Results from the genetic stability studies in which N, F, HN and SH genes of parent and P5 viruses were sequenced and aligned are summarised in Table 18 as amino acid changes. Full nucleotide and amino acid alignments are detailed in appendices 1-4.

Table 18 – Amino acid substitutions in P5 progeny Mu90 virus proteins from HGT-1 cells

Protein	**Mu90**
Nucleoprotein (N)	N/A
Fusion (F)	R537T Y538H
Haemagglutinin-neuraminidase (HN)	T24A
Small hydrophobic (SH)	F48L H50R

N/A – not applicable, no substitutions

No amino acid substitutions were observed in the N protein, and overall, a total of five substitutions were observed in the four proteins investigated. This low number indicates that the Mu90 MuV is relatively genetically stable under serial passage in HGT-1 cells.

3.2.9 RD

P1 to P5 titres of Mu90 progeny viruses from RD (human muscle rhabdomyosarcoma) cells are shown in Figure 21. These cells did not produce high enough titres of RIT 4385 progeny virus (> 3.3 $\log_{10}$ pfu/mL) at P1 to be investigated further with this MuV.

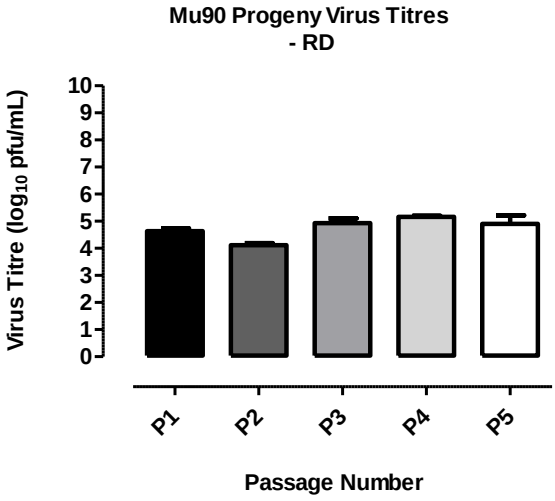

Figure 21 – Titres of Mu90 progeny viruses over 5 serial passages in RD cells. Infection and titration details as per Figure 5.

Mu90 progeny viruses from RD cells maintained steady titres throughout the serial passages, with the lowest recorded as 4.1 $\log_{10}$ pfu/mL (P2) and the highest 5.2 $\log_{10}$ pfu/mL (P4).

Figure 22 demonstrates the plaque morphologies from P1 to P5 of Mu90 progeny viruses.

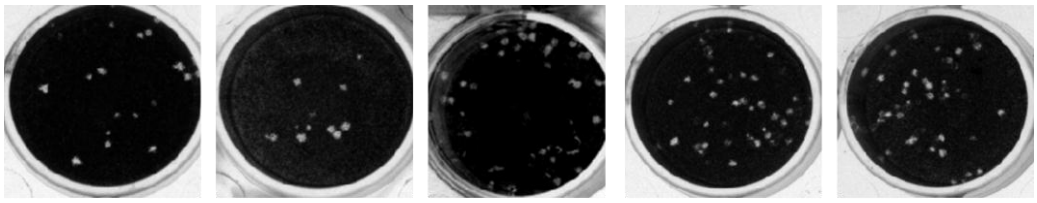

Figure 22 – Plaque morphologies of Mu90 progeny viruses over 5 serial passages in RD cells. As per Figure 6.

Mu90 P1 plaques appear to contain a mixture of medium sized and smaller morphologies, with the smaller plaques becoming the more dominant size by P5.

Results from the genetic stability studies in which N, F, HN and SH genes of parent and P5 viruses were sequenced and aligned are summarised in Table 19 as amino acid changes. Full nucleotide and amino acid alignments are detailed in appendices 1-4.

Table 19 – Amino acid substitutions in P5 progeny Mu90 virus proteins from RD cells

Protein	**Mu90**
Nucleoprotein (N)	N/A
Fusion (F)	I221M
	R537T
Haemagglutinin-neuraminidase (HN)	T24A
	H94Y
	N142K
	L576S
	T577N
	R578Q
	L579I
	T580D
	I581Y
	T582H
	-583L (extra amino acid)
Small hydrophobic (SH)	F48L
	H50R

Amino acid substitutions were present three out of four proteins investigated in these experiments with none present in the nucleoprotein. There are a total of eleven amino acid substitutions in the P5 Mu90 HN protein, making it one amino acid (position 583, leucine) longer than the parent.

3.2.10 BSC-1

P1 to P5 titres of Mu90 progeny viruses from BSC-1 (African Green Monkey kidney) cells are shown in Figure 23. These cells did not produce high enough titres of RIT 4385 progeny virus (> 3.3 log_{10} pfu/mL) at P1 to be investigated further with this MuV.

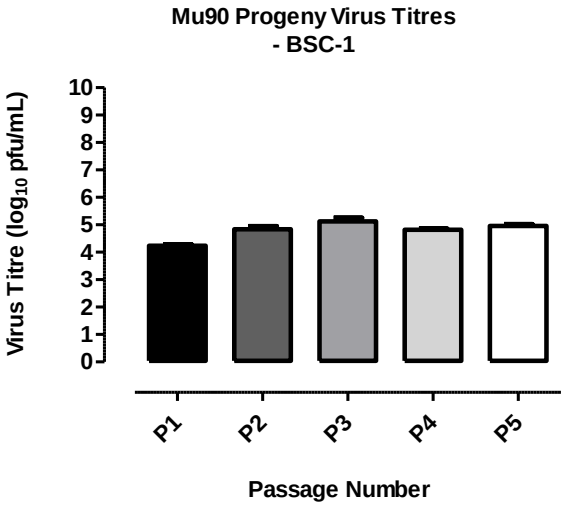

Figure 23 – Titres of Mu90 progeny viruses over 5 serial passages in BSC-1 cells. Infection and titration details as per Figure 5.

Mu90 progeny viruses from BSC-1 cells maintained steady titres throughout the serial passages, with the lowest recorded as 4.2 log_{10} pfu/mL (P1) and the highest 5.1 log_{10} pfu/mL (P3).

Figure 24 demonstrates the plaque morphologies from P1 to P5 of Mu90 progeny viruses.

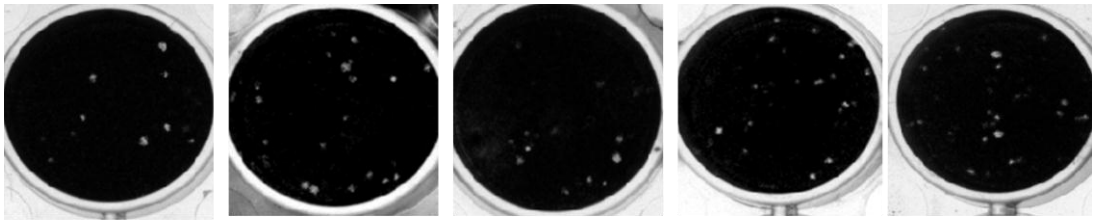

Figure 24 – Plaque morphologies of Mu90 progeny viruses over 5 serial passages in BSC-1 cells. As per Figure 6.

Mu90 P1 plaques appear to contain a mixture of medium sized and smaller morphologies, which is maintained throughout the five serial passages.

Results from the genetic stability studies in which N, F, HN and SH genes of parent and P5 viruses were sequenced and aligned are summarised in Table 20 as amino acid changes. Full nucleotide and amino acid alignments are detailed in appendices 1-4.

Table 20 – Amino acid substitutions in P5 progeny Mu90 virus proteins from BSC-1 cells

Protein	Mu90
Nucleoprotein (N)	E235K
	G264S
Fusion (F)	I536H
	R537Q
	Y538V
	-539L (extra amino acid)
Haemagglutinin-neuraminidase (HN)	T24A
	N142K
	L576S
	T577N
	R578Q

	L579I
	T580D
	I581Y
	T582H
	-583L (extra amino acid)
Small hydrophobic (SH)	F48L
	H50R

Amino acid substitutions were present in all four proteins investigated in these experiments. F and HN proteins of the P5 progeny virus were one amino acid (position 539, leucine and position 583, leucine, respectively) longer when compared with the parent virus.

3.2.11 COS-7

P1 to P5 titres of Mu90 and RIT 4385 progeny viruses from COS-7 (African Green Monkey kidney, SV-40 transformed) cells are shown in Figure 25.

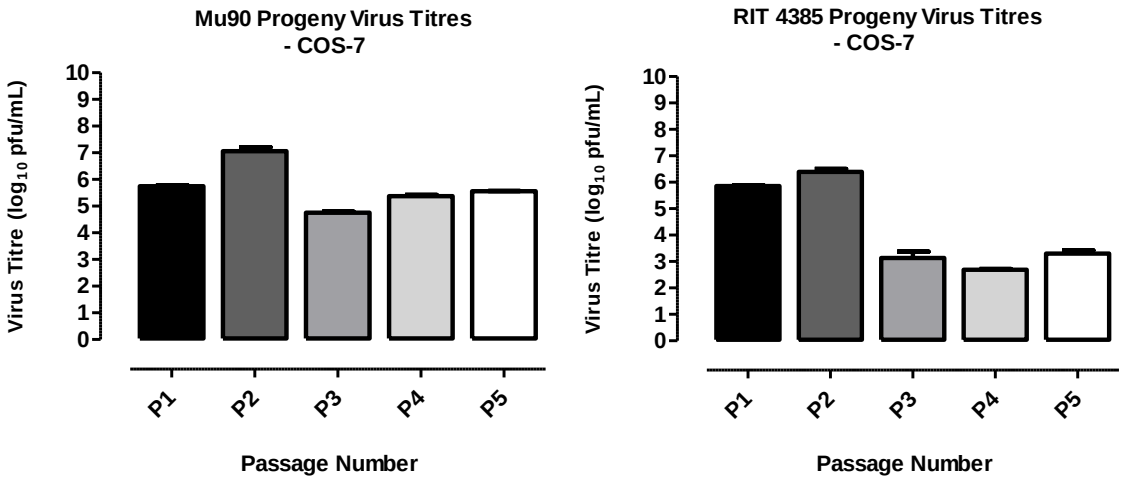

Figure 25 – Titres of Mu90 and RIT 4385 progeny viruses over 5 serial passages in COS-7 cells.

Infection and titration details as per Figure 5.

Mu90 and RIT 4385 P1 to P5 progeny viruses from COS-7 cells follow the same trend. The virus titres peak at P2 and then decrease at P3, before increasing again at P5, with P5 titres being lower than P1. Mu90 titres range from a minimum of 4.8 $\log_{10}$ pfu/mL (P3) to a maximum of 7.1 $\log_{10}$ pfu/mL (P2), and RIT 4385 titres from 2.7 $\log_{10}$ pfu/mL (P4) to 6.4 $\log_{10}$ pfu/mL (P2).

Figure 26 demonstrates the plaque morphologies from P1 to P5 of Mu90 and RIT 4385 progeny viruses.

a) Mu90 plaque morphologies

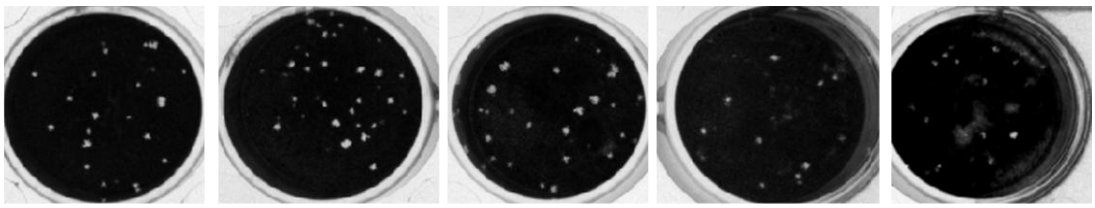

b) RIT 4385 plaque morphologies

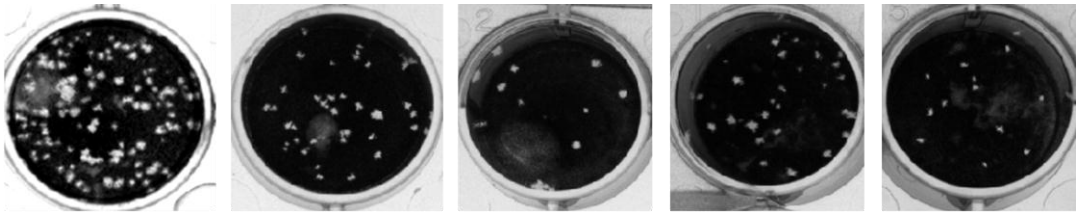

Figure 26 – Plaque morphologies of Mu90 (a) and RIT 4385 (b) progeny viruses over 5 serial passages in COS-7 cells. As per Figure 6.

Mu90 P1 plaques appear to contain a mixture of medium sized and smaller morphologies, with the smaller plaques becoming the more dominant size by P5. RIT 4385 P1 plaques are medium-sized

with fewer small plaques evident however as for Mu90, the small plaque morphology is more dominant by P5.

Results from the genetic stability studies in which N, F, HN and SH genes of parent and P5 viruses were sequenced and aligned are summarised in Table 21 as amino acid changes. Full nucleotide and amino acid alignments are detailed in appendices 1-8.

Table 21 – Amino acid substitutions in P5 progeny Mu90 and RIT 4385 virus proteins from COS-7 cells

Protein	Mu90	RIT 4385
Nucleoprotein (N)	N/A	S264L G265R R513Q E516K
Fusion (F)	Q268L	I244T -539R (extra amino acid)
Haemagglutinin-neuraminidase (HN)	T24A H94Y L576S T577N R578Q L579I T580D I581Y T582H -583L (extra amino acid)	N/A
Small hydrophobic (SH)	K35N A42S F48L H50R	N/A

N/A – not applicable, no substitutions

Although the F protein of P5 RIT 4385 progeny MuV is one amino acid (position 539, arginine) longer than the parent and there are four amino acid substitutions in the N protein, RIT 4385 appears to be more genetically stable during serial passage in COS-7 cells compare to Mu90. There are a total of nine amino acid substitutions in the P5 Mu90 HN protein, making it one amino acid (position 583, leucine) longer than the parent.

3.2.12 LLC-MK2

P1 to P5 titres of Mu90 progeny viruses from LLC-MK2 (Rhesus Monkey kidney) cells are shown in Figure 27. These cells did not produce high enough titres of RIT 4385 progeny virus (> 3.3 $\log_{10}$ pfu/mL) at P1 to be investigated further with this MuV.

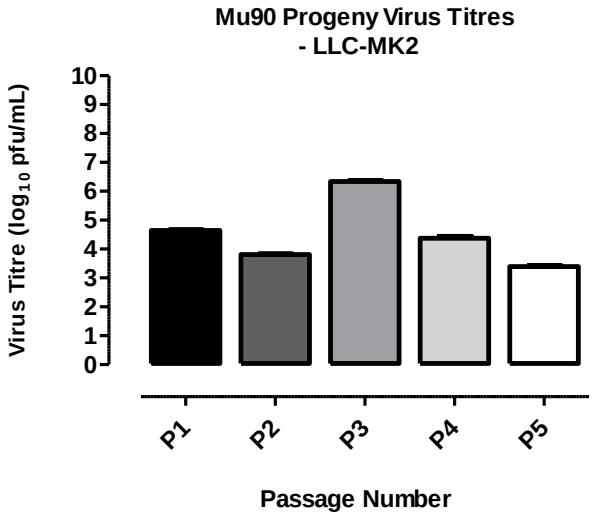

Figure 27 – Titres of Mu90 progeny viruses over 5 serial passages in LLC-MK2 cells. Infection and titration details as per Figure 5.

Titres of Mu90 progeny MuV from LLC-MK2 cells do not increase or decrease at a steady rate over 5 serial passages. The lowest titres were recorded at P5 (3.4 log_{10} pfu/mL) and the highest at P3 (6.3 log_{10} pfu/mL).

Figure 28 demonstrates the plaque morphologies from P1 to P5 of Mu90 progeny viruses.

Figure 28 – Plaque morphologies of Mu90 progeny viruses over 5 serial passages in LLC-MK2 cells.

As per Figure 6.

Mu90 P1 plaques appear to contain a mixture of medium sized and smaller morphologies, which is maintained throughout serial passage to P5.

Results from the genetic stability studies in which N, F, HN and SH genes of parent and P5 viruses were sequenced and aligned are summarised in Table 22 as amino acid changes. Full nucleotide and amino acid alignments are detailed in appendices 1-4.

Table 22 – Amino acid substitutions in P5 progeny Mu90 virus proteins from LLC-MK2 cells

Protein	**Mu90**
Nucleoprotein (N)	N/A
Fusion (F)	A3D F4I

Haemagglutinin-neuraminidase (HN)	T24A
	L576S
	T577N
	R578Q
	L579I
	T580D
	I581Y
	T582H
	-583L (extra amino acid)
Small hydrophobic (SH)	F48L
	H50R

Amino acid substitutions were present in three out of four proteins investigated in these experiments with none present in the N protein. The HN protein of the P5 progeny virus was one amino acid (position 583, leucine) longer when compared with the parent virus.

3.2.13 MA-104

P1 to P5 titres of Mu90 and RIT 4385 progeny viruses from MA-104 (foetal Rhesus Monkey kidney) cells are shown in Figure 29.

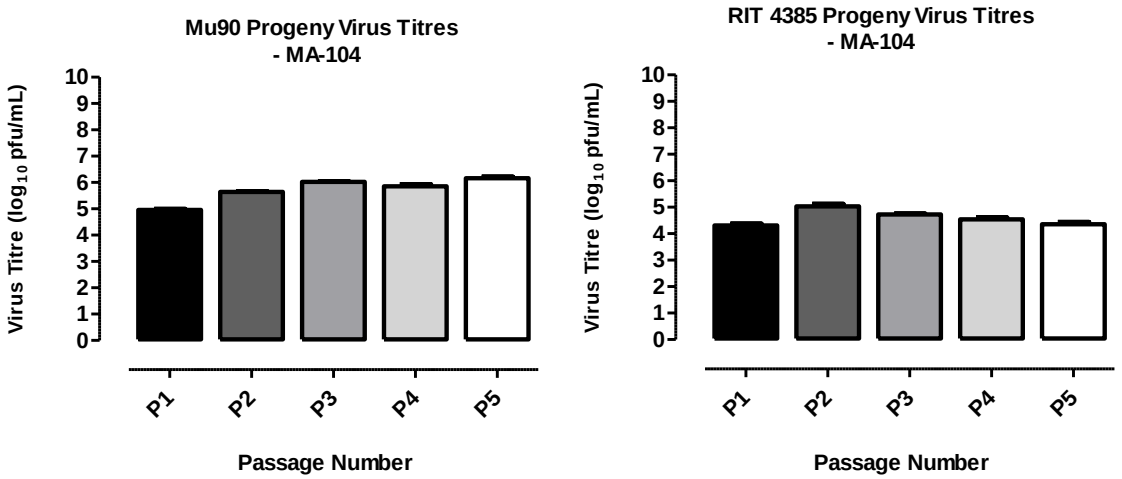

Figure 29 – Titres of Mu90 and RIT 4385 progeny viruses over 5 serial passages in MA-104 cells.

Infection and titration details as per Figure 5.

Mu90 progeny viruses from MA-104 cells increase in titre steadily from P1 (5.0 $\log_{10}$ pfu/mL) to P5 (6.2 $\log_{10}$ pfu/mL) with a slight decrease from P3 to P4 (6.0 $\log_{10}$ pfu/mL and 5.9 $\log_{10}$ pfu/mL respectively). RIT 4385 progeny virus titres maintain a steady rate with a slight peak at P2 (5.0 $\log_{10}$ pfu/mL) and a minimum titre of 4.5 $\log_{10}$ pfu/mL at P1.

Figure 30 demonstrates the plaque morphologies from P1 to P5 of Mu90 and RIT 4385 progeny viruses.

a) Mu90 plaque morphologies

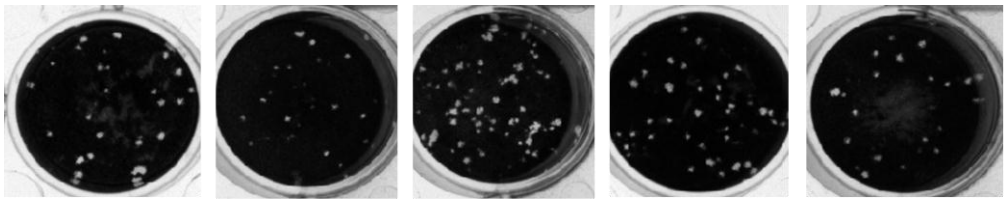

b) RIT 4385 plaque morphologies

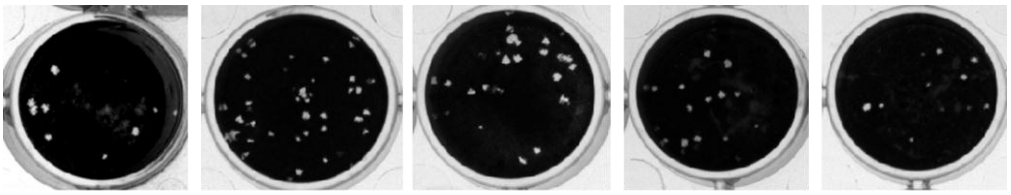

Figure 30 – Plaque morphologies of Mu90 (a) and RIT 4385 (b) progeny viruses over 5 serial passages in MA-104 cells. As per Figure 6.

Mu90 P1 plaques appear to contain a mixture of medium sized and smaller morphologies, with the smaller plaques becoming the more dominant size by P5. RIT 4385 P1 plaques are medium-sized with fewer small plaques evident however as for Mu90, the small plaque morphology is more dominant by P5.

Results from the genetic stability studies in which N, F, HN and SH genes of parent and P5 viruses were sequenced and aligned are summarised in Table 23 as amino acid changes. Full nucleotide and amino acid alignments are detailed in appendices 1-8.

Table 23 – Amino acid substitutions in P5 progeny Mu90 and RIT 4385 virus proteins from MA-104 cells

Protein	Mu90	RIT 4385
Nucleoprotein (N)	N/A	N/A
Fusion (F)	R381Q	I244T
	C505L	R537S
	C506L	Y538R
	W507L	
	A508G	
	Y509L	
	I510V	
	A511C	
	T512N	
Haemagglutinin-neuraminidase (HN)	T24A	Y152C
	L576S	S553G
	T577N	I566M
	R578Q	
	L579I	
	T580D	
	I581Y	
	T582H	
	-583L (extra amino acid)	
Small hydrophobic (SH)	F48L	N/A
	H50R	

N/A – not applicable, no substitutions

Although there are three amino acid substitutions in both the F and HN proteins of the P5 progeny virus from MA-104 cells, RIT 4385 appears to be more genetically stable during serial passage compared to Mu90. There are a total of nine amino acid substitutions in the P5 Mu90 HN protein, making it one amino acid (position 583, leucine) longer than the parent. There are also nine substitutions in the F protein and it is 26 amino acids shorter than the parent virus protein. There are no alterations in the N protein.

3.2.14 B95a

P1 to P5 titres of Mu90 progeny viruses from B95a (Marmoset lymphoblast) cells are shown in Figure 31. These cells did not produce high enough titres of RIT 4385 progeny virus (> 3.3 log_{10} pfu/mL) at P1 to be investigated further with this MuV.

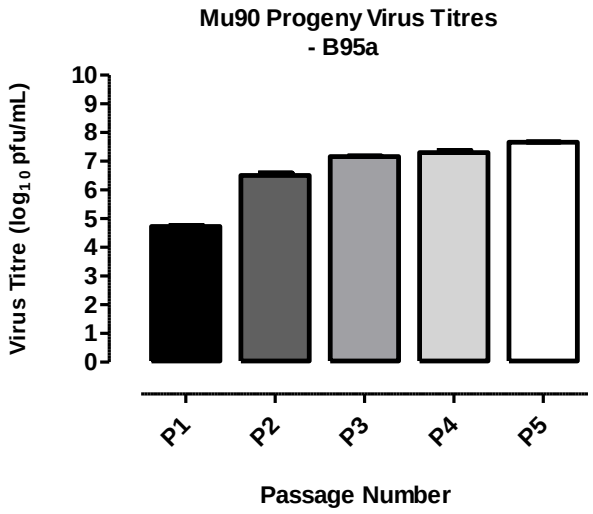

Figure 31 – Titres of Mu90 progeny viruses over 5 serial passages in B95a cells. Infection and titration details as per Figure 5.

Mu90 progeny viruses from B95a cells increase steadily in titre from P1 (4.7 log_{10} pfu/mL) to P5 (7.7 log_{10} pfu/mL).

Figure 32 demonstrates the plaque morphologies from P1 to P5 of Mu90 progeny viruses.

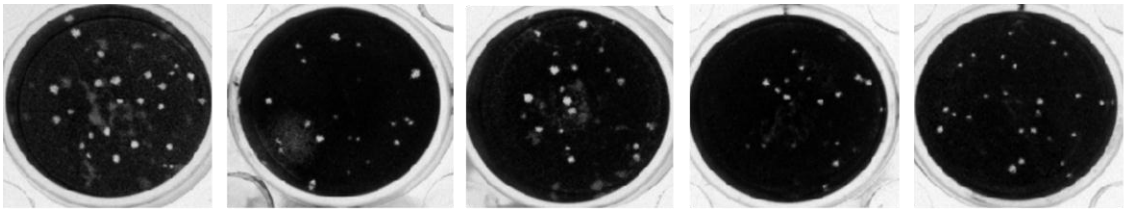

P1 – 1 in 100 P2 – 1 in 10,000 P3 – 1 in 10,000 P4 – 1 in 10,000 P5 – 1 in 100,000

Figure 32 – Plaque morphologies of Mu90 progeny viruses over 5 serial passages in B95a cells. As per Figure 6.

Mu90 P1 plaques appear to contain a mixture of medium sized and smaller morphologies, with the smaller plaques becoming the more dominant size from P2 to P5.

Results from the genetic stability studies in which N, F, HN and SH genes of parent and P5 viruses were sequenced and aligned are summarised in Table 24 as amino acid changes. Full nucleotide and amino acid alignments are detailed in appendices 1-4.

Table 24 – Amino acid substitutions in P5 progeny Mu90 virus proteins from B95a cells

Protein	Mu90
Nucleoprotein (N)	F481L
Fusion (F)	A3D
	F4I
	T7N
	A12V
	I18K
	F420L
Haemagglutinin-neuraminidase (HN)	T24A
	L576S
	T577N
	R578Q

	L579I
	T580D
	I581Y
	T582H
	-583L (extra amino acid)
Small hydrophobic (SH)	F48L
	H50R

There are a total of nine amino acid substitutions in the P5 Mu90 HN protein, making it one amino acid (position 583, leucine) longer than the parent. The N, F and SH proteins all contain a single phenylalanine (F) to leucine (L) substitution.

3.2.15 BHK-21

P1 to P5 titres of Mu90 progeny viruses from BHK-21 (Syrian Hamster kidney) cells are shown in Figure33. These cells did not produce high enough titres of RIT 4385 progeny virus (> 3.3 $\log_{10}$ pfu/mL) at P1 to be investigated further with this MuV.

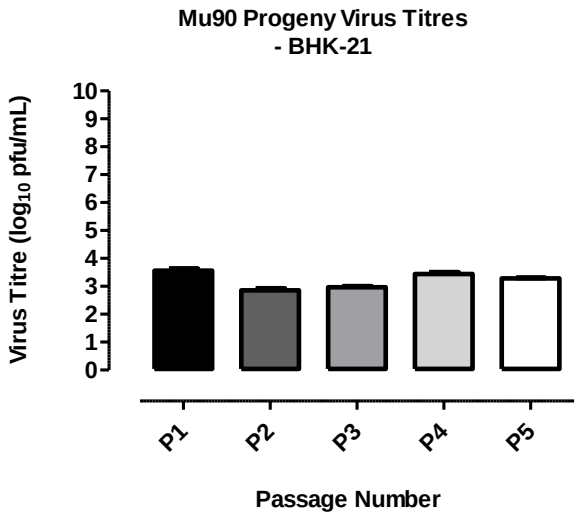

Figure 33 – Titres of Mu90 progeny viruses over 5 serial passages in BHK-21 cells. Infection and titration details as per Figure 5.

Titres of Mu90 progeny virus from BHK-21 cells are at a maximum at P1 (3.6 log_{10} pfu/mL) before decreasing at P2 (2.9 log_{10} pfu/mL) and then increasing to titres of 3.4 log_{10} pfu/mL and 3.3 log_{10} pfu/mL at P4 and P5 respectively.

Figure 34 demonstrates the plaque morphologies from P1 to P5 of Mu90 progeny viruses.

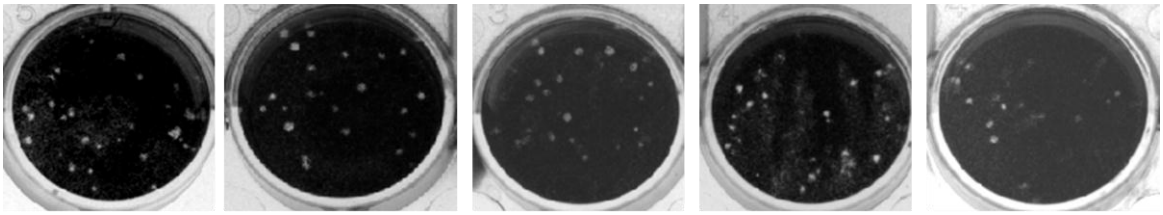

Figure 34 – Plaque morphologies of Mu90 progeny viruses over 5 serial passages in BHK-21 cells.

As per Figure 6.

Mu90 P1 plaques appear to contain a mixture of medium sized and smaller morphologies, which is maintained through to P5.

Results from the genetic stability studies in which N, F, HN and SH genes of parent and P5 viruses were sequenced and aligned are summarised in Table 25 as amino acid changes. Full nucleotide and amino acid alignments are detailed in appendices 1-4.

Table 25 – Amino acid substitutions in P5 progeny Mu90 virus proteins from BHK-21 cells

Protein	Mu90
Nucleoprotein (N)	G264R
Fusion (F)	N/A
Haemagglutinin-neuraminidase (HN)	T24A
	H94Y
	L576S
	T577N
	R578Q
	L579I
	T580D
	I581Y
	T582H
	-583L (extra amino acid)
Small hydrophobic (SH)	F48L
	H50R

N/A – not applicable, no substitutions

There are a total of nine amino acid substitutions in the P5 Mu90 HN protein, making it one amino acid (position 583, leucine) longer than the parent. There are no substitutions in the F protein.

3.2.16 JH4 Clone 1

P1 to P5 titres of Mu90 progeny viruses from JH4 Clone 1 (Guinea Pig lung) cells are shown in Figure 35. These cells did not produce high enough titres of RIT 4385 progeny virus (> 3.3 $\log_{10}$ pfu/mL) at P1 to be investigated further with this MuV.

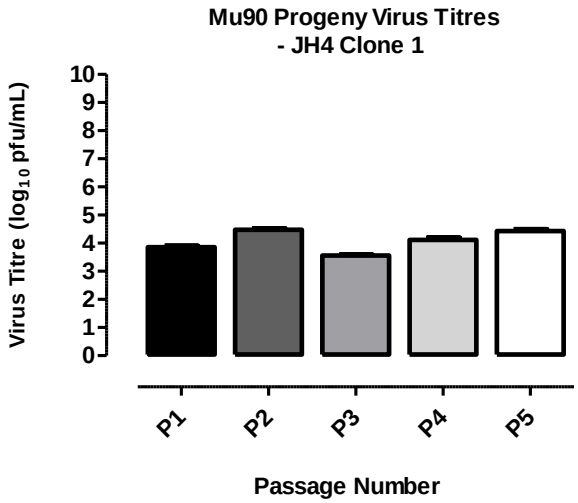

Figure 35 – Titres of Mu90 progeny viruses over 5 serial passages in JH4 Clone 1 cells. Infection and titration details as per Figure 5.

Titres of Mu90 progeny virus from JH4 Clone 1 cells increase from P1 to P2 (4.5 $\log_{10}$ pfu/mL) before decreasing at P3 (3.6 $\log_{10}$ pfu/mL) and then increasing to titres of 4.1 $\log_{10}$ pfu/mL and 4.4 $\log_{10}$ pfu/mL at P4 and P5 respectively.

Figure 36 demonstrates the plaque morphologies from P1 to P5 of Mu90 progeny viruses.

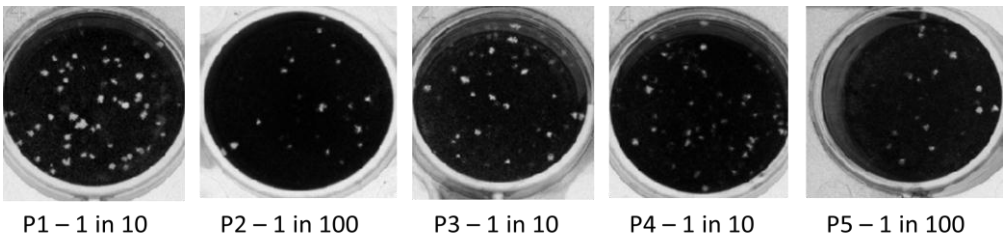

Figure 36 – Plaque morphologies of Mu90 progeny viruses over 5 serial passages in JH4 Clone 1 cells. As per Figure 6.

Mu90 P1 plaques appear to contain a mixture of medium sized and smaller morphologies, which is maintained through to P5.

Results from the genetic stability studies in which N, F, HN and SH genes of parent and P5 viruses were sequenced and aligned are summarised in Table 26 as amino acid changes. Full nucleotide and amino acid alignments are detailed in appendices 1-4.

Table 26 – Amino acid substitutions in P5 progeny Mu90 virus proteins from JH4 Clone 1 cells

Protein	**Mu90**
Nucleoprotein (N)	N/A
Fusion (F)	L535F
Haemagglutinin-neuraminidase (HN)	T24A
	L576S
	T577N
	R578Q
	L579I
	T580D
	I581Y
	T582H
	-583L (extra amino acid)
Small hydrophobic (SH)	F48L
	H50R

N/A – not applicable, no substitutions

There are a total of nine amino acid substitutions in the P5 Mu90 HN protein, making it one amino acid (position 583, leucine) longer than the parent.

3.2.17 MDCK

P1 to P5 titres of Mu90 and RIT 4385 progeny viruses from MDCK (canine kidney) cells are shown in Figure 37.

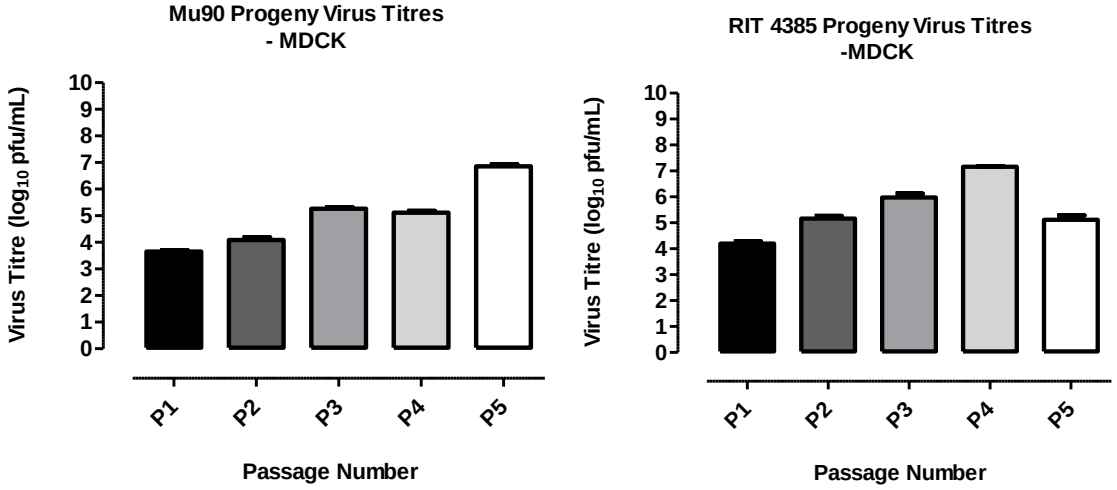

Figure 37 – Titres of Mu90 and RIT 4385 progeny viruses over 5 serial passages in MDCK cells.

Infection and titration details as per Figure 5.

Mu90 progeny viruses from MDCK cells increase in titre steadily from P1 (3.7 $\log_{10}$ pfu/mL) to P5 (6.9 $\log_{10}$ pfu/mL) with a slight decrease from P3 to P4 (5.3 $\log_{10}$ pfu/mL and 5.1 $\log_{10}$ pfu/mL respectively). RIT 4385 progeny virus titres increase a steady rate from P1 4.2 $\log_{10}$ pfu/mL) to P4 (7.2 $\log_{10}$ pfu/mL) and then decrease to 5.1 $\log_{10}$ pfu/mL at P5.

Figure 38 demonstrates the plaque morphologies from P1 to P5 of Mu90 and RIT 4385 progeny viruses.

a) Mu90 plaque morphologies

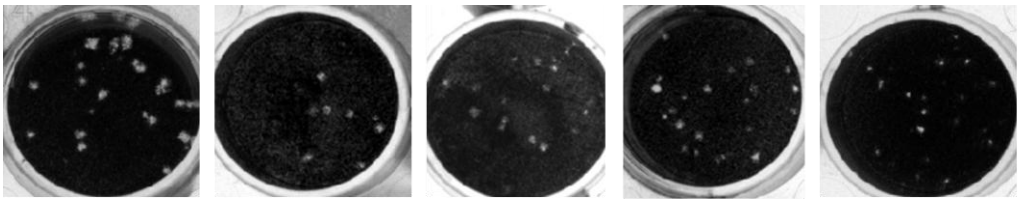

P1 – 1 in 10 P2 – 1 in 100 P3 – 1 in 1000 P4 – 1 in 100 P5 – 1 in 10,000

b) RIT 4385 plaque morphologies

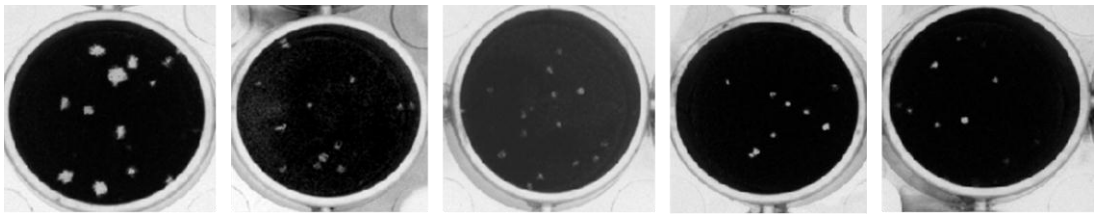

P1 – 1 in 100 P2 – 1 in 1000 P3 – 1 in 1000 P4 – 1 in 10,000 P5 – 1 in 1000

Figure 38 – Plaque morphologies of Mu90 (a) and RIT 4385 (b) progeny viruses over 5 serial passages in MDCK cells. As per Figure 6.

Mu90 P1 plaques appear to contain a mixture of medium sized and smaller morphologies, with the smaller plaques becoming the more dominant size by P5. RIT 4385 P1 plaques are heterogeneous and contain large, medium and small morphologies, however as for Mu90, the small plaque morphology is more dominant by P5.

Results from the genetic stability studies in which N, F, HN and SH genes of parent and P5 viruses were sequenced and aligned are summarised in Table 27 as amino acid changes. Full nucleotide and amino acid alignments are detailed in appendices 1-8.

Table 27 – Amino acid substitutions in P5 progeny Mu90 and RIT 4385 virus proteins from MDCK cells

Protein	Mu90	RIT 4385
Nucleoprotein (N)	N/A	N/A
Fusion (F)	I536L	I244T
Haemagglutinin-neuraminidase (HN)	T24A L576S T577N R578Q L579I T580D I581Y T582H -583L (extra amino acid)	N/A
Small hydrophobic (SH)	F48L H50R	N/A

N/A – not applicable, no substitutions

There are a total of nine amino acid substitutions in the MDCK P5 Mu90 HN protein, making it one amino acid (position 583, leucine) longer than the parent. No amino acid substitutions were evident in the N, HN and SH RIT 4385 MDCK P5 progeny virus proteins, and there was only one (I244T) in the F protein indicating that the virus is highly genetically stable when undergoing serial passage in MDCK cells.

3.3 Assessment of Plaque Formation on Various Cell Lines

Plaque assays were performed directly on each of the "successful" cell lines (section 3.2.2, Table 11) using the parent Mu90 virus (MOI 0.001) in order to determine whether or not they were able to support MuV plaque formation. These assays were performed in triplicate in order to obtain a mean plaque count to determine how sensitive each cell line was. All mock-infected controls were valid.

From the 17 cell lines investigated, 6 were capable of supporting plaque formation. These cells were Vero, A549 (BVDV), A549 (PIV5-V), LtK-, L20B and LLC-MK2, and are shown in Figure 39.

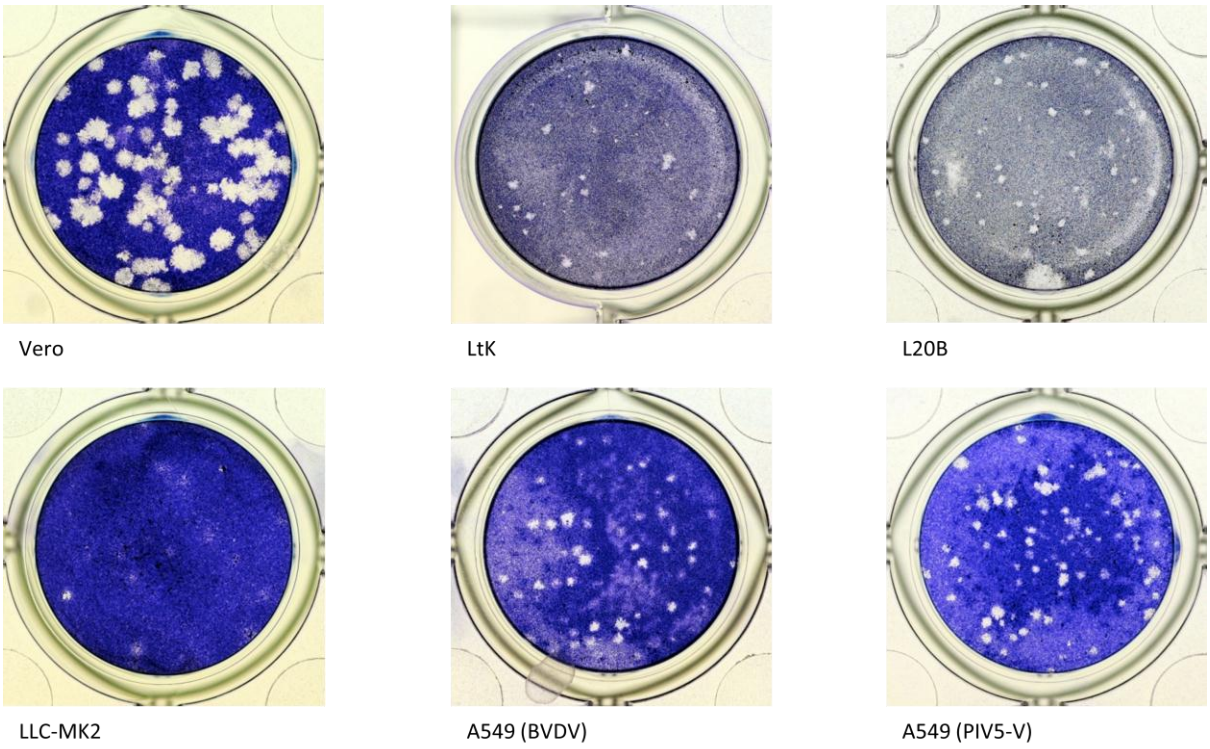

Figure 39 – Plaques formed by Mu90 on Vero, LtK-, L20B, LLC-MK2, A549 (BVDV) and A549 (PIV5-V) cells. Cells were infected with MuV Mu90 at an MOI of 0.001 pfu per cell in triplicate and incubated for 10 days before staining with methyl violet. Images are of a 1 in 100 virus dilution at day 10 post infection.

With regards to the other cell lines included in these experiments, some did not form confluent monolayers (CaCO2, B95a, HGT-1, PANC-1, MCF-7, RD, and Hep 2C) and those that did form confluent monolayers showed no evident plaques (COS-7, MA-104, JH4 Clone 1, BHK-21, BSC-1 and MDCK). LtK and L20B cells demonstrated similar plaque morphology and “faded” stain appearance, both with smaller and more circular plaques than the Vero control, and both types of A549 cells also

had similar plaque morphologies to one another. The plaques exhibited by these cells are alike in shape to the Vero control, however smaller in size.

Table 28 – Mean plaque counts from cell lines (Figure 39)

Cell Line	Mean Number of Plaques
Vero	63
A549 (BVDV)	40
A549 (PIV5-V)	61
L20B	42
LtK-	30
LLC-MK2	1.7

From Table 28, A549 (PIV5-V) cells are the only ones to be as sensitive for plaque formation as the Vero control. Although still able to form plaques, A549 (BVDV), L20B and LtK- cells appear to be less sensitive and LLC-MK2 cells formed only 1 to 2 plaques in each of the triplicate wells.

3.4 Sialic Acid Investigations

3.4.1 Sialic Acid Bioassay

A colorimetric bioassay technique was employed in order to quantify the relative amount of total sialic expressed on the cell surface of a panel of cell lines. Cells were chosen to include representatives from high, low and no GFP expressers, high and low titres and no infectious progeny virus, and human, non-human primate and other origins.

Experiments were performed in triplicate, optical density (OD) measured at 570 nm and values blank-corrected. OD is directly proportional to quantity of total sialic acid in the sample ($2x10^5$ cells),

and the concentration in mM was calculated by linear regression analysis of the assay standard in GraphPad Prism® 5.0 software. Data is shown in Figure 40.

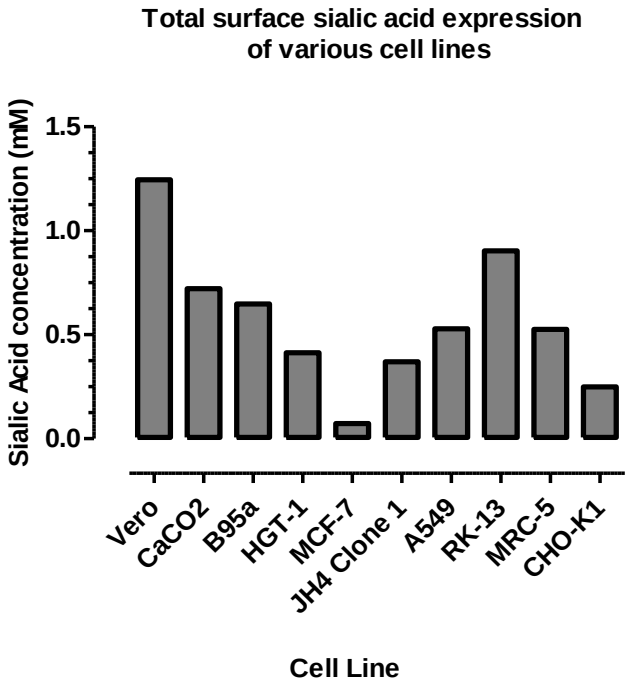

Figure 40 – Concentration of total sialic acid (mM) expressed on the surface of various cell lines.

Total cell surface sialic acid was quantified using the EnzyChrom™ Sialic Acid Bioassay kit according to manufacturer's instructions. The concentrations of the unknown cell lines were calculated using a sialic acid standard and linear regression analysis of the absorbance at 450 nm of these standards. Values displayed represent the mean of triplicate measurements.

Vero cells contained the highest concentration of total sialic acid (1.245 mM) and MCF-7 the lowest (0.073 mM). There appeared to be no correlation between quantities of sialic acid and how efficient a cell line is at propagating MuV. For example, RK-13 cells expressed the highest amount of sialic acid after Vero cells (0.903 mM) however they demonstrated no GFP expression and did not

propagate MuV efficiently. MRC-5 cells did not produce any infectious progeny virus or express GFP yet they contain a similar quantity of total sialic acid (0.526 mM) to HGT-1 cells (0.458 mM), which generated the highest titres of infectious Mu90 virus at P1.

3.4.2 FACS Analysis

DIG glycan differentiation FACS analysis was performed on a panel of cell lines in order to determine the relative quantity of α2,3 and α2,6-linked sialic acid expressed on cell surfaces ($2x10^5$ cells per sample). Cells were chosen to include representatives from high, low and no GFP expressers, high and low titres and no infectious progeny virus, and human, non-human primate and other origins. DIG-labelled lectins and DIG-FITC antibodies were used for detection of α2,3 and α2,6 and experiments were performed in triplicate with values blank-corrected. Vero and MDCK-SIAT1 cells were included as experimental controls, as they have been reported to express slightly more α2,3 sialic acid (Govorkova *et al.*, 1996) or more α2,6 sialic acid (Matrosovich *et al.*, 2003) respectively. The control data is shown in Figure 41, and Figure 42 summarises the data for the remaining cell lines.

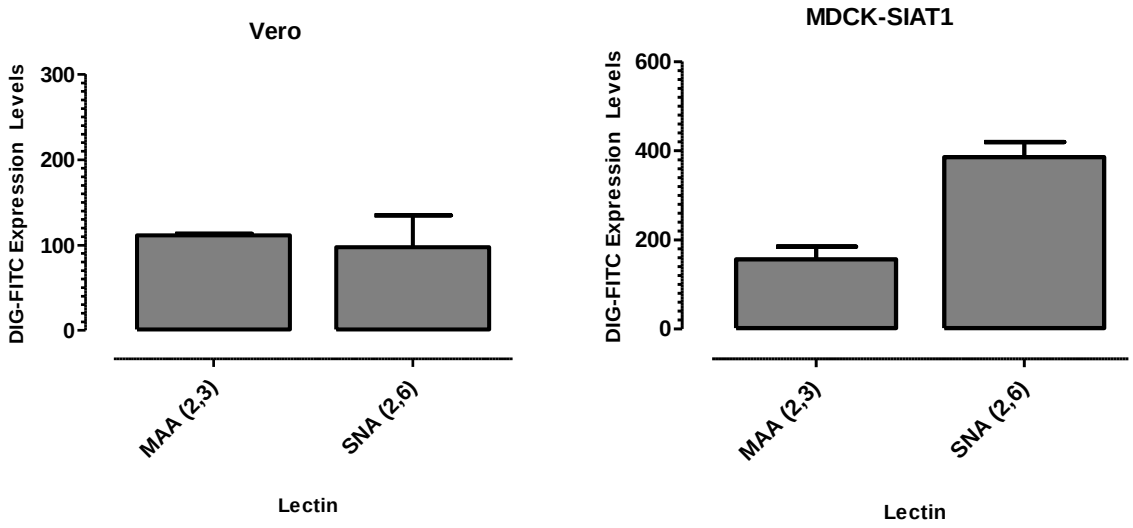

Figure 41 – DIG-FITC expression levels for experimental control cells Vero and MDCK-SIAT1. Data was obtained by FACS analysis and the values displayed represent the mean and standard variation of triplicate measurements for each lectin.

Controls were deemed to be valid as the Vero cells expressed slightly higher levels of α2,3 linked sialic acid (111 – α2,3 and 97 – α2,6), and MDCK-SIAT1 cells expressed higher levels of α2,6 linked sialic acid (α2,6 – 385 and α2,3 – 156) as expected.

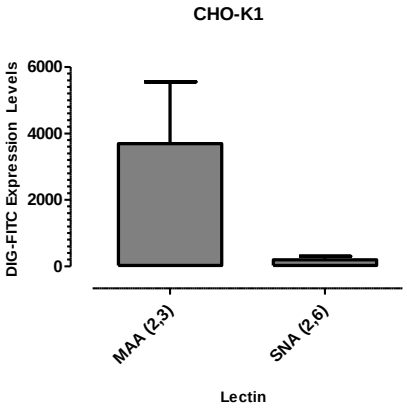
CHO-K1
DIG-FITC Expression Levels
6000
4000
2000
0
MAA (2,3)
SNA (2,6)
Lectin

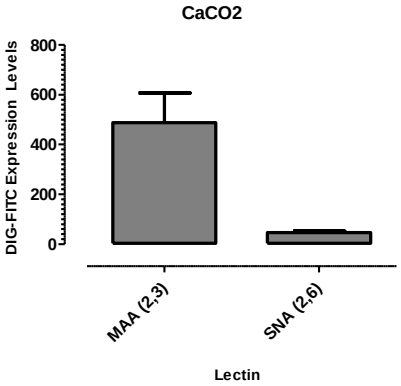
CaCO2
DIG-FITC Expression Levels
800
600
400
200
0
MAA (2,3)
SNA (2,6)
Lectin

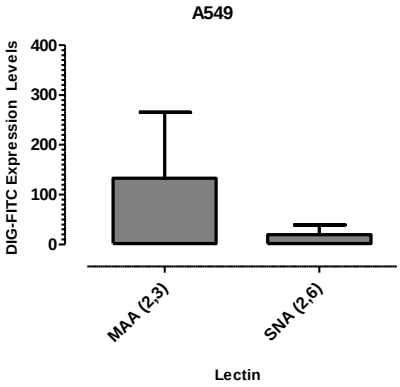
A549
DIG-FITC Expression Levels
400
300
200
100
0
MAA (2,3)
SNA (2,6)
Lectin

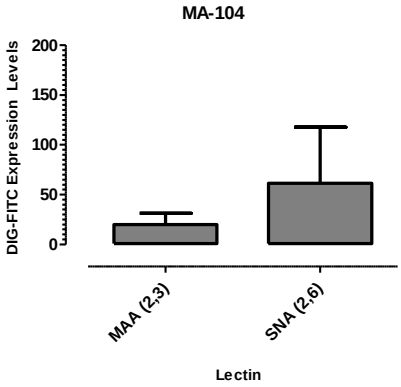
MA-104
DIG-FITC Expression Levels
200
150
100
50
0
MAA (2,3)
SNA (2,6)
Lectin

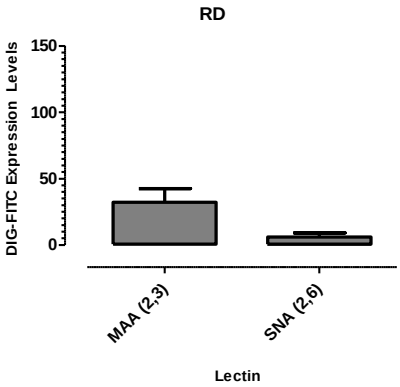
RD
DIG-FITC Expression Levels
150
100
50
0
MAA (2,3)
SNA (2,6)
Lectin

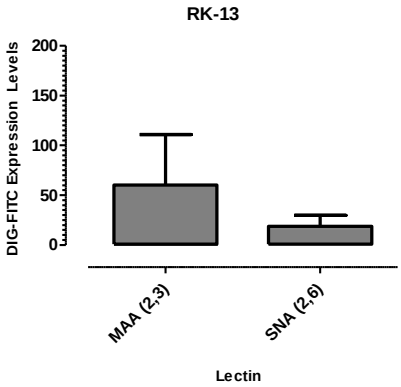
RK-13
DIG-FITC Expression Levels
200
150
100
50
0
MAA (2,3)
SNA (2,6)
Lectin

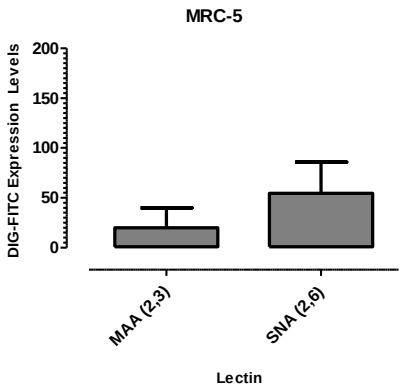
MRC-5
DIG-FITC Expression Levels
200
150
100
50
0
MAA (2,3)
SNA (2,6)
Lectin

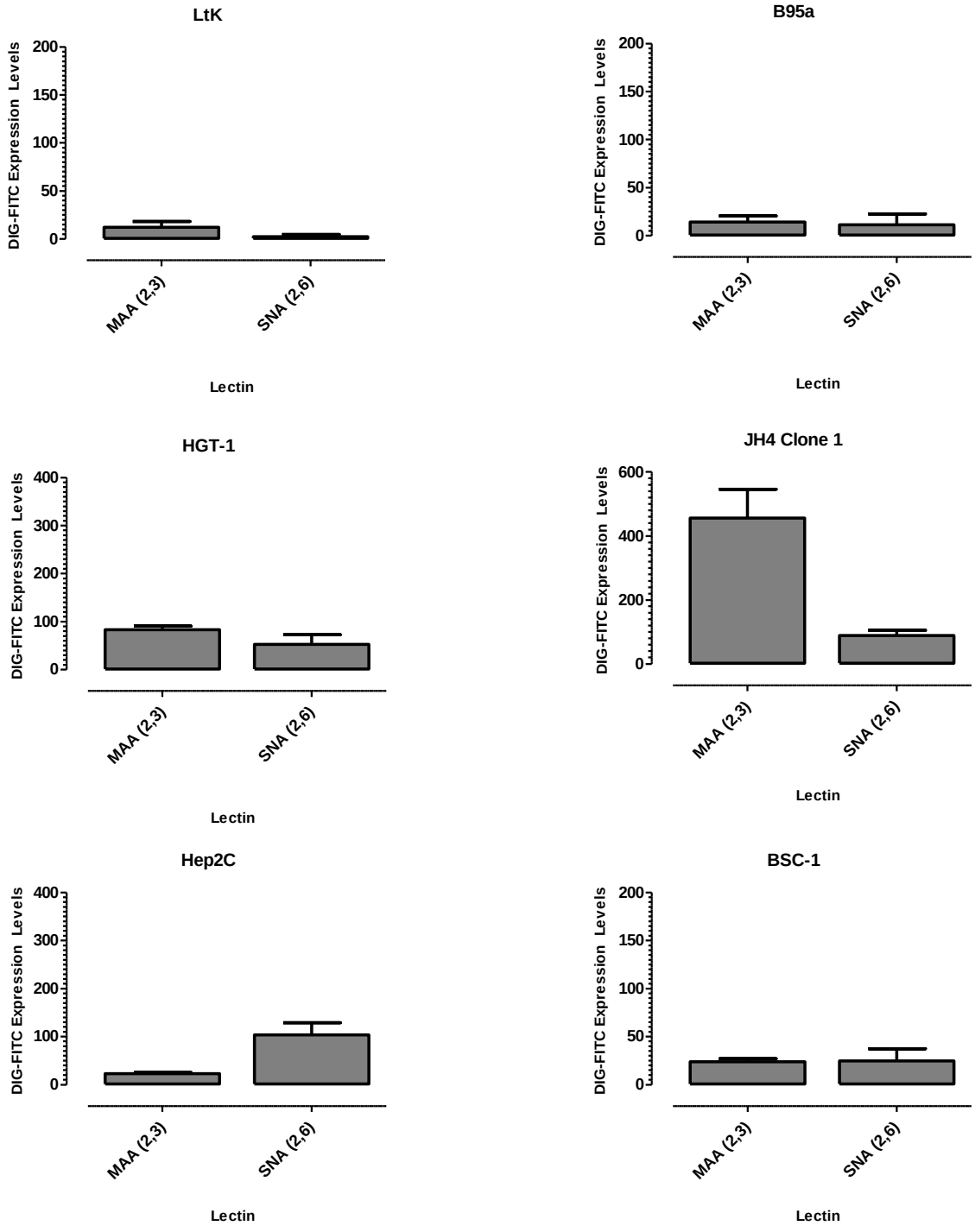

Figure 42 – DIG-FITC expression levels demonstrating relative quantities of α2,3 and α2,6 linked sialic acid expressed on surface of various cell lines. Data was obtained by FACS analysis and the values displayed represent the mean and standard variation of triplicate measurements for each lectin.

There appeared to be no correlation between type of sialic acid expressed and how efficient a cell line is at propagating MuV. For example, CaCO2 and MA-104 cells both demonstrated high levels of GFP expression and generated high titres of progeny Mu90 and RIT 4385 viruses however, CaCO2 express relatively more α2,3 (489) than α2,6 (47) linked sialic acid, and MA-104 express relatively more α2,6 (61) than α2,3 (20) linked sialic acid. No GFP expression or infectious progeny MuV was detected in MRC-5 and CHO-K1 cells. MRC-5 were shown to express relatively more α2,6 (55) than α2,3 (20) linked sialic acid, whereas CHO-K1 expressed relatively more α2,3 (3692 than α2,6 (199) linked sialic acid.

3.4.3 Infection of MDCK-SIAT1 cells with MuV

MDCK-SIAT1 cells have been reported to express increased quantities of α2,6 sialic acid with reduced levels of α2,3 sialic acid (Matrosovich *et al.*, 2003) and demonstrate improved influenza isolation when compared with parental MDCK cells (Oh *et al.*, 2008). MDCK-SIAT1 cells were infected with Mu90 or RIT 4385 viruses at an MOI of 0.001.This experiment was performed to investigate where or not an increased amount of α2,6 linkages has any effect on virus infection or production of progeny virus. MDCK and Vero cells were infected in the same way to act as controls. Virus was harvested from cell supernatants at 7 days post infection and titrated by plaque assay on Vero cells in triplicate. Mock-infected controls were valid. These data are shown in Figure 43.

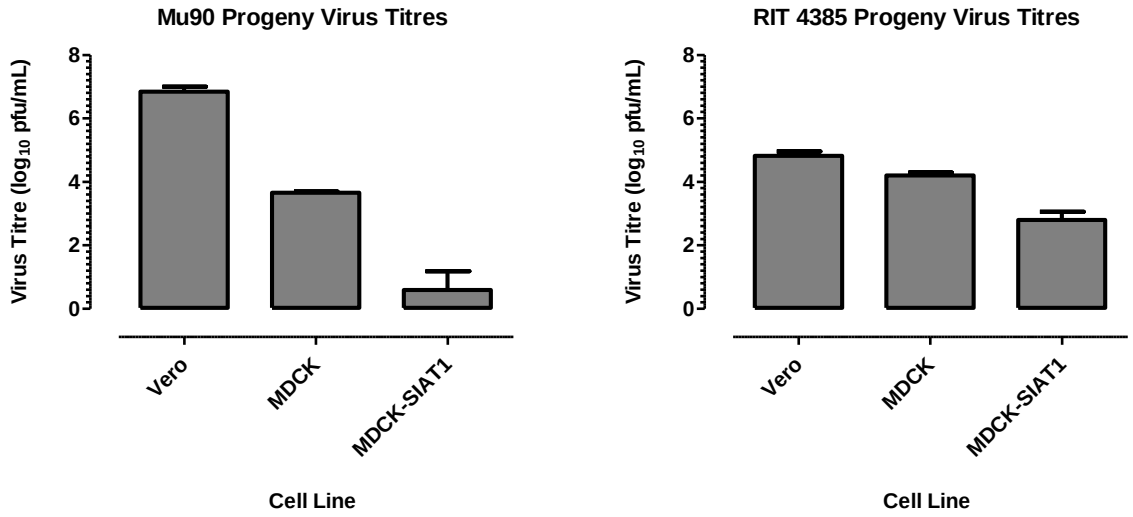

Figure 43 – Mu90 and RIT 4385 progeny virus titres after 1 passage on Vero, MDCK and MDCK-SIAT cells. Cells were infected at an MOI of 0.001 pfu per cell and viruses were harvested on day 7 post infection by freeze-thaw of cells and lysate clarification. Titres were obtained by plaque assay on Vero cells in triplicate and the values displayed represent the mean and standard deviation.

Infectious progeny virus was produced from MDCK-SIAT1 cells however Mu90 (0.59 log_{10}pfu/mL) and RIT 4385 (2.8 log_{10}pfu/mL) titres were significantly lower than those from parental MDCK cells (3.66 log_{10}pfu/mL and 4.2 log_{10}pfu/mL respectively). This may indicate that the increase in α2,6 and resultant decrease in α2,3 sialic acid linkages has a negative effect on MuV cellular infection and perhaps more α2,3 is required for efficient infection.

3.4.4 Sialic Acid Blocking

A panel of cell lines were treated with lectin from *Maackia amurensis* (MAA) to block α2,3 sialic acid residues and infected with Mu90 at an MOI of 0.001. This experiment was carried out in order to determine if blocking these sialic acid molecules would inhibit MuV infection. Cells were chosen that produced high titres of infectious progeny virus so that any differences could be easily identified.

Virus was harvested from cell supernatants every 24 hours post infection for 5 days and titrated by plaque assay on Vero cells in triplicate. Mock-infected and PBS controls were valid. These data are shown in Figure 44.

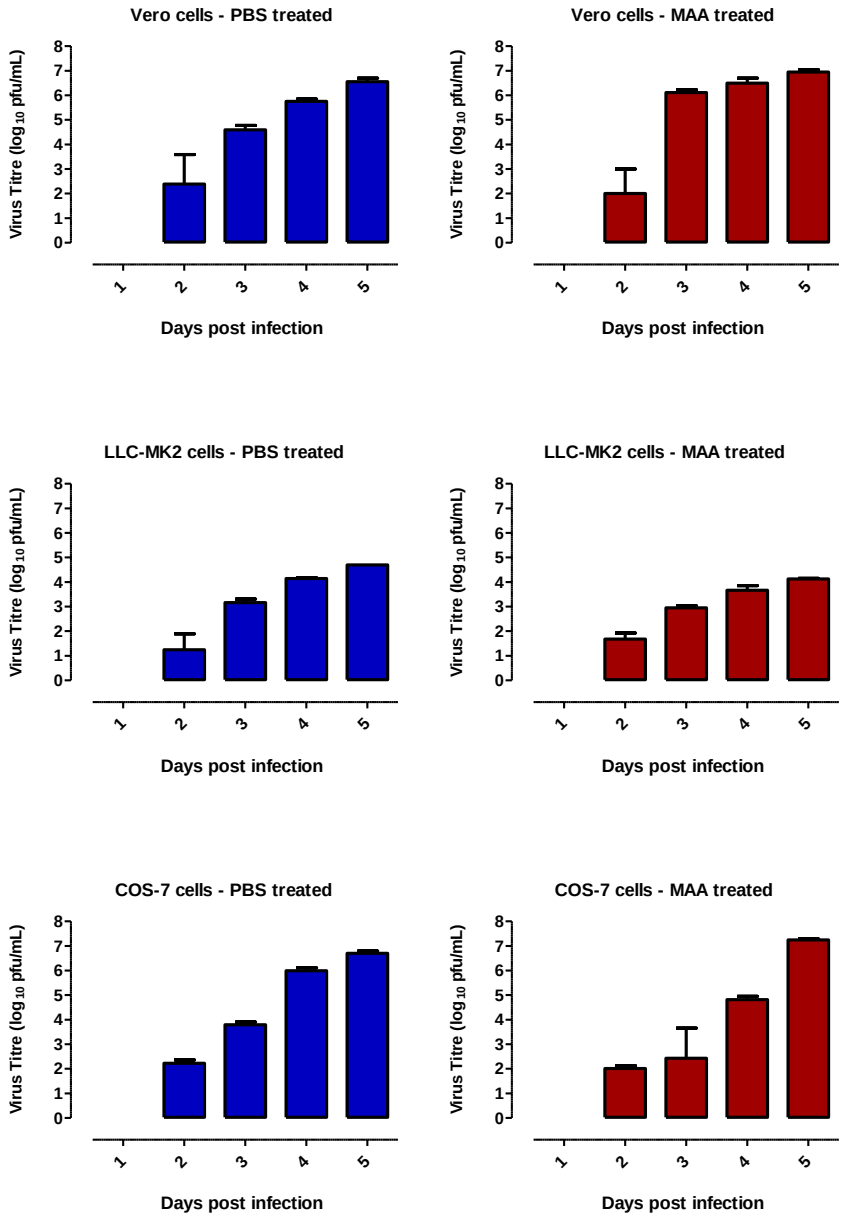

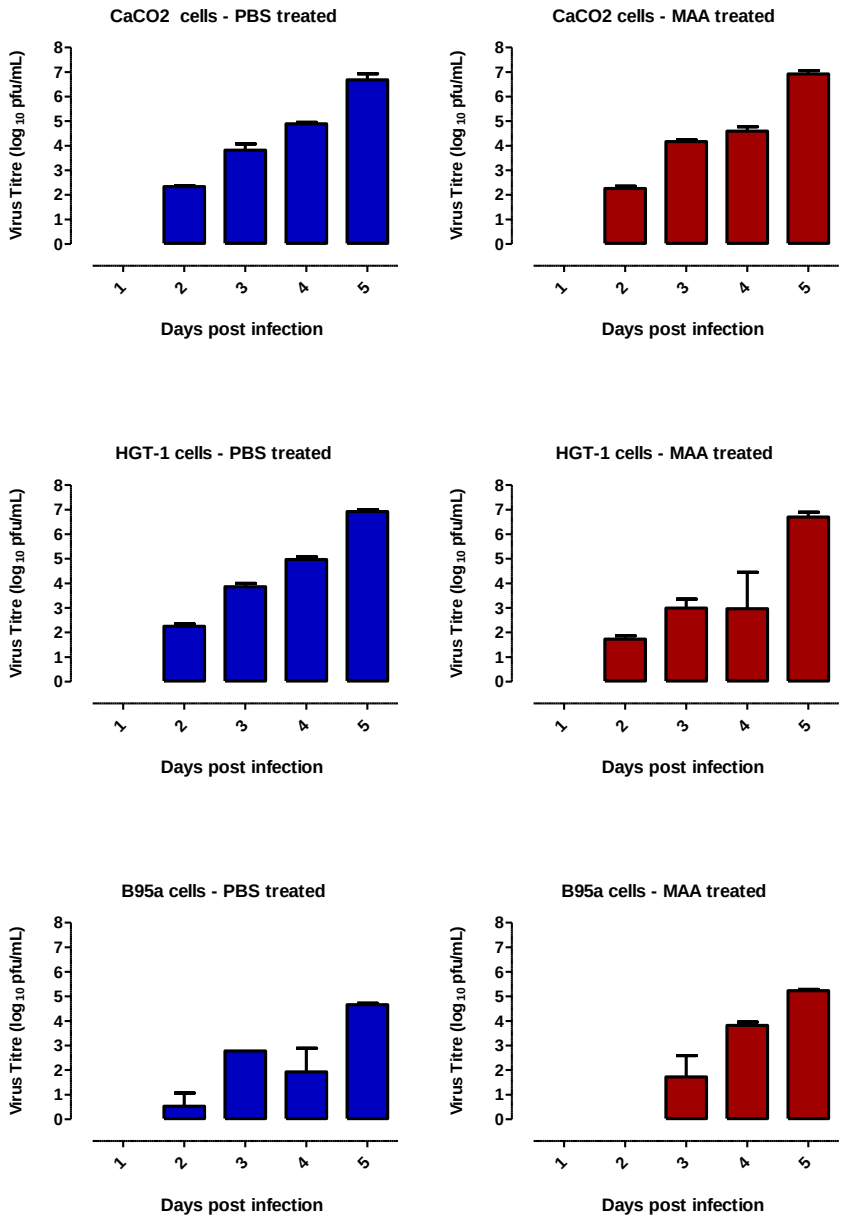

Figure 44 – Mu90 progeny virus titres from various cell lines treated with either PBS (blue) or lectin from MAA (red) prior to infection. Cells were incubated with either PBS or MAA lectin and then infected with MuV Mu90 at an MOI of 0.001 pfu per cell. Cell supernatant was harvested every 24 hours for 5 days post infection and titrated on Vero cells in triplicate. Data displayed represent the mean and standard deviation.

Treatment of cells with lectin from MAA prior to infection does not appear to have a significant effect on production of infectious progeny virus when compared with the PBS treatment control. However, progeny virus was detected in supernatant from PBS-treated B95a cells 24 hours earlier than MAA-treated B95a cells. In order to confirm if this treatment of cells was an efficient blocking mechanism, Vero cells were treated with lectin from *Sambucus nigra agglutinin* (SNA) to block α2,6 residues, and from MAA and SNA simultaneously. Data from this experiment is shown in Figure 45.

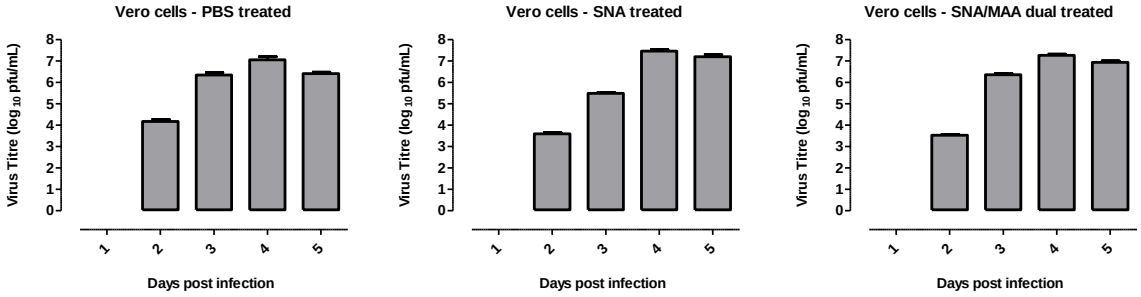

Figure 45 – Mu90 progeny virus titres from Vero cells treated with PBS, SNA or SNA and MAA prior to infection. Cells were incubated with either PBS, SNA lectin or a mixture of SNA and MAA lectins, and then infected with MuV Mu90 at an MOI of 0.001 pfu per cell. Cell supernatant was harvested every 24 hours for 5 days post infection and titrated on Vero cells in triplicate. Data displayed represent the mean and standard deviation.

Treatment of Vero cells with only SNA or SNA plus MAA prior to infection appears to have no effect on production of progeny virus when compared with the PBS treatment control.

The data from these sialic acid blocking experiments indicates that either this type of lectin blocking treatment does not form a tight enough block, or that MuV is capable of entry into the cell by another means.

3.5 Experimental Infection of MucilAir™ HAE with MuV

3.5.1 Infection of HAE with Representative Wild-Type and Vaccine MuV's

HAE cells were infected via the apical membrane with Mu90 (wild-type) or RIT 4385 (vaccine) viruses at an MOI of 0.0001 pfu per cell in order to determine if these cells were capable of being infected with MuV and supporting MuV replication. Viruses released from apical and basal membranes were harvested at 6, 12, and then every 24 hours post infection for 10 days and titrated by plaque assay on Vero cells in triplicate. Mock-infected controls were valid. These data are demonstrated in Figure 46.

a) Apically harvested viruses

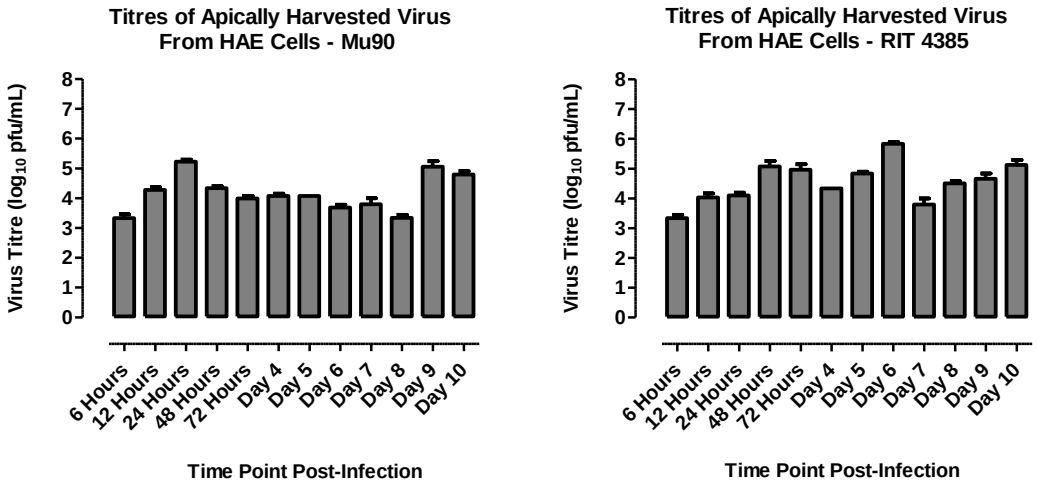

b) Basally harvested viruses

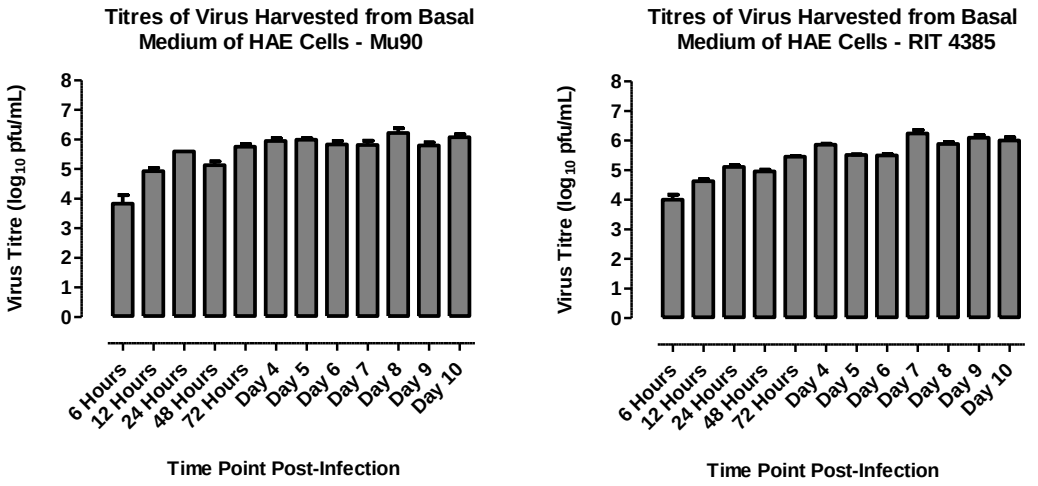

Figure 46 – Titres of viruses harvested from apical (a) and basal (b) membranes of HAE cells infected with Mu90 or RIT 4385 over a 10 day time course. After washing mucus from cell surfaces, cells were infected via the apical membrane at an MOI of 0.0001 pfu per cell and samples were harvested from both apical and basal compartments at 6, 12 and then every 24 hours for 10 days post infection. Virus titres were obtained by plaque assay on Vero cells in triplicate and the data displayed represents the mean and standard deviation.

Mu90 and RIT 4385 progeny virus was detected in apical samples by plaque assay at every measured time point from 6 hours to 10 days post infection. Mu90 titres ranged from 3.3 $\log_{10}$ pfu/mL (6 hours) to 5.2 $\log_{10}$ pfu/mL (24 hours). RIT 4385 titres ranged from 3.3 $\log_{10}$ pfu/mL (6 hours) to 5.8 $\log_{10}$ pfu/mL (day 6). For both viruses, the 6 hour time point titre was equal to that of the input virus suggesting recovery of the inoculum and not replicating virus. Mu90 and RIT 4385 progeny virus was also detected in basal samples by plaque assay at every measured time point. Mu90 titres ranged from a minimum of 3.8 $\log_{10}$pfu/mL (6 hours) to 6.2 $\log_{10}$pfu/mL (day 8). RIT 4385 titres ranged from 4.0 $\log_{10}$ pfu/mL (6 hours) to 6.24 $\log_{10}$ pfu/mL (day 7).

To confirm that the plaques formed on Vero cells were caused by infectious MuV, RNA was isolated from Mu90 and RIT 4385 apical and basal samples from days 1 and 5 post infection and analysed by RT-PCR and gel electrophoresis for presence of MuV SH gene mRNA using JLSH1Fw and JLSH2Rv primers. Bands of expected size were generated for all apical samples examined. No RT-PCR products were obtained for any of the basal samples. This may indicate that what was observed on Vero cells from basal samples when compared to the apical viruses (Figure 47) were not viral plaques caused by MuV infection. Negative and positive controls included in RT-PCR were valid.

a) **b)**

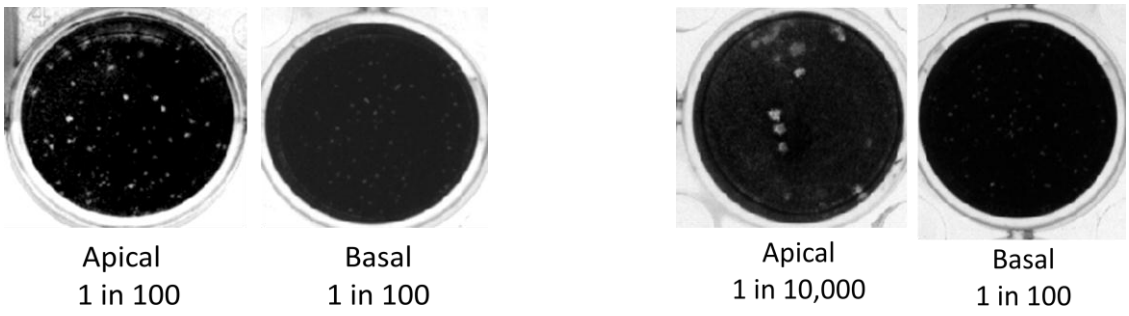

Figure 47 – Morphologies of plaques from progeny virus harvested from apical and basal surfaces of HAE cells infected with Mu90 (a) and RIT 4385 (b) at 7 days post infection. Dilutions of viruses photographed for each example of morphology of apical and basal samples are noted below each image.

These findings indicate that HAE cells are susceptible to MuV infection and are capable of supporting replication and release of progeny virus via the apical membrane, but possibly not the basal cell membrane.

3.5.2 Isolation of Clinical MuV Using HAE Cells

HAE cells were infected via the apical membrane with neat clinical MuV AFZ315 in order to determine if these cells can be used for isolation of MuV from un-passaged clinical samples. Viruses were harvested from apical and basal surfaces at 6, 12 and then every 24 hours post infection for 10 days and were titrated by plaque assay on Vero cells in triplicate. Mock infected controls were valid. These data are shown in Figure 48.

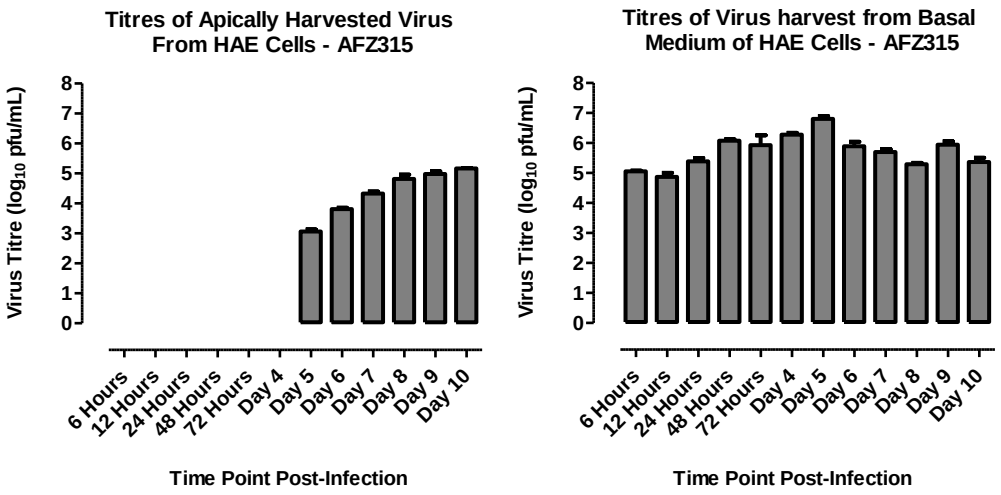

Figure 48 – Titres of clinical progeny virus AFZ315 harvested from apical or basal cell HAE membrane surfaces over a 10 day time course. After washing mucus from cell surfaces, cells were infected via the apical membrane with clinical sample AFZ315 and samples were harvested from both apical and basal compartments at 6, 12 and then every 24 hours for 10 days post infection. Virus titres were obtained by plaque assay on Vero cells in triplicate and the data displayed represents the mean and standard deviation.

Infectious MuV from HAE cells inoculated with AFZ315 was detected in apical samples from day 5 to day 10 post infection with titres increasing from 3.1 log_{10} pfu/mL (day 5) to 5.2 log_{10} pfu/mL (day 10). Plaques were also evident on assays inoculated with basal samples from every measured time point, from 6 hours to 10 days post infection. Titres ranged from a minimum of 4.0 log_{10} pfu/mL (6 hours) to a maximum of 6.24 log_{10} pfu/mL (day 7). However, these were very small in size when compared to those from apical samples (Figure 49) and it was not possible to generate RT-PCR products from RNA isolated from any basal samples. RNA was isolated from apical samples and selected genes sequenced, the results of which are summarised in section 3.4.5.

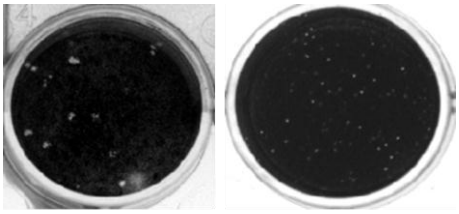

Apical
1 in 100

Basal
1 in 1000

Figure 49 – Morphologies of plaques from progeny virus harvested from apical and basal surfaces of HAE cells infected with AFZ315 at 7 days post infection. Dilutions of viruses photographed for each example of morphology of apical and basal samples are noted below each image.

These results indicate that HAE cells can be used for isolation of clinical MuV directly from a patient sample via the apical membrane however MuV may not be released from basal cell membranes.

3.5.3 Immunohistochemistry of HAE Cell Sections Infected with MuV

3.5.3.1 Optimisation of Antibody Dilutions

Prior to staining HAE cells, primary antibodies MuV anti-F protein, mouse anti-β-tubulin and their respective secondary antibodies Goat Anti-Rabbit IgG-FITC and Goat Anti-Mouse TEXAS RED® were titrated to achieve the optimal dilutions. All were diluted in either 1% (w/v) BSA/PBS A or 5% (w/v) non-fat dried milk/PBS A. MuV antibodies were titrated on infected LLC-MK2 cells and mouse antibodies on uninfected MCF-7 cells.

After titration, MuV primary anti-F antibody was decided to be diluted 1 in 10,000 in 5% (w/v) non-fat dried milk/PBS A and secondary antibody 1 in 200 in 1% (w/v) BSA/PBS A. Mouse anti-β-tubulin antibody was decided to be diluted 1 in 200 and secondary antibody 1 in 50, both in 1% (w/v) BSA/PBS A. These are shown in Figure 50.

a) MuV anti-F antibody (1°) and Goat Anti-Rabbit IgG-FITC (2°)

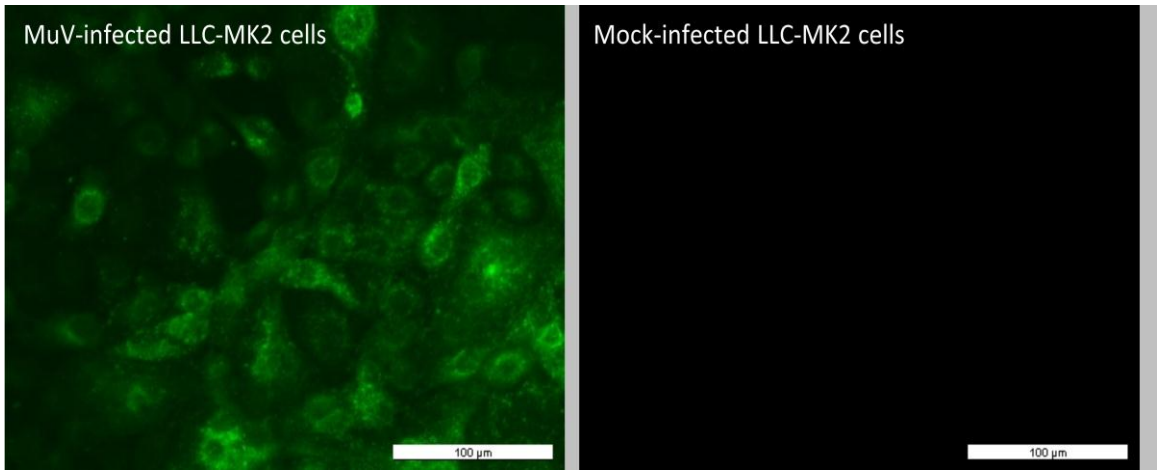

b) Mouse anti-β-tubulin antibody (1°) and Goat Anti-Mouse TEXAS RED® (2°)

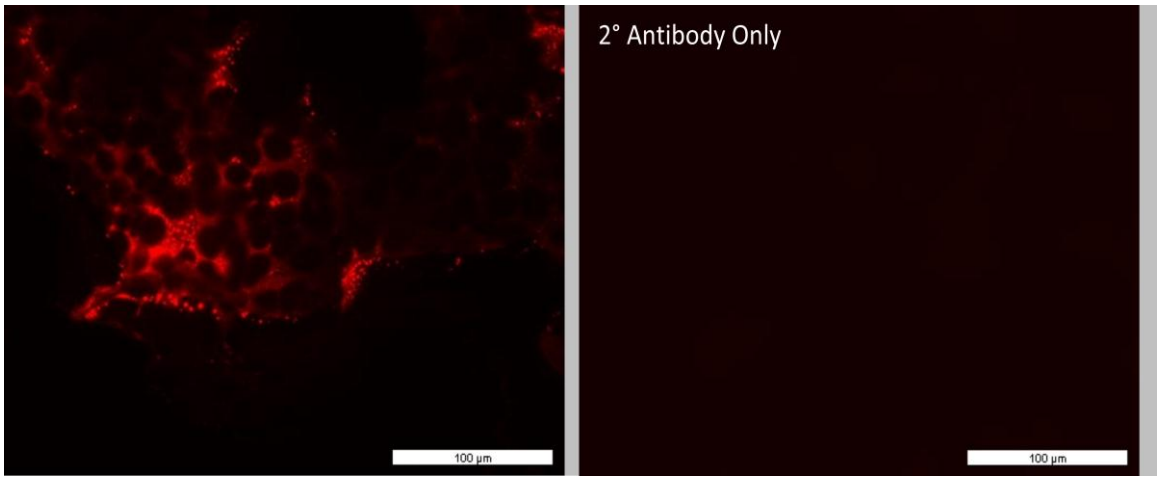

Figure 50 – Optimal dilutions for immunofluorescence antibodies. Antibody dilutions selected for immunofluorescence staining of MuV F protein (a) and ciliated cell types (tubulin) (b). Figure (a) shows 1° and 2° antibodies diluted 1 in 10,000 and 1 in 200 respectively on MuV infected and mock-infected LLC-MK2 cells. Figure (b) demonstrates 1° and 2° antibodies diluted 1 in 200 and 1 in 50 respectively. Cells stained with 2° antibody only is also shown here.

3.5.3.2 Immunofluorescence Staining of HAE Cell Sections

HAE cells infected with clinical MuV AFZ315 were fixed, sectioned and stained at day 7 post infection in order to visualise MuV protein location in infected cells. Antibodies and dilutions used were as described in section 3.4.3.1 and confocal images of infected and mock-infected cells are shown in Figure 51.

a) HAE cells infected with clinical MuV

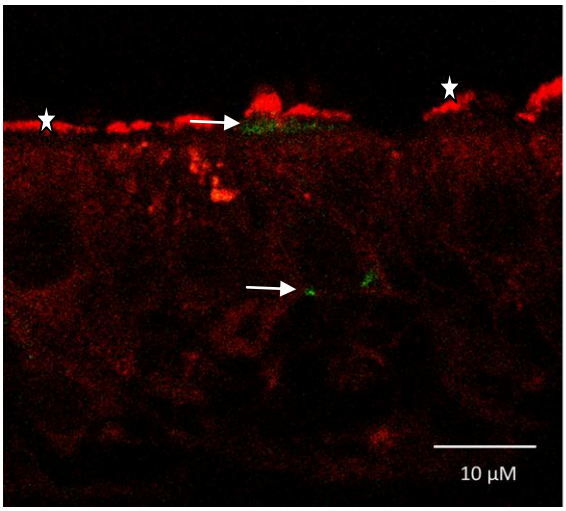

b) HAE cells infected with clinical MuV

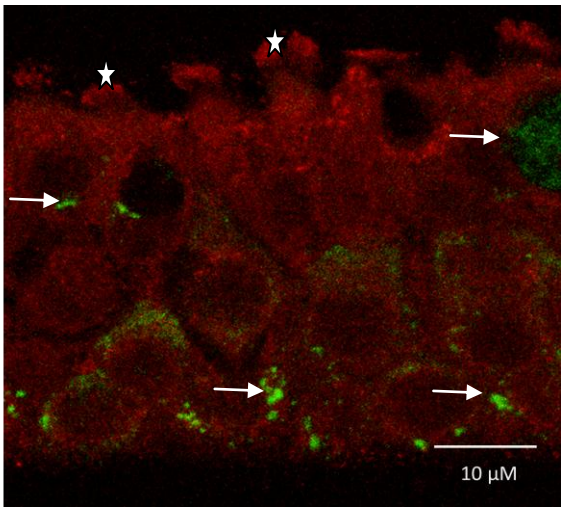

c) Mock-infected HAE cells

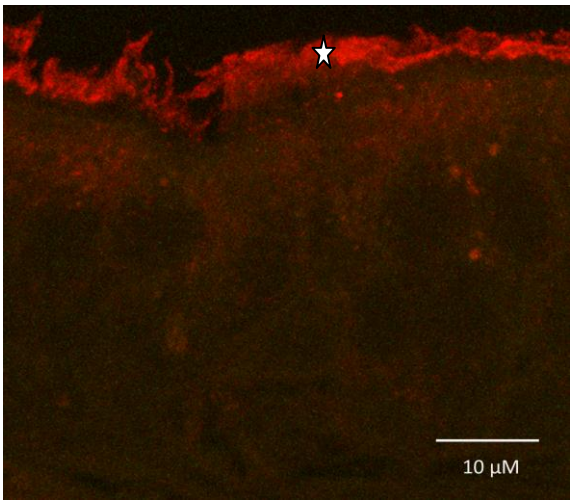

Figure 51 – HAE sections from day 7 post infection either infected with clinical MuV AFZ315 (a, b) or mock-infected (c). Cells were fixed at day 7 post-infection after infection with neat clinical sample AFZ315 or MEM (mock), and histological cross-sections were prepared by Propath UK before staining in-house. Confocal images show MuV F protein staining is green and indicated by arrows, and tubulin (ciliated cells) red and is highlighted by stars.

The photomicrographs show the localisation of the F protein in the microvilli of apical, ciliated cells (Figure 51 a) and basal cells (Figure 51 b). The MuV F protein is excluded from cell nuclei and has a primarily cytoplasmic location. Mock-infected cells show tubulin staining of ciliated cells only (Figure 51 c).

3.5.4 Comparison of HAE and Vero Cells for Isolation of Clinical MuV

HAE and Vero cells were inoculated with clinical MuV AFZ315 in triplicate under the same experimental conditions, and virus harvested from apical cell membranes or cell supernatant respectively at 6, 12 and then 24 hours for 10 days post infection. Released viruses were titrated by plaque assay on Vero cells and mock-infected controls were valid. This experiment was carried out as a direct comparison of the “gold-standard” Vero cells and the HAE model to see which, if either, was more efficient at isolating clinical MuV. The data are presented in Figure 52.

a) HAE cells **b) Vero cells**

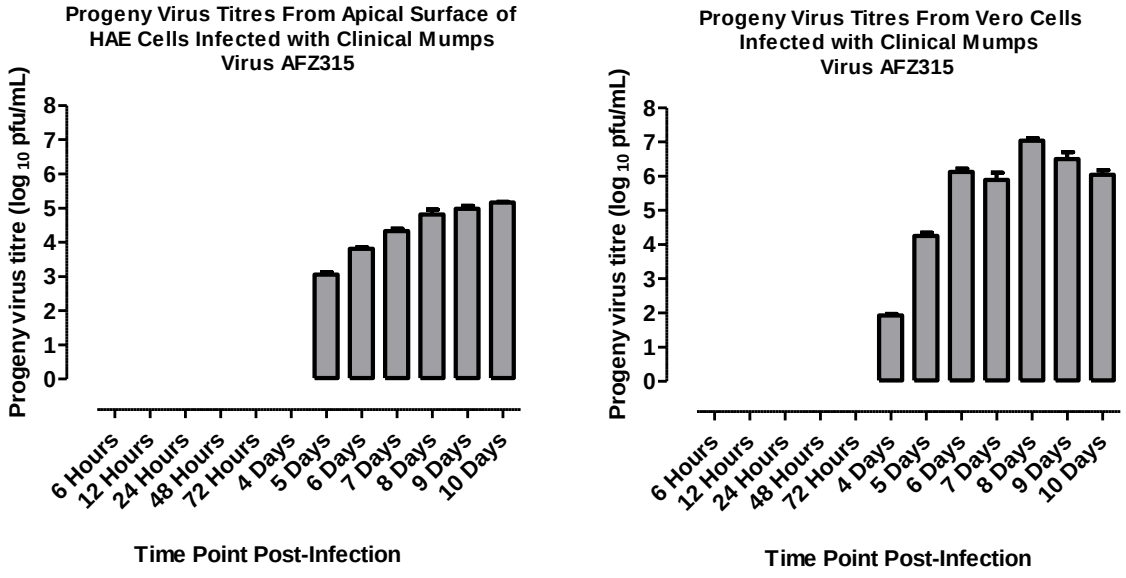

Figure 52 – Titres of clinical progeny virus AFZ315 harvested from the apical surface of HAE cells (a) or cell supernatant from Vero cells (b) over 10 days. Confluent monolayers of Vero cells or the apical surface of HAE cells were infected with clinical MuV AFZ315 in triplicate. Apical HAE samples and Vero cell supernatant were harvested at 6, 12 and then every 24 hours for 10 days post infection and virus titres were obtained by plaque assay on Vero cells. Data displayed represents the mean and standard deviation.

Progeny MuV from HAE cells was detected in apical samples from day 5 to day 10 post infection with titres increasing from 3.1 $\log_{10}$ pfu/mL (day 5) to 5.2 $\log_{10}$ pfu/mL (day 10). MuV was detected in Vero supernatant from day 4 to day 10 post infection with infectious virus titres from 1.9 $\log_{10}$ pfu/mL (day 4) to 7.0 $\log_{10}$ pfu/mL (day 8). These results indicate that Vero cells are capable of propagating and efficiently releasing clinical MuV 24 hours earlier than HAE cells and that the infectious titres are higher in Vero cells.

RNA was extracted from HAE apical and Vero supernatant virus samples harvested at 5, 6 and 7 days post infection and analysed by RT-PCR. Nucleoprotein, fusion, haemagglutinin-neuraminidase and small hydrophobic genes were sequenced and aligned with the parent virus sequences. Negative and positive controls included in RT-PCR were valid. This was carried out in order to assess and compare the genetic stability of a clinical MuV when propagated in either HAE or Vero cells.

In viruses from HAE cells, nucleotide, and therefore amino acid sequences of N and SH genes were identical in all cases. Nucleotide change thymine (t) to cytosine (c) at position 1548 of the HN gene of days 5, 6 and 7 viruses resulted in an amino acid change from tyrosine to cysteine at position 539 (Y539C). Nucleotide change adenine (a) to guanine (g) at position 1613 of the F gene of these viruses caused an amino acid change from Y to C at position 538 (Y538C). In viruses from Vero cells there were nucleotide, and amino acid alterations in all four genes and proteins analysed, and all of these mutations were identical in days 5, 6 and 7 viruses. Table 29 summarises the amino acid changes observed in the Vero and HAE progeny virus proteins and the full nucleotide and amino acid sequences are detailed in Appendices 9-16.

Table 29 – Amino acid substitutions in N, F, HN and SH proteins of HAE and Vero AFZ315 progeny viruses

Protein	HAE	Vero
Nucleoprotein (N)	N/A	I121V
		Q450H
		M500I
		P502H
Fusion (F)	Y538C	S4P
		T21I
		E61D
		S95P
		S181N
		Q329H

		R464K
		A475S
		A489T
		I492V
		I498M
		D534V
Haemagglutinin-neuraminidase (HN)	Y539C	A13T
		F69S
		T71I
		R76K
		H94Y
		S121N
		V125A
		A126S
		T130I
		S131N
		N203K
		N266D
		V287I
		I402T
		T473I
		A511T
		L538P
		S540P
		N542H
Small hydrophobic (SH)	N/A	V16I
		I28V
		I29V
		L30S
		A31T
		Q39R
		G46R
		F57L

N/A – not applicable, no substitutions

These results suggest that propagation of clinical MuV in Vero cells induces many mutations in the genome and that HAE cells produce more genetically stable progeny virus with very similar or identical genotypic properties to those of the parent virus.

3.6 Results Summary

A panel of human, non-human primate, murine and other cell lines were screened using a GFP-expressing MuV and then infected with representative wild-type (Mu90) and attenuated vaccine (RIT 4385) MuVs. Data that included levels of GFP expression and progeny virus titres after one passage allowed for the selection of a group of 17 (Table 11) out of a total of 41 cell lines which were deemed as being capable of efficiently supporting MuV growth and replication, however, GFP expression and virus titres from the various cell lines did not correlate (i.e. high levels of GFP expression did not necessarily mean high progeny virus titres in the same cell line). More cell lines were capable of successfully generating Mu90 progeny virus (17 cell lines) compared with RIT 4385 (6 cell lines), and only Vero, COS-7, MA-104, CaCO2, A549 (BVDV) and MDCK cells efficiently propagated both wild-type and attenuated vaccine viruses.

The highest levels of GFP expression were recorded for LLC-MK2 cells, followed by COS-7 and then the “gold-standard” Vero cells. HGT-1 cells produced the highest titre of wild-type MuV, with Vero cells producing the second highest. CEFs produced the highest titre of vaccine MuV followed by COS-7. Parental A549 cells were not capable of propagating Mu90 or RIT 4385 MuVs, however A549 cells expressing the V protein of hPIV5 produced high titres of both progeny viruses and those expressing the NPro protein of BVDV generated high titres of Mu90.

Analysis of P1 to P5 progeny virus titres of Mu90 and RIT 4385 MuVs showed varying trends in different cell lines. Some cells exhibited an increase in virus titres (A549 (BVDV), A549 (PIV5-V), Hep 2C, MA-104, B95a and MDCK – Mu90 only) while others showed a slight decrease (Vero – RIT 4385

only, CaCO2, LLC-MK2, BHK-21 and MDCK – RIT 4385 only). The remaining cell lines maintained relatively stable MuV titres throughout P1 to P5.

N, F, HN and SH genes of Mu90 and RIT 4385 parent MuVs and those passaged through cell lines five times were sequenced and compared. Nucleotide mutations resulting in amino acid changes were found in all four genes from P5 Mu90 viruses from all cell lines apart from A549 (PIV5-V) – N protein, CaCO2 - N protein, Hep 2C - N and F proteins, HGT-1 - N protein, RD – N protein, LLC-MK2 – N protein, MA-104 N protein, COS-7 - N protein, JH4 Clone 1 – N protein, MDCK – N protein and BHK-21 – N and F proteins. RIT 4385 appeared to be more stable during serial passage as there were fewer protein amino acid substitutions. However there were still a number of nucleotide mutations resulting in amino acid substitutions in N, F and HN genes from the majority of P5 RIT 4385 viruses apart from Vero - N protein, CaCO2 - HN protein, COS-7 - HN protein, MA-104 - N protein and MDCK – N and HN proteins. The SH protein sequences from all P5 RIT 4385 viruses were identical to the parent sequence in all cell lines. In some cases, the amino acid substitutions were found to be the same throughout several cell lines, and these are summarised in Tables 30 and 31.

Table 30 – Summary of identical amino acid substitutions in P5 Mu90 MuVs from various cell lines

		Cell Lines			
Protein	Amino Acid Change	Human	Non-Human Primate	Murine	Other
N	R194I		Vero	N/A	
	Q199H		Vero		
	E235K	A549 (BVDV)	BSC-1		
	R241Q	A549 (BVDV)			
	G264R	A549 (BVDV) MCF-7	BSC-1		BHK-21
	F481L		B95a		
	Q508K	A549 (BVDV)			
	D509X	A549 (BVDV)			
	G544A		Vero		
	D545T		Vero		
	W546G		Vero		
F	A3D	MCF-7	LLC-MK2 B95a	N/A	
	F4I	MCF-7	LLC-MK2 B95a		
	T7N		B95a		
	A12V		B95a		
	I18K		B95a		
	I28M	A549 (BVDV)			
	M140I		Vero		
	E153K		Vero		
	I221M	MCF-7 RD			
	Q268L		COS-7		
	R381Q		Vero MA-104		
	F420L		B95a		
	C505L		MA-104		
	C506L		MA-104		
	W507L		MA-104		
	A508G		MA-104		
	Y509L		MA-104		
	I510V		MA-104		
	A511C		MA-104		
	T512N		MA-104		
	L535F				JH4 Clone 1
	I536H		BSC-1		
	I536L I536S				MDCK
	R537Q		BSC-1		
	R537T	HGT-1 RD			

	Y538H	A549 (PIV5-V) HGT-1			
	Y538V -539L	 CaCO2	BSC-1 BSC-1		
HN	T24A	A549 (BVDV) A549 (PIV5-V) CaCO2 Hep 2C HGT-1 MCF-7 RD	Vero BSC-1 COS-7 LLC-MK2 MA-104	N/A	BHK-21 JH4 Clone 1 MDCK
	H94Y	A549 (BVDV) A549 (PIV5-V) CaCO2 Hep 2C MCF-7 RD	COS-7		BHK-21
	N142K V575F	MCF-7			
	L576S	A549 (BVDV) A549 (PIV5-V) CaCO2 Hep 2C RD	BSC-1 COS-7 LLC-MK2 MA-1014		BHK-21 JH4 Clone 1 MDCK
	T577N	A549 (BVDV) A549 (PIV5-V) CaCO2 Hep 2C RD	BSC-1 COS-7 LLC-MK2 MA-104		BHK-21 JH4 Clone 1 MDCK
	R578Q	A549 (BVDV) A549 (PIV5-V) CaCO2 Hep 2C RD	BSC-1 COS-7 LLC-MK2 MA-104		BHK-21 JH4 Clone 1 MDCK
	L579I	A549 (BVDV) A549 (PIV5-V) CaCO2 Hep 2C RD	BSC-1 COS-7 LLC-MK2 MA-104		BHK-21 JH4 Clone 1 MDCK
	T580D	A549 (BVDV) A549 (PIV5-V) CaCO2 Hep 2C RD	BSC-1 COS-7 LLC-MK2 MA-104		BHK-21 JH4 Clone 1 MDCK
	I581Y	A549 (BVDV) A549 (PIV5-V) CaCO2 Hep 2C RD	BSC-1 COS-7 LLC-MK2 MA-104		BHK-21 JH4 Clone 1 MDCK
	T582H	A549 (BVDV) A549 (PIV5-V)	BSC-1 COS-7		BHK-21 JH4 Clone 1

		CaCO2	LLC-MK2		MDCK
		Hep 2C	MA-104		
		RD			
	-583L	A549 (BVDV)	BSC-1		BHK-21
		A549 (PIV5-V)	COS-7		JH4 Clone 1
		CaCO2	LLC-MK2		MDCK
		Hep 2C			
		RD			
SH	K35N		COS-7	N/A	
	A42S		COS-7		
	Q45H	CaCO2			
	F48L	A549 (BVDV)	Vero		BHK-21
		A549 (PIV5-V)	BSC-1		JH4 Clone 1
		CaCO2	COS-7		MDCK
		Hep 2C	LLC-MK2		
		HGT-1	MA-104		
		MCF-7			
		RD			
	H50R	A549 (BVDV)	Vero		BHK-21
		A549 (PIV5-V)	BSC-1		JH4 Clone 1
		CaCO2	COS-7		MDCK
		Hep 2C	LLC-MK2		
		HGT-1	MA-104		
		MCF-7			
		RD			

N/A – not applicable

Cell lines deficient in IFN production or insensitive to IFN highlighted in blue

Table 31 – Summary of identical amino acid substitutions in P5 RIT 4385 MuVs from various cell lines

		Cell Lines			
Protein	Amino Acid Change	Human	Non-Human Primate	Murine	Other
N	S246L		COS-7	N/A	N/A
	G265R		COS-7		
	F451L	A549 (PIV5-V)			
		CaCO2			
	I433T	A549 (PIV5-V)			
	F451L	A549 (PIV5-V)			
	V455A	A549 (PIV5-V)			
	L457S	A549 (PIV5-V)			
	V460A	A549 (PIV5-V)			
	F468P	A549 (PIV5-V)			
	R513Q		COS-7		
	E516K		COS-7		
F	I244T	CaCO2	Vero	N/A	MDCK
			COS-7		
			MA-104		
	R537S		MA-104		
	Y538R		MA-104		
	-539Q	A549 (PIV5-V)			
	-539R		COS-7		
HN	F15S		Vero	N/A	N/A
	V43A		Vero		
	D151E		Vero		
	Y152C		MA-104		
	F157L		Vero		
	S509N	A549 (PIV5-V)			
	S553G		MA-104		
	I566M		MA-104		
	V575C	A549 (PIV5-V)			
	L576A	A549 (PIV5-V)			
	A577S	A549 (PIV5-V)			
	R578Q	A549 (PIV5-V)			
	L579I	A549 (PIV5-V)			
	T580D	A549 (PIV5-V)			
	I581H	A549 (PIV5-V)			
	T582H	A549 (PIV5-V)			
	-583L	A549 (PIV5-V)			
SH	N/A	N/A	N/A	N/A	N/A

N/A – not applicable

Cell lines deficient in IFN production or insensitive to IFN highlighted in blue

Only six out of the 17 cell lines subject to further investigation were capable of supporting MuV plaque formation. These were Vero, A549 (BVDV), A549 (PIV5-V), LLC-MK2, L20B and LtK-. A549 (PIV5-V) cells appeared to be as sensitive for plaque formation as Vero cells.

Sialic acid receptor studies of various cell lines using bioassay, FACS and SA-blocking lectin assay methodologies indicated that the concentration of total SA or relative quantities of α2,3 and α2,6 SA linkage expressed on the surface of a cell does not affect the ability of a cell line to support efficient MuV growth. The data also suggested that MuV may not exhibit a preference for type of SA when binding to the host cell receptor.

Infection of HAE cultures with clinical (AFZ315), laboratory wild-type (Mu90) and attenuated vaccine viruses (RIT 4385) demonstrated that these types of primary cells are susceptible to MuV infection and that the viruses bud successfully from the apical cell surface. Smaller plaques were formed on Vero cells from basal HAE samples which initially suggested that the virus might also bud basolaterally, however no MuV RT-PCR products could be generated to confirm that the tiny plaques were as a result of MuV infection of the Vero cells. Direct inoculation of HAE cells with saliva taken from a mumps patient (AFZ315) established that these cells could also be used for isolation of MuV from a clinical sample. Vero and HAE cells were compared by inoculation with the same saliva sample and progeny viruses analysed which showed that both are capable of producing reasonably high progeny virus titres, with those from Vero cells being slightly higher. However, sequencing of N, F, HN and SH genes from parent and progeny viruses revealed that MuV from HAE is highly genetically similar to the parent virus, with no amino acid substitutions in N or SH genes, and only one substitution in the F and HN genes (Y538C and Y539C respectively), whereas Vero cell progeny MuV exhibited many amino acid substitutions in all four proteins examined.

3.7 Discussion

3.7.1 Cell Line Screen

One of the aims of this project was to investigate the effect of different cell substrates on MuV growth and replication, in order to identify cell lines which are permissive for MuV infection and can produce high titre progeny virus with similar genotypic and phenotypic properties to the parent virus in a clinical specimen. The data presented in this thesis show that propagation of MuV in Vero cells, which are most commonly used for growing MuV in laboratories worldwide, introduces a large number of mutations throughout the genome of the virus. Any other cell lines fitting the criteria above could therefore potentially be used as an alternative to Vero cells in diagnostic laboratories and would also be of use for propagating stock viruses in research laboratories.

As GFP has been shown to be an early and sensitive indicator of cellular infection (Duprex *et al.*, 1999), cell lines were screened with a GFP-expressing MuV in order to identify those permissive for MuV infection. The results demonstrated no correlation between levels of GFP and ability to produce high titre progeny virus. This could potentially be due to the rate at which new viruses are being assembled and released from the host cell. Expression of GFP is not only indicative of cellular infection but also viral protein expression, therefore it may be the case that cell lines exhibiting high GFP expression but low or no infectious progeny virus (e.g. L929 and L20B) express a large quantity of viral proteins but very few virus particles are fully assembled and released from the host cells. These types of abortive infection have already been described for MuV in cell lines of murine origin (Tsurudome *et al.*, 1984; Yamada *et al.*, 1984). The reverse may then be true of cell lines exhibiting low GFP expression but high titres of progeny virus (e.g. HGT-1 and A549 (PIV5-V)). New MuV particles could be fully assembled and released from host cells at a quicker rate, therefore it would be more difficult to visualise and measure an accumulation of viral proteins.

The data show a significant difference in the ability of cell lines to produce infectious progeny Mu90 and RIT 4385 viruses, suggesting profound differences between the attenuated MuV vaccine and representative wild-type virus. All of the cell lines included in this study demonstrated a decreased ability to produce infectious progeny RIT 4385 virus compared to Mu90 and fewer numbers and types of cell lines were capable of supporting efficient RIT 4385 growth. This can be explained in part by the fact that RIT 4385 has been attenuated by serial passage in tissue culture which means that the virus will be less likely to exhibit cytopathic effects and may have restricted or selective cell line tropisms. An exception to this was observed in the CEF cells which produced a higher titre of progeny RIT 4385 virus than Mu90. This result was expected due to the Jeryl-Lynn mumps strain used in the GSK vaccine being developed by attenuation through passage in embryonated hen eggs (Buynak & Hilleman, 1966). If CEF cells had been more freely available during this project, it would have been of great interest to have serially passaged both Mu90 and RIT 4385 MuVs through these cells to examine progeny virus titres, plaque morphologies and genetic stability. The mechanisms of MuV attenuation to produce vaccine strains are currently unknown.

Three general trends were observed with regards to the P1 to P5 progeny virus titres, which were increase, decrease or maintaining a relatively steady titre throughout. Viral fitness can be defined as the ability of a virus to reproduce itself, so to replicate and efficiently generate progeny viruses. MuV can be considered to show an increase in fitness in those cell lines that demonstrate an increase in MuV titre from P1 to P5, and this could be caused by the virus adapting to the cell substrate under the selective pressures that will be exerted by different host cells. A decrease in progeny virus titres from P1 to P5 may be due to the presence of DI particles. Although the initial MOI (0.003) for producing P1 Mu90 and RIT 4385 viruses was low, the MOIs for the passages that followed may have been too high, as a standard dilution of 1 in 50 was employed (section 2.3.3). This could have resulted in the formation of DI particles due to the Von Magnus phenomenon (Von Magnus, 1954), which in turn would have caused further induction of RIG-I leading to increased anti-viral IFN signalling and therefore reduced titres of infectious progeny virus. If a cell line is capable of

maintaining steady virus titres through to P5, MuV may not require adaptation and so genetic stability would be more likely to be maintained also.

N, F, HN and SH genes from passage level five viruses from various cell lines were sequenced and compared to the parental MuV sequences in order to assess the genetic stability of the virus upon serial passage. It was hypothesised that as MuV is a solely human virus it may be more genetically stable in cell lines of human origin. It is true that the cell lines producing the lowest numbers of mutations in Mu90 progeny are human (HGT-1, MCF-7 and Hep 2C), however some human cell lines also generated progeny viruses with a large quantity of amino acid mutations (A549 (BVDV) and RD) and RIT 4385 progeny virus from A549 (PIV5-V) cells also had many alterations present. All of the non-human primate cell lines investigated produced P5 progeny Mu90 viruses with a relatively high number of amino acid alterations, and cells of hamster, guinea pig and canine origin were similar to Vero which may indicate that overall, human cell lines are better are retaining wild-type MuV genetic stability but there will be exceptions to this and it will vary between cell types. MuV may not have required as extensive adaptation in HGT-1, MCF-7 and Hep 2C host cell environments, therefore keeping any mutations to a minimum. With respect to the numbers of amino acid alterations, RIT 4385 appears to be more stable during serial passage which may be because the virus is attenuated having become adapted to tissue culture through extensive serial passage during vaccine strain development.

The P5 progeny viruses from twelve out of seventeen cell lines showed an altered C-terminus amino acid sequence in the HN protein resulting in it being one residue longer than that of the parent virus. This group of cell lines were of human, non-human primate, guinea pig and canine origin so it appears these mutations are not specific to a certain host or cell type. The addition of an extra amino acid in all of these cell lines is likely to be due to the insertion of a nucleotide (thymine) at gene position 1725 (appendix III, page 300). Although this insertion is present in all seventeen cell lines, those not exhibiting the altered C-terminus amino acid sequence (MCF-7, HGT-1 and Vero) had

a nucleotide deletion at position 1716 (appendix III, page 300) which may have compensated for the thymine insertion. The additional residue was leucine (L), whereas the terminal HN parental virus protein is Threonine (T). With regards to the properties of these amino acids, L is hydrophobic and T has a hydrophilic-neutral charge, therefore the addition of an extra residue and the differences in biochemical properties may have an effect on the folding or conformation of the protein. Carboxyl methylation can occur on C-terminal L residues resulting in alterations to protein-protein interactions and/or protein function. T residues are also subject to post-translational modifications. If this happened it could cause problems for the virus binding to the host cell or for initiating fusion activity of the F protein which would affect the infection process. On the other hand the observed changes may be due to adaptation to the host cell and give the virus an advantage. The insertion of one nucleotide does suggest that the progeny P5 Mu90 MuV from these twelve cell lines no longer complies with the rule of six however this may have been compensated for in one of the other genes not sequenced in this project. It has not been possible to associate this HN protein alteration with viral fitness and/or plaque phenotype as no clear trend has emerged. These twelve cell lines are a group which demonstrate increase and decreases in progeny virus titre through P1 to P5, some show alterations in plaque morphology where others maintain the same plaque phenotype.

A similar amino acid addition was observed in the F protein of P5 Mu90 progeny virus from BSC-1 cells. One L residue was added on, making the terminal residue L instead of tyrosine (Y), which has similar properties to threonine. This extra amino acid was likely to be caused by the insertion of an extra nucleotide (cytosine) at position 1603 (appendix II, page 274). The addition of the L residue appears not to have had an effect on viral fitness (Figure 23) or plaque phenotype (Figure 24) therefore may have not had a detrimental effect on the virus. The insertion of one nucleotide does suggest that the Mu90 MuV from BSC-1 cells no longer complies with the rule of six however this may have been compensated for in one of the other genes not sequenced in this project.

The F proteins of Mu90 P5 progeny virus from A549 (BVDV) and MA-104 cells were shorter than the parental F protein by 18 and 26 amino acids respectively. This observed alteration in the A549 (BVDV) viruses may be as a result of mutations at the nucleotide level, specifically, a thymine insertion at gene position 1561 (appendix II, page 273) and two deletions at positions 1574 and 1584 (appendix II, page 274). The shortened F protein amino acid sequence in Mu90 MuV from MA-104 cells is likely to be due to a nucleotide substitution at positions 1539 (appendix II, page 273) which results in a stop codon (TAA). Mutations such as these have the potential to affect protein folding, binding and protein-protein interactions and in the case of the F protein could affect virus-cell and cell-cell membrane fusion. Mu90 MuV in A549 (BVDV) cells demonstrates an increase in virus titre by P5 and there is no significant change in plaque phenotype, therefore this protein mutation may be providing the virus with a replicative or infective advantage. The Mu90 progeny virus from MA-104 cells also increases in titre and therefore viral fitness, however a small plaque phenotype becomes more dominant by P5 which may be as a result of the shortened F protein amino acid sequence.

Another interesting mutation observed in progeny Mu90 from the twelve cell lines exhibiting the altered C-terminal HN amino acid sequence was an L to serine (S) substitution at position 576. This could potentially be the introduction of a site for serine protease activity which causes protein cleavage. A T to asparagine (N) substitution at position 24 of the Mu90 P5 HN protein was present in progeny viruses from all cell lines indicating that this mutation may be specific to Mu90 virus during passage and not caused by a certain cell line or type.

Phenylalanine (F) to L and isoleucine (I) to T substitutions were observed in the SH protein from Mu90 progeny viruses from all cell lines also. These amino acids have similar biochemical properties to one another and are likely to substitute for one another therefore it is possible the change had a minimal effect on structure and function of the proteins. The other amino acid substitutions that were present throughout the Mu90 and RIT 4385 progeny viruses appear to be unrelated and may be of a spurious relationship.

It has been reported many times that RNA viruses exist as quasispecies which have been defined as a population of the same viruses consisting of a so-called “master sequence” with a collection of mutant versions (Ruiz-Jarabo *et al.*, 2000). These quasispecies are thought to be formed as a result of the high mutation rates of RNA viruses brought about by internal replication errors and their fast growth kinetics, which is reviewed in (Lauring & Andino, 2010). In theory if a virus population exists like this, then it would be possible for certain variants to be selected by the host cell environment over others, and this would result in this selected variant being the more predominant one through passage. It may be that this was not the case in the P5 viruses sequenced in the experiments in this project as analysis of the nucleotide sequences showed the traces were “clean” and did not consist of more than one peak. However, variant selection may have taken place before P5 and it would have been of interest to sequence the N, F, HN and SH genes at P2, P3 and P4.

If time had permitted it would have been useful to have sequenced the remainder of the genome of the progeny Mu90 and RIT 4385 viruses to assess any nucleotide and amino acid mutations being introduced by serial passage through cell culture in the V/P/I, M and L proteins.

Plaque assays were carried out on designated “successful” cell lines (Table 11), using Mu90 as the inocula. Interestingly, all of the cells capable of supporting MuV plaque formation apart from LLC-MK2 are known to be deficient in an aspect of interferon production. Vero cells are well-known for this trait (Desmyter *et al.*, 1968) (Emeny & Morgan, 1979). A549 (PIV5-V) cells constitutively express the V protein of hPIV5, and A549 (BVDV) cells constitutively express the NPro protein of BVDV. The hPIV5 V protein has been demonstrated to inhibit production of IL-6 (Lin *et al.*, 2007), and to inhibit interferon signalling by targeting STAT-1 for proteosome-mediated degradation (Didcock *et al.*, 1999), whilst the BVDV NPro protein inhibits DNA binding by IRF-3 and targets this factor for degradation (Hilton *et al.*, 2006). LtK- cells have been reported not to induce an IFN response when treated with IFN-α (Mengheri *et al.*, 1983) and IFN-β (Shan & Lewis, 1989) which suggests that these cells are deficient somehow in interferon production. L20B cells are derived from LtK- (Mendelsohn

et al., 1989) so would be assumed to have this same characteristic. Although murine cells did support plaque formation, a smaller number of plaques were formed (42 and 30 respectively) compared to Vero cells (63), which could also indicate abortive infection. These data suggest that the ability of a cell line to support efficient MuV plaque formation is dependent upon whether or not the cells are able to produce IFN. This is in line with data observed for Foot-and-Mouth Disease virus plaque formation, which has also been reported to be dependent upon IFN suppression in cell cultures (Chinsangaram *et al.*, 1999) as has vaccinia virus plaque formation (Gifford *et al.*, 1963).

Despite the high GFP expression levels and reasonably high titres of progeny virus production, LLC-MK2 cells did not support plaque formation as efficiently as the other five cell lines and only 1 to 2 plaques were evident in each of the triplicate wells. When observed microscopically using bright field, CPE can be seen in cultures of LLC-MK2 cells from 72 hours post infection as syncytia formation. However, over the seven days after the onset of CPE, no cell lysis is observed and the cell monolayer remains intact. This could potentially be due to the action of the SH protein which has recently been demonstrated to play a major role in preventing apoptosis of the host cells by targeting ataxin-1 ubiquitin-like interacting protein 4 (Woznik *et al.*, 2010). It could also be as a result of the cells growing faster than the virus. A549 (PIV5-V) were the only cells to be as sensitive for plaque formation as the Vero control, and both formed plaques of a similar morphology although those on A549 (PIV5-V) were smaller in size. A549 (BVDV) cells also produced plaques of a similar morphology to this although the cells appeared to be less sensitive. These cells also gave slightly different results with regards to GFP expression and progeny virus titres, with the PIV5-V cells expressing lower levels of GFP but producing slightly higher titres of progeny RIT 4385 and Mu90 viruses when compared with the BVDV cells. The differences do not appear to be statistically significant, but they are noticeable from the data.

Both of these cell lines have been genetically engineered to be insensitive to interferon (Young *et al.*, 2003) using A549 as the parent cell line. A549 cells were included in the experiments to act as a

control for the IFN-sensitive cells, and did not show any evidence of GFP expression or CPE and produced significantly lower titres of progeny virus than the genetically engineered cells. The differences in results may be due to the activities of the V and NPro proteins, for instance does one exert a stronger anti-viral effect than the other, or the levels of protein expression. This method of engineering cells has also been successfully carried out to allow increased viral replication in MRC-5 and Hep2 cells (Young *et al.*, 2003), and there is potential for these techniques to be used on other candidate cell lines, for example, engineering a cell line that produced no infectious MuV and demonstrated no GFP expression such as Mpf (ferret brain) to constitutively express an accessory protein known to interfere with the host cell IFN response. The data obtained from infection of the three A549 cell lines with GFP-MuV, Mu90 and RIT 4385 have demonstrated how important the anti-viral response of a host cell is and that interfering with this response at a constant rate as in the genetically engineered cells, makes a cell line more permissive for MuV infection and replication.

From the data obtained in these *in vitro* studies, A549 (PIV5-V) cells could be used as an alternative cell line to Vero's for assessing plaque formation and morphology. It may be that there is not just one cell line suitable for all aspects of MuV propagation, but a few cell lines, which can be of value depending upon the purpose they are to be used for. For example, LLC-MK2 cells could be used for expressing large quantities of viral proteins, whereas HGT-1 cells could be used for producing high titres of wild-type or clinical progeny MuV. The data also suggests that cell lines of human origin maintain MuV genetic stability better than non-human primate cells, and that Hep 2C, HGT-1 and MCF-7 cells proved most successful in these experiments. One of these cell lines could be used as an alternative to Vero cells for propagating MuV stocks and if samples had been readily available, it would have been very interesting to find out how successful these cells are at isolating MuV from clinical patient samples.

3.7.2 Sialic Acid Studies

The molecular reasons for a cell line being able to support successful MuV growth and replication are unclear. Virus infection of a host cell is a complex, multifactoral process and there are undoubtedly many elements involved. One aim of this project was to assess whether or not concentration of total sialic acid or type of linkage (α2,3 or α2,6) was one of these molecular determinants.

The results from the sialic acid quantification bioassay suggested that concentration of total SA expressed (mM) does not correlate with how efficient a cell line is at propagating MuV, therefore it was hypothesised that the type of SA linkage present on a cells surface may be a factor involved in successful MuV infection and perhaps the virus demonstrates a preference for either α2,3 or α2, 6 moieties. Receptor-binding SA preferences are well-characterised in human and avian influenza viruses. It has been shown that Adenovirus Type 37 binds preferentially to α2,3 SA (Arnberg *et al.*, 2000) and polyoma virus JC binds to both types of SA linkage (Dugan *et al.*, 2008). In this thesis, DIG glycan differentiation FACS analysis was performed on a panel of 15 cell lines, including two controls (Vero and MDCK-SIAT1) and the results indicate that the type of SA linkage expressed on a cell surface does also not correlate with the success of a cell line at supporting MuV growth.

Infection of MDCK-SIAT1 cells expressing increased α2,6 and reduced α2,3 moieties (Matrosovich *et al.*, 2003) with Mu90 and RIT 4385 produced lower titres of progeny virus compared with parental MDCK cells expressing an approximately equal amount of both SA types (Matrosovich *et al.*, 2003). This suggested that a lower amount of available α2,3 SA has a negative effect on the MuV host cell infection and/or replication process, which may indicate a preference for α2,3 SA despite the bioassay and FACS data. Treatment of various cell lines with lectin from MAA to block α2,3 residues did not significantly decrease progeny MuV titres or the time point at which MuV was released from the host cells when compared with PBS-treated cells, and the results were the same when cells were blocked with lectin from SNA to block α2,6 residues or with a mixture of both. There are several

potential explanations for the observed results from the blocking assays. The bonds formed between the lectins and SA molecules may not have been a tight enough "block" and the receptors may still have been exposed in some way for the MuVs to bind. If the lectin block had been effective, the virus possibly entered the cell by using another receptor molecule although this is unlikely due to the fact that treating cells with sialidase protects the cell from MuV infection (Markwell, 1991) and the HN glycoprotein possesses neuraminidase activity which specifically acts by cleaving sialic acid as part of the virus life cycle. SA also exists as an α2,8 analogue and if MuV binds non-preferentially to SA molecules then the virus may have entered the cell via α2,8 residues when α2,3 and α2,6 were blocked by the lectins. It would have been useful to treat several continuous cell lines and HAE cultures with a neuraminidase to confirm that the destruction of SA residues completely prevents MuV infection. If time had permitted, the Biacore (GE Healthcare) surface plasmon resonance (SPR) facility which is newly available at NIBSC could have been employed as a means of studying the molecular interaction between the different types of SA receptor residue and the HN glycoprotein. SPR operates on the basis of measuring changes in the refractive index of optical waves extremely close to a sensor surface, which is normally the protein or ligand of interest (E.g. MuV HN) immobilised on a chip. The other molecule of interest (E.g. sialic acid-containing compounds) is passed over the chip in solution and the binding and release of the compounds changes the refractive index, therefore the kinetics of binding can be measure to a highly precise level (reviewed in (McDonnell, 2001)). SPR has previously been used successfully for identification of a panel of human glycoproteins using lectins (Safina *et al.*, 2011) and the Biacore system has recently been applied to analysing the binding kinetics of RNA aptamers to the haemagglutinin protein of influenza virus (Misono & Kumar, 2005). This technique would provide new and interesting data on MuV receptor binding.

3.7.3 Investigation of HAE Cells

HAE cells have been used to generate data on – ssRNA viruses however have not been previously used to investigate MuV infection. RIT4385, Mu90 and clinical AFZ315 MuVs were used to demonstrate that HAE cells are susceptible to MuV infection and are capable of effectively propagating clinical, laboratory wild-type strain, and attenuated vaccine MuVs, as well as being able to isolate the virus directly from a clinical sample. The delay in clinical virus replication and/or release when compared with Mu90 and RIT 4385 may be due to the fact that the latter two viruses have both become adapted to *in vitro* cell systems whereas the clinical isolate came from a patient and required a certain adaptation period to the cell culture environment. The titre of the virus in the saliva could also have been of an extremely low titre and therefore a much lower MOI. This is a common problem when attempting to isolate MuV in a diagnostic setting.

In stained sections of infected HAE cells, the F protein was shown to be located in both apical and basal cells, but appears to be more prominent in the basal cell section. As the presence of a protein does not automatically infer viral replication, the clinical MuV may have a greater affinity for replication in basal cell types or it may be visualised in this area as a result of virus 'leaking' from apical cells caused by the breakdown of tight junctions. As a means of confirming if this was a factor in the accumulation of MuV in basal cells, the HAE sections could have been counter-stained with an antibody against the tight junction protein zonula occludens (ZO)-1 (Stevenson *et al.*, 1986). If the virus was replicating efficiently in the basolateral cells, it would be expected that MuV would be released from these cells into the basal medium otherwise the progeny viruses may need to traverse back up to the apical cells to be released. When the basal medium was titrated on Vero cells, tiny plaques were observed from samples at every time point from 6 hours to 10 days post infection. MuV typically takes on average 48 to 72 hours to start showing signs of CPE in tissue culture therefore it was a surprise to find evidence of infectious progeny virus at such early time points. No MuV RNA was detected by RT-PCR in any of the basal samples therefore it is possible that the small

plaques observed were not caused by the virus. They may have been artefactual plaques caused by a molecule(s) that was being secreted by the HAE cells in response to infection. Another possibility is that there were inhibitory compounds present in the basal medium that exerted their effect during RNA isolation or RT-PCR, and the tiny plaques were indeed caused by MuV. The small plaque phenotype could be due to the effect of cytokines or IFNs being secreted by the cell which would be present in the sample upon inoculation onto Vero cells. Although these cells are known not to be capable of producing IFN (Emeny & Morgan, 1979), they can be treated with IFN. Vero cells treated with IFN have previously been demonstrated to have an inhibitory effect on Herpes Simplex Virus (HSV)-2 plaque formation (Petrera & Coto, 2006). To investigate this further, the HAE basal samples from various time points could have been inoculated onto Vero or other cell cultures and observed for formation of MuV CPE.

Ciliated cells are known to express more α-2,3 than α-2,6-linked sialic acid, whereas non-ciliated cells express a higher quantity of α-2,6-linked sialic acid molecules (Thompson *et al.*, 2006). The images do not conclusively indicate that MuV is capable of infecting both ciliated and non-ciliated cells, and further studies of this type at earlier time points with different MuVs would be useful to validate the sialic acid assay results obtained in this project which indicate that MuV does not exhibit a preference for one type over the other.

It has recently been suggested that Vero cells may produce viruses with altered gene sequences that are unsuitable for research purposes (Afzal *et al.*, 2005), however this had not yet been established. MuV titres from Vero cells were higher than those from HAE cells, but this was at a price. The data in these experiments has shown that propagating a clinical MuV in Vero cells results in mutations of varying severity in at least four (N, F, HN and SH) out of seven MuV genes, indicating that Vero cells should not be used for growth of clinical isolates that will be used for research. In contrast, HAE cells produce more genetically stable progeny virus with very similar or identical genotypic properties to those of the parent virus, albeit with infectious progeny viruses detected 24 hours later and with

slightly lower infectious titres. Nucleotide substitutions at positions 1548 and 1613 of the progeny virus HN and F genes respectively both resulted in tyrosine to cysteine amino acid residue alterations. Both have polar, uncharged side chains and due to their similar biochemical properties, are likely to substitute for each other in a situation where mutations may arise.

Due to the similarities between tyrosine and cysteine, the mutations seen in the day 5, 6 and 7 progeny virus HN and F proteins may be ineffectual to protein function and structure. The MuV HN envelope glycoprotein is responsible for binding to the cellular sialic acid receptor and therefore plays a major role in infection. The N terminus contains a hydrophobic sequence of 19 amino acids responsible for the anchoring of the protein in the virus envelope (Waxham *et al.*, 1988) and potential glycosylation sites of the HN protein have also been identified (Kovamees *et al.*, 1989). Amino acid change S466D was shown to reduce receptor binding affinity and neuraminidase activity in a wild-type MuV (Malik *et al.*, 2007) and amino acid change E335K in the HN protein has also been demonstrated to alter receptor binding specificity of the Urabe strain of MuV (Reyes-Leyva *et al.*, 2007). The Y539C substitution was not located in the vicinity of or upstream of any known significant sites. The F envelope glycoprotein of MuV drives virus to cell and cell to cell fusion, resulting in entry of viral genomic information into the host cell which are essential activities for virus spread. A protease-dependent cleavage site is known to be located between amino acids 102 and 103, with a membrane anchor region of 30 hydrophobic residues in the C terminus (Waxham *et al.*, 1987). A leucine residue at position 383 of a wild-type MuV was shown to confer fusogenicity in B95a cells (Yoshida & Nakayama, 2010), and this amino acid is present in the parent and progeny clinical viruses from this study. The Y538 mutation identified in the F protein is not located in any of the known regions significant for function.

In conclusion, the *in vitro* MucilAir™ HAE cell model is capable of efficient propagation of both wild-type and vaccine mumps viruses. These cells can be used for direct MuV isolation from a clinical sample, producing high titre progeny virus with highly similar genotypic properties to that of the

parent titre when compared with “gold standard” Vero cells. If time had permitted, it would have been of value to have sequenced the entire genome of the parent AFZ315 and HAE progeny viruses in order to determine if there were any significant amino acid alterations in any of the other viral proteins not included in these experiments (V/P/I, M and L). It would have been of interest to infect these cells with a large panel of MuVs representing different genotypes, phenotypes and also to determine if HAE cells are capable of isolating clinical MuV from different types of patient samples (E.g. urine or nose/throat swabs) in order to further confirm and elaborate on the data obtained in this PhD project. The data demonstrate for the first time that growth of MuV in Vero cells results in mutations in genes important in virus transcription, entry and spread, and these mutations are introduced not only through serial passage but also during persistent replication in a single culture. HAE cells have a potential to be a very valuable tool for diagnostic and mumps research laboratories.

CHAPTER 4 – IN VIVO RESULTS

There is currently no animal model for mumps virus, and one of the aims of this project was to assess ferrets as an *in vivo* model for experimental MuV infection.

Ferrets have been used effectively as an animal model for many pathogenic organisms including strains of Campylobacter (Bell & Manning, 1990) and Helicobacter (Fox *et al.*, 1990) bacteria, and the viruses SARS (Martina *et al.*, 2003) and CDV as model for human Measles virus (Pillet *et al.*, 2009). The ferret may be best known within the field of virology for its use as an experimental model for influenza infection, pathogenesis and transmission, which is reviewed in (Maher & DeStefano, 2004).

Influenza and MuV are both negative-sense ssRNA viruses and share other biological properties such as the use of sialic acid-containing molecules as a cellular receptor, and both contain proteins with haemagglutinin and neuraminidase activities. The respiratory tract of the ferret is known to present cells with similar sialic acid patterns as that of the human respiratory tract (van Riel *et al.*, 2007), and this has recently been extensively characterised using multiplex staining with various plant lectins and human adapted influenza haemagglutinins (Jayaraman *et al.*, 2012). These data indicate that ferrets may be a suitable model for mumps virus.

Four separate ferret studies were carried out in this project, using male animals in all experiments.

The initial study designated A was performed with clinical and vaccine strains of MuV over 28 days to assess clinical signs of infection, virus shedding in nasal washes, urine and faeces, production of neutralising antibodies and ability to recover virus from tissues on day 28 post infection. The second study designated B was carried out in order to investigate whether or not the antibodies produced by ferrets in A were specific to MuV, by using a heat-inactivated vaccine virus. The purpose of the study designated C, was to investigate virus shedding in oral fluid, cytokine mRNA levels in PBMCs and ability to recover virus from tissues at days 1, 4, 7 and 14 post infection with the same clinical virus used in study A. The final *in vivo* study designated D, was carried out in order to assess whether

or not a higher titre of inoculum virus would increase the likelihood of virus recovery from tissues at days 4 and 7 post infection.

4.1 Ferret Study A

4.1.1 Clinical Signs of Infection

Two groups of 3 male ferrets (designated 1, 2 and 3) were inoculated intranasally with either clinical mumps sample AFZ315 or RIT 4385 vaccine strain mumps virus (designated 4, 5 and 6). For 28 days post infection, body weight, temperature, testes width and depth, and parotid swelling around the head and from ear to ear were measured and values recorded. Figure 53 provides a summary of Study A.

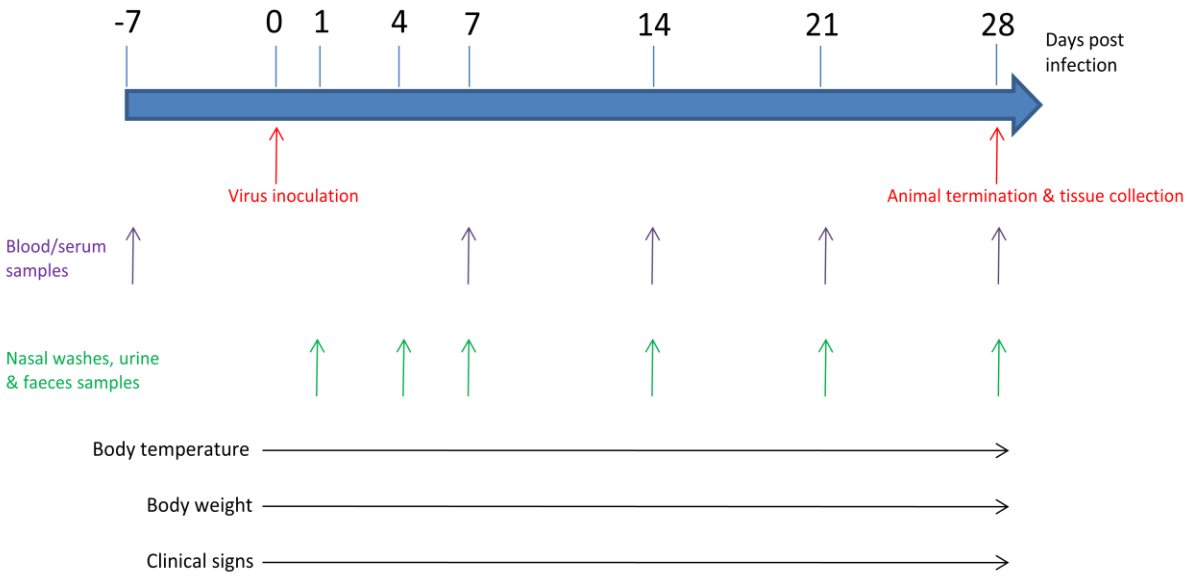

Figure 53 – Ferret study A summary. Clinical observations made and samples collected from ferrets inoculated with either clinical or attenuated vaccine MuV over a 28 day period.

Clinical data are presented in Figure 54. No significant increases or decreases in body weight or temperature were recorded for any of the ferrets. The recorded increase in testes width and depth was due to the fact that the ferrets were at an age associated with reaching sexual maturity and the testes were growing in size, however, it was noted by NIBSC BSD staff that on day 4 post infection the testes of ferret 3 were noticeably redder. Testes width and depth could not be measured on ferrets 1 and 2 as no testes were visible on these 2 males. The recorded increases in parotid swelling of all ferrets at various time points throughout the study were also due to growth of the ferrets. No changes in behaviour were noticed in any of ferrets 1 to 6 and the animals appeared healthy, and with no loss of appetite for the entire 28 days of the study.

a) Ferrets 1-3, clinical mumps virus

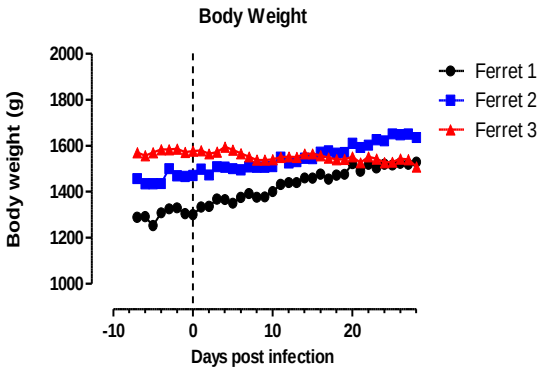

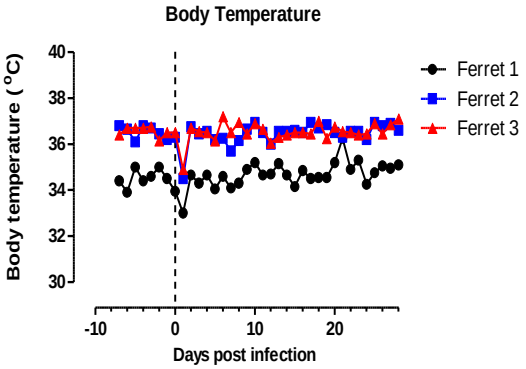

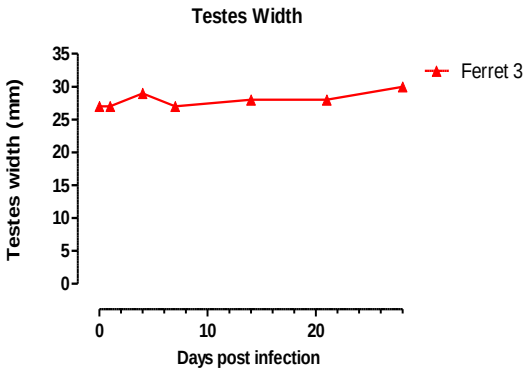

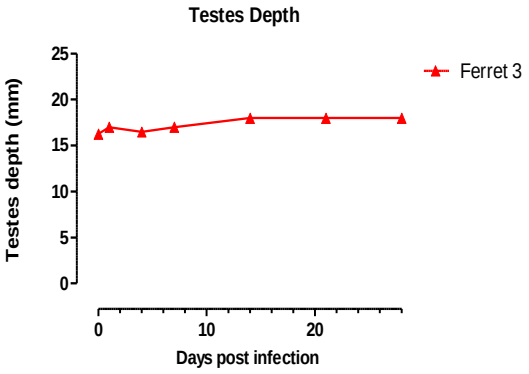

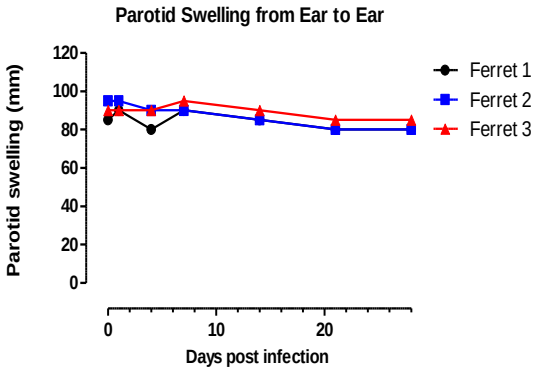

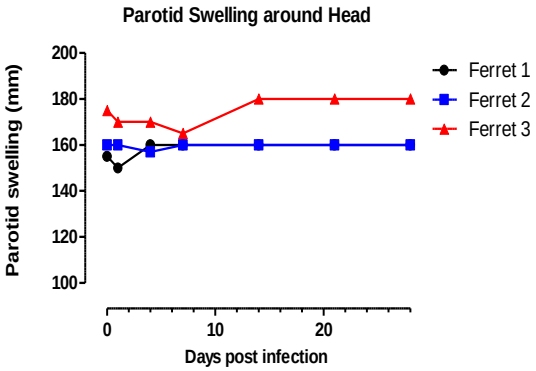

b) Ferrets 4-6, vaccine mumps virus

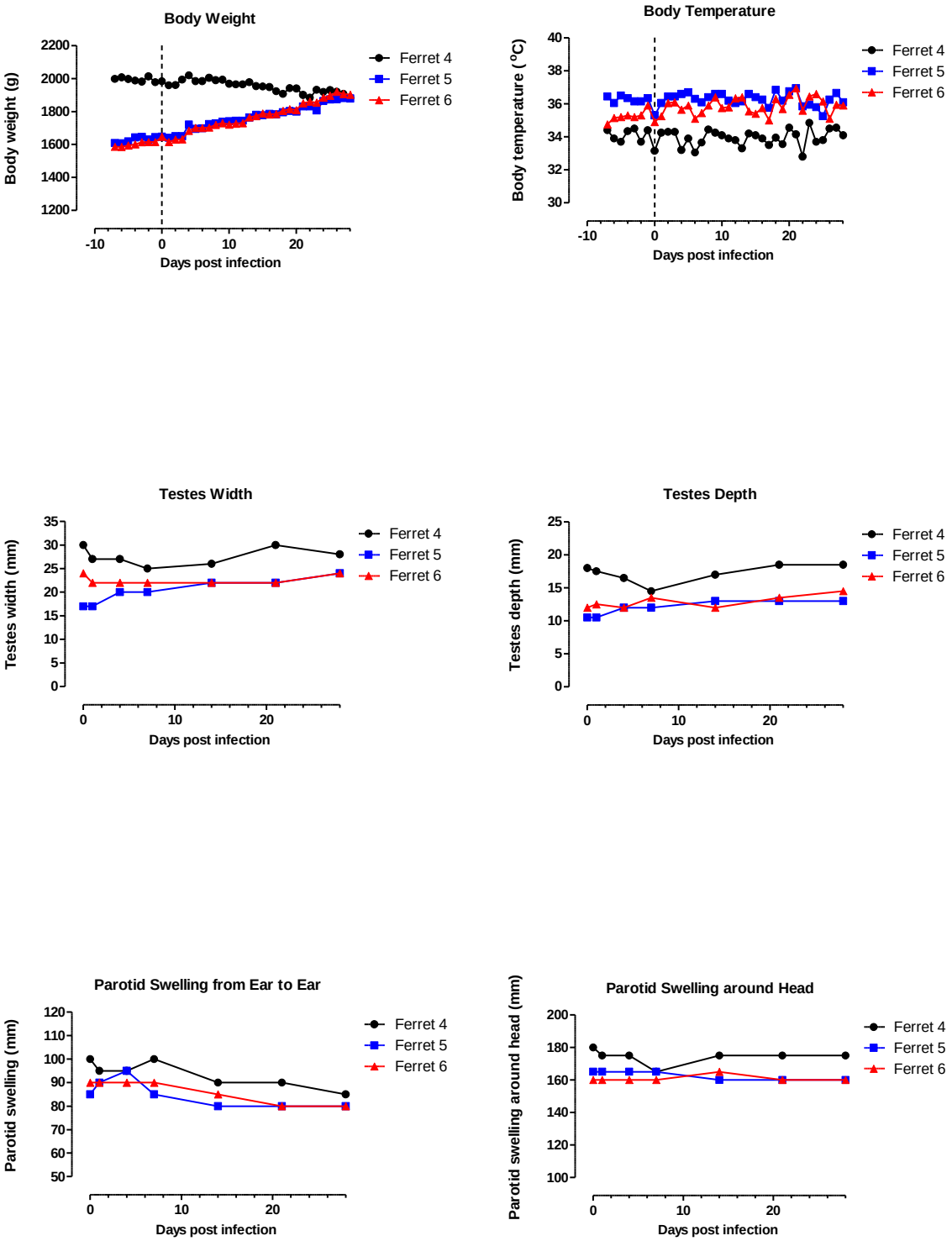

Figure 54 – Ferret Study A Clinical Symptoms Observations. Body weight, temperature, size of testes and parotid swelling of animals inoculated with 7 x 10^3 pfu in saliva from a mumps patient (a) or with 2 x 10^4 pfu of the RIT 4385 mumps vaccine (b).

4.1.2 Isolation of Virus from Nasal Washes, Urine and Faeces

Processed and clarified nasal washes, urine and faeces samples from ferrets 1-6 were inoculated onto Vero cells, incubated at 35°C, 5% CO_2 for 10 days and examined daily for signs of CPE. The resulting cell lysates were blind-passaged once onto Vero cells and incubated and examined as before. None of the inoculated cell cultures demonstrated evidence of CPE.

RNA was isolated from all cell lysates from nasal wash, urine and faces samples and analysed by standard RT-PCR and then nested PCR for presence of MuV SH gene mRNA. This was done using primers JLSH1Fw and JLSH2Rv, and JLSH3Fw and JLSH4Rv respectively. All RT and nested PCR products were found to be negative when electrophoresed on a 1% agarose gel.

RNA was also extracted from neat nasal washes, urine and faeces samples, and analysed by real-time RT-PCR for presence of MuV SH gene mRNA using either AFZ315SHF, AFZ315SHR and AFZ315P primers and probe for ferrets 1 to 3, or JLSHF, JLSHR and JLSHP primers and probe for ferrets 4 to 6. All of the test samples were found to be negative.

Negative and positive controls included in these experiments were valid, and all were performed in triplicate.

No clinical or vaccine mumps viruses were detected by cell culture or PCR methods in nasal washes, urine or faeces at 1, 4, 7, 14, 21 or 28 days post infection.

4.1.3 PRN Assays

PRN assays measure the serum dilution required to reduce plaque formation by the virus in cell cultures by 50%. These were carried out in order to determine whether or not the test ferrets elicited an antibody response to infection with MuV. The average plaque count obtained from the positive control (no sera, challenge vaccine virus only) was 50. Figure 55 shows the results obtained.

All animals produced anti-mumps antibodies by day 28 as demonstrated by increased ND_{50} values (Figure 55). The ND_{50} value of the human mumps serum 93/582 was lower than any of these values, which showed that the antibodies produced by the ferrets had a higher neutralising activity than the human serum. For example, the serum from ferret 1, day 28 post infection would require an approximate 1 in 42 dilution to reduce plaque formation by 50%, whereas 93/582 would require being more concentrated, with an approximate 1 in 11 dilution.

Pre-bleed samples were taken from all ferrets 7 days prior to inoculation to act as a control, yet they also showed a reduction in plaque number, and had ND_{50} values similar to those obtained from day 7 and day 14 sera samples.

a) Ferrets 1-3, clinical mumps virus and human reference serum

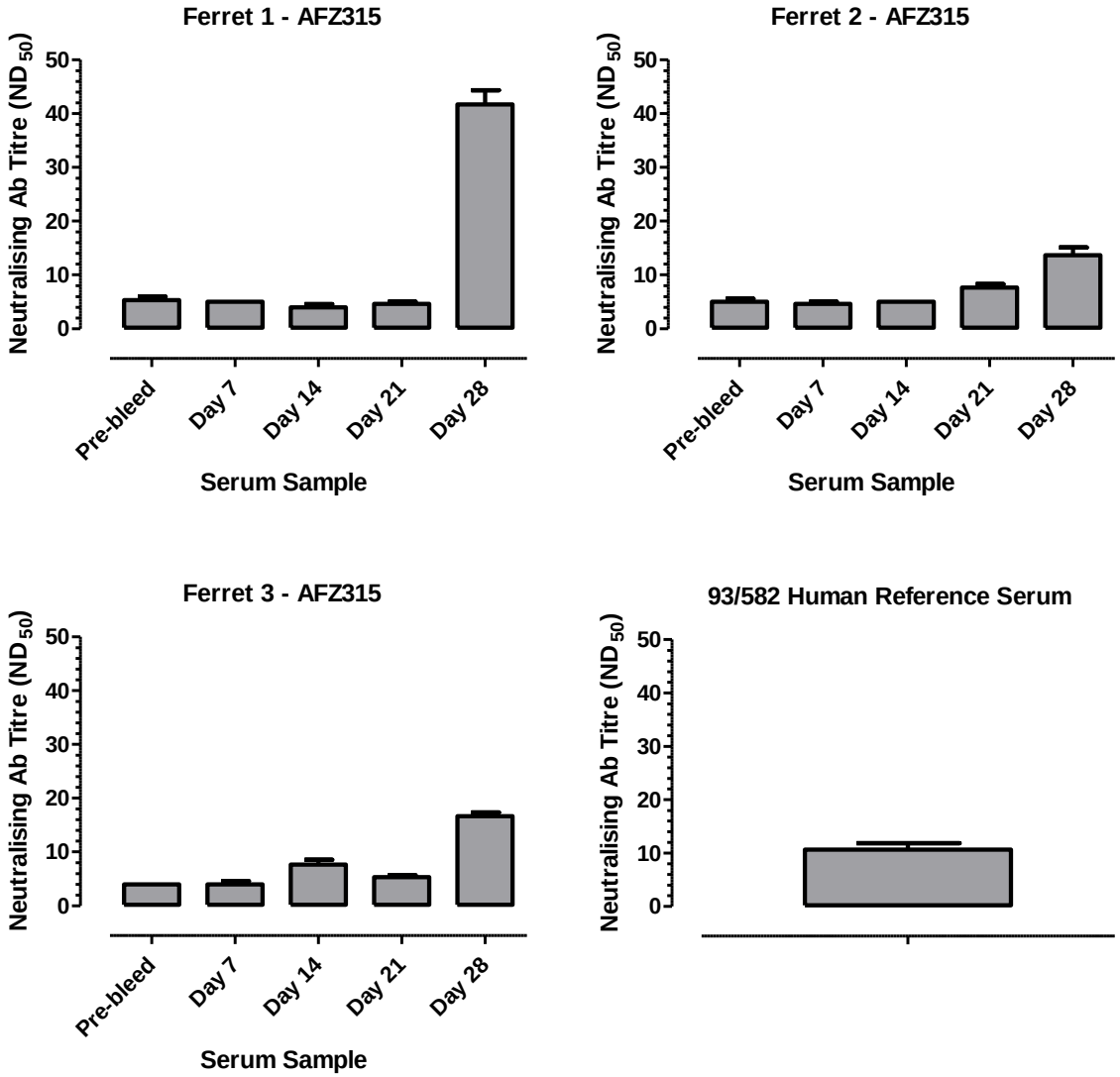

b) Ferrets 4-6, vaccine mumps virus and human reference serum

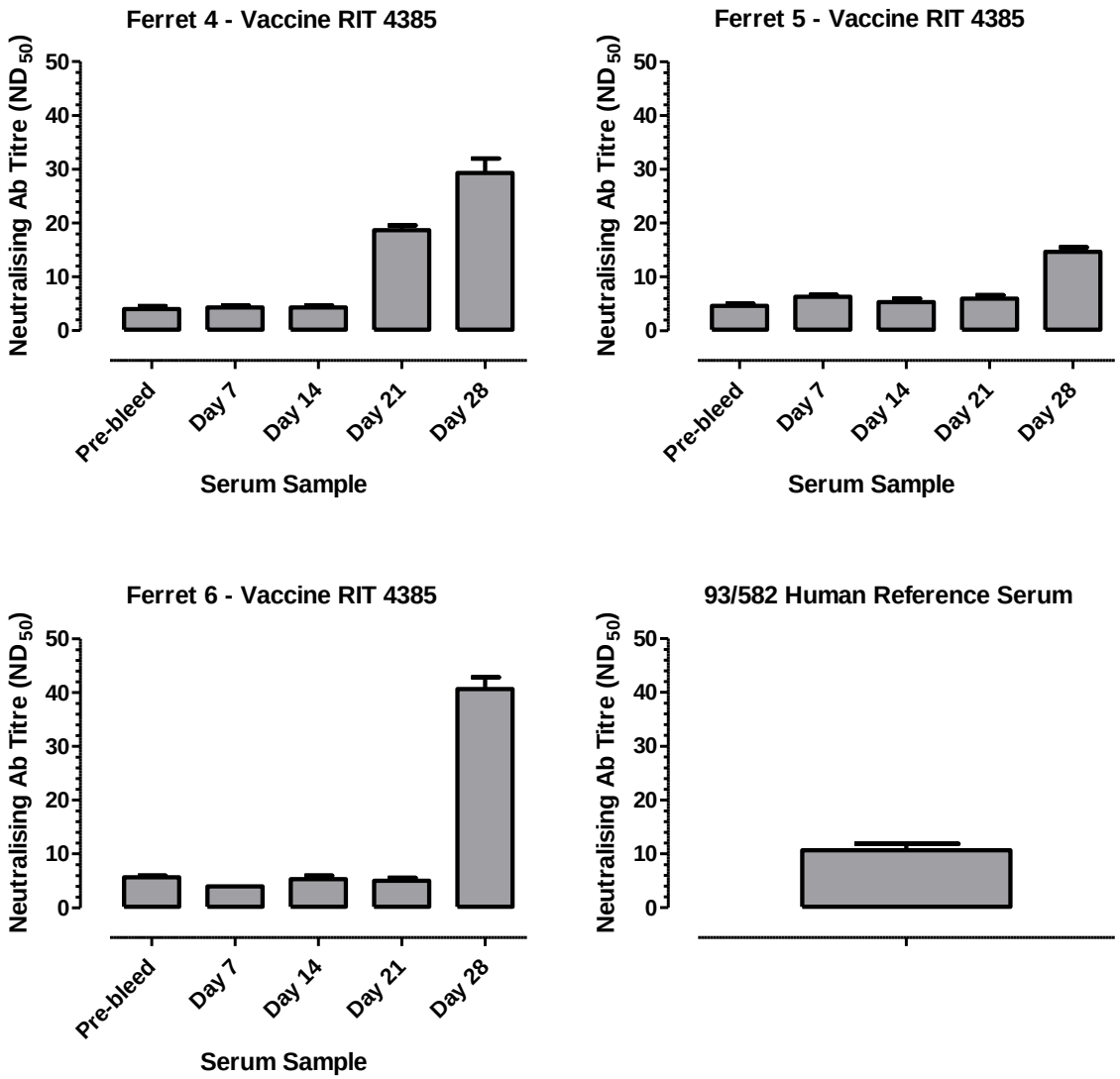

Figure 55 – Ferret study A Mean ND_{50} values of neutralising antibodies produced in response to infection with clinical AFZ315 (a) or attenuated RIT 4385 vaccine (b) mumps viruses. Sera obtained from ferrets inoculated with AFZ315 or RIT 4385 were challenged with MuVs LO-1 or RIT 4385 respectively and the dilution required to reduce number of plaques by 50% (ND_{50} titre) was calculated. A human reference standard (93/582) used in MMR batch release assays at NIBSC was included as a reference control. All PRN assays were performed in triplicate and the data represents the mean and standard deviation.

4.1.4 Recovery of Virus from day 28 Ferret Tissues

Ferrets infected with clinical or vaccine mumps viruses were terminated on day 28 post infection and tissues harvested (Table 10). The tissues were chosen based on those that have been implicated in mumps cases in humans, and several others that are often affected during viral infection in general. Whole tissues were used to prepare 20% homogenates and these were analysed for presence of cultivable MuV and viral RNA which would give an indication of the tropism of these viruses.

Clarified homogenates were inoculated onto Vero cells, incubated at 35°C, 5% CO_2 for 10 days and examined daily for signs of CPE. The resulting cell lysates were blind-passaged once onto Vero cells and incubated and examined as before. None of the inoculated cell cultures demonstrated evidence of CPE. RNA was isolated from all cell lysates from tissue homogenate samples and analysed by standard RT-PCR and nested PCR for presence of MuV SH gene mRNA using JLSH1Fw and JLSH2Rv, or JLSH3Fw and JLSH4Rv respectively. All RT-PCR products were found to be negative when electrophoresed on a 1% agarose gel. Negative (H_2O) and positive (AFZ315 or RIT 4385 parent viruses) controls included in these experiments were valid.

RNA was also extracted directly from the 20% tissue homogenates and analysed for the presence of MuV SH gene mRNA using either AFZ315SHF, AFZ315SHR and AFZ315P primers and probe for ferrets 1 to 3, or JLSHF, JLSHR and JLSHP primers and probe for ferrets 4 to 6. Glyceraldehyde 3-phosphate dehydrogenase (GAPDH) gene mRNA was measured using GAPDH535Fw, GAPDH680Rv and GAPDH primers and probe. GAPDH is an enzyme involved in carbohydrate metabolism and due to its ubiquitous presence in eukaryotic organisms, is often referred to as a "housekeeping" gene. GAPDH was included in these experiments as a control to confirm that the total RNA extracted from each sample was present and amplifiable. Each RT-PCR reaction was performed in triplicate.

GAPDH mRNA was detected in varying quantities in all of the tissue samples from ferrets 1-6, apart from ferrets 1, 2 and 3 colon, and ferrets 4, 5 and 6 small intestine homogenates. Salivary glands

from ferrets 2 and 3 were unable to be located and removed at the time of tissue harvest, so there is no data available for these. The data is shown in Figure 56. This demonstrates that the total RNA isolated was capable of being amplified by the real-time RT-PCR method used.

RNA extractions and real-time PCR reactions were performed three times on the colon and small intestine samples and were unsuccessful on all occasions, which may have been due to the large amounts of faeces present in the tissues upon harvest.

The MuV positive controls included were standard dilution curves of clinical AFZ315 and vaccine RIT 4385 viruses. The dilutions ranged from neat virus to 10^{-7} and each contained a known quantity of virus measured in plaque-forming units (pfu). Both of these virus controls were valid and the values are shown in Figure 56. All negative non-template controls (NTC) were valid.

All of the day 28 tissue homogenate samples from ferrets 1-6 were negative when analysed by real-time RT-PCR.

In summary, no cultivable clinical or vaccine mumps viruses or viral RNA were recovered from any of the ferret tissues by the methods employed here.

a) Ferrets 1-3, clinical mumps virus, GAPDH internal control mRNA levels

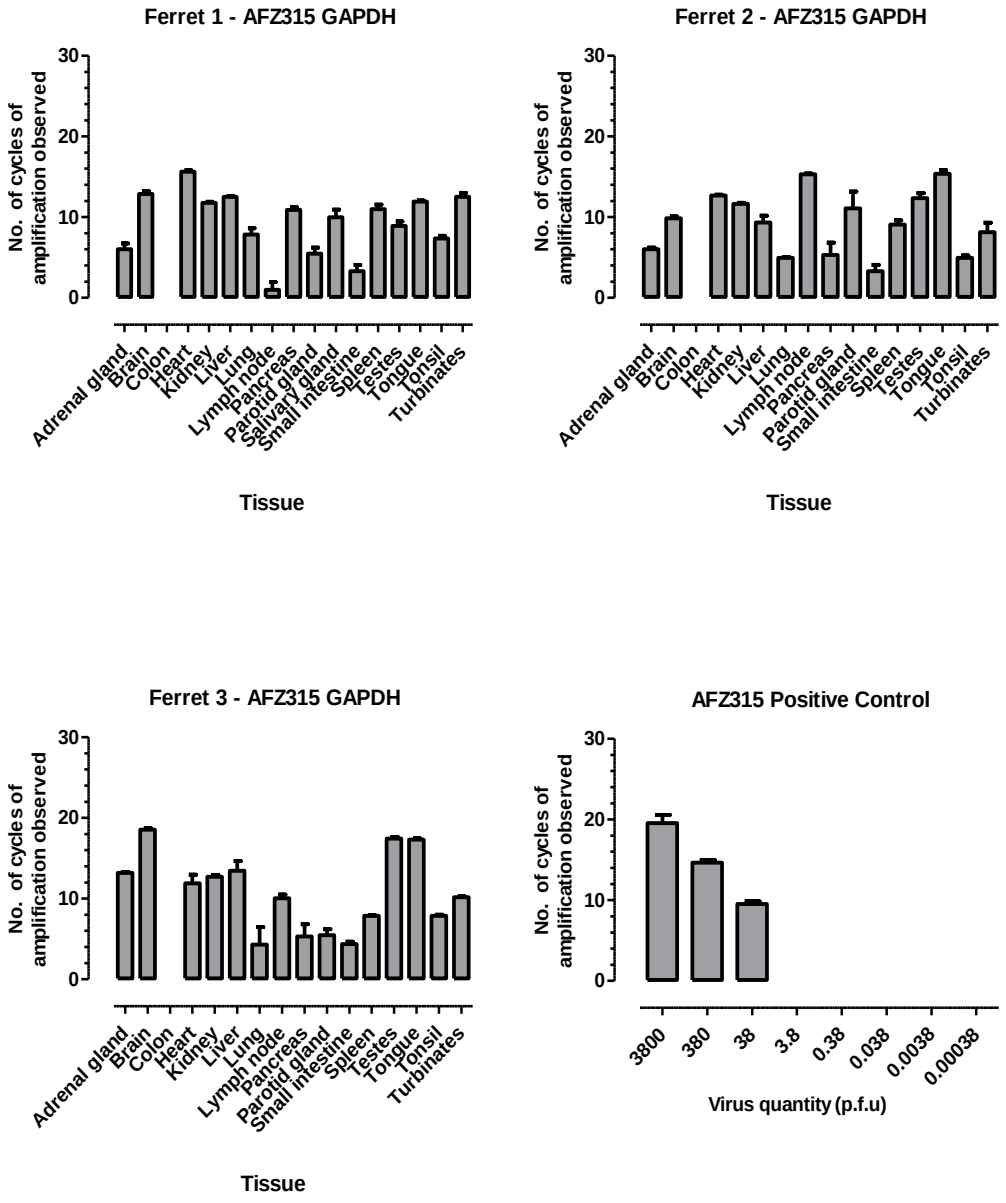

Figure 56 – Ferret study A, ferrets 1 to 3 inoculated with AFZ315 day 28 tissues real-time PCR data.

GAPDH mRNA levels in 20% tissue homogenates from ferrets infected with MuV AFZ315 were measured by real-time PCR as an internal control. No MuV mRNA was detected in any of the ferret tissues, and the positive control included demonstrates that the lowest virus quantity which could be detected by this method is 38 pfu. Assays were performed in triplicate and the data displayed represents the mean and standard deviation.

b) Ferrets 4-6, vaccine mumps virus, GAPDH internal control mRNA levels

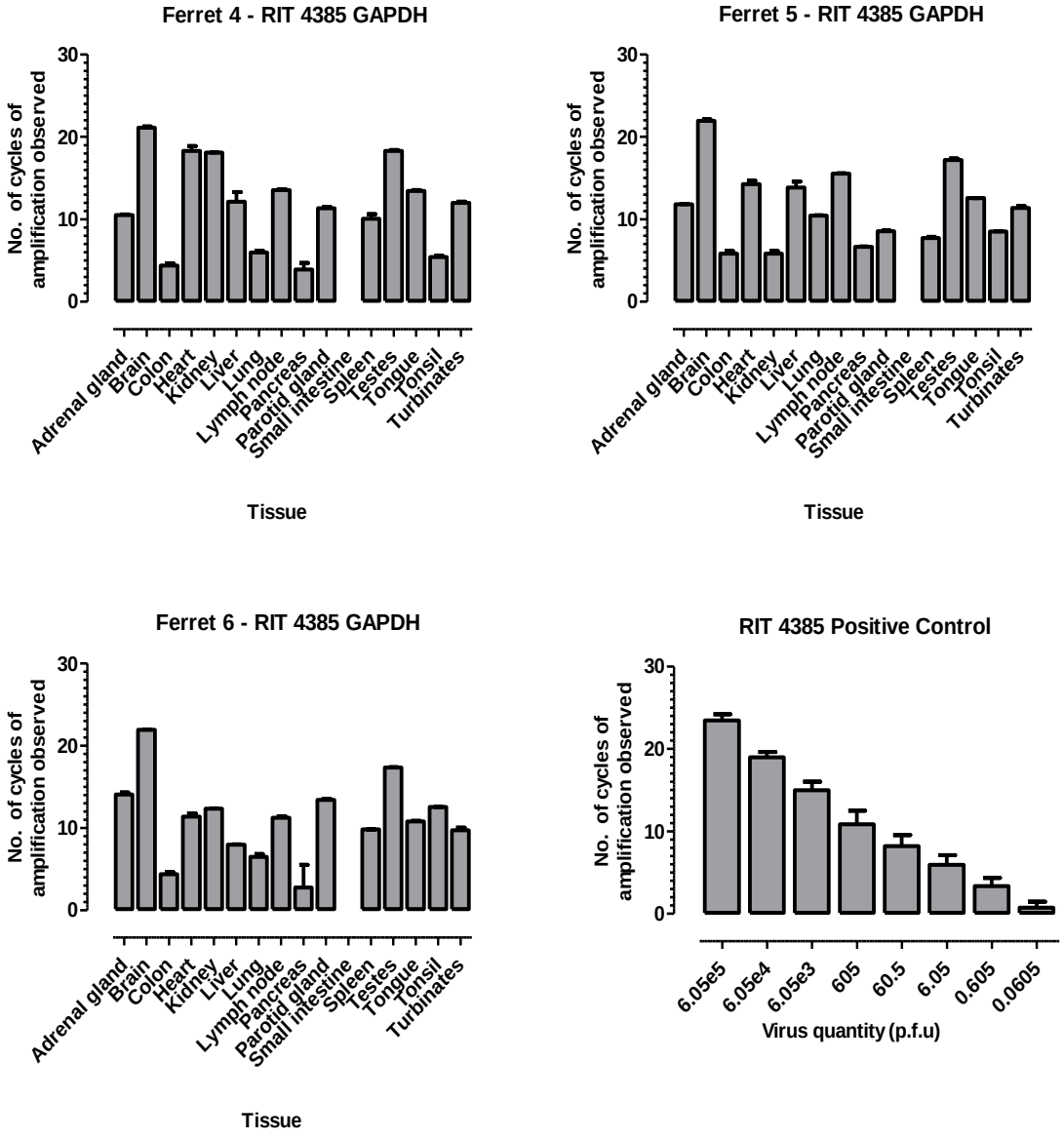

<u>Figure 56 – Ferret study A, ferrets 4 to 6 inoculated with RIT 4385 day 28 tissues real-time PCR data.</u> GAPDH mRNA levels in 20% tissue homogenates from ferrets infected with MuV RIT 4385 were measured by real-time PCR as an internal control. No MuV mRNA was detected in any of the ferret tissues, and the positive control included demonstrates that the lowest virus quantity which could be detected by this method is 38 pfu. Assays were performed in triplicate and the data displayed represents the mean and standard deviation.

4.2 Ferret Study B

4.2.1 Heat-inactivation of MuV

Mumps vaccine virus RIT 4385 was heat-inactivated by incubating at 56°C for 30 min. To confirm that this process had eliminated the infectivity of the virus a plaque assay on Vero cells was performed, including a live RIT 4385 as a positive control.

No plaques or CPE were evident by day 10 post infection on the Vero cells inoculated with the heat-inactivated virus, and the positive and negative controls were valid.

RNA was extracted from 10-fold dilution series of live and heat-inactivated RIT 4385 containing known quantities of virus and analysed by real-time RT-PCR using JLSHF, JLSHR and JLSHP primers and probe to confirm that the heat-inactivated virus was still genetically stable and intact. Each reaction was performed in triplicate and all negative NTC controls were valid.

The real-time PCR data from this experiment is shown in Figure 57.

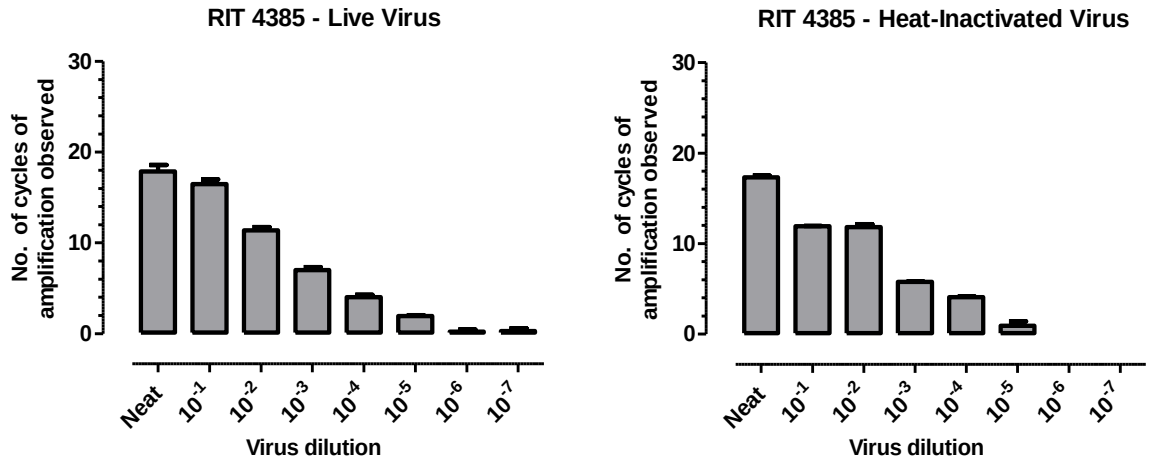

Figure 57 – Live versus heat-inactivated MuV RIT 4385 real-time PCR data. Real-time RT-PCR was performed on 10-fold serial dilutions of live and heat-inactivated RIT 4385 MuV vaccine virus and levels of detectable MuV RIT 4385 SH gene mRNA were compared. Assays were performed in triplicate and data displayed represents the mean and standard deviation.

4.2.2 PRN Assays

Three male ferrets were inoculated intranasally with heat-inactivated RIT 4385 attenuated vaccine virus, and blood samples were collected every 7 days until day 28 post infection. Figure 58 provides a summary of Study B.

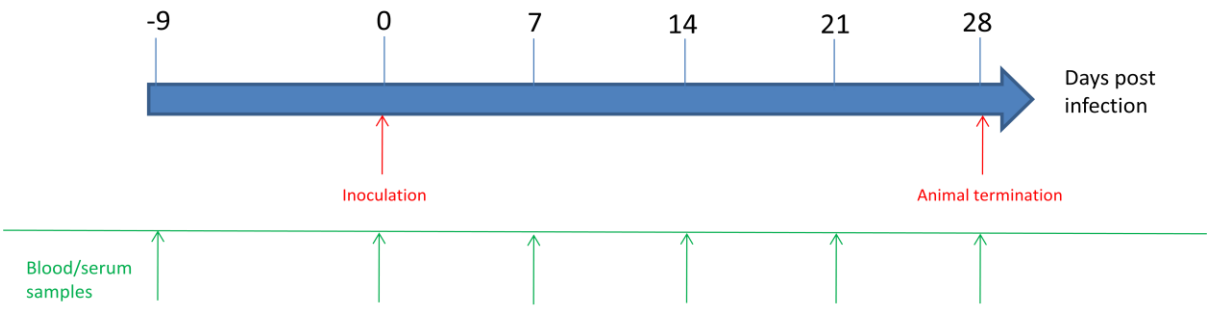

Figure 58 – Ferret study B summary. Samples collected from ferrets inoculated with heat-inactivated attenuated vaccine MuV over a 28 day period.

PRN assays were performed and ND_{50} values calculated as described in section 4.1.3, using serum samples from 3 male ferrets (designated A, B and C) inoculated with *ca* $2x10^4$ pfu heat-inactivated RIT 4385. Live RIT 4385 mumps vaccine virus was used as the challenge virus. The average plaque count obtained from the positive control (no sera, challenge vaccine virus only) was 10. The data obtained were compared against those for the live RIT 4385 virus (section 4.1.3, Figure 55 b) and are shown in Figure 59.

The ND_{50} titres calculated for ferrets A to C showed a slight increase at day 28 compared to the pre-bleed samples. To establish if the ND_{50} values obtained for day 28 sera from ferrets A to C were significantly increased, unpaired two-tail T tests were performed using GraphPad Prism 5.0 to compare the day 28 and pre-bleed data from each animal. This statistical analysis was also performed on the data from ferrets 4 to 6 (study A).

P values for ferrets A, B and C were 0.0640, 0.5126 and 0.2711 respectively, and the differences between pre-bleed and day 28 sera samples were not statistically significant. However, the P values for ferrets 4, 5 and 6 were 0.0007, 0.0004 and >0.0001 respectively, and the increase in ND_{50} values from pre-bleed to 28 days were statistically significant.

These results indicate that the neutralising antibody response exhibited by ferrets 1 to 6 in study A, was specific to mumps virus.

To confirm this result further, PRN assays were performed on day 28 sera from ferrets 1 to 6 (study A) using a high growth influenza laboratory strain (PR8) or a clinical MuV isolate (HPA1.1/P1V) as challenge viruses. As mumps is thought to be serologically monotypic, the animal sera should neutralise HPA1.1/P1V but not PR8.

The results in Figure 60 demonstrate that the day 28 sera from all 6 animals are not capable of effectively neutralising the influenza virus, however did show neutralising activity when challenged with clinical MuV HPA1.1/P1V.

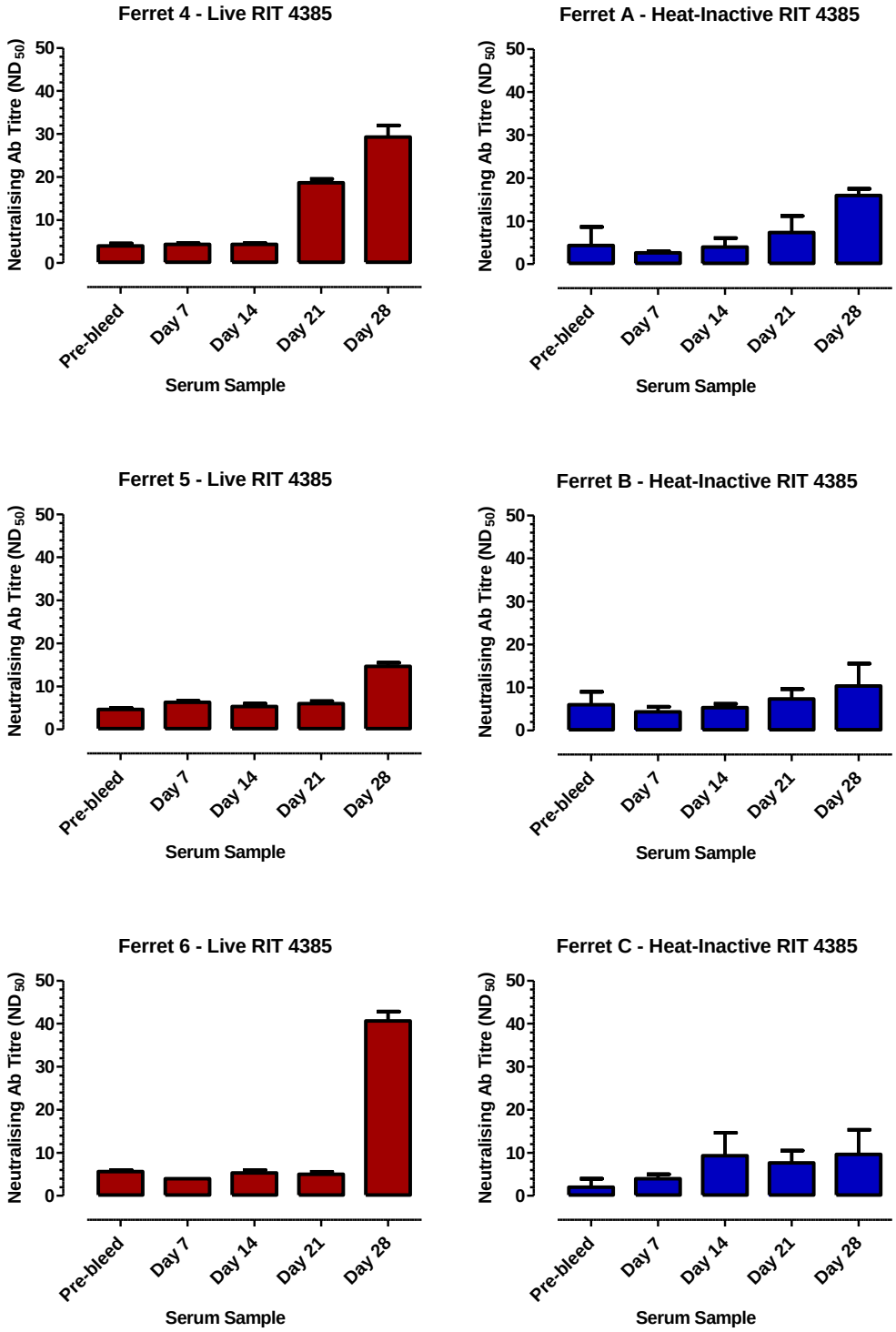

Figure 59 – Ferret study B, plaque reduction neutralisation assay data. Sera obtained from ferrets inoculated with live (red) or heat-inactivated (blue) RIT 4385 were challenged with RIT 4385 and the dilution required to reduce number of plaques by 50% (ND_{50} titre) was calculated. All PRN assays were performed in triplicate and the data represents the mean and standard deviation.

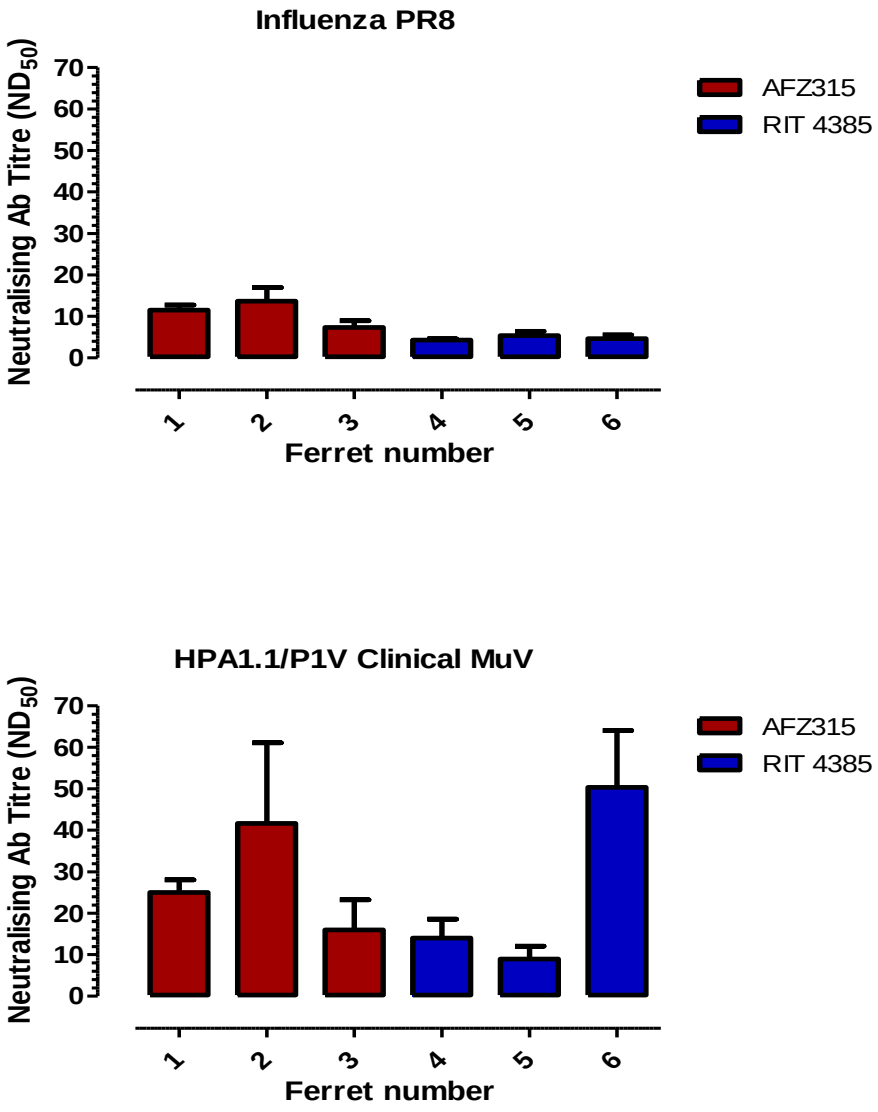

Figure 60 – Ferret study B, Influenza PR8 and MuV HPA1.1/P1V challenge plaque reduction neutralisation assay data. Day 28 sera obtained from ferrets inoculated with AFZ315 (red) or RIT 4385 (blue) in study A, were challenged with influenza PR8 or MuV HPA1.1/P1V and the dilution required to reduce number of plaques by 50% (ND_{50} titre) was calculated. All PRN assays were performed in triplicate and the data represents the mean and standard deviation.

4.3 Ferret Study C

Eight male ferrets were inoculated intranasally with clinical MuV AFZ315. Oral swabs were collected daily and 2 animals sacrificed with tissues collected on days 1, 4, 7 and 14 post infection. Figure 61 provides a summary of Study C.

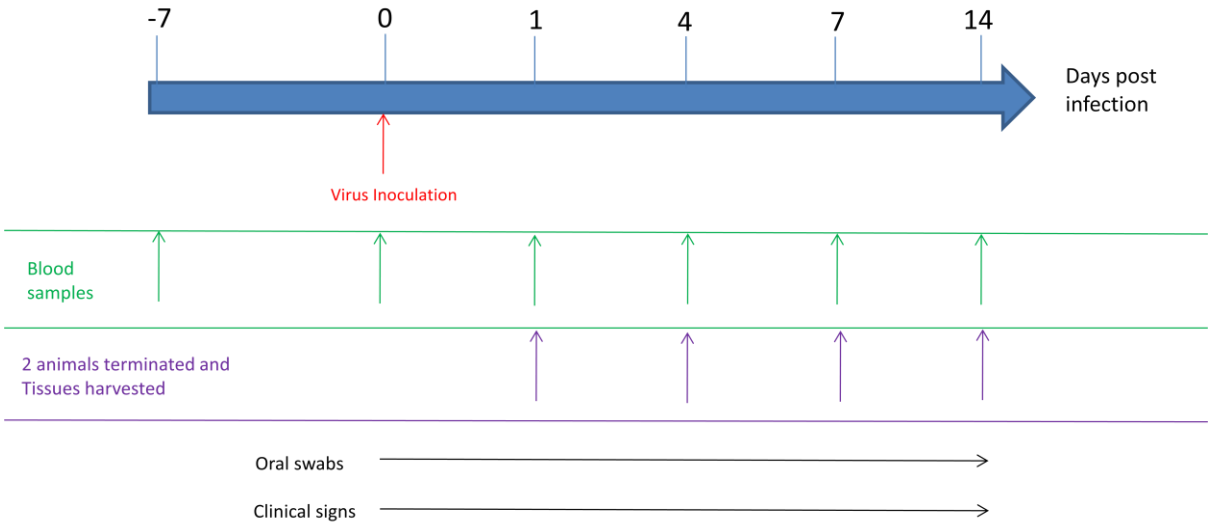

Figure 61 – Ferret study C summary. Clinical observations and samples collected from ferrets inoculated with clinical MuV over a 14 day period.

4.3.1 Isolation of Virus from Oral Swabs

Processed and clarified oral swab samples from ferrets 1.1 to 1.8 were inoculated onto Vero cells, incubated at 35°C, 5% CO_2 for 10 days and examined daily for signs of CPE. The resulting cell lysates were blind-passaged once onto Vero cells and incubated and examined as before. None of the inoculated cell cultures demonstrated evidence of CPE.

RNA was isolated from all cell lysates from oral swab samples and analysed by standard RT-PCR and then nested PCR for presence of MuV SH gene mRNA. This was done using primers JLSH1Fw and

JLSH2Rv, and JLSH3Fw and JLSH4Rv respectively. All RT and nested PCR products were found to be negative when electrophoresed on a 1% agarose gel.

RNA was also extracted directly from oral swabs and analysed by real-time RT-PCR for presence of MuV SH gene mRNA using AFZ315SHF, AFZ315SHR and AFZ315P primers and probe. All of the test samples were found to be negative.

Negative and positive controls included in these experiments were valid, and all were performed in triplicate.

No mumps virus was detected by cell culture or PCR methods in oral swabs from days at 1 to 14 post infection.

4.3.2 Recovery of Virus from Ferret Tissues

Two ferrets infected with clinical mumps virus AFZ315 were terminated on days 1, 4, 7 and 14 post infection and tissues harvested (Table 10). The tissues were chosen based on those that have been implicated in mumps cases in humans. Whole tissues were used to prepare 20% homogenates and these were analysed for presence of cultivable MuV and viral RNA which would give an indication of the biological distribution of the virus at specific time points.

Clarified homogenates were inoculated onto Vero cells, incubated at 35°C, 5% CO_2 for 10 days and examined daily for signs of CPE. The resulting cell lysates were blind-passaged once onto Vero cells and incubated and examined as before. None of the inoculated cell cultures demonstrated evidence of CPE. RNA was isolated from all cell lysates from tissue homogenate samples and analysed by standard RT-PCR and nested PCR for presence of MuV SH gene mRNA using JLSH1Fw and JLSH2Rv, or JLSH3Fw and JLSH4Rv respectively. All RT-PCR products were found to be negative when electrophoresed on a 1% agarose gel. Negative and positive controls included in these experiments were valid.

RNA was also extracted directly from the 20% tissue homogenates and analysed for presence of MuV SH gene mRNA using AFZ315SHF, AFZ315SHR and AFZ315P primers and probe. GAPDH gene mRNA was measured using GAPDH535Fw, GAPDH680Rv and GAPDH primers and probe, and was included as an internal control to confirm that the total RNA extracted from each sample was present and amplifiable. Each RT-PCR reaction was performed in triplicate.

GAPDH mRNA was detected in varying quantities in all of the tissue samples from ferrets 1.1 to 1.8 and this data is shown in Figure 62. Lymph nodes were unable to be located and removed from ferrets 1.4 and 1.7 at the time of tissue harvest therefore there is no data available for these. This demonstrates that the total RNA isolated was capable of being amplified by the real-time RT-PCR method used.

The MuV positive control included was a standard dilution curve of clinical AFZ315 MuV. The dilutions ranged from neat virus to 10^{-7} and contained a known quantity of virus measured in pfu. The virus control was valid and the values are shown in Figure 62. All negative NTC controls were valid.

All of the tissue homogenate samples from ferrets 1.1 to 1.8 were negative when analysed by real-time RT-PCR.

No cultivable mumps virus or viral RNA was recovered from any of the ferret tissues by the methods used in these experiments.

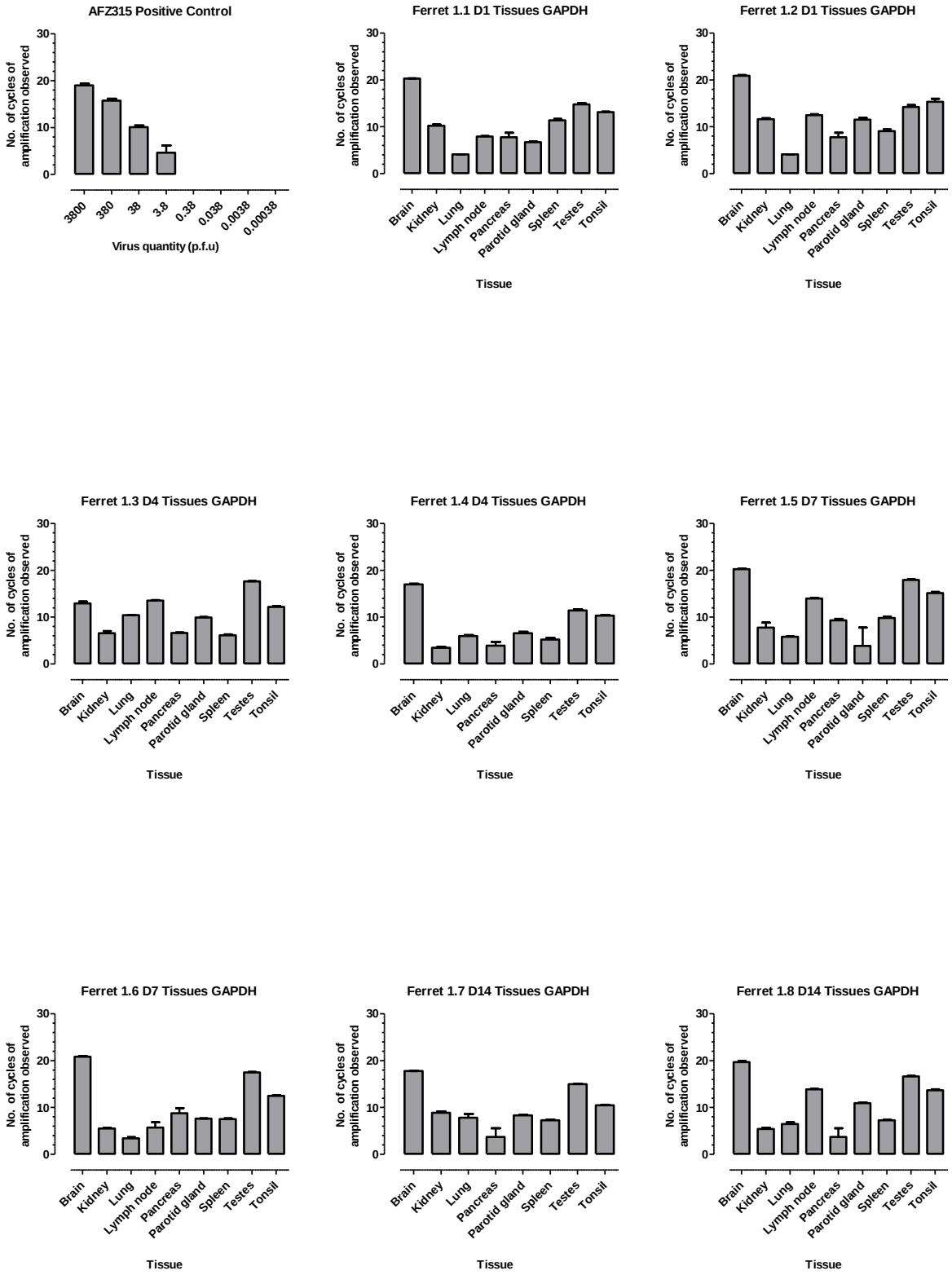

Figure 62 – Ferret study C, Ferrets 1.1 to 1.8 tissues real-time PCR data. GAPDH mRNA levels in day 1, 4, 7 and 14 20% tissue homogenates from ferrets infected with MuV AFZ315 were measured by real-time PCR as an internal control. No MuV mRNA was detected in any of the ferret tissues, and

the positive control included demonstrates that the lowest virus quantity which could be detected by this method is 3.8 pfu. Assays were performed in triplicate and the data displayed represents the mean and standard deviation.

4.3.3 Spiking of Uninfected Ferret Tissue Homogenates with MuV

Clinical MuV AFZ315 virus was used to spike 20% brain, kidney and spleen homogenates from ferret 1.1 and serial dilutions up to 10^{-7} were prepared in each homogenate. The same virus dilutions were prepared in MEM to act as a control. This was carried out to determine the ability of MuV to be extracted from ferret tissues and to obtain an approximate limit of detection for the real-time PCR assays performed throughout the *in vivo* studies.

Brain, spleen and kidney were chosen due to the differences between each of the tissue types. For example the brain is a fatty tissue, the spleen contains a large quantity of blood and the kidney represents a tissue which proved reasonably difficult to homogenate.

RNA was isolated from the spiked 20% tissue homogenate dilution series and the MEM/virus control, and analysed for presence of MuV SH gene mRNA using AFZ315SHF, AFZ315SHR and AFZ315P primers and probe. Each reaction was performed in triplicate and the real-time RT-PCR data is shown in Figure 63. All negative NTC controls were valid.

The data indicates that by this method, the assay is capable of detecting 3.8 pfu of MuV per µL of template RNA when diluted in MEM only, and can detect 38 pfu of MuV per µL of template RNA isolated from the tissue homogenates. The limit of detection was shown to be the same for all 3 tissues types. Based upon the weight of the animal and tissue and volume of media added to result in a 20% homogenate, the minimum amount of clinical mumps virus that can be detected by this method can be calculated to be approximately 6000 pfu per gram of ferret.

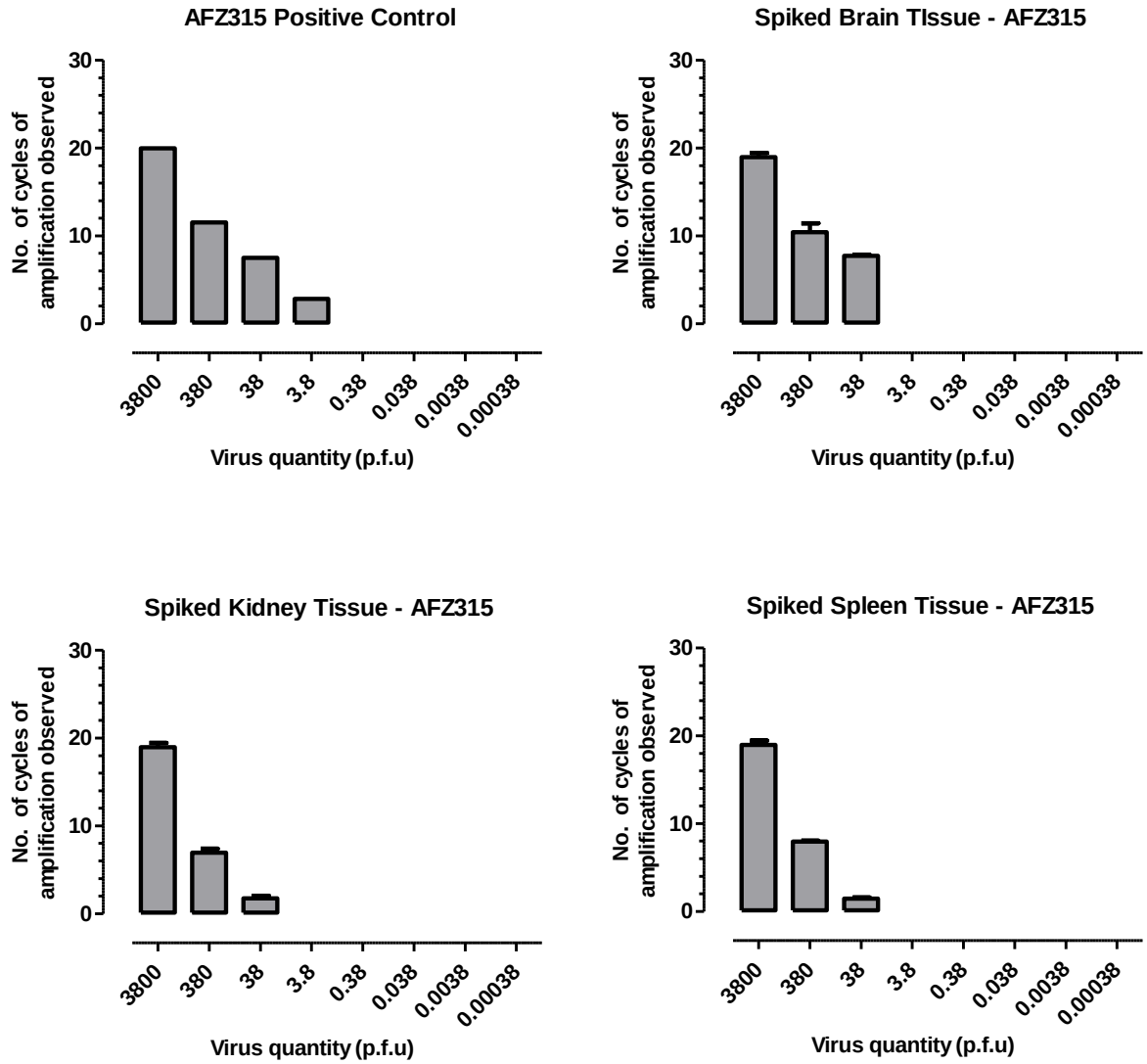

Figure 63 – Limit of detection of mumps virus AFZ315 in ferret tissues by real-time RT-PCR. MEM and uninfected ferret brain, spleen and kidney 20% homogenates were spiked with serial dilutions of a known quantity of MuV AFZ315 to compare MuV SH gene mRNA levels detectable by real-time RT-PCR. Assays were performed in triplicate and the data displayed represents the mean and standard deviation.

4.3.4 Detection of MuV in Ferret PBMCs

PBMCs were isolated from ferret terminal bleeds at 1, 4, 7 and 14 days post infection and were analysed for the presence of MuV mRNA. This was carried out to determine whether or not clinical MuV is lymphotropic in ferrets.

RNA was extracted from PBMCs isolated from ferret terminal bleeds and analysed for presence of MuV SH gene mRNA using AFZ315SHF, AFZ315SHR and AFZ315P primers and probe. GAPDH gene mRNA was measured using GAPDH535Fw, GAPDH680Rv and GAPDH primers and probe, and was included as an internal control to confirm that the total RNA extracted from each sample was present and amplifiable. Each RT-PCR reaction was performed in triplicate.

GAPDH mRNA was detected in varying quantities in all of the PBMC samples from ferrets 1.1 to 1.8 and this data is shown in Figure 64. This demonstrates that the total RNA isolated was capable of being amplified by the real-time RT-PCR method used.

The MuV positive control included was a standard dilution curve of clinical AFZ315 MuV. The dilutions ranged from neat virus to 10^{-7} and contained a known quantity of virus measured in pfu. The virus control was valid and the values are shown in Figure 64. All negative NTC controls were valid.

All of the samples from ferrets 1.1 to 1.8 were negative for MuV when analysed by real-time RT-PCR.

No viral RNA was recovered from any of the ferret PBMCs by the methods used in this experiment.

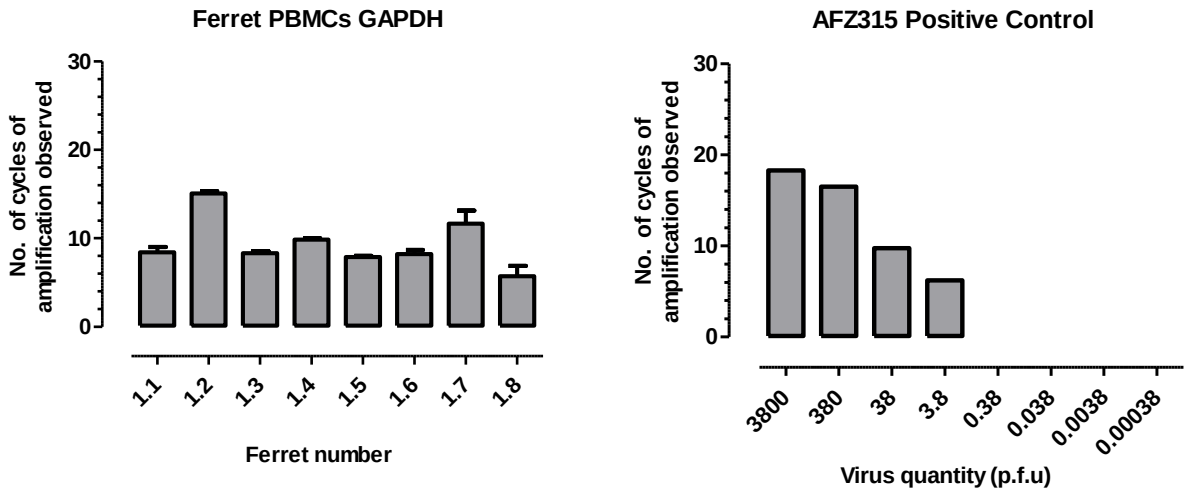

Figure 64 – Ferret study C, ferrets 1.1 to 1.8 PBMCs real-time PCR data. GAPDH mRNA levels in PBMCs isolated from terminal bleeds of ferrets infected with MuV AFZ315 were measured by real-time PCR as an internal control. No MuV mRNA was detected in any PBMCs, and the positive control included demonstrates that the lowest virus quantity which could be detected by this method is 3.8 pfu. Assays were performed in triplicate and the data displayed represents the mean and standard deviation.

4.3.5 Detection of Cytokines in Ferret PBMCs

RNA isolated from ferret PBMCs was analysed by SYBR® Green real-time RT-PCR for the presence of IFN-γ, IL-2, IL-6 and IL-10 at various time points post infection with clinical MuV. These cytokines were chosen for this experiment as they have been previously shown to increase significantly in CSF of patients with mumps meningitis (Ichiyama *et al.*, 2005), and due to the availability of ferret PCR primers at the time (Svitek & von Messling, 2007).

Cytokine mRNA levels were detected using IFNGAMMAFw, IFNGAMMARv, IL2Fw, IL2Rv, IL6Fw, IL6Rv and IL10Fw and IL10Rv primer pairs. GAPDH gene mRNA was measured using GAPDHFw, GAPDHRv

primers, and was included as an internal control to confirm that the total RNA extracted from each sample was present and amplifiable. Each RT-PCR reaction was performed in duplicate.

GAPDH mRNA was detected in varying quantities in all of the PBMC samples from ferrets 1.1 to 1.8. This demonstrates that the total RNA isolated was capable of being amplified by the SYBR® Green PCR method used.

The fold change in mRNA levels between pre-bleed and test bleeds for each cytokine gene was calculated using the level of GAPDH for each sample as a control. To do this, the Ct value for GAPDH is first subtracted from the Ct value of the unknown gene (ΔCt) from the pre-bleed sample. The mRNA fold change is then calculated by subtracting the pre-bleed ΔCt value of the gene of interest from the ΔCt values of the gene at each time point (days 1, 4, 7 and 14). These values were then changed into absolute values by using the equation: fold mRNA change = $2^{-\Delta\Delta Ct}$ (Svitek & von Messling, 2007)

IFN-γ levels showed no change on days 1 (ferrets 1.1 and 1.2), 4 (ferrets 1.3 and 1.4) or 7 (ferrets 1.5 and 1.6) post infection, however a mean fold increase of 2.0 on day 14 post infection (ferrets 1.7 and 1.8) was observed. IL-2, IL-6 and IL-10 levels peaked on day 4 post infection as demonstrated by a mean increase in fold mRNA change of 20, $2x10^4$ and 600, respectively. This data is shown in Figure 65.

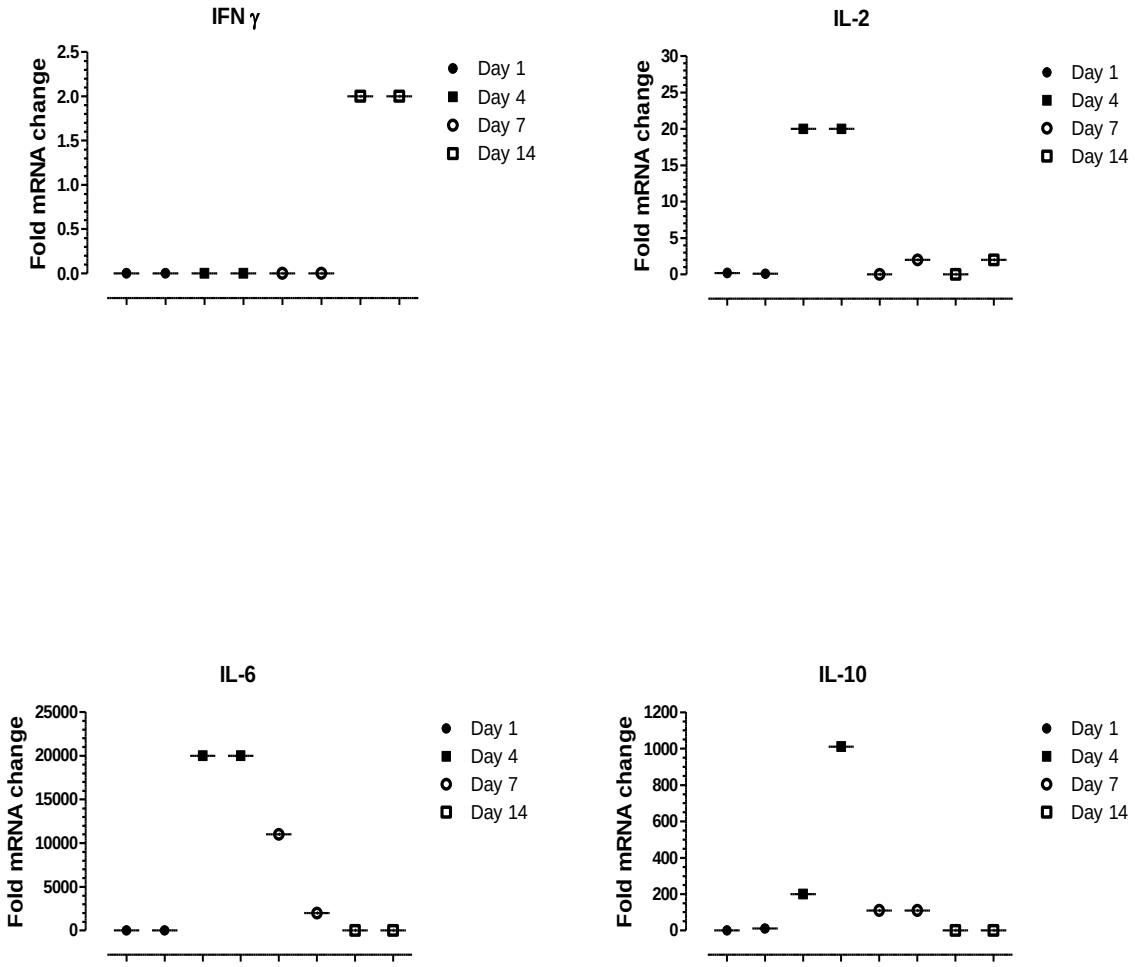

Figure 65 – Ferret study C, detection of cytokines in ferret PBMCs at various time points SYBR® Green real-time PCR data. Fold change of IFN-γ, IL-2, IL-6 and IL-10 mRNA levels in PBMCs isolated from ferret blood at days 1, 4, 7 and 14 post infection with clinical MuV AFZ315 was calculated using the differences in Ct values in the equation: fold mRNA change = $2^{-\Delta\Delta Ct}$

4.3.6 Human Cytokine ELISA

Basal samples from MucilAir™ HAE cells infected with clinical MuV AFZ315 were assayed using a Multi-Analyte ELISArray™ Kit for human inflammatory cytokines. Included in the panel of cytokines were IL-2, IL-6, IL-10 and IFN-γ and this assay was carried out in order to assess any correlation

between the cytokine levels observed in ferret PBMCs and those secreted from infected HAE cells at similar time points (days 1, 4, 7 and 10 post infection).

The absorbance was measured at 450 nm and the data analysed using Ascent® software (Thermo Scientific, UK), where the value for optical density (OD_{450}) is proportional to the quantity of cytokine present in the experimental sample.

Quantities of IL-2 and IL-10 peak at day 7 post infection with a noticeable decrease by day 10 post infection. IL-6 levels appear to be highest at day 1 post infection and decrease steadily until 10 days post infection. Levels of IFN-γ peak at day 1 post infection, followed by a sharp decrease at day 4 and an increase by day 7, and this level is maintained at day 10 post infection. The data is shown in Figure 66.

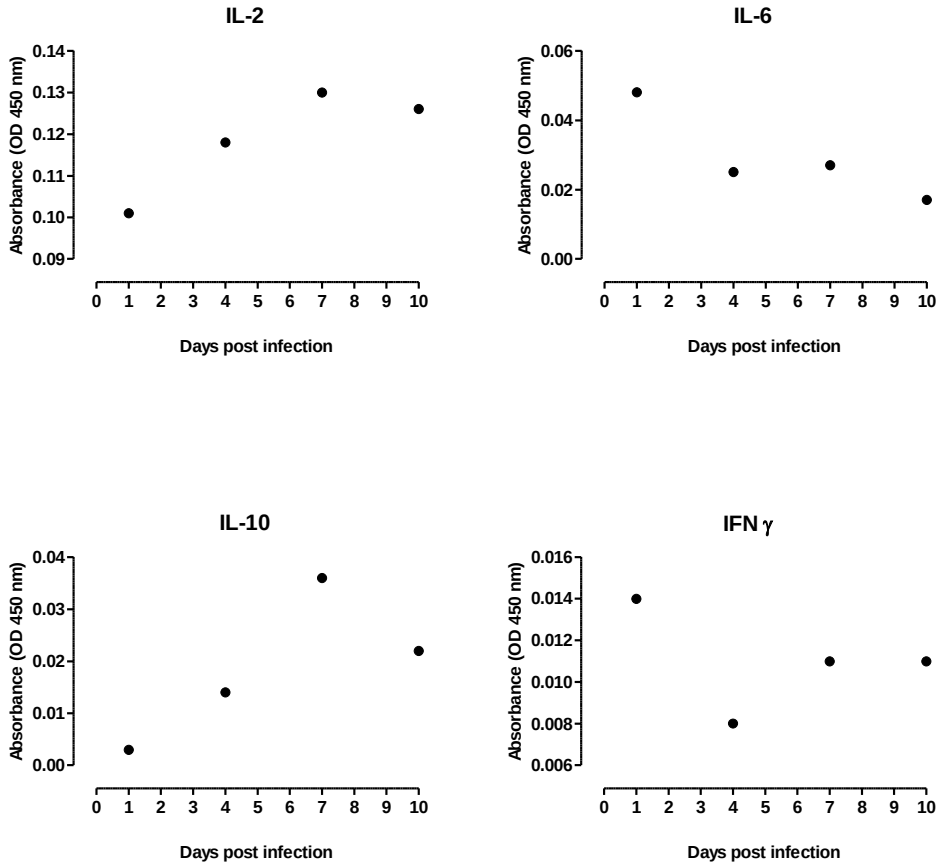

Figure 66 – Measurement of cytokine levels in basal HAE cell samples at various time points, ELISA data. IL-2, IL-6, IL-10 and IFN-γ levels in basal samples from MucilAir™ HAE cells at days 1, 4, 7 and 10 post infection with clinical MuV AFZ315 were measured using a Multi-Analyte ELISArray™ Kit for human inflammatory cytokines and reading absorbance at 450nm.

4.4 Ferret Study D

4.4.1 Recovery of Virus from Ferret Tissues

Two ferrets infected with clinical mumps virus AFZ315 harvested from the apical surface of MucilAir™ HAE at day 10, were terminated on days 4 and 7 post infection and tissues harvested (Table 10). Figure 67 provides a summary of Study D. The tissues were chosen based on those that have been implicated in mumps cases in humans. Whole tissues were used to prepare 20%

homogenates and these were analysed for presence of cultivable MuV and viral RNA which would give an indication of the biological distribution of the virus at specific time points.

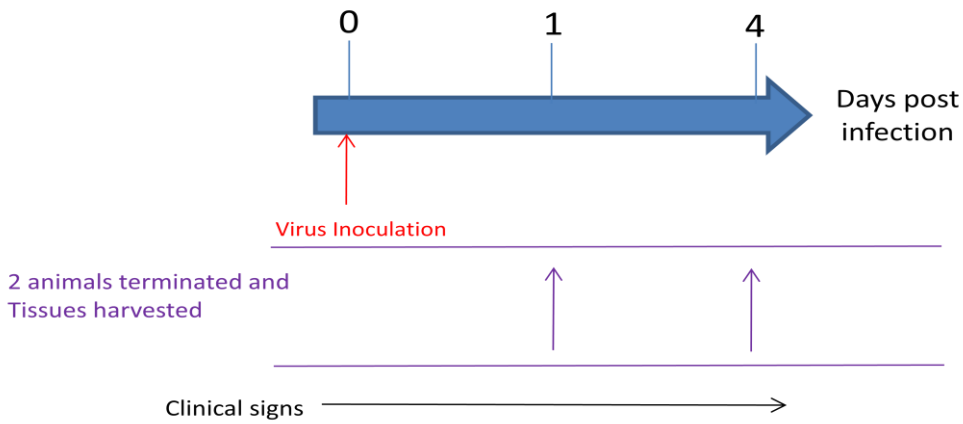

Figure 67 – Ferret study D summary. Clinical observations and samples collected from ferrets inoculated with clinical MuV isolated from HAE cells over a 4 day period.

Clarified homogenates were inoculated onto Vero cells, incubated at 35°C, 5% CO_2 for 10 days and examined daily for signs of CPE. The resulting cell lysates were blind-passaged once onto Vero cells and incubated and examined as before. None of the inoculated cell cultures demonstrated evidence of CPE. RNA was isolated from all cell lysates from tissue homogenate samples and analysed by standard RT-PCR and nested PCR for presence of MuV SH gene mRNA using JLSH1Fw and JLSH2Rv, or JLSH3Fw and JLSH4Rv respectively. All RT-PCR products were found to be negative when electrophoresed on a 1% agarose gel. Negative and positive controls included in these experiments were valid.

RNA was also extracted directly from the 20% tissue homogenates and analysed for presence of MuV SH gene mRNA using AFZ315SHF, AFZ315SHR and AFZ315P primers and probe. GAPDH gene

mRNA was measured using GAPDH535Fw, GAPDH680Rv and GAPDH primers and probe, and was included as an internal control to confirm that the total RNA extracted from each sample was present and amplifiable. Each RT-PCR reaction was performed in triplicate.

GAPDH mRNA was detected in varying quantities in all of the tissue samples from ferrets 1 to 4 and this data is shown in Figure 68. This demonstrates that the total RNA isolated was capable of being amplified by the real-time RT-PCR method used.

The MuV positive control included was a standard dilution curve of clinical AFZ315 MuV. The dilutions ranged from neat virus to 10^{-7} and contained a known quantity of virus measured in pfu. The virus control was valid and the values are shown in Figure 68. All negative NTC controls were valid.

All of the tissue homogenate samples from ferrets 1 to 4 were negative when analysed by real-time RT-PCR.

In summary, no cultivable mumps virus or viral RNA was recovered from any of the ferret tissues by the methods used in these experiments.

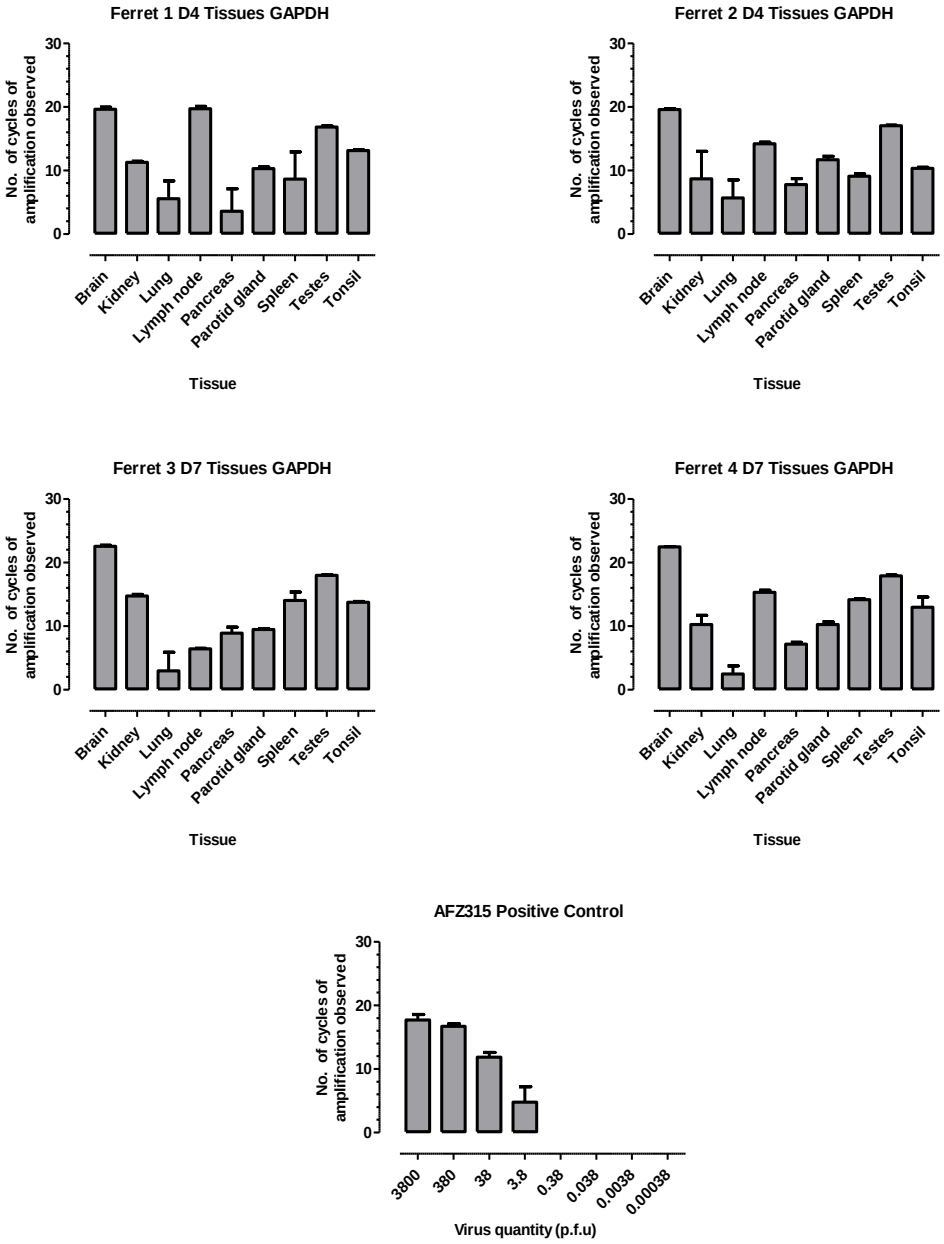

Figure 68 – Ferret study D, ferrets 1 to 4 tissues real-time PCR data. GAPDH mRNA levels in day 4 and 7 20% tissue homogenates from ferrets infected with MuV AFZ315 harvested from the apical surface of HAE cells at day 10 post infection were measured by real-time PCR as an internal control. No MuV mRNA was detected in any of the ferret tissues, and the positive control included demonstrates that the lowest virus quantity which could be detected by this method is 3.8 pfu. Assays were performed in triplicate and the data displayed represents the mean and standard deviation.

4.5 Summary of Results

Clinical symptoms including temperature, body weight, appetite, alertness, physical appearance, and swelling of parotid gland areas and testes were recorded on a daily basis for all of the ferrets included in studies A to D. No signs were observed at any point during these studies that would indicate mumps-like disease or any other type of illness.

PRN assays were performed using sera from ferrets inoculated with clinical MuV AFZ315 or attenuated vaccine virus RIT 4385 (study A) and these tests showed that the animals were all capable of producing antibodies that neutralised MuV by day 28 post infection. PRN assays were then carried out using sera from ferrets inoculated with heat-inactivated RIT 4385 (study B), which was not able to effectively neutralise MuV. Sera from animals on day 28 (study A) were also capable of neutralising another clinical MuV (HPA1.1/P1V) but not a laboratory strain of influenza.

In studies A, C and D attempts were made to recover infectious virus or viral RNA from nasal washes, urine, faeces, oral swabs, PBMCs and 20% tissue homogenates by culture on Vero cells and real-time quantitative RT-PCR. However, no MuV RNA or live virus was detected by these methods. A spiking experiment as part of study C in which uninfected brain, kidney and spleen homogenates were "spiked" with known quantities of clinical MuV AFZ315 demonstrated that it is possible to detect this virus in ferret tissues if present at a minimum of 38 pfu per µL of RNA template.

PBMCs from ferret terminal bleeds (study C) were used to determine levels of IFN-γ, IL-2, IL-6 and IL-10 present over 14 days by SYBR® Green RT-PCR. The results were calculated to represent the fold change in mRNA and demonstrated no change in IFN-γ mRNA levels until a peak at day 14, whereas IL-2, IL-6 and IL-10 mRNA levels all peaked at day 4 post infection. In an attempt to correlate these results with a human infection, a human cytokine ELISA was performed using the basal media from HAE cells infected with the same clinical MuV over 10 days. Levels of IFN-γ, IL-2, IL-6 and IL-10 were

all found to change over the time course, however a different time course trend was observed than that seen in ferret PBMCs.

4.6 Discussion

As previously mentioned, no animals in any of the studies A to D exhibited any clinical symptoms of illness. However the fact that they elicited a serum antibody response after inoculation with a live clinical or vaccine MuV indicates that although the ferrets did not demonstrate physical signs of disease, suggests that they probably were infected. Guinea pigs have been shown to be an efficient model for studying influenza virus infection and transmission, yet they have been reported not to display clinical signs (Palese *et al.*, 2006). The levels of IFN and cytokine production observed in the PBMCs also indicate a response to viral infection.

Male ferrets were chosen for these studies to aid observation of external clinical symptoms by measurement of testicular swelling, as orchitis is common in mumps disease in male patients. The equivalent in female patients is oophoritis, however this occurs at a less frequent rate than orchitis and it would not have been feasible in this project to examine animals' ovaries as a means of observing clinical symptoms. Female mice have been reported to have a more severe reaction to influenza A infection than males, with increased hypothermia, loss of body weight and mortality rates (Robinson *et al.*, 2011). This was associated with sex-specific hormones and differences in viral infection outcome between males and females have also been reported for HIV and herpes viruses (Klein & Huber, 2010). Performing the studies described in this thesis using female ferrets may have been of interest and produced different results, however there has not been any evidence reported that mumps occurs with higher incidence in males or females, or that either of the sexes is more prone to mumps disease with complications (Hviid *et al.*, 2008).

The neutralising antibodies (NAb's) produced by the ferrets in response to infection with clinical or attenuated vaccine MuVs (study A) can be said to be mumps-specific as sera from ferrets inoculated with the heat-inactivated vaccine virus RIT 4385 (study B) were not capable of significantly neutralising MuV. Also, the day 28 sera from study A effectively neutralised another clinical MuV as well as Mu90 and RIT 4385 challenge viruses, but had no neutralising effect when challenged with a laboratory strain of influenza. MuV is reported to be serologically monotypic (Rubin *et al.*, 2006) which means that antibodies effective against one strain or genotype of the virus should be able to neutralise all other MuVs. This was shown to be the case with the ferret NAb's as they successfully neutralised RIT 4385 (genotype A), Mu90 (genotype D) and clinical virus HPA1.1/P1V (genotype G). All of these data taken together indicate that the neutralising antibody response elicited by ferrets during these studies was mumps-specific. This data correlates with that produced from a previously documented study in which antibodies that neutralised MuV were detected in the sera of ferrets after intranasal inoculation with the Enders strain of MuV (Gordon *et al.*, 1956).

Analysis of PBMCs from terminal bleeds of animals infected with clinical MuV AFZ315 demonstrated increases in the mRNA levels of IFN-γ (day 14), IL-2, IL-6 and IL-10 (all day 4) which correlates with previous studies in which the concentrations of these immune molecules were found to be elevated in patients CSF in cases of mumps meningitis (Ichiyama *et al.*, 2005). In a similar experiment, mRNA levels of IFN-γ, IL-2, IL-6 and IL-10 in PBMCs from ferrets infected with non-lethal CDV have also been demonstrated to increase at days 3 or 7 post-infection (Svitek & von Messling, 2007). The authors suggested that elevations in mRNA levels of these genes in the CDV study indicated that innate (IL-6), T helper cell 1 (Th1) (IFN-γ and IL-2) and T helper cell 2 (Th-2) (IL-10) types of immune responses were all stimulated, which suggests that this may also be the case in ferrets after infection with clinical MuV. It would have been useful to have carried out the same PBMC analysis from the ferrets inoculated with heat-inactivated MuV as a comparison, and also to have further confirmed the lack of serum antibody response observed in study B from animals infected with heat-inactivated RIT 4385.

The functions of IL-2, IL-6, IL-10 and IFN-γ are extensive and varied and are reviewed in (Meager & Wadhu, 2007) and (Schroder *et al.*, 2004). IL-6 is involved in the acute phase of innate immunity and the direct induction of acute-phase proteins such as C-reactive protein (CRP), and sharp increases in serum CRP levels correlate with IL-6 levels after infection (Heinrich *et al.*, 2003). This would have been interesting to measure using ferret sera that had not been heat-inactivated, perhaps using ELISA methodology, in order to determine whether or not there was a correlation with the results from the PBMCs, and it would have also provided another indicator of infection. CRP has previously been found to become elevated in plasma of mumps patients with orchitis (Niizuma *et al.*, 2004). IL-2 is produced by T lymphocytes and is heavily involved with T-cell proliferation, causing them to produce IFN-γ, among other cytokines. IL-10 has many suppressive activities and is reported to act as a negative regulator of IFN-γ and inhibit its synthesis by Th1 cells (Schroder *et al.*, 2004) (Fiorentino *et al.*, 1991), which would provide an explanation as to why in the ferret PBMCs, IFN-γ mRNA levels did not increase until the IL-10 mRNA levels decreased at day 7. If IL-2 is involved in stimulating induction of IFN-γ, this would suggest why it was detected earlier than IFN-γ. IFN-γ has also previously been demonstrated to be of importance at later stages of the immune response to coordinate a longer-term anti-viral state in the host (Cantin *et al.*, 1999).

The levels of IL-2, IL-6, IL-10 and IFN-γ proteins measured in basal media from HAE cells infected with MuV AFZ315 differed from the trends observed in the measured fold mRNA changes calculated from the ferret PBMCs. Increased levels of IL-6 at day 1 post infection correlates with its involvement in acute-phase immune activities, however, in the HAE cells more IFN-γ is present initially as opposed to IL-2 and IL-10. Once again though, IFN-γ and IL-10 do not reach peak levels at the same time which may be another demonstration of the negative regulation of IFN-γ by IL-10. Unfortunately there is only one data point available for each sample and time point due to lack of sample availability, so it would be of interest to repeat this experiment using more HAE cells in order to have a greater sample volume for testing in triplicate. There are many possible reasons as to why the trends observed for the HAE cells and PBMCs were different. The substances being measured were

different (mRNA and protein) and were done so by different means (real-time RT-PCR and ELISA) which could have an effect on the outcomes for comparison. The PBMCs came from an *in vivo* animal system where intranasal inoculation was used, and the HAE cells were washed thoroughly and inoculated directly onto the apical surface, and one system was ferret and the other human. Also, as the HAE cultures are lacking in types of immune cells such as Th1 and Th2 (Huang *et al.*, 2011) it is likely that the responses measured from the basal medium were basic cellular infection responses, whereas the PBMCs analysis revealed an actual immune response. It would be of interest in the future to carry out similar experiments, when more ferret reagents are available, in order to obtain a full cytokine profile for ferrets infected with MuV.

The immune response data from these *in vivo* studies is highly indicative that although the ferrets did not become ill, they were infected with MuV. As no infectious virus or viral RNA was detected in any of the clinical samples (no shedding) or tissue homogenates, this raised the question of what happened to the virus and where did it go? Wild-type MuVs are known to spread in saliva or respiratory droplets, and oral swabs are the most common means of obtaining a sample from a mumps patient, therefore it was expected that the clinical MuV AFZ315 would be detected in oral fluid and/or nasal washes. The fact that no attenuated vaccine virus was recovered was less of a concern as there is no reported connection between RIT 4385 and virus shedding, and the fact that this MuV is attenuated may account for low levels or lack of replication in tissues. After study A, the working hypothesis was that perhaps no virus was detected in tissues at day 28 because by this time point, the virus had been cleared from the animals' system by the strong NAb response. The results from study C indicated that this was not the case, as no virus was recovered from tissues at 1, 4, 7, or 14 days post infection. After obtaining these results, the hypothesis was that the lack of recoverable clinical MuV was due to a low titre of input virus and so the inoculum titre was increased in study D, by infecting ferrets with progeny AFZ315 from HAE cells which were found to be of a higher titre and highly genetically similar to the parent virus (section 3.5.4). The virus inoculum titre increase from 7×10^3 pfu/ferret to 1×10^5 pfu/ferret in study D did not aid virus

recovery in any of the tissue homogenates therefore it was concluded that a low inoculum titre was likely not to be the reason for this. The results of these experiments were not in agreement with those from a previous study in which infectious MuV was recovered from nasal washings, turbinates and lung samples at days 3 and 4 post infection (Gordon *et al.*, 1956). However, the virus used in the afore-mentioned investigation had been serially passaged through allantoic fluid of embryonated hen's eggs 19 to 23 times prior to inoculation which may have caused selective adaptations in the virus.

This conclusion resulted in the formation of a new hypothesis, this being that perhaps there was an issue with the detection capabilities and limits of the real-time RT-PCR assay. To address this, brain, kidney and spleen homogenates previously demonstrated to be negative for MuV were spiked with known quantities (pfu) of clinical MuV AFZ315 and compared with AFZ315 diluted in MEM only by real-time RT-PCR. The virus was successfully detected in all three of the spiked tissues with a sensitivity limit of 38 pfu per µL of RNA template. The MEM-diluted virus assay showed a higher sensitivity limit of 3.8 pfu per µL of RNA template, which may be due to the presence of compounds in the starting material of the spiked tissue samples known to be inhibitory in PCR reactions such as haemoglobin and lactoferrin (Al-Soud & Radstrom, 2001). The sensitivity limit for this PCR assay using ferret tissue homogenates was calculated to mean that for MuV RNA to be detected, the virus would need to be present in a quantity of approximately 6000 pfu per gram of ferret. This is a high quantity of virus, therefore the inoculum MuV would need to be concentrated in one or two tissues or be replicating efficiently to produce high titres of progeny virus in order to be detected by the method used here. With regards to the limit of detection of the RIT 4385 MuV, if it is considered that the lowest quantity of virus detected decreases by approximately 10-fold due to the presence of potential PCR inhibitors in tissue (as seen for clinical MuV), it can be assumed that the detection limit would be approximately 0.605 pfu per µL of RNA template making it more sensitive than for clinical MuV AFZ315.

The fact that no live MuV or viral RNA was detected may be as a result of host restriction factor(s) in the ferret. The virus may have been capable of only replicating at very low levels or inefficiently in tissues and organs. Virus restriction factors of the host organism are commonly related to the availability of a suitable receptor for binding and/or host anti-viral response. As ferret cells of the respiratory tract have been demonstrated to express similar SA patterns to those found in human cells (van Riel *et al.*, 2007) (Jayaraman *et al.*, 2012) it is unlikely that the receptor type or availability posed a problem. Studies on the SA content of ferret and human salivary or parotid glands are lacking, however SA-containing mucous, a common barrier to viral and bacterial infection, has been shown to be present in the parotid glands of ferrets (Jacob & Poddar, 1978).

The antiviral response of the animals may play a role in inhibiting MuV replication or restricting viral tropism. IL-2, IL-6, IL-10 and IFN-γ all activate several signalling pathways including the JAK-STAT cascade which the V protein of MuV is known to interfere with by targeting STATs for degradation (discussed in section 1.8.2), however there is a chance that this may affect only IFN α/β signalling and not that of IFN-γ, as has previously been reported to be the case for MV (Takeuchi *et al.*, 2003). IFN-γ has been implicated in to act in a tissue-dependent manner during clearance of vaccinia and alpha-viruses (Kundig *et al.*, 1993) (Binder & Griffin, 2001). It also upregulates several anti-viral genes including dsRNA-specific adenosine deaminase (ADAR) which may cause the translation of non-functional proteins by an mRNA editing function (Patterson *et al.*, 1995), and protein kinase dsRNA-regulated (PKR) which can inhibit viral replication and activate NF-κB (Zamanian-Daryoush *et al.*, 2000). These may have a restrictive effect on MuV replication in ferret tissues. The MuV V protein may also not be fully functional in ferret cells and tissues, and could play a role in determining host range as has been described for the V protein of RSV (Bossert & Conzelmann, 2002) and NDV (Park *et al.*, 2003).

It is worth considering the possibility that the immune responses observed in the ferret sera and PBMCs were generated in response to the MuV viral antigen, the HN glycoprotein, and not

replicating virus. If this is the case, the insignificant neutralising antibody response from ferrets inoculated with heat-inactivated vaccine virus (study B) could be explained by the denaturation or irreversible conformational change of the antigen brought about by the high temperature treatment during the inactivation process. To test this theory, ferrets could be inoculated in the same way as described in this project with a virus vector expressing the HN protein of MuV.

If the outcome of the virus recovery experiments in ferrets had been different and either live MuV or viral RNA had been successfully detected, a technique to detect viral proteins in tissue sections such as fluorescent in situ hybridisation could also have been carried out. This procedure has previously been used to successfully detect RSV proteins in infected cells of the lungs of cotton rats (Murphy *et al.*, 1990). Any recovered MuV would have been titrated by plaque assay and sequenced to compare with the inoculum virus in order to determine if any changes at the nucleotide and amino acid level had been brought about by replication and adaptation to the host tissues.

In conclusion, the *in vivo* data presented here provides evidence that ferrets are capable of producing mumps-specific neutralising antibodies after intranasal inoculation with clinical or attenuated vaccine MuVs, and that they appear to elicit a cytokine response to clinical MuV. These results alone are not conclusive as to whether or not the ferrets were infected with MuV, and experimental infection of *ex-vivo* ferret airway epithelial cells similar in set-up to the HAE cells used here would be useful to confirm whether or not ferret cells are capable of being infected with MuV. No live virus or viral RNA was recovered from any nasal washes, urine, faeces, PBMCs or tissues at any of the time points included. This indicates that the virus was not shedding from the animals and that it is unlikely that it was replicating in any ferret tissues. If virus is not being shed, transmission studies are not possible, and a lack of clinical symptoms and recovery of virus from samples make fundamental *in vivo* mumps research using the ferret model extremely difficult. This model would also be very limited in its uses for investigating attenuated vaccine viruses. The data raise more

questions than they answer, however do not provide evidence that the ferret is a suitable animal model for investigative MuV research.

CHAPTER 5 – CONCLUDING DISCUSSION

Although mumps cases have been documented for hundreds of years, and vaccines have been available for over 60 years, specific virological data on MuV is somewhat lacking. Much of the knowledge available from the literature is inferred from research carried out on other paramyxoviruses, in particular the closely related hPIV5 which is often referred to as a prototypical rubulavirus and paramyxovirus. The lack of a sensitive cell culture model and an effective animal model are two reasons contributing to this lack of knowledge in the field of mumps research, and this PhD project was carried out in an attempt to tackle these issues.

The project was divided into two concurrent parts. The first focussed on *in vitro* work to investigate the growth of MuV in various cell substrates, and the second addressed the assessment of ferrets as an *in vivo* model for mumps.

Studies have been carried out in the past to assess the use of certain cell lines for MuV propagation, and a brief preliminary screen of eight cell lines has previously been carried out (Afzal *et al.*, 2005). However this project is the largest screen that has been performed to investigate MuV growth and genetic stability in cell lines, including genetically engineered interferon-insensitive cells. Data on sialic acid receptor binding specificity of MuV was unavailable at the time of designing this PhD project and the SA studies described in this thesis are the first to provide data indicating that MuV may not exhibit any preferential binding. This is also the first investigation of mumps using an *ex-vivo* culture system which mimics the human respiratory epithelia (MucilAir™) and has demonstrated that HAE cells are capable of supporting efficient infection, replication and release of wild-type laboratory and attenuated MuV vaccine strains, and can be used for clinical MuV isolation producing genetically stable progeny virus with titres only slightly lower than Vero cells. Vero cells had previously been accused of producing genetically altered viruses during growth and serial passage however this had never been confirmed until now.

Ferrets had been experimentally infected prior to this PhD project (Gordon *et al.*, 1956) with interesting results suggesting that they are susceptible to MuV infection and elicit an immune response, yet despite these findings, no other mumps studies using the ferret model have been documented. The *in vivo* data described here further validates the historical findings that ferrets generate a serum antibody response specific to MuV and also reports for the first time on the cytokine and IFN response in this animal model to MuV infection.

The findings from both the *in vitro* and *in vivo* studies have provided new information in the area of mumps research and may further advance related research. For example, the cell lines identified as being suitable for propagating high titre, genetically stable representative wild-type MuV (Mu90) are widely available and easy to manipulate (Hep 2C, HGT-1 and MCF-7) so could be routinely used for growing stocks of virus in research laboratories and have potential to be used for cultivation of clinical isolates. These cells would also be useful for investigating MuV-host cell interactions by proteomics techniques such as stable isotope labelling of amino acids in cell culture (SILAC) coupled with mass spectrometry, or transcriptome analyses by human microarray and RNAseq. All of these techniques require the infection of a human cell line with the virus of interest as the annotated genome of the host cell must be fully available. It also makes the results of these types of experiments more meaningful as the data can be translated to provide information on the human infection. Now that the susceptibility of HAE cells to MuV infection has been confirmed, these types of cultures will be valuable for future mumps research and although they may not be as readily available as continuous cell lines such as Hep 2C, they are commercially available, produced under strict quality control, and have been demonstrated in this project to be the superior *in vitro* system for maintaining the genetic stability of MuV.

As discussed in section 4.6, the ferret model appears not to be of value for studying virus pathogenesis, tropism, persistence and transmission of MuV *in vivo*. The guinea pig model may prove to be effective for these aspects of MuV infection as these animals have previously been

demonstrated to elicit a serum antibody response and infectious virus was recovered after intracerebral inoculation (Tokuda, 1957). From a technical point of view, guinea pigs are smaller, cheaper and also easier to handle than ferrets. Studies validating and elaborating on these findings are lacking and a systematic evaluation of the guinea pig as a mumps animal model should be carried out in the future in a similar manner to the experiments described in this thesis.

The results obtained from infection of A549 cells constitutively expressing the V protein of hPIV5 or the NPro protein of BVDV (discussed in section 3.7) provided a proof of principle that expression of a molecule that will allow a virus to circumvent the host IFN response allows for enhanced virus replication. Transgenic mice expressing the human poliovirus receptor (Ren *et al.*, 1990) have been successfully developed and used in polio research for many years, and in theory transgenic mice expressing a protein such as hPIV5-V or indeed MuV-V could be useful for MuV research. A transgenic mouse model expressing human STAT-2 has been developed and utilised for experimental hPIV5 infection (Kraus *et al.*, 2008) and it would be interesting to infect mice like these or other IFN-knockout mice with MuV.

The results generated during this PhD project including the “negative” findings, will be of interest to scientists in the field of paramyxovirus research and have made a significant contribution to mumps research. The data described for the assessment of ferrets as an *in vivo* MuV model have been submitted for publication. Therefore, this project has formed a distinct contribution to the knowledge of the subject and provides evidence of originality shown by the discovery of new facts and the exercise of independent critical power.

REFERENCES

Afzal, M., Pickford, A. R., Forsey, T., Heath, A. B. & Minor, P. D. (1993). The Jeryl Lynn vaccine strain of mumps virus is a mixture of two distinct isolates. *Journal of General Virology* **74**, 917-920.

Afzal, M. A., Elliott, G. D., Rima, B. K. & Orvell, C. (1990). Virus and host cell-dependent variation in transcription of the mumps virus genome. *J Gen Virol* **71 (Pt 3)**, 615-619.

Afzal, M. A., Buchanan, J., Heath, A. B. & Minor, P. D. (1997). Clustering of mumps virus isolates by SH gene sequence only partially reflects geographical origin. *Arch Virol* **142**, 227-238.

Afzal, M. A., Marsden, S. A., Hull, R. M., Pipkin, P. A., Bentley, M. L. & Minor, P. D. (1999). Evaluation of the neurovirulence test for mumps vaccines. *Biologicals* **27**, 43-49.

Afzal, M. A., Dussupt, V., Minor, P. D., Pipkin, P. A., Fleck, R., Hockley, D. J. & Stacey, G. N. (2005). Assessment of mumps virus growth on various continuous cell lines by virological, immunological, molecular and morphological investigations. *Journal of Virological Methods* **126**, 149-156.

Al-Soud, W. A. & Radstrom, P. (2001). Purification and characterization of PCR-inhibitory components in blood cells. *J Clin Microbiol* **39**, 485-493.

Andrejeva, J., Childs, K. S., Young, D. F., Carlos, T. S., Stock, N., Goodbourn, S. & Randall, R. E. (2004). The V proteins of paramyxoviruses bind the IFN-inducible RNA helicase, mda-5, and inhibit its activation of the IFN-beta promoter. *Proc Natl Acad Sci U S A* **101**, 17264-17269.

Andrewes, C. H., Bang, F. B. & Burnet, F. M. (1955). A short description of the Myxovirus group (influenza and related viruses). *Virology* **1**, 176-184.

Andrews, P. W., Damjanov, I., Simon, D., Banting, G. S., Carlin, C., Dracopoli, N. C. & Fogh, J. (1984). Pluripotent embryonal carcinoma clones derived from the human teratocarcinoma cell line Tera-2. Differentiation in vivo and in vitro. *Lab Invest* **50**, 147-162.

Andzhaparidze, O. G., Boriskin Yu, S., Bogomolova, N. N. & Drynov, I. D. (1982). Mumps virus-persistently infected cell cultures release defective interfering virus particles. *J Gen Virol* **63**, 499-503.

Arnberg, N., Edlund, K., Kidd, A. H. & Wadell, G. (2000). Adenovirus type 37 uses sialic acid as a cellular receptor. *J Virol* **74**, 42-48.

Asano, T., Ichiki, K., Koizumi, S., Kaizu, K., Hatori, T., Fujino, O., Mashiko, K., Sakamoto, Y., Miyasho, T. & other authors (2011). Enhanced expression of cytokines/chemokines in cerebrospinal fluids in mumps meningitis in children. *Pediatr Int* **53**, 143-146.

Atrasheuskaya, A. V., Neverov, A. A., Rubin, S. & Ignatyev, G. M. (2006). Horizontal transmission of the Leningrad-3 live attenuated mumps vaccine virus. *Vaccine* **24**, 1530-1536.

Bakker, W. & Mathias, R. (2001). Mumps caused by an inadequately attenuated measles, mumps and rubella vaccine. *Can J Infect Dis* **12**, 144-148.

Balraj, V. & Miller, E. (1995). Complications of mumps vaccines. *Reviews in Medical Virology* **5**, 219-227.

Bankamp, B., Fontana, J. M., Bellini, W. J. & Rota, P. A. (2008). Adaptation to cell culture induces functional differences in measles virus proteins. *Virol J* **5**, 129.

Banks-Schlegel, S. P., Gazdar, A. F. & Harris, C. C. (1985). Intermediate filament and cross-linked envelope expression in human lung tumor cell lines. *Cancer Res* **45**, 1187-1197.

Bastien, N., Bowness, D., Burton, L., Bontovics, E., Winter, A. L., Tipples, G., Minielly, D., Gregg, B., Cramer, C. & other authors (2009). Parotitis in a child infected with triple-reassortant influenza A virus in Canada in 2007. *J Clin Microbiol* **47**, 1896-1898.

Beale, A. J., Christofinis, C. G. & Furminger, I. G. S. (1963). Rabbit cells susceptible to rubella virus. *The Lancet* **2**, 640.

Beck, M., Welszmalecek, R., Meskoprejac, M., Radman, V., Juzbasic, M., Rajningermiholic, M., Prislinmusklic, M., Dobrovsaksourek, V., Smerdel, S. & other authors (1989). Mumps Vaccine L-Zagreb, Prepared in Chick Fibroblasts .1. Production and Field Trials. *J Biol Stand* **17**, 85-90.

Bell, J. A. & Manning, D. D. (1990). A domestic ferret model of immunity to Campylobacter jejuni-induced enteric disease. *Infect Immun* **58**, 1848-1852.

Binder, G. K. & Griffin, D. E. (2001). Interferon-gamma-mediated site-specific clearance of alphavirus from CNS neurons. *Science* **293**, 303-306.

Bose, S., Welch, B. D., Kors, C. A., Yuan, P., Jardetzky, T. S. & Lamb, R. A. (2011). Structure and mutagenesis of the parainfluenza virus 5 hemagglutinin-neuraminidase stalk domain reveals a four-helix bundle and the role of the stalk in fusion promotion. *J Virol* **85**, 12855-12866.

Bossert, B. & Conzelmann, K. K. (2002). Respiratory syncytial virus (RSV) nonstructural (NS) proteins as host range determinants: a chimeric bovine RSV with NS genes from human RSV is attenuated in interferon-competent bovine cells. *Journal of virology* **76**, 4287-4293.

Brown, E. G. & Wright, K. E. (1998). Genetic studies on a mumps vaccine strain associated with meningitis. *Rev Med Virol* **8**, 129-142.

Buynak, E. B. & Hilleman, M. R. (1966). Live attenuated mumps virus vaccine. 1. Vaccine development. *Proc Soc Exp Biol Med* **123**, 768-775.

Calain, P. & Roux, L. (1993). The rule of six, a basic feature for efficient replication of Sendai virus defective interfering RNA. *J Virol* **67**, 4822-4830.

Cantin, E., Tanamachi, B. & Openshaw, H. (1999). Role for gamma interferon in control of herpes simplex virus type 1 reactivation. *J Virol* **73**, 3418-3423.

Carbone, K. M. & Rubin, S. (2007). Mumps virus in:. In *Fields Virology*, 6 edn, pp. 1527-1550. Edited by D. M. Knipe & P. M. Howley. Philadelphia: Lippincott, Williams and Wilkins.

Carney, D. N., Gazdar, A. F., Bepler, G., Guccion, J. G., Marangos, P. J., Moody, T. W., Zweig, M. H. & Minna, J. D. (1985). Establishment and Identification of Small Cell Lung-Cancer Cell-Lines Having Classic and Variant Features. *Cancer Res* **45**, 2913-2923.

Carter, S. D., Dent, K. C., Atkins, E., Foster, T. L., Verow, M., Gorny, P., Harris, M., Hiscox, J. A., Ranson, N. A. & other authors (2010). Direct visualization of the small hydrophobic protein of human respiratory syncytial virus reveals the structural basis for membrane permeability. *Febs Lett* **584**, 2786-2790.

Castells, E., George, V. G. & Hierholzer, J. C. (1990). Nci-H292 as an Alternative Cell-Line for the Isolation and Propagation of the Human Paramyxoviruses. *Archives of Virology* **115**, 277-288.

Chambers, P., Rima, B. K. & Duprex, W. P. (2009). Molecular differences between two Jeryl Lynn mumps virus vaccine component strains, JL5 and JL2. *Journal of General Virology* **90**, 2973-2981.

Chen, S., Short, J. A., Young, D. F., Killip, M. J., Schneider, M., Goodbourn, S. & Randall, R. E. (2010). Heterocellular induction of interferon by negative-sense RNA viruses. *Virology* **407**, 247-255.

Chiba, Y., Horino, K., Umetsu, M., Wataya, Y. & Chiba, S. (1973). Virus excretion and antibody response in saliva in natural mumps. *Tohoku J Exp Med* **111**, 229-238.

Childs, K., Randall, R. & Goodbourn, S. (2012). Paramyxovirus V proteins interact with the RNA Helicase LGP2 to inhibit RIG-I-dependent interferon induction. *J Virol* **86**, 3411-3421.

Chinsangaram, J., Piccone, M. E. & Grubman, M. J. (1999). Ability of foot-and-mouth disease virus to form plaques in cell culture is associated with suppression of alpha/beta interferon. *J Virol* **73**, 9891-9898.

Cizman, M., Mozetic, M., Radescek-Rakar, R., Pleterski-Rigler, D. & Susec-Michieli, M. (1989). Aseptic meningitis after vaccination against measles and mumps. *Pediatr Infect Dis J* **8**, 302-308.

Cohen, C., White, J. M., Savage, E. J., Glynn, J. R., Choi, Y., Andrews, N., Brown, D. & Ramsay, M. E. (2007). Vaccine effectiveness estimates, 2004-2005 mumps outbreak, England. *Emerg Infect Dis* **13**, 12-17.

Connaris, H., Takimoto, T., Russell, R., Crennell, S., Moustafa, I., Portner, A. & Taylor, G. (2002). Probing the sialic acid binding site of the hemagglutinin-neuraminidase of Newcastle disease virus: identification of key amino acids involved in cell binding, catalysis, and fusion. *J Virol* **76**, 1816-1824.

Connor, R. J., Kawaoka, Y., Webster, R. G. & Paulson, J. C. (1994). Receptor specificity in human, avian, and equine H2 and H3 influenza virus isolates. *Virology* **205**, 17-23.

Conzelmann, K. K. (1998). Nonsegmented negative-strand RNA viruses: genetics and manipulation of viral genomes. *Annu Rev Genet* **32**, 123-162.

Cordey, S. & Roux, L. (2006). Transcribing paramyxovirus RNA polymerase engages the template at its 3' extremity. *J Gen Virol* **87**, 665-672.

Crennell, S., Takimoto, T., Portner, A. & Taylor, G. (2000). Crystal structure of the multifunctional paramyxovirus hemagglutinin-neuraminidase. *Nat Struct Biol* **7**, 1068-1074.

Cusi, M. G., Santini, L., Bianchi, S., Valassina, M. & Valensin, P. E. (1998). Nucleotide sequence at position 1081 of the hemagglutinin-neuraminidase gene in wild-type strains of mumps virus is the most relevant marker of virulence. *Journal of Clinical Microbiology* **36**, 3743-3744.

da Cunha, S. S., Rodrigues, L. C., Barreto, M. L. & Dourado, I. (2002). Outbreak of aseptic meningitis and mumps after mass vaccination with MMR vaccine using the Leningrad-Zagreb mumps strain. *Vaccine* **20**, 1106-1112.

Darnell, J. E., Jr., Kerr, I. M. & Stark, G. R. (1994). Jak-STAT pathways and transcriptional activation in response to IFNs and other extracellular signaling proteins. *Science* **264**, 1415-1421.

Dayan, G. H., Quinlisk, M. P., Parker, A. A., Barskey, A. E., Harris, M. L., Schwartz, J. M., Hunt, K., Finley, C. G., Leschinsky, D. P. & other authors (2008). Recent resurgence of mumps in the United States. *N Engl J Med* **358**, 1580-1589.

Desmyter, J., Melnick, J. L. & Rawls, W. E. (1968). Defectiveness of interferon production and of rubella virus interference in a line of African green monkey kidney cells (Vero). *J Virol* **2**, 955-961.

Didcock, L., Young, D. F., Goodbourn, S. & Randall, R. E. (1999). The V protein of simian virus 5 inhibits interferon signalling by targeting STAT1 for proteasome-mediated degradation. *J Virol* **73**, 9928-9933.

Dugan, A. S., Gasparovic, M. L. & Atwood, W. J. (2008). Direct correlation between sialic acid binding and infection of cells by two human Polyomaviruses (JC virus and BK virus). *J Virol* **82**, 2560-2564.

Dunlevy, F., McElvaney, N. G. & Greene, C. M. (2010). TLR3 Sensing of Viral Infection. *The Open Infectious Diseases Journal* **4**, 1-10.

Duprex, W. P., McQuaid, S., Hangartner, L., Billeter, M. A. & Rima, B. K. (1999). Observation of measles virus cell-to-cell spread in astrocytoma cells by using a green fluorescent protein-expressing recombinant virus. *J Virol* **73**, 9568-9575.

Elango, N., Varsanyi, T. M., Kovamees, J. & Norrby, E. (1988). Molecular cloning and characterization of six genes, determination of gene order and intergenic sequences and leader sequence of mumps virus. *J Gen Virol* **69 (Pt 11)**, 2893-2900.

Elliot, G. D., Afzal, M. A., Martin, S. J. & Rima, B. K. (1989). Nucleotide sequence of the matrix, fusion and putative SH protein genes of mumps virus and their deduced amino acid sequences. *Virus Research* **12**, 61-75.

Elliott, G. D., Yeo, R. P., Afzal, M. A., Simpson, E. J., Curran, J. A. & Rima, B. K. (1990). Strain-variable editing during transcription of the P gene of mumps virus may lead to the generation of non-structural proteins NS1 (V) and NS2. *J Gen Virol* **71 (Pt 7)**, 1555-1560.

Emeny, J. M. & Morgan, M. J. (1979). Regulation of the Interferon System - Evidence That Vero Cells Have a Genetic Defect in Interferon-Production. *Journal of General Virology* **43**, 247-252.

Enders, J. F., Kane, L. W., Cohen, S. & Levens, J. H. (1945). Immunity in mumps I. Experiments with Monkeys (Macacus mulatta). The Development of complement-fixing antibody following infection and experiments on immunization by means of inactivated virus and convalescent human serum. *Journal of Experimental Medicine* **81**, 93-117.

Engelhorn, M., Stricker, R. & Roux, L. (1993). Molecular cloning and characterization of a Sendai virus internal deletion defective RNA. *J Gen Virol* **74 (Pt 1)**, 137-141.

Fehrholz, M., Kendl, S., Prifert, C., Weissbrich, B., Lemon, K., Rennick, L., Duprex, P. W., Rima, B. K., Koning, F. A. & other authors (2012). The innate antiviral factor APOBEC3G targets replication of measles, mumps and respiratory syncytial viruses. *J Gen Virol* **93**, 565-576.

Ferm, V. H. & Kilham, L. (1963). Mumps Virus Infection of the Pregnant Hamster. *J Embryol Exp Morphol* **11**, 659-665.

Finney, D. J. (1971). *Probit Analysis*, 3rd edn.: Cambridge University Press.

Fiorentino, D. F., Zlotnik, A., Vieira, P., Mosmann, T. R., Howard, M., Moore, K. W. & O'Garra, A. (1991). IL-10 acts on the antigen-presenting cell to inhibit cytokine production by Th1 cells. *J Immunol* **146**, 3444-3451.

Fleischer, B. & Kreth, H. W. (1982). Mumps virus replication in human lymphoid cell lines and in peripheral blood lymphocytes: preference for T cells. *Infect Immun* **35**, 25-31.

Fogh, J., Wright, W. C. & Loveless, J. D. (1977a). Absence of HeLa cell contamination in 169 cell lines derived from human tumors. *J Natl Cancer Inst* **58**, 209-214.

Fogh, J., Fogh, J. M. & Orfeo, T. (1977b). One hundred and twenty-seven cultured human tumor cell lines producing tumors in nude mice. *J Natl Cancer Inst* **59**, 221-226.

Foster, K. A., Oster, C. G., Mayer, M. M., Avery, M. L. & Audus, K. L. (1998). Characterization of the A549 cell line as a type II pulmonary epithelial cell model for drug metabolism. *Exp Cell Res* **243**, 359-366.

Fox, J. G., Ackerman, J. I., Taylor, N., Claps, M. & Murphy, J. C. (1987). Campylobacter jejuni infection in the ferret: an animal model of human campylobacteriosis. *Am J Vet Res* **48**, 85-90.

Fox, J. G., Correa, P., Taylor, N. S., Lee, A., Otto, G., Murphy, J. C. & Rose, R. (1990). Helicobacter mustelae-associated gastritis in ferrets. An animal model of Helicobacter pylori gastritis in humans. *Gastroenterology* **99**, 352-361.

Foy, H. M., Cooney, M. K., Hall, C. E., Bor, E. & Maletzky, A. J. (1971). Isolation of mumps virus from children with acute lower respiratory tract disease. *Am J Epidemiol* **94**, 467-472.

Fu, C. X., Nie, J., Liang, J. H. & Wang, M. (2009). Evaluation of live attenuated S79 mumps vaccine effectiveness in mumps outbreaks: a matched case-control study. *Chin Med J (Engl)* **122**, 307-310.

Furesz, J. & Contreras, G. (1990). Vaccine-related mumps meningitis--Canada. *Can Dis Wkly Rep* **16**, 253-254.

Gardner, A. E., Martin, K. L. & Dutch, R. E. (2007). A conserved region between the heptad repeats of paramyxovirus fusion proteins is critical for proper F protein folding. *Biochemistry-Us* **46**, 5094-5105.

Gavitt, F. & Bird, T. J. (1967). Cytopathic effect of mumps and other viruses in guinea pig heart cells. *Appl Microbiol* **15**, 448-450.

Gifford, G. E., Toy, S. T. & Lindenmann, J. (1963). Studies on vaccinia virus plaque formation and its inhibition by interferon. II. Dynamics of plaque formation by vaccinia virus in the presence of interferon. *Virology* **19**, 294-301.

Gil, L. H., Ansari, I. H., Vassilev, V., Liang, D., Lai, V. C., Zhong, W., Hong, Z., Dubovi, E. J. & Donis, R. O. (2006). The amino-terminal domain of bovine viral diarrhea virus Npro protein is necessary for alpha/beta interferon antagonism. *J Virol* **80**, 900-911.

Gluck, R., Hoskins, J. M., Wegmann, A., Just, M. & Germanier, R. (1986). Rubini, a new live attenuated mumps vaccine virus strain for human diploid cells. *Dev Biol Stand* **65**, 29-35.

Gluzman, Y. (1981). SV40-transformed simian cells support the replication of early SV40 mutants. *Cell* **23**, 175-182.

Goh, K. T. (1999). Resurgence of mumps in Singapore caused by the Rubini mumps virus vaccine strain. *Lancet* **354**, 1355-1356.

Gordon, I., Pavri, K. & Cohen, S. M. (1956). Response of ferrets to mumps virus. *J Immunol* **76**, 328-333.

Gotoh, B., Komatsu, T., Takeuchi, K. & Yokoo, J. (2002). Paramyxovirus strategies for evading the interferon response. *Rev Med Virol* **12**, 337-357.

Gotoh, H., Shioda, T., Sakai, Y., Mizumoto, K. & Shibuta, H. (1989). Rescue of Sendai virus from viral ribonucleoprotein-transfected cells by infection with recombinant vaccinia viruses carrying Sendai virus L and P/C genes. *Virology* **171**, 434-443.

Govorkova, E. A., Murti, G., Meignier, B., de Taisne, C. & Webster, R. G. (1996). African green monkey kidney (Vero) cells provide an alternative host cell system for influenza A and B viruses. *J Virol* **70**, 5519-5524.

Graham, F. L., Smiley, J., Russell, W. C. & Nairn, R. (1977). Characteristics of a human cell line transformed by DNA from human adenovirus type 5. *J Gen Virol* **36**, 59-74.

Gravel, K. A. & Morrison, T. G. (2003). Interacting domains of the HN and F proteins of newcastle disease virus. *J Virol* **77**, 11040-11049.

Habel, K. (1945). Cultivation of mumps virus in the developing chick embryo and its application to studies of immunity to mumps in man. *Public Health Reports* **60**, 201-212.

Hamaguchi, M., Yoshida, T., Nishikawa, K., Naruse, H. & Nagai, Y. (1983). Transcriptive complex of Newcastle disease virus. I. Both L and P proteins are required to constitute an active complex. *Virology* **128**, 105-117.

Hamilton, R. (1790). An account of a distemper by the common people of England vulgarly called the mumps. *London Medical Journal* **11**, 190-211.

Hausmann, S., Garcin, D., Delenda, C. & Kolakofsky, D. (1999). The versatility of paramyxovirus RNA polymerase stuttering. *Journal of virology* **73**, 5568-5576.

Heinrich, P. C., Behrmann, I., Haan, S., Hermanns, H. M., Muller-Newen, G. & Schaper, F. (2003). Principles of interleukin (IL)-6-type cytokine signalling and its regulation. *Biochem J* **374**, 1-20.

Henle, G. & Deinhardt, F. (1955). Propagation and primary isolation of mumps virus in tissue culture. *Proc Soc Exp Biol Med* **89**, 556-560.

Herrler, G. & Compans, R. W. (1982). Synthesis of mumps virus polypeptides in infected Vero cells. *Virology* **119**, 430-438.

Hilton, L., Moganeradj, K., Zhang, G., Chen, Y. H., Randall, R. E., McCauley, J. W. & Goodbourn, S. (2006). The NPro product of bovine viral diarrhea virus inhibits DNA binding by interferon regulatory factor 3 and targets it for proteasomal degradation. *J Virol* **80**, 11723-11732.

Hishiyama, M., Tanabayashi, K., Takeuchi, K. & Yamada, A. (1996). Establishment of cell lines stably expressing mumps virus glycoproteins. *Jpn J Med Sci Biol* **49**, 29-38.

Hopps, H. E., Bernheim, B. C., Nisalak, A., Tjio, J. H. & Smadel, J. E. (1963). Biologic Characteristics of a Continuous Kidney Cell Line Derived from the African Green Monkey. *J Immunol* **91**, 416-424.

Hornung, V., Ellegast, J., Kim, S., Brzozka, K., Jung, A., Kato, H., Poeck, H., Akira, S., Conzelmann, K. K. & other authors (2006). 5 '-triphosphate RNA is the ligand for RIG-I. *Science* **314**, 994-997.

Horvath, C. M. (2004a). Weapons of STAT destruction. Interferon evasion by paramyxovirus V protein. *Eur J Biochem* **271**, 4621-4628.

Horvath, C. M. (2004b). Silencing STATs: lessons from paramyxovirus interferon evasion. *Cytokine Growth Factor Rev* **15**, 117-127.

Hoying, J. (1975). Selection and histochemical identification of epithelial-like cells from guinea pig lung *MSc Thesis, Wright State University*.

HPA, U. (2012). Laboratory confirmed cases of measles, mumps and rubella (Engaldn and Wales): April-June 2012. In *Immunisation*: Health Protection Agency UK.

Hsu, C. H., Re, G. G., Gupta, K. C., Portner, A. & Kingsbury, D. W. (1985). Expression of Sendai virus defective-interfering genomes with internal deletions. *Virology* **146**, 38-49.

Hsu, M., Scheid, A. & Choppin, P. W. (1981). Activation of the Sendai virus fusion protein (f) involves a conformational change with exposure of a new hydrophobic region. *J Biol Chem* **256**, 3557-3563.

Huang, A. S. & Baltimore, D. (1970). Defective viral particles and viral disease processes. *Nature* **226**, 325-327.

Huang, S., Wiszniewski, L. & Constant, S. (2011). The use of In Vitro 3D Cell Models in Drug Development for Respiratory Diseases. In *Drug Discovery and Development - Present and Future*. Edited by I. M. Kapetanovic: InTech.

Hull, R. N., Cherry, W. R. & Johnson, I. S. (1956). The adaption and maintenance of mammalian cells to continuous growth in tissue culture. *Anat Rec* **124**, 490.

Hull, R. N., Cherry, W. R. & Tritch, O. J. (1962). Growth characteristics of monkey kidney cell strains LLC-MK1, LLC-MK2, and LLC-MK2(NCTC-3196) and their utility in virus research. *J Exp Med* **1**, 903-918.

Hviid, A., Rubin, S. & Muhlemann, K. (2008). Mumps. *Lancet* **371**, 932-944.

Ichiyama, T., Maeba, S., Suenaga, N., Saito, K., Matsubara, T. & Furukawa, S. (2005). Analysis of cytokine levels in cerebrospinal fluid in mumps meningitis: comparison with echovirus type 30 meningitis. *Cytokine* **30**, 243-247.

Iorio, R. M. & Mahon, P. J. (2008). Paramyxoviruses: different receptors - different mechanisms of fusion. *Trends Microbiol* **16**, 135-137.

Irie, T., Kiyotani, K., Igarashi, T., Yoshida, A. & Sakaguchi, T. (2012). Inhibition of Interferon Regulatory Factor 3 Activation by Paramyxovirus V Protein. *J Virol* **86**, 7136-7145.

Ivancic, J., Forcic, D., Gulija, T. K., Zgorelec, R., Repalust, L., Baricevic, M., Mesko-Prejac, M. & Mazuran, R. (2004). Genetic characterization of a mumps virus isolate during passaging in the amniotic cavity of embryonated chicken eggs. *Virus Res* **99**, 121-129.

Jacob, S. & Poddar, S. (1978). The histochemistry of mucosubstances in ferret salivary glands. *Acta Histochem* **61**, 142-154.

Jacobs, J. P., Jones, C. M. & Baille, J. P. (1970). Characteristics of a human diploid cell designated MRC-5. *Nature* **227**, 168-170.

Jayaraman, A., Chandrasekaran, A., Viswanathan, K., Raman, R., Fox, J. G. & Sasisekharan, R. (2012). Decoding the distribution of glycan receptors for human-adapted influenza A viruses in ferret respiratory tract. *PloS one* **7**, e27517.

Jensen, F. C., Girardi, A. J., Gilden, R. V. & Koprowski, H. (1964). Infection of Human and Simian Tissue Cultures with Rous Sarcoma Virus. *Proc Natl Acad Sci U S A* **52**, 53-59.

Jensen, S. & Thomsen, A. R. (2012). Sensing of RNA viruses: a review of innate immune receptors involved in recognizing RNA virus invasion. *J Virol* **86**, 2900-2910.

Jin, L., Rima, B., Brown, D., Orvell, C., Tecle, T., Afzal, M., Uchida, K., Nakayama, T., Song, J. W. & other authors (2005). Proposal for genetic characterisation of wild-type mumps strains: preliminary standardisation of the nomenclature. *Arch Virol* **150**, 1903-1909.

Johnson, C. D. & Goodpasture, E. W. (1934). An Investigation of the Etiology of Mumps. *J Exp Med* **59**, 1-19.

Johnson, C. D. & Goodpasture, E. W. (1935). The Etiology of Mumps. *Am J Hyg* **21**, 46-57.

Johnston, M. D. (1981). The characteristics required for a Sendai virus preparation to induce high levels of interferon in human lymphoblastoid cells. *J Gen Virol* **56**, 175-184.

Jokinen, S., Osterlund, P., Julkunen, I. & Davidkin, I. (2007). Cellular immunity to mumps virus in young adults 21 years after measles-mumps-rubella vaccination. *J Infect Dis* **196**, 861-867.

Kaic, B., Gjenero-Margan, I., Aleraj, B., Ljubin-Sternak, S., Vilibic-Cavlek, T., Kilvain, S., Pavic, I., Stojanovic, D. & Ilic, A. (2008). Transmission of the L-Zagreb mumps vaccine virus, Croatia, 2005-2008. *Euro Surveill* **13**.

Kao, F. T. & Puck, T. T. (1968). Genetics of somatic mammalian cells, VII. Induction and isolation of nutritional mutants in Chinese hamster cells. *Proc Natl Acad Sci U S A* **60**, 1275-1281.

Kato, T. (1981). [Growth of mumps virus in human stomach cancer cell lines. I. Establishment of persistent infections (author's transl)]. *Hokkaido Igaku Zasshi* **56**, 154-158.

Kawai, T., Takahashi, K., Sato, S., Coban, C., Kumar, H., Kato, H., Ishii, K. J., Takeuchi, O. & Akira, S. (2005). IPS-1, an adaptor triggering RIG-I- and Mda5-mediated type I interferon induction. *Nat Immunol* **6**, 981-988.

Kilham, L. (1951). Mumps virus in human milk and in milk of infected monkey. *J Am Med Assoc* **146**, 1231-1232.

Kilham, L. & Murphy, H. W. (1952). Propagation of mumps virus in suckling mice and in mouse embryo tissue cultures. *Proc Soc Exp Biol Med* **80**, 495-498.

Kit, S., Dubbs, D. R., Piekarski, L. J. & Hsu, T. C. (1963). Deletion of Thymidine Kinase Activity from L Cells Resistant to Bromodeoxyuridine. *Exp Cell Res* **31**, 297-312.

Klein, S. L. & Huber, S. (2010). In *Sex Hormones and Immunity to Infection*.

Klenk, H. D. & Garten, W. (1994). Host cell proteases controlling virus pathogenicity. *Trends Microbiol* **2**, 39-43.

Knowles, W. A. & Cohen, B. J. (2001). Efficient isolation of mumps virus from a community outbreak using the marmoset lymphoblastoid cell line B95a. *Journal of Virological Methods* **96**, 93-96.

Kobinger, G. P., Figueredo, J. M., Rowe, T., Zhi, Y., Gao, G., Sanmiguel, J. C., Bell, P., Wivel, N. A., Zitzow, L. A. & other authors (2007). Adenovirus-based vaccine prevents pneumonia in ferrets challenged with the SARS coronavirus and stimulates robust immune responses in macaques. *Vaccine* **25**, 5220-5231.

Kolakofsky, D., Pelet, T., Garcin, D., Hausmann, S., Curran, J. & Roux, L. (1998). Paramyxovirus RNA synthesis and the requirement for hexamer genome length: the rule of six revisited. *J Virol* **72**, 891-899.

Kong, W. S., Irie, T., Yoshida, A., Kawabata, R., Kadoi, T. & Sakaguchi, T. (2012). Inhibition of virus-like particle release of Sendai virus and Nipah virus, but not that of mumps virus, by tetherin/CD317/BST-2. *Hiroshima journal of medical sciences* **61**, 59-67.

Kovamees, J., Norrby, E. & Elango, N. (1989). Complete nucleotide sequence of the hemagglutinin-neuraminidase (HN) mRNA of mumps virus and comparison of paramyxovirus HN proteins. *Virus Res* **12**, 87-96.

Kraus, T. A., Garza, L. & Horvath, C. M. (2008). Enabled interferon signaling evasion in an immune-competent transgenic mouse model of parainfluenza virus 5 infection. *Virology* **371**, 196-205.

Krilov, L. R. & Swenson, P. (1985). Acute parotitis associated with influenza A infection. *J Infect Dis* **152**, 853.

Kubota, T., Yokosawa, N., Yokota, S. & Fujii, N. (2001). C terminal CYS-RICH region of mumps virus structural v protein correlates with block of interferon alpha and gamma signal transduction pathway through decrease of STAT 1-alpha. *Biochem Bioph Res Co* **283**, 255-259.

Kubota, T., Yokosawa, N., Yokota, S. & Fujii, N. (2002). Association of mumps virus V protein with RACK1 results in dissociation of STAT-1 from the alpha interferon receptor complex. *J Virol* **76**, 12676-12682.

Kubota, T., Yokosawa, N., Yokota, S., Fujii, N., Tashiro, M. & Kato, A. (2005a). Mumps virus V protein antagonizes degradation interferon without the complete of STAT1. *Journal of virology* **79**, 4451-4459.

Kubota, T., Yokosawa, N., Yokota, S., Fujii, N., Tashiro, M. & Kato, A. (2005b). Mumps virus V protein antagonizes interferon without the complete degradation of STAT1. *J Virol* **79**, 4451-4459.

Kulkarni, P. S., Phadke, M. A., Jadhav, S. S. & Kapre, S. V. (2005). No definitive evidence for L-Zagreb mumps strain associated aseptic meningitis: a review with special reference to the da Cunha study. *Vaccine* **23**, 5286-5288.

Kundig, T. M., Hengartner, H. & Zinkernagel, R. M. (1993). T cell-dependent IFN-gamma exerts an antiviral effect in the central nervous system but not in peripheral solid organs. *J Immunol* **150**, 2316-2321.

Laboisse, C. L., Augeron, C., Couturier-Turpin, M. H., Gespach, C., Cheret, A. M. & Potet, F. (1982). Characterization of a newly established human gastric cancer cell line HGT-1 bearing histamine H2-receptors. *Cancer Res* **42**, 1541-1548.

Lamb, R. A. & Parks, G. D. (2007). Paramyxoviridae: The Viruses and their Replication. In *Fields Virology*, 6 edn, pp. 1449-1496. Edited by D. M. Knipe & P. M. Howley. Phildadelphia: Lippincott, Williams and Wilkins.

Lauring, A. S. & Andino, R. (2010). Quasispecies theory and the behavior of RNA viruses. *PLoS Pathog* **6**, e1001005.

Lawrence, M. C., Borg, N. A., Streltsov, V. A., Pilling, P. A., Epa, V. C., Varghese, J. N., McKimm-Breschkin, J. L. & Colman, P. M. (2004). Structure of the haemagglutinin-neuraminidase from human parainfluenza virus type III. *J Mol Biol* **335**, 1343-1357.

Lazzarini, R. A., Keene, J. D. & Schubert, M. (1981). The origins of defective interfering particles of the negative-strand RNA viruses. *Cell* **26**, 145-154.

Lee, A. C., Lim, W. L. & So, K. T. (1997). Epstein-Barr virus associated parotitis. *J Paediatr Child Health* **33**, 177-178.

Li, M., Schmitt, P. T., Li, Z., McCrory, T. S., He, B. & Schmitt, A. P. (2009). Mumps virus matrix, fusion, and nucleocapsid proteins cooperate for efficient production of virus-like particles. *J Virol* **83**, 7261-7272.

Lieber, M., Mazzetta, J., Nelson-Rees, W., Kaplan, M. & Todaro, G. (1975). Establishment of a continuous tumor-cell line (panc-1) from a human carcinoma of the exocrine pancreas. *Int J Cancer* **15**, 741-747.

Lin, Y., Sun, M., Fuentes, S. M., Keim, C. D., Rothermel, T. & He, B. (2007). Inhibition of interleukin-6 expression by the V protein of parainfluenza virus 5. *Virology* **368**, 262-272.

Liu, Y., Xu, Y., Lou, Z., Zhu, J., Hu, X., Gao, G. F., Qiu, B., Rao, Z. & Tien, P. (2006). Structural characterization of mumps virus fusion protein core. *Biochem Biophys Res Commun* **348**, 916-922.

MacPherson, I. (1963). Characteristics of a hamster cell clone transformed by polyoma virus. *J Natl Cancer Inst* **30**, 795-815.

Madin, S. H. & Darby, N. B., Jr. (1958). Established kidney cell lines of normal adult bovine and ovine origin. *Proc Soc Exp Biol Med* **98**, 574-576.

Maher, J. A. & DeStefano, J. (2004). The ferret: an animal model to study influenza virus. *Lab Anim (NY)* **33**, 50-53.

Makino, S., Yamane, Y., Sasaki, K., Nagashima, T. & Higashihara, M. (1976). Studies on the development of a live attenuated mumps virus vaccine. II. Development and evaluation of the live "Hoshino" mumps vaccine. *Kitasato Arch Exp Med* **49**, 53-62.

Malik, T., Wolbert, C., Mauldin, J., Sauder, C., Carbone, K. M. & Rubin, S. A. (2007). Functional consequences of attenuating mutations in the haemagglutinin neuraminidase, fusion and polymerase proteins of a wild-type mumps virus strain. *J Gen Virol* **88**, 2533-2541.

Malik, T., Shegogue, C. W., Werner, K., Ngo, L., Sauder, C., Zhang, C., Duprex, W. P. & Rubin, S. (2011). Discrimination of mumps virus small hydrophobic gene deletion effects from gene translation effects on virus virulence. *J Virol* **85**, 6082-6085.

Malik, T. H., Wolbert, C., Nerret, L., Sauder, C. & Rubin, S. (2009). Single amino acid changes in the mumps virus haemagglutinin-neuraminidase and polymerase proteins are associated with neuroattenuation. *J Gen Virol* **90**, 1741-1747.

Markwell, M. A. K. (1991). New Frontiers Opened by the Exploration of Host Cell Receptors. In *The Paramyxoviruses*, pp. 407-425. Edited by D. W. Kingsbury. New York: Plenum Press.

Martin, R., Vallbracht, A. & Kreth, H. W. (1991). Interferon-gamma secretion by in vivo activated cytotoxic T lymphocytes from the blood and cerebrospinal fluid during mumps meningitis. *J Neuroimmunol* **33**, 191-198.

Martina, B. E., Haagmans, B. L., Kuiken, T., Fouchier, R. A., Rimmelzwaan, G. F., Van Amerongen, G., Peiris, J. S., Lim, W. & Osterhaus, A. D. (2003). Virology: SARS virus infection of cats and ferrets. *Nature* **425**, 915.

Mather, J. P. (1980). Establishment and characterization of two distinct mouse testicular epithelial cell lines. *Biol Reprod* **23**, 243-252.

Matrosovich, M., Matrosovich, T., Carr, J., Roberts, N. A. & Klenk, H. D. (2003). Overexpression of the alpha-2,6-sialyltransferase in MDCK cells increases influenza virus sensitivity to neuraminidase inhibitors. *J Virol* **77**, 8418-8425.

Matrosovich, M. N., Matrosovich, T. Y., Gray, T., Roberts, N. A. & Klenk, H. D. (2004). Human and avian influenza viruses target different cell types in cultures of human airway epithelium. *Proc Natl Acad Sci U S A* **101**, 4620-4624.

Matsuoka, Y., Lamirande, E. W. & Subbarao, K. (2009). The ferret model for influenza. *Curr Protoc Microbiol* **Chapter 15**, Unit 15G 12.

McAllister, R. M., Melnyk, J., Finkelstein, J. Z., Adams, E. C., Jr. & Gardner, M. B. (1969). Cultivation in vitro of cells derived from a human rhabdomyosarcoma. *Cancer* **24**, 520-526.

McCallan, L., Corbett, D., Andersen, P. L., Aagaard, C., McMurray, D., Barry, C., Thompson, S., Strain, S. & McNair, J. (2011). A New Experimental Infection Model in Ferrets Based on Aerosolised Mycobacterium bovis. *Vet Med Int* **2011**, 981410.

McCarthy, M., Jubelt, B., Fay, D. B. & Johnson, R. T. (1980). Comparative studies of five strains of mumps virus in vitro and in neonatal hamsters: evaluation of growth, cytopathogenicity, and neurovirulence. *J Med Virol* **5**, 1-15.

McDonnell, J. M. (2001). Surface plasmon resonance: towards an understanding of the mechanisms of biological molecular recognition. *Curr Opin Chem Biol* **5**, 572-577.

Meager, A. & Wadhu, M. (2007). Interleukins. In *Encyclopedia of Life Sciences (eLS)*: John Wiley & Sons, Ltd.

Mendelsohn, C., Johnson, B., Lionetti, K. A., Nobis, P., Wimmer, E. & Racaniello, V. R. (1986). Transformation of a Human Poliovirus Receptor Gene into Mouse Cells. *P Natl Acad Sci USA* **83**, 7845-7849.

Mendelsohn, C. L., Wimmer, E. & Racaniello, V. R. (1989). Cellular receptor for poliovirus: molecular cloning, nucleotide sequence, and expression of a new member of the immunoglobulin superfamily. *Cell* **56**, 855-865.

Mengheri, E., Esteban, M. & Lewis, J. A. (1983). Thymidine kinase genes and the induction of anti-viral responses by interferon. *Febs Lett* **157**, 301-305.

Merck & Co, I. (2004). M-M-R II (Measles, Mumps and Rubella Virus Vaccine Live).

Merz, D. C., Server, A. C., Waxham, M. N. & Wolinsky, J. S. (1983). Biosynthesis of mumps virus F glycoprotein: non-fusing strains efficiently cleave the F glycoprotein precursor. *J Gen Virol* **64 (Pt 7)**, 1457-1467.

Miller, E., Goldacre, M., Pugh, S., Colville, A., Farrington, P., Flower, A., Nash, J., MacFarlane, L. & Tettmar, R. (1993). Risk of aseptic meningitis after measles, mumps, and rubella vaccine in UK children. *Lancet* **341**, 979-982.

Miller, G., Shope, T., Lisco, H., Stitt, D. & Lipman, M. (1972). Epstein-Barr virus: transformation, cytopathic changes, and viral antigens in squirrel monkey and marmoset leukocytes. *Proc Natl Acad Sci U S A* **69**, 383-387.

Misono, T. S. & Kumar, P. K. R. (2005). Selection of RNA aptamers against human influenza virus hemagglutinin using surface plasmon resonance. *Analytical Biochemistry* **342**, 312-317.

Moore, A. E., Sabachewsky, L. & Toolan, H. W. (1955). Culture characteristics of four permanent lines of human cancer cells. *Cancer Res* **15**, 598-602.

Morrison, T. G. (2003). Structure and function of a paramyxovirus fusion protein. *Biochim Biophys Acta* **1614**, 73-84.

Murphy, B. R., Prince, G. A., Lawrence, L. A., Croen, K. D. & Collins, P. L. (1990). Detection of respiratory syncytial virus (RSV) infected cells by in situ hybridization in the lungs of cotton rats immunized with formalin-inactivated virus or purified RSV F and G glycoprotein subunit vaccine and challenged with RSV. *Virus Res* **16**, 153-162.

Murphy, S. K. & Parks, G. D. (1997). Genome Nucleotide Lengths that are Divisible by six are not Essential but Enhance Replication of Defective Interfering RNAs of the Paramyxovirus Simian Virus 5. *Virology* **232**, 145-157.

Nagai, Y., Ogura, H. & Klenk, H. (1976). Studies on the assembly of the envelope of Newcastle disease virus. *Virology* **69**, 523-538.

Nakayama, K. (1997). Furin: a mammalian subtilisin/Kex2p-like endoprotease involved in processing of a wide variety of precursor proteins. *Biochem J* **327 (Pt 3)**, 625-635.

Naniche, D., Variorkrishnan, G., Cervoni, F., Wild, T. F., Rossi, B., Rabourdincombe, C. & Gerlier, D. (1993). Human Membrane Cofactor Protein (Cd46) Acts as a Cellular Receptor for Measles-Virus. *J Virol* **67**, 6025-6032.

Naruse, H., Nagai, Y., Yoshida, T., Hamaguchi, M., Matsumoto, T., Isomura, S. & Suzuki, S. (1981). The Polypeptides of Mumps-Virus and Their Synthesis in Infected Chick-Embryo Cells. *Virology* **112**, 119-130.

Negrete, O. A., Levroney, E. L., Aguilar, H. C., Bertolotti-Ciarlet, A., Nazarian, R., Tajyar, S. & Lee, B. (2005). EphrinB2 is the entry receptor for Nipah virus, an emergent deadly paramyxovirus. *Nature* **436**, 401-405.

Nguyen, D. T., Ludlow, M., van Amerongen, G., de Vries, R. D., Yuksel, S., Verburgh, R. J., Osterhaus, A. D., Duprex, W. P. & de Swart, R. L. (2012). Evaluation of synthetic infection-enhancing lipopeptides as adjuvants for a live-attenuated canine distemper virus vaccine administered intra-nasally to ferrets. *Vaccine* **30**, 5073-5080.

Nichols, W. W., Murphy, D. G., Cristofalo, V. J., Toji, L. H., Greene, A. E. & Dwight, S. A. (1977). Characterization of a new human diploid cell strain, IMR-90. *Science* **196**, 60-63.

Niizuma, T., Terada, K., Kosaka, Y., Daimon, Y., Inoue, M., Ogita, S., Kataoka, N. & Tanaka, K. (2004). Elevated serum C-reactive protein in mumps orchitis. *Pediatr Infect Dis J* **23**, 971.

Nishio, M., Garcin, D., Simonet, V. & Kolakofsky, D. (2002). The carboxyl segment of the mumps virus V protein associates with stat proteins in vitro via a tryptophan-rich motif. *Virology* **300**, 92-99.

Novick, S. L. & Hoekstra, D. (1988). Membrane penetration of Sendai virus glycoproteins during the early stages of fusion with liposomes as determined by hydrophobic photoaffinity labeling. *Proc Natl Acad Sci U S A* **85**, 7433-7437.

Oh, D. Y., Barr, I. G., Mosse, J. A. & Laurie, K. L. (2008). MDCk SIAT-1 cells show improved isolation rates for recent human influenza viruses compared to conventional MDCK cells. *Journal of Clinical Microbiology* **46**, 2189-2194.

Okazaki, K., Tanabayashi, K., Takeuchi, K., Hishiyama, M., Okazaki, K. & Yamada, A. (1992). Molecular-Cloning and Sequence-Analysis of the Mumps-Virus Gene Encoding the L-Protein and the Trailer Sequence. *Virology* **188**, 926-930.

Ortmann, D., Ohuchi, M., Angliker, H., Shaw, E., Garten, W. & Klenk, H. D. (1994). Proteolytic cleavage of wild type and mutants of the F protein of human parainfluenza virus type 3 by two subtilisin-like endoproteases, furin and Kex2. *J Virol* **68**, 2772-2776.

Orvell, C. (1978). Immunological properties of purified mumps virus glycoproteins. *J Gen Virol* **41**, 517-526.

Orvell, C. (1984). The reactions of monoclonal antibodies with structural proteins of mumps virus. *J Immunol* **132**, 2622-2629.

Overman, J. R. (1954). Antibody response of suckling mice to mumps virus. II. Relation of onset of antibody production to susceptibility to mumps virus infection. *J Immunol* **73**, 249-255.

Palermo, L. M., Porotto, M., Yokoyama, C. C., Palmer, S. G., Mungall, B. A., Greengard, O., Niewiesk, S. & Moscona, A. (2009). Human parainfluenza virus infection of the airway epithelium: viral hemagglutinin-neuraminidase regulates fusion protein activation and modulates infectivity. *J Virol* **83**, 6900-6908.

Palese, P., Lowen, A. C., Mubareka, S., Tumpey, T. M. & Garcia-Sastre, A. (2006). The guinea pig as a transmission model for human influenza viruses. *P Natl Acad Sci USA* **103**, 9988-9992.

Pallister, J., Middleton, D., Crameri, G., Yamada, M., Klein, R., Hancock, T. J., A., F., B., S., Michalski, W. & other authors (2009). Chloroquine Administration Does Not Prevent Nipah Virus Infection and Disease in Ferrets. *J Virol* **83**, 11979-11982.

Parisien, J. P., Lau, J. F. & Horvath, C. M. (2002). STAT2 acts as a host range determinant for species-specific paramyxovirus interferon antagonism and simian virus 5 replication. *Journal of virology* **76**, 6435-6441.

Park, M. S., Garcia-Sastre, A., Cros, J. F., Basler, C. F. & Palese, P. (2003). Newcastle disease virus V protein is a determinant of host range restriction. *Journal of virology* **77**, 9522-9532.

Paterson, R. G. & Lamb, R. A. (1990). RNA editing by G-nucleotide insertion in mumps virus P-gene mRNA transcripts. *J Virol* **64**, 4137-4145.

Patterson, J. B., Thomis, D. C., Hans, S. L. & Samuel, C. E. (1995). Mechanism of interferon action: double-stranded RNA-specific adenosine deaminase from human cells is inducible by alpha and gamma interferons. *Virology* **210**, 508-511.

Pattillo, R. A., Hussa, R. O., Story, M. T., Ruckert, A. C., Shalaby, M. R. & Mattingly, R. F. (1977). Tumor antigen and human chorionic gonadotropin in CaSki cells: a new epidermoid cervical cancer cell line. *Science* **196**, 1456-1458.

Peterson, W. D., Stulberg, C. S. & Simpson, W. F. (1971). Permanent Heteroploid Human Cell Line with Type-B Glucose-6-Phosphate Dehydrogenase. *P Soc Exp Biol Med* **136**, 1187-&.

Petrera, E. & Coto, C. E. (2006). The synergistic effect of IFN-α and IFN-γ against HSV-2 replication in Vero cells is not interfered by the plant antiviral 1-cinnamoyl-3, 11-dihydroxymeliacarpin. *Virology Journal* **3**, 1-10.

Philip, R. N., Reinhard, K. R. & Lackman, D. B. (1959). Observations on a mumps epidemic in a virgin population. *Am J Hyg* **69**, 91-111.

Piazza, F. M., Carson, J. L., Hu, S. S. & Leigh, M. W. (1991). Attachment of Influenza-a Virus to Ferret Tracheal Epithelium at Different Maturational Stages. *Am J Resp Cell Mol* **4**, 82-87.

Pichlmair, A., Schulz, O., Tan, C. P., Naslund, T. I., Liljestrom, P., Weber, F. & Reis e Sousa, C. (2006). RIG-I-mediated antiviral responses to single-stranded RNA bearing 5'-phosphates. *Science* **314**, 997-1001.

Pillet, S., Svitek, N. & von Messling, V. (2009). Ferrets as a Model for Morbillivirus Pathogenesis, Complications, and Vaccines. *Curr Top Microbiol* **330**, 73-87.

Pipkin, P. A., Wood, D. J., Racaniello, V. R. & Minor, P. D. (1993). Characterisation of L cells expressing the human poliovirus receptor for the specific detection of polioviruses in vitro. *J Virol Methods* **41**, 333-340.

Plotkin, S. A. & Wharton, M. (1999). Mumps vaccine. In *Vaccines*, 4th edn, pp. 267-292. Edited by S. A. Plotkin & W. A. Orenstein. Philadelphia: WB Saunders.

Plotkin, S. A. & Rubin, S. (2008). Mumps Vaccine. In *Vaccines*, pp. 435-465. Edited by S. A. Plotkin, W. A. Orenstein & P. A. Offit: Saunders.

Pons, C., Pelayo, T., Pachon, I., Galmes, A., Gonzalez, L., Sanchez, C. & Martinez, F. (2000). Two outbreaks of mumps in children vaccinated with the Rubini strain in Spain indicate low vaccine efficacy. *Euro Surveill* **5**, 80-84.

Porotto, M., Fornabaio, M., Kellogg, G. E. & Moscona, A. (2007). A second receptor binding site on human parainfluenza virus type 3 hemagglutinin-neuraminidase contributes to activation of the fusion mechanism. *J Virol* **81**, 3216-3228.

Porotto, M., Salah, Z., DeVito, I., Talekar, A., Palmer, S. G., Xu, R., Wilson, I. A. & Moscona, A. (2012). The second receptor binding site of the globular head of the Newcastle disease virus hemagglutinin-neuraminidase activates the stalk of multiple paramyxovirus receptor binding proteins to trigger fusion. *J Virol* **86**, 5730-5741.

Puck, T. T., Cieciura, S. J. & Robinson, A. (1958). Genetics of somatic mammalian cells. III. Long-term cultivation of euploid cells from human and animal subjects. *J Exp Med* **108**, 945-956.

Ramachandran, A. & Horvath, C. M. (2009). Paramyxovirus disruption of interferon signal transduction: STATus report. *J Interferon Cytokine Res* **29**, 531-537.

Rassa, J. C. & Parks, G. D. (1998). Molecular basis for naturally occurring elevated readthrough transcription across the M-F junction of the paramyxovirus SV5. *Virology* **247**, 274-286.

Re, G. G., Gupta, K. C. & Kingsbury, D. W. (1983). Genomic and copy-back 3' termini in Sendai virus defective interfering RNA species. *J Virol* **45**, 659-664.

Reina, J., Ballesteros, F., Mari, M. & Munar, M. (2001). Evaluation of different continuous cell lines in the isolation of mumps virus by the shell vial method from clinical samples. *J Clin Pathol* **54**, 924-926.

Ren, R. B., Costantini, F., Gorgacz, E. J., Lee, J. J. & Racaniello, V. R. (1990). Transgenic mice expressing a human poliovirus receptor: a new model for poliomyelitis. *Cell* **63**, 353-362.

Reyes-Leyva, J., Banos, R., Borraz-Arguello, M., Santos-Lopez, G., Rosas, N., Alvarado, G., Herrera, I., Vallejo, V. & Tapia-Ramirez, J. (2007). Amino acid change 335 E to K affects the sialic-acid-binding and neuraminidase activities of Urabe AM9 mumps virus hemagglutinin-neuraminidase glycoprotein. *Microbes Infect* **9**, 234-240.

Rima, B. K., Roberts, M. W., McAdam, W. D. & Martin, S. J. (1980). Polypeptide synthesis i mumps virus-infected cells. *J Gen Virol* **46**, 501-505.

Robinson, D. P., Lorenzo, M. E., Jian, W. & Klein, S. L. (2011). Elevated 17beta-estradiol protects females from influenza A virus pathogenesis by suppressing inflammatory responses. *PLoS pathogens* **7**, e1002149.

Rogers, G. N. & Paulson, J. C. (1983). Receptor determinants of human and animal influenza virus isolates: differences in receptor specificity of the H3 hemagglutinin based on species of origin. *Virology* **127**, 361-373.

Rosas-Murrieta, N. H., Santos-Lopez, G., Reyes-Leyva, J., Jurado, F. S. & Herrera-Camacho, I. (2011). Modulation of apoptosis by V protein mumps virus. *Virol J* **8**, 224.

Rubin, S., Mauldin, J., Chumakov, K., Vanderzanden, J., Iskow, R. & Carbone, K. (2006). Serological and phylogenetic evidence of monotypic immune responses to different mumps virus strains. *Vaccine* **24**, 2662-2668.

Rubin, S. A., Snoy, P. J., Wright, K. E., Brown, E. G., Reeve, P., Beeler, J. A. & Carbone, K. M. (1999). The mumps virus neurovirulence safety test in Rhesus monkeys: a comparison of mumps virus strains. *J Infect Dis* **180**, 521-525.

Rubin, S. A., Afzal, M. A., Powell, C. L., Bentley, M. L., Auda, G. R., Taffs, R. E. & Carbone, K. M. (2005). The rat-based neurovirulence safety test for the assessment of mumps virus neurovirulence in humans: An international collaborative study. *J Infect Dis* **191**, 1123-1128.

Ruiz-Jarabo, C. M., Arias, A., Baranowski, E., Escarmis, C. & Domingo, E. (2000). Memory in viral quasispecies. *J Virol* **74**, 3543-3547.

Safina, G., Duran Iu, B., Alasel, M. & Danielsson, B. (2011). Surface plasmon resonance for real-time study of lectin-carbohydrate interactions for the differentiation and identification of glycoproteins. *Talanta* **84**, 1284-1290.

Sanderson, C. M., Wu, H. H. & Nayak, D. P. (1994). Sendai virus M protein binds independently to either the F or the HN glycoprotein in vivo. *J Virol* **68**, 69-76.

Sanford, K. K., Earle, W. R. & Likely, G. D. (1948). The growth in vitro of single isolated tissue cells. *J Natl Cancer Inst* **9**, 229-246.

Santos, C. L., Ishida, M. A., Foster, P. G., Sallum, M. A., Benega, M. A., Borges, D. B., Correa, K. O., Constantino, C. R., Afzal, M. A. & other authors (2008). Detection of a new mumps virus genotype during parotitis epidemic of 2006-2007 in the state of Sao Paulo, Brazil. *J Med Virol* **80**, 323-329.

Santra, G. (2009). HIV parotitis. *J Assoc Physicians India* **57**, 517.

Sauder, C. J., Zhang, C. X., Ngo, L., Werner, K., Lemon, K., Duprex, W. P., Malik, T., Carbone, K. & Rubin, S. A. (2011). Gene-specific contributions to mumps virus neurovirulence and neuroattenuation. *J Virol* **85**, 7059-7069.

Scheid, A. & Choppin, P. W. (1974). Identification of biological activities of paramyxovirus glycoproteins. Activation of cell fusion, hemolysis, and infectivity of proteolytic cleavage of an inactive precursor protein of Sendai virus. *Virology* **57**, 475-490.

Schmitt, A. P., He, B. & Lamb, R. A. (1999). Involvement of the cytoplasmic domain of the hemagglutinin-neuraminidase protein in assembly of the paramyxovirus simian virus 5. *J Virol* **73**, 8703-8712.

Schmitt, H. J., Just, M. & Neiss, A. (1993). Withdrawal of a mumps vaccine: reasons and impacts. *Eur J Pediatr* **152**, 387-388.

Schroder, K., Hertzog, P. J., Ravasi, T. & Hume, D. A. (2004). Interferon-gamma: an overview of signals, mechanisms and functions. *J Leukoc Biol* **75**, 163-189.

Server, A. C., Merz, D. C., Waxham, M. N. & Wolinsky, J. S. (1982). Differentiation of mumps virus strains with monoclonal antibody to the HN glycoprotein. *Infect Immun* **35**, 179-186.

Shah, D., Vidal, S., Link, M. A., Rubin, S. A. & Wright, K. E. (2009). Identification of genetic mutations associated with attenuation and changes in tropism of Urabe mumps virus. *J Med Virol* **81**, 130-138.

Shan, B. & Lewis, J. A. (1989). Interferon-Induced Expression of Different Genes Is Mediated by Distinct Regulatory Pathways. *Virology* **170**, 277-281.

Shuai, K. & Liu, B. (2003). Regulation of JAK-STAT signalling in the immune system. *Nat Rev Immunol* **3**, 900-911.

Smorodintsev, A. A. (1960). New live vaccines against virus diseases. *Am J Public Health Nations Health* **50(6)Pt 2**, 40-45.

Soule, H. D., Vazguez, J., Long, A., Albert, S. & Brennan, M. (1973). A human cell line from a pleural effusion derived from a breast carcinoma. *J Natl Cancer Inst* **51**, 1409-1416.

Stephensen, C. B., Welter, J., Thaker, S. R., Taylor, J., Tartaglia, J. & Paoletti, E. (1997). Canine distemper virus (CDV) infection of ferrets as a model for testing Morbillivirus vaccine strategies: NYVAC- and ALVAC-based CDV recombinants protect against symptomatic infection. *J Virol* **71**, 1506-1513.

Stevenson, B. R., Siliciano, J. D., Mooseker, M. S. & Goodenough, D. A. (1986). Identification of ZO-1: a high molecular weight polypeptide associated with the tight junction (zonula occludens) in a variety of epithelia. *J Cell Biol* **103**, 755-766.

Strahle, L., Garcin, D. & Kolakofsky, D. (2006). Sendai virus defective-interfering genomes and the activation of interferon-beta. *Virology* **351**, 101-111.

Strober, W. (2001). Trypan blue exclusion test of cell viability. *Curr Protoc Immunol* **Appendix 3**, Appendix 3B.

Strohle, A., Eggenberger, K., Steiner, C. A., Matter, L. & Germann, D. (1997). [Mumps epidemic in vaccinated children in West Switzerland]. *Schweiz Med Wochenschr* **127**, 1124-1133.

Subbarao, E. K., London, W. & Murphy, B. R. (1993). A single amino acid in the PB2 gene of influenza A virus is a determinant of host range. *Journal of virology* **67**, 1761-1764.

Suzuki, Y., Ito, T., Suzuki, T., Holland, R. E., Chambers, T. M., Kiso, M., Ishida, H. & Kawaoka, Y. (2000). Sialic acid species as a determinant of the host range of influenza A viruses. *Journal of virology* **74**, 11825-11831.

Svitek, N. & von Messling, V. (2007). Early cytokine mRNA expression profiles predict Morbillivirus disease outcome in ferrets. *Virology* **362**, 404-410.

Takeuchi, K., Hishiyama, M., Yamada, A. & Sugiura, A. (1988). Molecular cloning and sequence analysis of the mumps virus gene encoding the P protein: mumps virus P gene is monocistronic. *J Gen Virol* **69 (Pt 8)**, 2043-2049.

Takeuchi, K., Tanabayashi, K., Hishiyama, M. & Yamada, A. (1996). The Mumps Virus SH Protein is a Membrane protein and Not Essential for Virus Growth. *Virology* **225**, 156-162.

Takeuchi, K., Kadota, S. I., Takeda, M., Miyajima, N. & Nagata, K. (2003). Measles virus V protein blocks interferon (IFN)-alpha/beta but not IFN-gamma signaling by inhibiting STAT1 and STAT2 phosphorylation. *Febs Lett* **545**, 177-182.

Takeuchi, K., Tanabayashi, K., Hishiyama, M., Yamada, Y. K., Yamada, A. & Sugiura, A. (1990). Detection and characterization of mumps virus V protein. *Virology* **178**, 247-253.

Takeuchi, O. & Akira, S. (2008). MDA5/RIG-I and virus recognition. *Curr Opin Immunol* **20**, 17-22.

Takimoto, T. & Portner, A. (2004). Molecular mechanism of paramyxovirus budding. *Virus Res* **106**, 133-145.

Tanabayashi, K., Takeuchi, K., Okazaki, K., Hishiyama, M. & Yamada, A. (1993). Identification of an Amino-Acid That Defines the Fusogenicity of Mumps-Virus. *J Virol* **67**, 2928-2931.

Tanabayashi, K., Takeuchi, K., Hishiyama, M., Yamada, A., Tsurudome, M., Ito, Y. & Sugiura, A. (1990). Nucleotide sequence of the leader and nucleocapsid protein gene of mumps virus and epitope mapping with the in vitro expressed nucleocapsid protein. *Virology* **177**, 124-130.

Tatsuo, H., Ono, N., Tanaka, K. & Yanagi, Y. (2000). SLAM (CDw150) is a cellular receptor for measles virus. *Nature* **406**, 893-897.

Thompson, C. I., Barclay, W. S., Zambon, M. C. & Pickles, R. J. (2006). Infection of human airway epithelium by human and avian strains of influenza a virus. *J Virol* **80**, 8060-8068.

Tillieux, S. L., Halsey, W. S., Sathe, G. M. & Vassilev, V. (2009). Comparative analysis of the complete nucleotide sequences of measles, mumps, and rubella strain genomes contained in Priorix-Tetra and ProQuad live attenuated combined vaccines. *Vaccine* **27**, 2265-2273.

Tokuda, M. (1957). Studies on mumps virus. III. Experimental studies in guinea pigs. *J Immunol* **79**, 355-360.

Trowbridge, R. S., Lehmann, J. & Brophy, P. (1982). Establishment and characterization of ferret cells in culture. *In Vitro* **18**, 952-960.

Trowbridge, R. S., Lehmann, J., Brown, H. R., Brophy, P. & Haddad, R. (1985). Morphology, organelles and susceptibility to viruses of cultured ferret cells. *Microbios* **43**, 157-168.

Tsurudome, M., Yamada, A., Hishiyama, M. & Ito, Y. (1984). Replication of mumps virus in murine cells. *Arch Virol* **81**, 13-24.

Tsurudome, M., Yamada, A., Hishiyama, M. & Ito, Y. (1987). Replication of mumps virus in mouse: transient replication in lung and potential of systemic infection. *Arch Virol* **97**, 167-179.

Ueda, K., Miyazaki, C., Hidaka, Y., Okada, K., Kusuhara, K. & Kadoya, R. (1995). Aseptic meningitis caused by measles-mumps-rubella vaccine in Japan. *Lancet* **346**, 701-702.

Ukkonen, P., Granstrom, M. L. & Penttinen, K. (1981). Mumps-Specific Immunoglobulin-M and G-Antibodies in Natural Mumps Infection as Measured by Enzyme-Linked Immunosorbent-Assay. *Journal of Medical Virology* **8**, 131-142.

Ulane, C. M., Rodriguez, J. J., Parisien, J. P. & Horvath, C. M. (2003). STAT3 ubiquitylation and degradation by mumps virus suppress cytokine and oncogene signaling. *Journal of virology* **77**, 6385-6393.

Utz, J. P., Szwed, C. F. & Kasel, J. A. (1958). Clinical and laboratory studies of mumps. II. Detection and duration of excretion of virus in urine. *Proc Soc Exp Biol Med* **99**, 259-261.

van der Veen, J. & Sonderkamp, H. J. (1965). Secondary antibody response of guinea pigs to parainfluenza and mumps viruses. *Arch Gesamte Virusforsch* **15**, 721-734.

van Riel, D., Munster, V. J., de Wit, E., Rimmelzwaan, G. F., Fouchier, R. A., Osterhaus, A. D. & Kuiken, T. (2007). Human and avian influenza viruses target different cells in the lower respiratory tract of humans and other mammals. *Am J Pathol* **171**, 1215-1223.

Villar, E. & Barroso, I. M. (2006). Role of sialic acid-containing molecules in paramyxovirus entry into the host cell: a minireview. *Glycoconj J* **23**, 5-17.

Von Magnus, P. (1954). Incomplete forms of influenza virus. *Adv Virus Res* **2**, 59-79.

von Messling, V., Milosevic, D., Devaux, P. & Cattaneo, R. (2004). Canine distemper virus and measles virus fusion glycoprotein trimers: partial membrane-proximal ectodomain cleavage enhances function. *J Virol* **78**, 7894-7903.

Wallace, R. E., Vasington, P. J., Petricciani, J. C., Hopps, H. E., Lorenz, D. E. & Kadanka, Z. (1973a). Development of a diploid cell line from fetal rhesus monkey lung for virus vaccine production. *In Vitro* **8**, 323-332.

Wallace, R. E., Vasingto.Pj, Petricci.Jc, Hopps, H. E., Lorenz, D. E. & Kadanka, Z. (1973b). Development and Characterization of Cell Lines from Subhuman Primates. *In Vitro Cell Dev B* **8**, 333-341.

Watanabe, M., Hirano, A., Stenglein, S., Nelson, J., Thomas, G. & Wong, T. C. (1995). Engineered serine protease inhibitor prevents furin-catalyzed activation of the fusion glycoprotein and production of infectious measles virus. *J Virol* **69**, 3206-3210.

Waxham, M. N., Server, A. C., Goodman, H. M. & Wolinsky, J. S. (1987). Cloning and sequencing of the mumps virus fusion protein gene. *Virology* **159**, 381-388.

Waxham, M. N., Aronowski, J., Server, A. C., Wolinsky, J. S., Smith, J. A. & Goodman, H. M. (1988). Sequence determination of the mumps virus HN gene. *Virology* **164**, 318-325.

Whitaker, A. M. & Hayward, C. J. (1985). The characterization of three monkey kidney cell lines. *Dev Biol Stand* **60**, 125-131.

WHO (1994). Requirements for measles mumps and rubella vaccines and combined vaccine (live). In *Technical Report Series*, pp. 100-176: World Health Organisation (WHO).

WHO (2007). Immunizations, Vaccines and Biologicals - The Mumps Vaccines, pp. 51-60: World Health Organisation.

Wollstein, M. (1916). An Experimental Study of Parotitis (Mumps). *J Exp Med* **23**, 353-375.

Woznik, M., Rodner, C., Lemon, K., Rima, B., Mankertz, A. & Finsterbusch, T. (2010). The mumps virus small hydrophobic protein targets ataxin-1 ubiquitin-like interacting protein (ubiquilin 4). *J Gen Virol*.

Xu, P., Luthra, P., Li, Z., Fuentes, S., D'Andrea, J. A., Wu, J., Rubin, S., Rota, P. A. & He, B. (2012). The V protein of mumps virus plays a critical role in pathogenesis. *J Virol* **86**, 1768-1776.

Yamada, A., Tsurudome, M., Hishiyama, M. & Ito, Y. (1984). Abortive infection of mumps virus in murine cell lines. *J Gen Virol* **65 (Pt 5)**, 973-980.

Yamanishi, K., Takahashi, M., Kurimura, T., Ueda, S. & Minekawa, Y. (1970). Studies on live mumps virus vaccine. 3. Evaluation of newly developed live mumps virus vaccine. *Biken J* **13**, 157-161.

Yasumura, Y. & Kawakita, Y. (1963). Studies on SV40 in tissue culture - preliminary step for cancer research in vitro. *Nihon Rinsho* **21**, 1201-1205.

Yates, P. J. (1995). *Immunity to Paramyxoviruses*. PhD thesis, National Institute for Biological Standards and Control.

Yeo, R. P., Afzal, M. A., Forsey, T. & Rima, B. K. (1993). Identification of a new mumps virus lineage by nucleotide sequence analysis of the SH gene of ten different strains. *Arch Virol* **128**, 371-377.

Yoneyama, M., Kikuchi, M., Natsukawa, T., Shinobu, N., Imaizumi, T., Miyagishi, M., Taira, K., Akira, S. & Fujita, T. (2004). The RNA helicase RIG-I has an essential function in double-stranded RNA-induced innate antiviral responses. *Nature Immunology* **5**, 730-737.

Yoshida, N. & Nakayama, T. (2010). Leucine at Position 383 of Fusion Protein Is Responsible for Fusogenicity of Wild-Type Mumps Virus in B95a Cells. *Intervirology* **53**, 193-202.

Young, D., Andrejeva, J., Livingstone, A., Goodbourn, S., Lamb, R. A., Collins, P. L., Elliot, R. M. & Randall, R. E. (2003). Virus Replication in Engineered human Cells That Do Not Respond to Interferons. *J Virol* **77**, 2174-2181.

Young, D. F., Galiano, M. C., Lemon, K., Chen, Y. H., Andrejeva, J., Duprex, W. P., Rima, B. K. & Randall, R. E. (2009). Mumps Virus Enders strain is sensitive to interferon (IFN) despite encoding a functional IFN antagonist. *Journal of General Virology* **90**.

Yuan, P., Thompson, T. B., Wurzburg, B. A., Paterson, R. G., Lamb, R. A. & Jardetzky, T. S. (2005). Structural studies of the parainfluenza virus 5 hemagglutinin-neuraminidase tetramer in complex with its receptor, sialyllactose. *Structure* **13**, 803-815.

Yuan, P., Swanson, K. A., Leser, G. P., Paterson, R. G., Lamb, R. A. & Jardetzky, T. S. (2011). Structure of the Newcastle disease virus hemagglutinin-neuraminidase (HN) ectodomain reveals a four-helix bundle stalk. *Proc Natl Acad Sci U S A* **108**, 14920-14925.

Zamanian-Daryoush, M., Mogensen, T. H., DiDonato, J. A. & Williams, B. R. (2000). NF-kappaB activation by double-stranded-RNA-activated protein kinase (PKR) is mediated through NF-kappaB-inducing kinase and IkappaB kinase. *Mol Cell Biol* **20**, 1278-1290.

Zhang, L., Collins, P. L., Lamb, R. A. & Pickles, R. J. (2011). Comparison of differing cytopathic effects in human airway epithelium of parainfluenza virus 5 (W3A), parainfluenza virus type 3, and respiratory syncytial virus. *Virology* **421**, 67-77.

Zhang, L., Bukreyev, A., Thompson, C. I., Watson, B., Peeples, M. E., Collins, P. L. & Pickles, R. J. (2005). Infection of ciliated cells by human parainfluenza virus type 3 in an in vitro model of human airway epithelium. *J Virol* **79**, 1113-1124.

Zhang, L. Q., Peeples, M. E., Boucher, R. C., Collins, P. L. & Pickles, R. J. (2002). Respiratory syncytial virus infection of human airway epithelial cells is polarized, specific to ciliated cells, and without obvious cytopathology. *J Virol* **76**, 5654-5666.